

COMMUNAUTÉ FRANÇAISE DE BELGIQUE
UNIVERSITÉ DE LIÈGE – GEMBLOUX AGRO-BIO TECH

**The Chemistry of New Garlic-Derived Organosulfur Compounds
and the Molecular Basis of Olfaction**

Bérénice Dethier

Essai présenté en vue de l'obtention du grade de docteur en sciences agronomiques et ingénierie biologique

Promoteurs: Prof. Marie-Laure FAUCONNIER, Prof. Eric BLOCK

2016

COMMUNAUTÉ FRANÇAISE DE BELGIQUE
UNIVERSITÉ DE LIÈGE – GEMBLOUX AGRO-BIO TECH

**The Chemistry of New Garlic-Derived Organosulfur Compounds
and the Molecular Basis of Olfaction**

Bérénice Dethier

Essai présenté en vue de l'obtention du grade de docteur en sciences agronomiques et ingénierie biologique

Promoteurs: Prof. Marie-Laure FAUCONNIER, Prof. Eric BLOCK

2016

Copyright. Aux termes de la loi belge du 30 juin 1994, sur le droit d'auteur et les droits voisins, seul l'auteur a le droit de reproduire partiellement ou complètement cet ouvrage de quelque façon et forme que ce soit ou d'en autoriser la reproduction partielle ou complète de quelque manière et sous quelque forme que ce soit. Toute photocopie ou reproduction sous autre forme est donc faite en violation de la dite loi et des modifications ultérieures.

The Chemistry of New Garlic-Derived Organosulfur Compounds and the Molecular Basis of Olfaction.

Doctorat en Sciences Agronomiques et Ingénierie Biologique – Université de Liège – 2016

Doctor of Philosophy in Chemistry – State University of New York at Albany – 2016

(Joint PhD program)

Professor Marie-Laure Fauconnier and Professor Eric Block, Advisors.

Bérénice Dethier

Abstract

Garlic is a very popular condiment that has been used around the world for centuries. It is also a source of a remarkably extensive range of organosulfur compounds, whose chemistry is the focus of this thesis. The central reaction in formation of these compounds is the enzymatic cleavage of alk(en)yl cysteine sulfoxides by alliinases, which leads to sulfenic acids. The latter can then undergo condensation and rearrangement into various organosulfur compounds. Three aspects of the chemistry of garlic have been investigated in this thesis.

First, little studied, minor organosulfur compounds in extracts of freshly chopped garlic were studied. These higher molecular weight compounds (MW 150–550) can be conveniently studied using state-of-the-art Liquid Chromatography-Mass Spectrometry (LC-MS) and Direct Analysis in Real Time-Mass Spectrometry (DART-MS) techniques. Novel garlic-derived compounds were studied and the structure of one representative compound containing a five-membered thiolane ring, ajothiolane, was determined by spectroscopic methods, using synthetic analogues as spectroscopic standards. The fate of compounds in a garlic extract over time was also studied, since the new, higher mass sulfur compounds are slowly formed by rearrangement of smaller metabolites a few days after maceration of the garlic.

A second part of this thesis provides hands-on methods for the analysis and preparation of key garlic metabolites. The isolation and/or synthesis of alliin, alliinase and vinylidithiins have been optimized, and are proposed as turnkey procedures for future work.

Finally, in an effort to explain the unique odor of garlic-related thiols and sulfides (in garlic breath, sweat, etc.), the interactions between odorants and olfactory receptors have been studied. Work described in this thesis contributed to this larger project by designing and synthesizing model macrocyclic odorants to resolve the mechanism of olfaction at the receptor level. The conclusions, arguing against the plausibility of the so-called “vibration theory of olfaction”, have been published as a foundation for future work on olfactory detection of thiols and other sulfur-containing compounds.

Chimie de Nouvelles Molécules Dérivées de l'Ail et Bases Moléculaires de l'Olfaction.

Doctorat en Sciences Agronomiques et Ingénierie Biologique – Université de Liège – 2016

Doctor of Philosophy in Chemistry – State University of New York at Albany – 2016

(Thèse en cotutelle)

Professor Marie-Laure Fauconnier and Professor Eric Block, Promoteurs.

Bérénice Dethier

Résumé

L'ail, aliment populaire utilisé de par le monde depuis des siècles, est aussi la source d'une grande variété de molécules organosoufrées. La réaction principale lors de la formation des molécules d'intérêt est le clivage enzymatique d'alk(én)yl cystéine sulfoxydes par des alliinases, réaction qui libère des acides alcan/ènesulféniques. Ces derniers se condensent puis se réarrangent en d'autres composés organosoufrés, dont la chimie est étudiée dans cette thèse en trois axes.

Dans un premier temps, des molécules mineures, relativement peu décrites et présentes dans un macérât d'ail sont examinées. Celles-ci sont caractérisées par une masse moléculaire plus élevée (entre 150 et 550) et peuvent être analysées par LC-MS et DART-MS (Direct Analysis in Real Time-Mass Spectrometry). Le suivi de l'évolution de la composition d'un extrait d'ail au fil du temps, et en particulier des composés soufrés de haute masse moléculaire, suggère que ceux-ci résultent du réarrangement de plus petites molécules après plusieurs jours de macération. L'une de ces nouvelles molécules contenant un thiolane (cycle à cinq atomes dont un soufre), l'ajothiolane, a été étudiée comme modèle. L'utilisation de méthodes spectroscopiques classiques ainsi que la comparaison à des analogues synthétisés ont permis de déterminer sa structure.

Dans un deuxième temps, des méthodes de préparation et d'analyse de trois composés importants dans l'étude de la chimie de l'ail ont été développées. L'optimisation de l'extraction, de la purification et/ou de l'analyse de l'alliine, de l'alliinase et des vinyldithiines fournit des procédures clé-sur-porte pour de futures études.

Enfin, dans le cadre d'un projet visant à expliquer l'odeur caractéristique des thiols et sulfures liés à l'ail (haleine, sueur, etc.), les interactions entre composés organiques volatils et récepteurs olfactifs ont été étudiées. Des molécules modèles (macrocycles carbonylés) ont été synthétisées afin de comprendre le mécanisme de reconnaissance moléculaire, au niveau des récepteurs. Les conclusions, qui infirment la théorie vibrationnelle de l'olfaction, servent de base à la construction d'un modèle général qui inclura les thiols et autres molécules organosoufrées.

Contents

Abstract	ii
Contents	vi
List of Figures	x
Table of Abbreviations	xv
Acknowledgments	xvii
1 The chemistry of genus <i>Allium</i> plants	1
1.1 Overview of the chemistry of garlic secondary metabolites	1
1.1.1 “Don’t eat me!”	1
1.1.2 Rearrangements of thiosulfinate	6
1.1.3 What about onion? Chemistry of zwiebelanes and thiolanes	9
1.2 Smelling sulfur compounds	11
2 Extraction and purification of thiolane-containing natural products from processed genus <i>Allium</i> plants	18
2.1 Novel compounds identified in garlic extracts	18
2.2 DART-MS as a semi-quantitative tool	24
2.2.1 Critical aspects of DART-MS	25
2.2.2 Validation of the method	27
2.2.3 Improving the yield: starting from an enriched extract	33
2.3 Purification of thiolane-containing compounds from garlic extracts	35

2.4	Characterization and stereochemistry of ajothiolane	39
2.4.1	Why is the NMR data so confusing?	41
2.4.2	Functional groups confirmation	42
2.4.3	Mass spectrometry	44
2.4.4	Characterization of stereoisomers	46
2.5	Identification of methylisoajoene	49
2.6	Conclusions	52
2.7	Experimental	52
3	Chemistry of thiolane-containing natural products from processed plants of the genus <i>Allium</i>	60
3.1	Introduction	60
3.1.1	Sulfenic acids	62
3.1.2	Biosynthetic routes of secondary metabolites of <i>Allium</i>	62
3.2	Synthesis of thiolane analogues	64
3.2.1	Insertion of functional groups in the α -position of thiolanes	65
3.2.2	Synthesis of 3,4-dimethylthiolane	69
3.3	Attempted syntheses of ajothiolane	70
3.3.1	Synthesis of bis-1-propenyl disulfide	73
3.3.2	Synthesis of ajothiolane by oxidation of bis-1-propenyl disulfide	76
3.3.3	Synthesis of ajothiolane by heating bis-1-propenyl disulfide	77
3.3.4	Ideas for future work	81
3.4	Synthesis of methylisoajoene	81
3.5	Thiolactone sulfoxides	82
3.5.1	Literature review	82
3.5.2	Attempts to synthesize a thiolactone sulfoxide	85
3.6	Conclusions	86
3.7	Experimental	88
4	Alliin, the precursor: analytical and preparative study	105
4.1	Alliin: origin and interest	105

4.2	Analytical separation of the diastereoisomers of alliin	106
4.2.1	Method development on porous graphitic carbon (PGC)	107
4.2.2	Method validation by the accuracy profiles	110
4.2.3	Conclusions	115
4.3	Preparation of pure stereoisomers of alliin	116
4.3.1	Extraction and purification of (+)-alliin from garlic cloves	116
4.3.2	Chemical synthesis followed by separation	119
4.3.3	Stereospecific synthesis	122
4.3.4	Conclusions	123
4.4	Alliinase purification	125
4.5	Extraction of vinylidithiins from garlic	126
4.5.1	Extraction optimization	128
4.5.2	Conclusions	131
4.6	Conclusion	131
4.7	Experimental	132
5	The chemistry of smell	148
5.1	Introduction	148
5.1.1	Overview of the olfactory system	149
5.1.2	(Bio)chemistry and theories of olfaction	153
5.1.3	Interactions of musk-related compounds and the olfactory receptors	157
5.1.4	Designing olfactory reception experiments: challenges	158
5.2	Results and discussion	160
5.2.1	Synthesis of musk derivatives	161
5.2.2	Interactions at the receptors: in vitro testing and computational study	168
5.2.3	Connection with previous work: could a kinetic isotope effect explain the difference in perception?	170
5.3	Conclusions	172
5.4	Experimental	174
6	General conclusions and perspectives	185

7 Appendices	187
7.1 Extraction and purification of thiolane-containing natural products from processed genus <i>Allium</i> plants	187
7.2 Chemistry of thiolane-containing natural products from processed plants of the genus <i>Allium</i>	212
7.3 Alliin, the precursor: analytical and preparative study	246
7.3.1 Deoxyalliin	246
7.3.2 Alliin	253
7.4 The chemistry of smell	266

List of Figures

1.1	Overview of the alliinase reaction when an <i>Allium</i> cell is cut	2
1.2	Distribution of the major alk(en)yl cysteine sulfoxides in alliums	3
1.3	Biosynthetic routes for the formation of alliin	4
1.4	Mechanism of the enzymatic cleavage of alk(en)yl cysteine sulfoxides	5
1.5	Mechanism of the condensation of two sulfenic acids to a thiosulfinate	5
1.6	Overview of the chemistry of garlic organosulfur compounds	7
1.7	Mechanism of formation of vinyldithiins from allicin.	8
1.8	Mechanism of formation of ajoenes	8
1.9	Mechanism of formation of polysulfides	9
1.10	Chemistry of 1-propenesulfenic acid and the lachrymatory factor in onion	10
1.11	Thiolane compounds in <i>Allium</i> extracts	12
2.1	Thiolanes in petroleum and sediments	18
2.2	Cepathiolane	19
2.3	Formation of cepathiolane	20
2.4	Biosynthesis of thiolane-containing <i>Allium</i> compounds	21
2.5	Proposed mechanism of formation of thiolanes in <i>Allium</i> extracts	21
2.6	Proposed biosynthesis of ajothiolane	22
2.7	Summary of thiolanes reported in <i>Allium</i> extracts	23
2.8	Methylisoajoene and related structures	23
2.9	Comparison of the fragmentation of ajothiolane by DART-MS under different conditions	26
2.10	Fragmentation of ajothiolane ion by DART-MS	27

2.11	DART-MS linear rail	28
2.12	Experimental plan for validation of the quantification by DART-MS	29
2.13	Utilization of the DART-MS signal for quantification: example of data processing	30
2.14	Coefficients of variation of DART-MS analyses for selected garlic metabolite ions	31
2.15	Parameters in the extraction of ajothiolane are the rest time and the extraction time.	33
2.16	Amount of selected garlic metabolites depending on the rest time	34
2.17	Amount of selected garlic metabolites depending on the extraction time	35
2.18	Optimized purification of ajothiolane from garlic cloves.	37
2.19	Purification of ajothiolane: separation scheme.	38
2.20	Comparison of the ^1H NMR chemical shifts of key protons of selected synthesized species . .	40
2.21	Correlations observed by 2D NMR of ajothiolane (COSY, HMBC)	41
2.22	INADEQUATE NMR spectrum of ajothiolane	43
2.23	Correlations observed on the INADEQUATE NMR spectrum of ajothiolane	44
2.24	Summary of the NMR data of ajothiolane	45
2.25	Attempted oxidation of ajothiolane	45
2.26	Fragmentation of ion 221.06 (ajothiolane) by LC-MS/MS	46
2.27	Proposed structures of the fragment ions found in the MS/MS analysis of ajothiolane	47
2.28	Ajothiolane stereoisomers can be distinguished in the methyl region by ^1H NMR	48
2.29	LC-MS of a garlic extract, selected ions 221.06 and 234.04	49
2.30	Methylajoene and garlicin D	50
2.31	NMR of methylisoajoene: comparison of the chemical shifts in CDCl_3 and benzene- d_6	50
2.32	Overview of the ajoene compounds	51
2.33	Mechanism of formation of ajoene	51
3.1	Thiolanes reported in alliums extracts	61
3.2	Sulfenic acids tend to condense to form thiosulfinate	62
3.3	Sulfenic acid reactivity	63
3.4	Example of a stable sulfenic acid	63
3.5	Origin of the secondary metabolites in the <i>Allium</i> species.	64
3.6	Summary of the secondary metabolites extracted from garlic	64
3.7	Alkylation of thiolane sulfoxide	65

3.8 Pummerer reaction	66
3.9 Hydrolysis of the Pummerer product	66
3.10 Mechanism of the Pummerer reaction	66
3.11 Attempted Pummerer reaction on substituted thiolanes	67
3.12 Attempted thio-Pummerer reaction	67
3.13 Synthesis of 2-(allylthio)thiolane sulfoxide	68
3.14 Synthesis of 2-(allylthio)thiolane sulfoxide derivatives	69
3.15 Comparison of the chemical shifts of C ₂ -H of various 2-(allylthio)thiolane derivatives	70
3.16 Synthesis of 2-mercaptopthiolane	70
3.17 Attempted chlorination of 2-mercaptopthiolane	71
3.18 Synthesis of 3,4-dimethylthiolane	71
3.19 Influence of the stereochemistry of the double bonds in the rearrangement of <i>S</i> -(1-propenyl)-1-propenethiosulfinate	72
3.20 Synthesis of alkyl 1-propenyl sulfide	73
3.21 Synthesis of alkyl (<i>E</i>)-1-propenyl sulfide	73
3.22 Mechanism of the reduction of 1-propenyl propyl sulfide	74
3.23 Ammonia-free reduction of 1-propenyl propyl sulfide	75
3.24 Mechanism of the oxidation in the synthesis of bis 1-propenyl disulfide	76
3.25 Proposed synthesis of ajothiolane by oxidation of bis-1-propenyl disulfide	78
3.26 Isomerization of ajothiolane	79
3.27 Structure of the by-product of the synthesis of ajothiolane and deoxyajothiolane	79
3.28 Proposed synthesis of ajothiolane by thermal rearrangement of bis-1-propenyl disulfide	80
3.29 Ideas for future work: treatment of 2-thioacetoxythiolane with chlorine	81
3.30 Ideas for future work: trap the short-life double Pummerer product	81
3.31 Proposed synthesis of methylisoajoene	82
3.32 Thiolactone sulfoxides in the literature	83
3.33 Proposed pathway of the metabolism of Prasugrel including a thiolactone sulfoxide intermediate	84
3.34 Thiolactone sulfoxide trapped in the chemistry of Prasugrel	85
3.35 Synthesis of γ -thiobutyrolactone	85
3.36 Alternative structure for unknown compound with formula C ₉ H ₁₄ O ₂ S	86

3.37 Updated overview of the chemistry of garlic	89
4.1 Enzymatic reaction of alliin and subsequent condensation	105
4.2 Alliin synthesis	106
4.3 Alliin stereoisomers	106
4.4 Van Deemter plot of the HPLC method	109
4.5 Representative chromatogram of the optimized HPLC method	111
4.6 Chromatogram of a garlic extract	111
4.7 Accuracy profile methodology	112
4.8 Linearity profile	113
4.9 Accuracy profile	115
4.10 Suggested rearrangement of alliin by Mislow-Evans rearrangement	117
4.11 Extraction of alliin from garlic cloves	118
4.12 Alliin in the binding pocket of alliinase	120
4.13 Enzymatic resolution of stereoisomers of alliin: principle	120
4.14 Enzymatic resolution of (\pm) -alliin by alliinase: HPLC chromatograms	121
4.15 Enzymatic resolution of (\pm) -alliin by alliinase	121
4.16 Protection of the amine and carboxylic acid functions of deoxyalliin	124
4.17 Proposed stereospecific synthesis of alliin	124
4.18 Summary of the different approaches in the production of pure $(+)$ -alliin	125
4.19 Extraction and purification of alliinase: comparison	126
4.20 Mechanism of the biosynthesis of vinyldithiins	128
4.21 Extraction of vinyldithiins: optimization	129
4.22 Extraction of vinyldithiins: influence of the temperature	130
4.23 Extraction of vinyldithiins: assisted extractions	131
5.1 Olfactory system	150
5.2 Olfaction is the combination of the signal from multiple olfactory receptors	151
5.3 Biochemistry after activation of the olfactory receptors	154
5.4 Vibration theory of olfaction: overview	155
5.5 Example of molecular modeling of the olfactory receptor	156

5.6	Structure of musk-related compounds	157
5.7	Deuteration patterns of cyclopentadecanone isotopologues studied in this work.	161
5.8	Wash-out reaction: base catalyzed exchange of four hydrogens	161
5.9	Mechanism of the deuteration reaction	162
5.10	Rhodium-catalyzed deuteration reaction	162
5.11	Deuteration reaction: proportion of the products.	163
5.12	Recycling the reduced cyclopentadecanone by oxidation of the alcohol.	163
5.13	Inverted wash-out reaction: base catalyzed exchange of four deuteriums.	164
5.14	Infrared spectra of isotopologues of cyclopentadecanone	165
5.15	Mass spectra of isotopologues of cyclopentadecanone	166
5.16	NMR spectra of isotopologues of cyclopentadecanone	167
5.17	Luciferase assay results	169
5.18	Scheme of the electron tunneling phenomenon	170
5.19	Baeyer-Villiger oxidation of cyclopentadecanone	171
5.20	Kinetic isotope effect in Baeyer-Villiger oxidation of cyclopentadecanone	172
5.21	Kinetic isotope effect in Baeyer-Villiger oxidation of cyclopentadecanone: results	173

Table of Abbreviations

AA acetic anhydride

ACN acetonitrile

ACSO *S*-alk(en)yl cysteine sulfoxide

APCI atmospheric pressure chemical ionization

ANOVA ANalysis Of VAriance

BV Baeyer-Villiger

***n*-BuLi** *n*-butyllithium

COSY COrrelation SpectroscopY

CV coefficient of variation

DART-MS Direct Analysis in Real Time Mass Spectroscopy

DCM dichloromethane

ESI electrospray ionisation

EtOAc ethyl acetate

FDA Food and Drug Administration

GC-MS gas chromatography - mass spectroscopy

GPCR G protein-coupled receptor

HMBC Heteronuclear Multiple-Bond Correlation

HPLC high-performance liquid chromatography

INADEQUATE Incredible Natural Abundance Double QUAntum Transfer Experiment

IR infrared spectroscopy

KIE kinetic isotope effect

LDH lactate dehydrogenase

LF lachrymatory factor
mCPBA *m*-chloroperbenzoic acid
MS mass spectrometry
MeOH methanol
NCS *N*-chlorosuccinimide
NMR nuclear magnetic resonance
OBP odorant-binding protein
OE olfactory epithelium
OR olfactory receptor
OSN olfactory sensory neuron
PEG polyethylene glycol
PGC porous graphitic carbon
PLP pyridoxal phosphate
TFA trifluoroacetic acid
TLC thin-layer chromatography
TFAA trifluoroacetic anhydride
UV ultraviolet
VTO vibration theory of olfaction

Acknowledgments

I would like to express my sincere gratitude to my mentor Professor Eric Block for his guidance, creativity, support and scientific integrity. His knowledge of sulfur chemistry and dedication to the advancement of the field will always be a model for me. I could not have imagined having a better advisor for my PhD study.

Besides my advisor, I would like to thank the rest of my thesis committee: Robert Sheridan, Professors Rabi Musah, Maksim Royzen, Ting Wang and Qiang Zhang as well as other faculty members of the Chemistry Department for their insightful comments and encouragement.

I wish to gratefully acknowledge the following for their contribution during the course of the research described in this Thesis on the American side: Dr. Sivaji Gundala, Julien Ponchaux, Rama Yaghi, Dr. Sonia Flores-Penalba and Benjamin Bechand for their assistance in the laboratory; Professor Rabi Musah for many helpful discussions and her attention to details; Professor Alexander Shekhtman, Professor Zhang Wang and Robert Sheridan (New York State Agriculture and Markets lab) for their valued collaboration on portions of the research; and the Department staff: Brian, Dave and Nicole.

My sincere thanks also go to my colleagues in the Department for their timely assistance and friendship, especially Leah Seebald, Kelly Bonetti, Kristen Fowble and Juliana Agudelo. My years in Albany would not have had the same flavor without them.

I thank the Chemistry Department of the University at Albany, the National Science Foundation and Initiative for Women for their financial support.

On the Belgian side, I want to thank Professors Marie-Laure Fauconnier and Jean-Paul Wathelet for trusting me and giving me opportunities for carrying out this research project.

My labmates Nathalie, Morgan, Pierre-Patrick, Céline, Gaëtan, Katherine, Nadine, Djamel, Marie, Nicolas, Sandrine, Emilien, François and Pascal deserve many thanks for their assistance in the laboratory as well as the excellent atmosphere in the group. I also thank Danny, Franck and Vincent for educating me

in a new area of research and for many helpful discussions, and the Belgian Committee members Professor Aurore Richel, Michel Frederich, Steve Lanners, Georges Lognay and Daniel Portetelle for their informed advice. The following undergraduate students helped with the lab work, and I wish to thank them: Loic, Fabio, Julien, Virginie, Francesco, David and Lydia. Members of the following laboratories provided help and advices: Chimie Analytique, Chimie Biologique Industrielle, Chimie Organique de Synthèse (UNamur), and I am grateful for their contribution to this Thesis.

I want to acknowledge the assistance and support received from Nathalie le Maire, even from far away. Her dedication to teaching Chemistry and improving the understanding of our students sets an example for the rest of us. Thanks also to my two co-assistants, Marjolaine and Michael, for the lunches and good time, and Cédric, Marie-Laure and Coraline for the carpooling memories.

Furthermore, I thank the University of Liège, in particular the CURAGx of Gembloux Agro-Bio Tech, the Fédération Wallonie-Bruxelles and the Fonds National pour la Recherche Scientifique for their generous financial support.

Across continents, I have been blessed with the encouragements and support of my amazing family. My parents, Fabienne and Clément, my siblings Delphine, Martin and Colombe and my husband Ameen deserve so much acknowledgment. Their contribution to shaping the person I have become is immense. Thanks.

Finally, I want to thank you, Reader, for your interest in our work and the wonderful field of organosulfur chemistry.

*Aux femmes de ma vie
Colombe, Delphine, Fabienne, Félicie and Juliette*

Chapter 1

The chemistry of genus *Allium* plants

1.1 Overview of the chemistry of garlic secondary metabolites

During the first six months of 2016, “garlic” generated over 6000 hits in Google Scholar. Papers are constantly being published on the topic, mostly on the biological and therapeutic properties of garlic compounds. Interest in *Allium* chemistry does not seem to wane. Garlic is also known outside academia for its health properties, and is recommended in folk medicine. Most of these properties originate from the organosulfur compounds that are present in garlic. This chapter seeks to describe these compounds and their formation in garlic extracts. Onion chemistry will also be discussed. However, the therapeutic properties will not be treated in this chapter. Our focus is the chemistry leading to the formation of the molecules, not their applications. The abundant literature on the bioavailability and bioactivity of the compounds, assessed by sometimes controversial bioassays, are reviewed elsewhere^{1–6} (non-exhaustive list).

1.1.1 “Don’t eat me!”

Organosulfur compounds originate from a defense mechanism of the plant. The pungent garlic compounds are released when the cloves are damaged to repel the predator. From a chemical point of view, this happens because the precursors of the volatile compounds are physically separated in the garlic cells (Figure 1.1). The enzyme alliinase is stored in the vacuole, while its substrates, *S*-alk(en)yl cysteine sulfoxides (ACSOs), are stored in the cytosol. Each of the alk(en)yl group of ACSOs is present in different proportions in the

Allium plants (Figure 1.2). Allyl (2-propenyl) and 1-propenyl are the major alkenyl groups in garlic and onion, respectively.

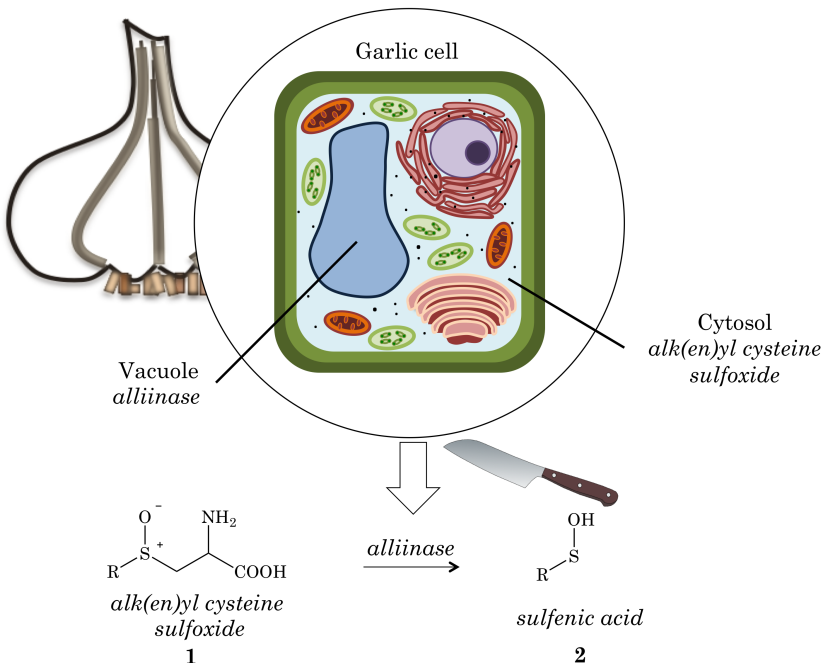


Figure 1.1: Overview of the alliinase reaction as a defense mechanism of the plant. In garlic cells, the substrate is stored in the cytosol and the enzyme in the vacuole. The substrate of the enzymatic reaction is an alk(en)yl cysteine sulfoxide (ACSO, **1**). Only when the plant is damaged can alliinase cleave the cysteine sulfoxide, leading to the formation of a sulfenic acid (**2**). The most abundant ACSO in garlic is alliin (**1a**, R = allyl).

S-Allyl cysteine sulfoxide is named alliin (**1a**), and *S*-methyl cysteine sulfoxide, methiin (**1b**). *S*-Propyl cysteine sulfoxide, propiin, is abundant in onion, but not in garlic, and will not be covered in this work.

Research on the biosynthesis of ACSOs was pioneered by Granroth who proposed two paths.⁸ The first one (Figure 1.3) starts with serine, to which 2-propenethiol is added. This was discovered by measuring ¹⁴C labeled *S*-allyl cysteine in plants fed with labeled serine. The second path involves γ -glutamyl peptides, also uncovered by feeding various alliums with ³⁵S-sulfate.⁹ These peptides are formed from glutathione, which loses glycine after alk(en)ylation, forming an alk(en)yl γ -glutamyl cysteine. Two enzymes are then involved in the synthesis of ACSOs: a γ -glutamyl trans-peptidase cleaves the glutamyl moiety, and an oxidase converts the sulfide to sulfoxide. Both routes are summarized in Figure 1.3 for alliin.

The reaction with alliinase requires a cofactor, pyridoxal phosphate (PLP), which forms an imine with the amino group of the cysteine moiety (Figure 1.4). Alliinases vary slightly between species, and so does their

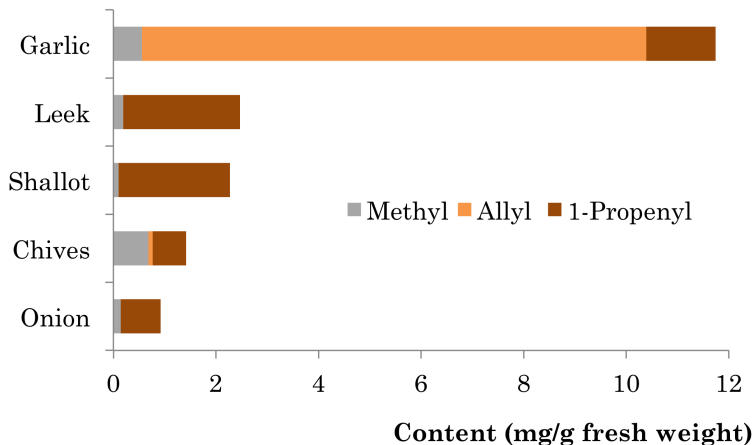


Figure 1.2: Distribution of the ak(en)yl groups of *S*-alk(en)yl cysteine sulfoxides (ACSOs, **1**) in selected *Allium* plants. *S*-Propyl cysteine sulfoxide, present in onion, has not been analyzed in the work of Sun Yoo et al.⁷

activity toward each of the ACSOs. In particular, the stereochemistry of the sulfoxide group is recognized by the enzyme. A difference in activity between (+)- and (-)-**1a** of up to 1.75-fold was reported in garlic.¹¹ Alliinases are mostly found in the genus *Allium*, but also in *Petiveria alliacea*¹² and *Ensifer adhaerens*.¹³

The products of the enzymatic reaction are one mole of sulfenic acid (**2**), pyruvate and ammonia per mole of substrate. The formation of pyruvate is directly proportional to the formation of sulfenic acid, which is used to indirectly measure the activity of alliinase. Pyruvate is transformed into lactate by lactate dehydrogenase (LDH), a reaction that consumes NADH. The disappearance of NADH is monitored by spectrometry (decrease of absorbance at 340 nm), and the formation of pyruvate and sulfenic acid can be inferred from these results.¹⁴

The condensation of two molecules of sulfenic acid leads to a thiosulfinate **3** (Figure 1.5). Table 1.1 reports the proportion in each thiosulfinate in a garlic extract. Logically, the thiosulfinate derived from the most abundant allyl group (diallyl thiosulfinate or allicin, **3a**) are present in larger amount, but mixed thiosulfinates are also formed. Thiosulfinates are highly reactive and quickly form a variety of compounds depending on the environment. The reported half-life of allicin in water at 25 °C is 6 days, but only 3.1 h in vegetable oil,¹⁵ which reflects the protective action of hydrogen bonding in water. Rearrangement products are likely responsible for the alleged biological properties of garlic.

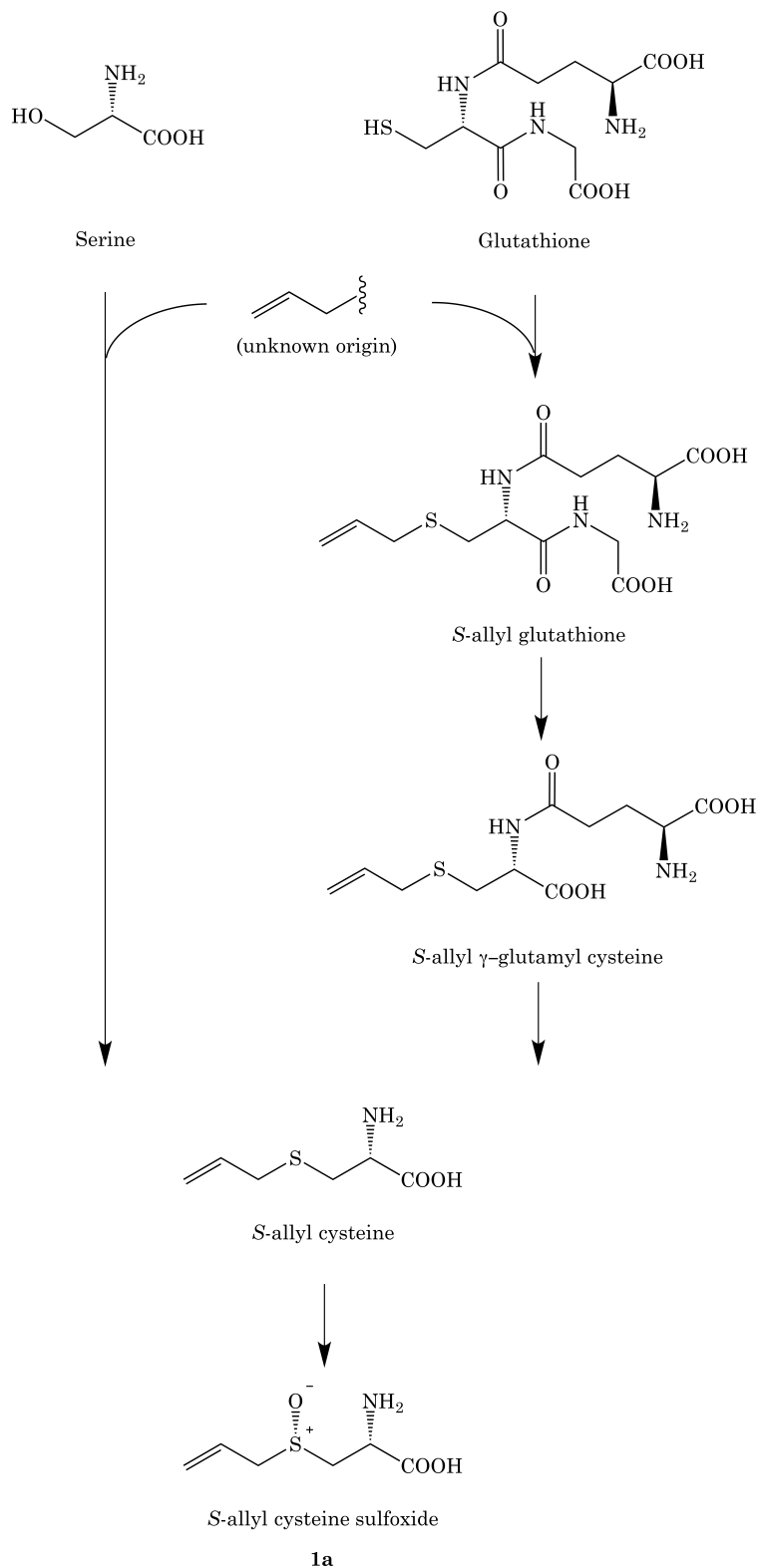


Figure 1.3: Two biosynthetic routes for the formation of alliin in *Allium* plants, the serine path on the left and the γ -glutamyl peptide path on the right.¹⁰

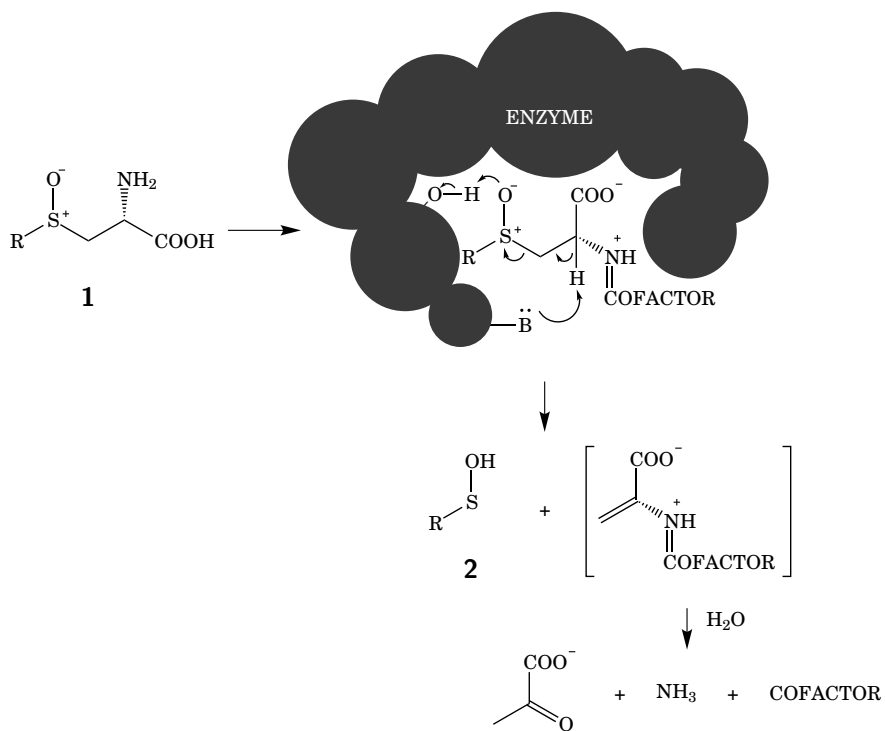


Figure 1.4: *S*-Alk(en)yl cysteine sulfoxides (ACSOs, **1**) are the precursors of garlic flavor compounds. They are cleaved by alliinase when the cell is crushed. A sulfenic acid (**2**), pyruvate and ammonia are released. R = allyl (**1a**), methyl (**1b**), 1-propenyl (**1c**, see Figure 1.2 for composition).

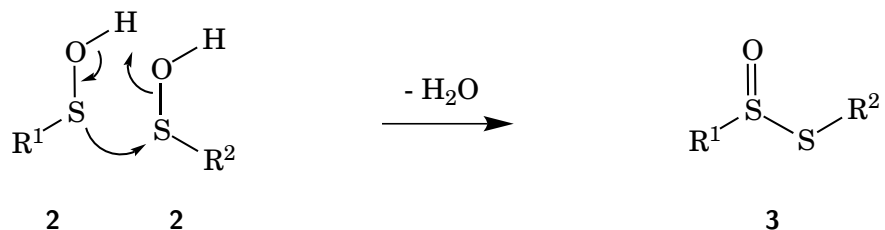


Figure 1.5: Two molecules of sulfenic acid **2** condense to form a thiosulfinate **3**.

Table 1.1: Composition in thiosulfinate of a garlic extract.¹⁶

	R ¹	R ²	mg/g dry wt.	Molar proportion
Allicin	allyl	allyl	12.1	73%
	1-propenyl	allyl	0.9	5%
	allyl	1-propenyl	0.33	2%
	allyl	methyl	2.3	16%
	methyl	allyl		
	1-propenyl	methyl	0.16	1%
	methyl	1-propenyl		
Dimethyl	methyl	methyl	0.26	2%
TOTAL			16.05	

1.1.2 Rearrangements of thiosulfinates

Products of thiosulfinate rearrangement are illustrated in Figure 1.6. The environment (temperature, solvent, etc.) plays a key role in the products formed. Block¹⁷ divides the compounds into three groups: primary volatiles (thiosulfinates **3**), secondary volatiles (such as polysulfides **4a** and **4b**) and secondary solution components or aged extract components. High temperatures lead mostly to the formation of (poly)sulfides. If allicin is dissolved in less polar, edible oils, vinyldithiins are formed (**5**). The production of each of these compounds is briefly outlined in this section. 1-Propenyl thiosulfinate (**3c**) undergoes different chemistry that is more specific to onion and will be discussed in Section 1.1.3.

Vinyldithiins (**5**)

Vinyldithiins were the object of a research project (and a publication¹⁸) in the context of a collaboration between BioXtract SA and the Unit of General and Organic Chemistry of Gembloux Agro Bio-Tech. Their extraction and chemistry will be developed in Chapter 4. Briefly, two types of vinyldithiins are formed by a Diels-Alder reaction between two molecules of thioacrolein (**6**), formed by decomposition of allicin (Figure 1.7). 1,3-Vinyldithiin (**5a**) is the most abundant isomer. The lipophilicity of thioacrolein and dithiins explains why they are formed in non-polar environment such as edible oils, and why their properties are related to the metabolism of fat.^{19,20}

Ajoenes (**7**)

A potent antithrombotic agent was discovered in garlic extracts by Apitz-Castro et al.,²¹ but the structure they proposed was incorrect. It was later corrected by Block, Apitz-Castro and other coworkers as 1-allyl-2-(3-(allylsulfinyl)prop-1-en-1-yl)disulfane (**7a**). The name "ajoene" was coined from *ajo*, the Spanish word for garlic, combined with "ene" signifying double bonds. The internal double bond is found in both *E* and *Z* configurations in a 4:1 ratio, which is consistent with the mechanism of its formation (Figure 1.8).

Ajoenes are formed from allylic thiosulfinates.²² The divalent sulfur of the thiosulfinate attacks an equivalent sulfur in a second molecule, leading to a triallyloxotrisulfan-2-ium ion (**11**). An alkenedisulfanum ion (**12**) is formed by rearrangement and loss of sulfenic acid. 1,4-Nucleophilic addition of a sulfenic acid leads to the final ajoene. Years after the identification of **7a**, equivalent compounds with methyl groups were discovered by Sendl et al.²³ Methyl- ($R^1 = \text{allyl}$, $R^4 = \text{methyl}$, **7b**) and dimethylajoene ($R^1 = R^4 = \text{methyl}$, **7c**) were both found in a different species of *Allium*, *Allium ursinum*, in which methiin (**1b**) is more abundant.

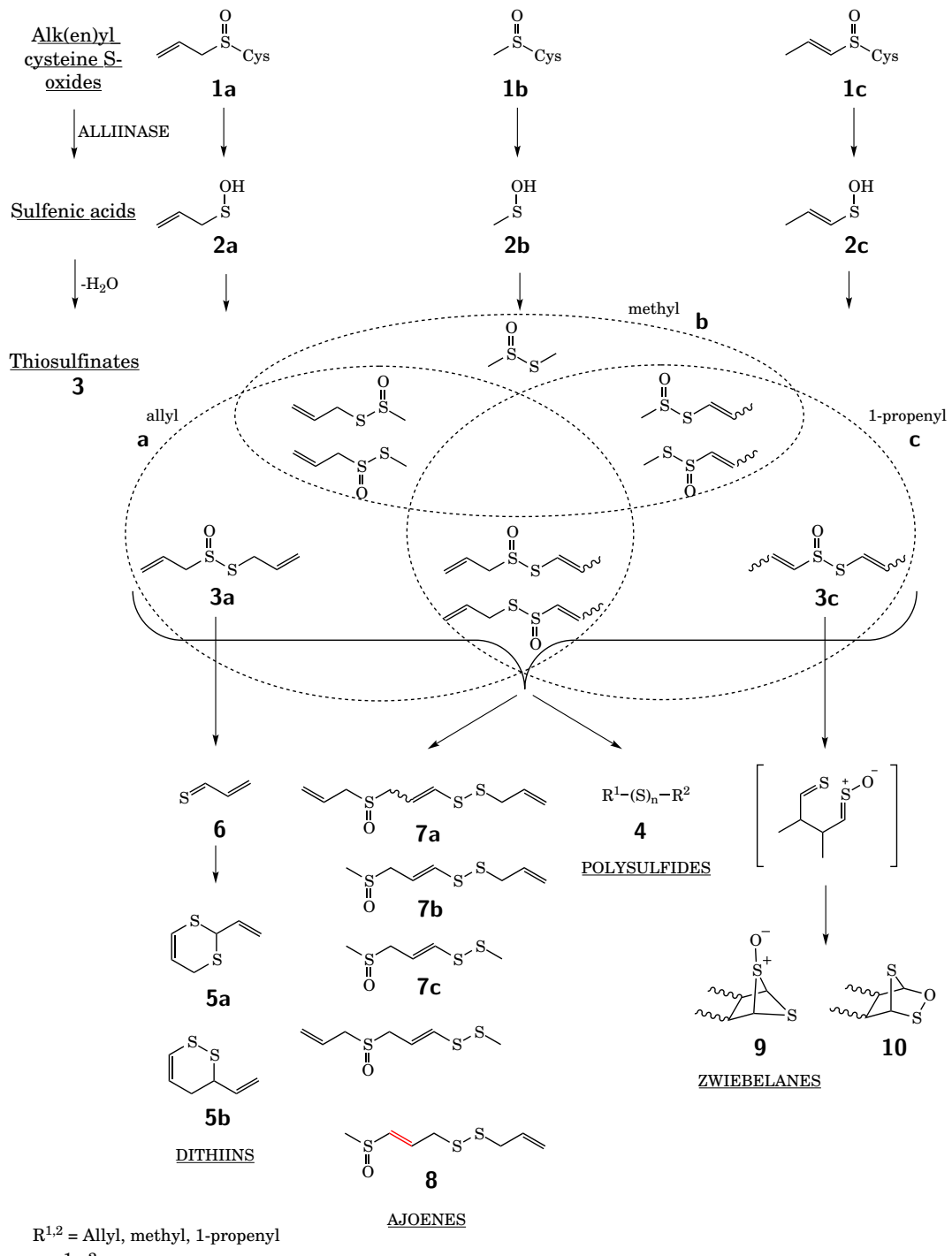


Figure 1.6: Overview of the chemistry of garlic organosulfur compounds. Alliin (**1a**) and other *S*-alk(en)yl cysteine sulfoxides (ACSOs, **1**) are cleaved by alliinase to the corresponding sulfenic acids (**2**), which then condense giving thiosulfinates (**3**), which in turn rearrange giving three main types of compounds: vinylidithiins (**5**), ajoenes (**7**) and (poly)sulfide (**4**). 1-Propenyl thiosulfinate (**3c**) can undergo a thio-Claisen rearrangement, followed by further rearrangements. This chemistry is described elsewhere (Section 1.1.3).

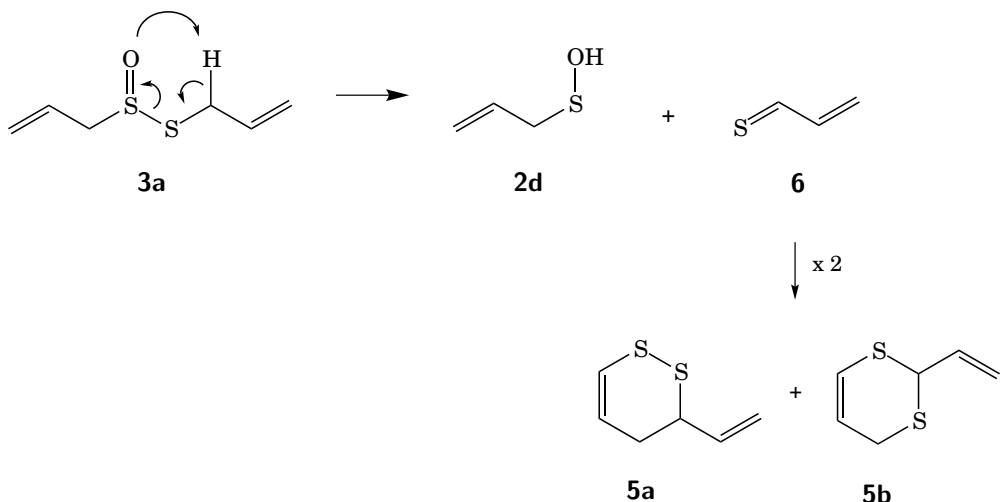


Figure 1.7: Mechanism of formation of vinyldithiins from allicin.

Confusion is possible here: ajoene is the name used for the first discovered diallyl ajoene **7a** ($R^1 = R^4 = \text{allyl}$), but also to the plural form for the group of compounds containing a $R\text{-S(O)}\text{-CH}_2\text{-CH=CH-S-S-R}'$ core. More recently, an isomer of methylajoene, **8** (Figure 1.6), has been reported by Yoshida et al.²⁴ Studies of this compound are described in Chapter 2.

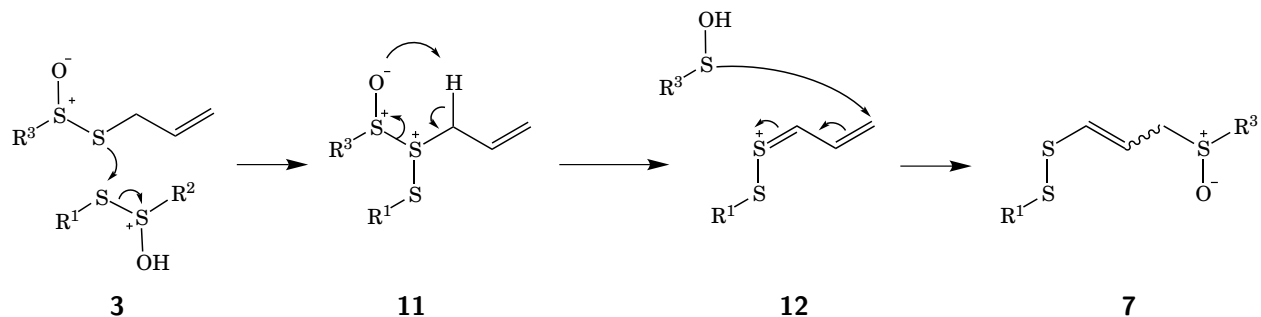


Figure 1.8: Ajoenes are formed by the reaction of two thiosulfinates. Allyl and methyl ajoenes have been reported (R^1 to $R^3 = \text{allyl or methyl}$). One isomer of methylajoene (**8**, Figure 1.6) had also been reported,²⁴ and will be discussed in Chapter 2.

Polysulfides (4)

Alk(en)yl mono- and polysulfides are mostly found in garlic oil, i.e. steam distilled garlic extracts. The mechanism for their formation (Figure 1.9) was postulated in 2010 based on Direct Analysis in Real Time Mass Spectroscopy (DART-MS) experiments.²⁵ Two key intermediates, 2-propenesulfenic acid (**13**) and diallyl trisulfane *S*-oxide (**14**), were identified by this technique. 2-Propenesulfenic acid (**2a**) was also directly

identified for the first time, even though its existence had been known for decades in *Allium* chemistry. Diallyl sulfide is thought to be produced by decomposition of diallyldi- and diallyltrisulfide with heat. One mole of allyl alcohol (**15**) is released by pathway a. This metabolite has been associated with the anti-yeast activity of garlic.^{26,27}

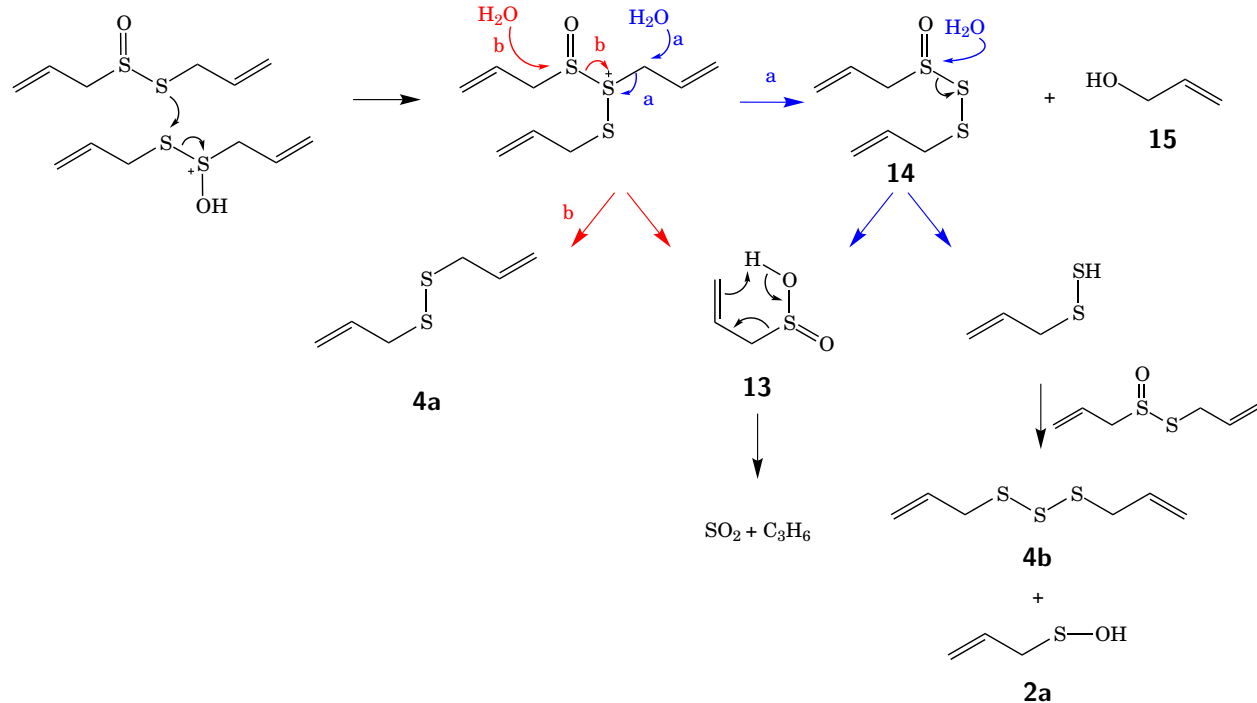


Figure 1.9: Biosynthetic route leading to the formation of allyl polysulfides **4a** and **4b**. The intermediate **14** and by-product **13** were identified by Direct Analysis in Real Time Mass Spectroscopy (DART-MS) by Block et al.²⁵

1.1.3 What about onion? Chemistry of zwiebelanes and thiolanes

The composition of alk(en)yl cysteine sulfoxides is different in onion, in which 1-propenyl cysteine sulfoxide (**1c**, isoalliin) predominates. Another crucial difference between onion and garlic is the presence of a second enzyme, the lachrymatory factor synthase (LFS), identified by Imai et al.²⁸ This enzyme converts 1-propenesulfenic acid (**2c**) into the lacrymatory factor (LF, **16**, Figure 1.10), which triggers tears in contact with the eyes. LF had been identified earlier, but was thought to be formed spontaneously from **2c** until LFS was isolated.²⁹ A consequence of this reaction is the low availability of **2c** and only small amounts of 1-propenyl thiosulfinate (**3c**) being formed.

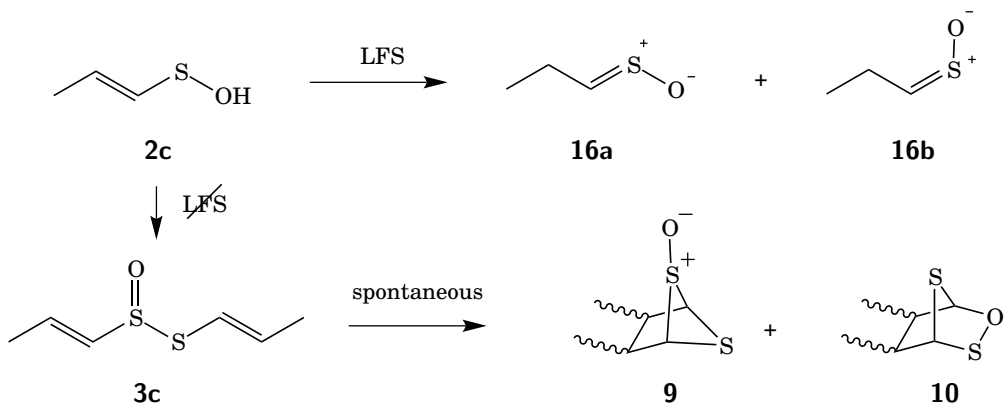


Figure 1.10: Lachrymatory factor (LF, **16**) is formed when enzyme LFS reacts with 1-propenesulfenic acid (**2c**). Stereoisomer **16a** is minor. If LFS is suppressed, the sulfenic acid condenses forming 1-propenyl thiosulfinate (**3c**), which rearranges to zwiebelane (**9**) or a bicyclic sultene **10** depending on the stereochemistry of the double bonds.³⁰

Recent work on LFS-suppressed onions by Aoyagi's research group sheds light on additional compounds derived from the rearrangement of thiosulfinate **3c** including thiolanes.³¹⁻³³ This rearrangement first leads to zwiebelane (**9**)³⁴ and a bicyclic sultene **10**. Thiolanes (five-membered rings with one sulfur) are formed when a nucleophile attacks the sultene sulfur of **10**, resulting in ring opening. This mechanism will be covered extensively in Chapter 3.

Interest in thiolanes arises from the concurrent publication of papers on structures termed "garlicnins" (**17**) and "onionins" (**18**) by Nohara's research group³⁵⁻³⁸ (Figure 1.11). Some functional groups present in the proposed structures seems to be implausible due to their high reactivity (sulfenic acids in **18** and **17a** and **17b**, thiolactone sulfoxide in **17c**). A review of the literature on these functional groups and synthesis of analogues of thiolanes is presented in Chapter 3.

A common feature of cepthiolane, garlicnins and onionin is a 3,4-dimethylthiolane core substituted at positions 2 and 5 (Figure 1.11). The nature of the substituents on these two carbons separates them into two groups: cepthiolane (**19**) and garlicnin C (**17d**), which have heteroatoms on both C₂ and C₅, whereas other garlicnins and onionin present a heteroatom on C₂ and an alkenyl group on C₅. Since there is no heteroatom between the six carbons of dimethylthiolane and the alkenyl group in the latter, the number of connected carbons equals nine. This raises a concern, since chains of more than six carbons have not been previously reported in garlic and onion degradation metabolites and seem to be inconsistent with their formation by known biosynthetic pathways. The likelihood of the formation of a carbon-carbon bond between the side chain and C₅ of the thiolane ring by biosynthesis is therefore an important question discussed in Chapter 2.

Another thiolane, ajothiolane (**20**, Figure 1.11), will also be discussed. The structure of ajothiolane is proposed based on the biosynthetic intermediates present in garlic by analogy to the formation of cepathiolane. These results, including findings on other natural products and their purification from garlic extracts, lay the foundation for a larger project on the analysis of higher mass compounds found in aged-garlic extracts, which can be analyzed with techniques previously unavailable.

Lastly, improvements to the protocols for isolation, purification and analysis of garlic natural products, including alliin and other ACSOs (**1**), alliinase, and vinyldithiins (**5**) are presented in Chapter 4.

1.2 Smelling sulfur compounds

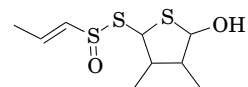
Another key feature of organosulfur compounds, including those from garlic, is their unique smell. Not only are sulfur compounds easily recognizable, but their threshold of olfactory detection is also very low. This property is notably used in natural gas distribution: odorless gas is odorized with thiols to sense leaks and prevent gas-related disasters. Furthermore, thiol and sulfide odors are perceived very differently from their oxygenated counterparts alcohols and ethers, respectively.

The mechanisms of olfaction at the molecular level are not well understood. Two models are invoked to explain the activation of a receptor by an odorant: a mechanism based on structural and stereo-electronic properties on the one hand, and a mechanism based on the vibrational properties of the odorant on the other hand. Better understanding of the mechanisms triggering a response from the olfactory receptor is needed.

Isotopologues (molecules differing only in their isotopic composition) represent an appropriate model to determine the plausibility of the vibration theory of olfaction if the response from the receptor can be measured: isotopologues have different vibrational properties, but similar shape and electronic properties. The use of deuterium in place of hydrogen is particularly interesting: the mass of the atom is double, so the vibrational frequencies are very different, with little impact on the shape. The level of interaction with the receptor should be drastically different for isotopologues to confirm the vibrational mechanism hypothesis.

Unfortunately, this method cannot be applied in the design of thiol odorants. The proton of a thiol is acidic, and a deuterium would exchange quickly under aqueous conditions (in a bioassay with the receptor for example), causing the results to be meaningless. Therefore, before investigating the particular case of thiols, macrocyclic ketones were studied. Macroyclic ketones interact with a only a few olfactory receptors (ORs) and, unlike thiols, do not have labile protons. Isotopologues were designed, synthesized and their interactions

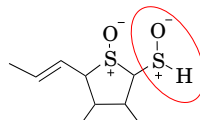
Structure proposed by Aoyagi et al.



Cepathiolane

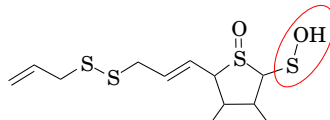
19

Structures proposed by Nohara et al.



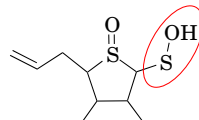
Onionin

18



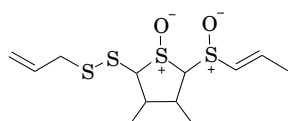
Garlicin A

17a



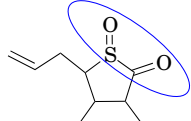
Garlicin B

17b



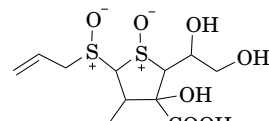
Garlicin C

17d



Garlicin K

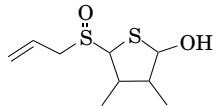
17c



Garlicin H

17e

Structure proposed in this work for garlicin B



Ajothiolane

20

Sulfenic acid

Thiolactone sulfoxide

Figure 1.11: Thiolane compounds reported in *Allium* extracts by the Aoyagi³¹⁻³³ and Nohara research groups.³⁵⁻³⁸ Ajothiolane (**20**) is proposed in this work as an alternative to **17b**. It is suggested here that **18**, **17a**, **b** and **c** are implausible because of the presence of highly reactive sulfenic acid and thiolactone sulfoxide moieties. The letters used for identification of the garlicins by Nohara et al. are capitalized; lower case letters are used in conjunction with the compound number **17**. Stereochemistry is omitted.

with one human receptor screened for musk odors, OR5AN1, were assessed via a luciferase bioassay. Chapter 5 presents these results.

The work on macrocyclic ketones may appear far from the chemistry of garlic. However, it was crucial to eliminate a mechanism of olfaction that could be generalized to all odorants.³⁹ Hydrogen bonds and polar interactions likely involved in the olfaction of ketones will eventually be linked to smelling organosulfur compounds in more complex systems with more than one OR. Since this work, thiol-specific ORs have been identified, and sulfur-containing small molecules were tested in mouse and human ORs.

References

- (1) Block, E., *Garlic and Other Alliums: the Lore and the Science*; Royal Society of Chemistry: Cambridge, UK, 2010.
- (2) Lawson, L. D.; Gardner, C. D. Composition, stability, and bioavailability of garlic products used in a clinical trial. *J. Agric. Food Chem.* **2005**, *53*, 6254–6261.
- (3) Bongiorno, P. B.; Fratellone, P. M.; LoGiudice, P. Potential health benefits of garlic (*Allium sativum*): a narrative review. *J. Complement. Integr. Med.* **2008**, *5*, 1.
- (4) Wilson, E. A.; Demmig-Adams, B. Antioxidant, anti-inflammatory, and antimicrobial properties of garlic and onions. *Nutr. Food Sci.* **2007**, *37*, 178–183.
- (5) Rahman, K.; Lowe, G. M. Garlic and cardiovascular disease: a critical review. *J. Nutr.* **2006**, *136*, 736S–740S.
- (6) Fleischauer, A. T.; Arab, L. Garlic and cancer: a critical review of the epidemiologic literature. *J. Nutr.* **2001**, *131*, 1032S–1040S.
- (7) Sun Yoo, K.; Pike, L. M. Determination of flavor precursor compound *S*-alk(en)yl-l-cysteine sulfoxides by an HPLC method and their distribution in *Allium* species. *Sci. Hortic. (Amsterdam)*. **1998**, *75*, 1–10.
- (8) Granroth, B. Biosynthesis and decomposition of cysteine derivatives in onion and other *Allium* species. *Ann. Acad. Sci. Fenn. Ser. A 2* **1970**, 1–71.
- (9) Lancaster, J. E.; Shaw, M. L. γ -Glutamyl peptides in the biosynthesis of *S*-alk(en)yl-l-cysteine sulphoxides (flavour precursors) in *Allium*. *Phytochemistry* **1989**, *28*, 455–460.
- (10) Borlinghaus, J.; Albrecht, F.; Gruhlke, C. M.; Nwachukwu, D. I.; Slusarenko, J. A. Allicin: chemistry and biological properties. *Molecules* **2014**, *19*, 12591–12618.
- (11) Krest, I.; Keusgen, M. Quality of herbal remedies from *Allium sativum*: differences between alliinase from garlic powder and fresh garlic. *Planta Med.* **1999**, *65*, 139–143.
- (12) Musah, R. A.; He, Q.; Kubec, R.; Jadhav, A. Studies of a novel cysteine sulfoxide lyase from *Petiveria alliacea*: the first heteromeric alliinase. *Plant Physiol.* **2009**, *151*, 1304–1316.
- (13) Yutani, M.; Taniguchi, H.; Borjihan, H.; Ogita, A.; Fujita, K.-i.; Tanaka, T. Alliinase from *Ensifer adhaerens* and its use for generation of fungicidal activity. *AMB Express* **2011**, *1*, 1–8.

(14) Schwimmer, S.; Mazelis, M. Characterization of alliinase of *Allium cepa* (onion). *Arch. Biochem. Biophys.* **1963**, *100*, 66–73.

(15) Fujisawa, H.; Suma, K.; Origuchi, K.; Seki, T.; Ariga, T. Thermostability of allicin determined by chemical and biological assays. *Biosci. Biotechnol. Biochem.* **2008**, *72*, 2877–2883.

(16) Lawson, L. D.; Hughes, B. G. Characterization of the formation of allicin and other thiosulfinate from garlic. *Planta Med.* **1992**, *58*, 345–350.

(17) Block, E. The organosulfur chemistry of the genus *Allium* - Implications for the organic chemistry of sulfur. *Angew. Chem. Int. Ed.* **1992**, *31*, 1135–1178.

(18) Dethier, B.; Hanon, E.; Maayoufi, S.; Nott, K.; Fauconnier, M.-L. Optimization of the formation of vinylidithiins, therapeutic compounds from garlic. *Eur. Food Res. Technol.* **2013**, *237*, 83–88.

(19) Egen-Schwind, C.; Eckard, R.; Jekat, F. W.; Winterhoff, H. Pharmacokinetics of vinylidithiins, transformation products of allicin. *Planta Med.* **1992**, *58*, 8–13.

(20) Egen-Schwind, C.; Eckard, R.; Kemper, F. H. Metabolism of garlic constituents in the isolated perfused rat liver. *Planta Med.* **1992**, *58*, 301–305.

(21) Apitz-Castro, R.; Cabrera, S.; Cruz, M. R.; Ledezma, E.; Jain, M. K. Effects of garlic extract and of three pure components isolated from it on human platelet aggregation, arachidonate metabolism, release reaction and platelet ultrastructure. *Thromb. Res.* **1983**, *32*, 155–169.

(22) Block, E.; Ahmad, S.; Jain, M. K.; Crecely, R. W.; Apitz-Castro, R.; Cruz, M. R. The chemistry of alkyl thiosulfate esters. 8. (*E,Z*)-ajoene: a potent antithrombotic agent from garlic. *J. Am. Chem. Soc.* **1984**, *106*, 8295–8296.

(23) Sendl, A.; Wagner, H. Isolation and identification of homologues of ajoene and alliin from bulb-extracts of *Allium ursinum*. *Planta Med.* **1991**, *57*, 361–362.

(24) Yoshida, H.; Katsuzaki, H.; Ohta, R.; Ishikawa, K.; Fukuda, H.; Fujino, T.; Suzuki, A. An organosulfur compound isolated from oil-macerated garlic extract, and its antimicrobial effect. *Biosci. Biotechnol. Biochem.* **1999**, *63*, 588–590.

(25) Block, E.; Dane, A. J.; Thomas, S.; Cody, R. B. Applications of direct analysis in real time mass spectrometry (DART-MS) in *Allium* chemistry. 2-Propenesulfenic and 2-propenesulfinic acids, diallyl trisulfane *S*-oxide, and other reactive sulfur compounds from crushed garlic and other alliums. *J. Agric. Food Chem.* **2010**, *58*, 4617–4625.

(26) Lee, S.; Woo, Y.; Kyung, K. H. Allyl alcohol found in heated garlic is a potent selective inhibitor of yeasts. *J. Microbiol. Biotechnol.* **2006**, *16*, 1236.

(27) Chung, I.; Kwon, S. H.; Shim, S.-T.; Kyung, K. H. Synergistic antiyeast activity of garlic oil and allyl alcohol derived from alliin in garlic. *J. Food Sci.* **2007**, *72*, M437–M440.

(28) Imai, S.; Tsuge, N.; Tomotake, M.; Nagatome, Y.; Sawada, H.; Nagata, T.; Kumagai, H. Plant biochemistry: an onion enzyme that makes the eyes water. *Nature* **2002**, *419*, 685.

(29) Brodnitz, M. H.; Pascale, J. V. Thiopropanal *S*-oxide: a lachrymatory factor in onions. *J. Agric. Food Chem.* **1971**, *19*, 269–272.

(30) Block, E.; Thiruvazhi, M.; Toscano, P. J.; Bayer, T.; Grisoni, S.; Zhao, S.-H. *Allium* chemistry: structure, synthesis, natural occurrence in onion (*Allium cepa*), and reactions of 2,3-dimethyl-5,6-dithiabicyclo[2.1.1]hexane *S*-oxides. *J. Am. Chem. Soc.* **1996**, *118*, 2790–2798.

(31) Aoyagi, M.; Kamoi, T.; Kato, M.; Sasako, H.; Tsuge, N.; Imai, S. Structure and bioactivity of thiosulfinates resulting from suppression of lachrymatory factor synthase in onion. *J. Agric. Food Chem.* **2011**, *59*, 10893–10900.

(32) Eady, C. C.; Kamoi, T.; Kato, M.; Porter, N. G.; Davis, S.; Shaw, M.; Kamoi, A.; Imai, S. Silencing onion lachrymatory factor synthase causes a significant change in the sulfur secondary metabolite profile. *Plant Physiol.* **2008**, *147*, 2096–2106.

(33) Kato, M.; Kamoi, T.; Sasaki, R.; Sakurai, N.; Aoki, K.; Shibata, D.; Imai, S. Structures and reactions of compounds involved in pink discolouration of onion. *Food Chem.* **2013**, *139*, 885–892.

(34) Bayer, T.; Wagner, H.; Block, E.; Grisoni, S.; Zhao, S. H.; Neszmelyi, A. Zwiebelanes: novel biologically active 2,3-dimethyl-5,6-dithiabicyclo[2.1.1]hexane 5-oxides from onion. *J. Am. Chem. Soc.* **1989**, *111*, 3085–3086.

(35) El-Aasr, M.; Fujiwara, Y.; Takeya, M.; Ono, M.; Nakano, D.; Okawa, M.; Kinjo, J.; Ikeda, T.; Miyashita, H.; Yoshimitsu, H.; Nohara, T. Garlicnin A from the fraction regulating macrophage activation of *Allium sativum*. *Chem. Pharm. Bull.* **2011**, *59*, 1340–1343.

(36) Nohara, T.; Kiyota, Y.; Sakamoto, T.; Manabe, H.; Ono, M.; Ikeda, T.; Fujiwara, Y.; Nakano, D.; Kinjo, J. Garlicnins B1, C1, and D, from the fraction regulating macrophage activation of *Allium sativum*. *Chem. Pharm. Bull.* **2012**, *60*, 747–751.

(37) Nohara, T.; Fujiwara, Y.; Ikeda, T.; Murakami, K.; Ono, M.; Nakano, D.; Kinjo, J. Cyclic sulfoxides garlicnins B2, B3, B4, C2, and C3 from *Allium sativum*. *Chem. Pharm. Bull.* **2013**, *61*, 695–699.

(38) Nohara, T.; Fujiwara, Y.; Komota, Y.; Kondo, Y.; Saku, T.; Yamaguchi, K.; Komohara, Y.; Takeya, M. Cyclic sulfoxides-garlicnins K 1, K 2, and H 1-extracted from *Allium sativum*. *Chem. Pharm. Bull.* **2015**, *63*, 117–121.

(39) Block, E.; Jang, S.; Matsunami, H.; Sekharan, S.; Dethier, B.; Ertem, M. Z.; Gundala, S.; Pan, Y.; Li, S.; Li, Z.; Lodge, S. N.; Ozbil, M.; Jiang, H.; Penalba, S. F.; Batista, V. S.; Zhuang, H. Implausibility of the vibrational theory of olfaction. *Proc. Natl. Acad. Sci. U.S.A.* **2015**, *112*, E2766–E2774.

Chapter 2

Extraction and purification of thiolane-containing natural products from processed genus *Allium* plants

2.1 Novel compounds identified in garlic extracts

Apart from the bicyclic thiolane derivative biotin, naturally occurring thiolanes are little known, particularly as plant secondary metabolites. Before 2008, thiolane-containing natural products had mostly been reported in petroleum and sediments (Figure 2.1).¹⁻⁶

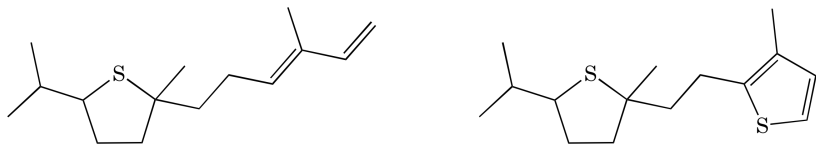


Figure 2.1: Examples of natural thiolanes found in petroleum and sediments.¹⁻⁶

The first plant-based thiolane described was cepathiolane (**19a**, Figure 2.2), extracted from Welsh onion by Yoshida et al. in 2008.⁷ The name is a portmanteau of the botanical term for onion (*Allium cepa*) and the main structural feature, a thiolane (5-membered heterocycle with one sulfur). This compound was patented for its flavor and Welsh onion scent.⁷

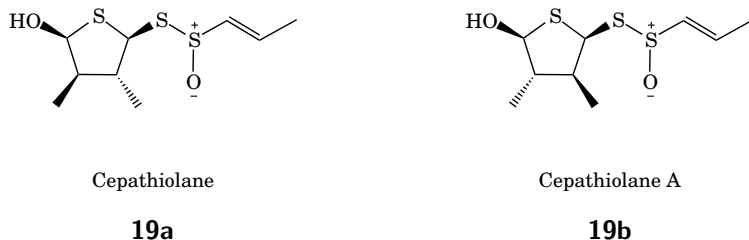


Figure 2.2: Stereoisomers of cepathiolane extracted from Welsh onion (**19a**)⁷ and lachrymatory factor synthase-suppressed onion (**19b**).⁸

The IUPAC name of **19** is *S*-(5-hydroxy-3,4-dimethyltetrahydrothiophen-2-yl) (*E*)-prop-1-ene-1-sulfinothiolate. Stereoisomer (*2S,3R,4R,5S*) (**19a**) was the first to be identified. With five chiral centers, $2^5 = 32$ stereoisomers are possible. A second stereoisomer (**19b**) was then reported with the stereochemistry (*2R,3R,4R,5R*), and named “cepatherolane A”.⁸ The latter was isolated from onion genetically modified to silence lachrymatory factor synthase (LFS) gene expression (Figure 2.3). In the absence of LFS, the lachrymatory factor (LF, **16**) is not formed. Thus, 1-propenesulfenic acid can condense and the resulting thiosulfinate **3c** rearranges (Figure 2.4, rearrangement described in the next paragraph). Prior to its isolation, **19** was postulated by Block in 1992 as an onion chemistry intermediate.⁹ Subsequently, a mechanism for the formation of these compounds was proposed and proven by the Block group.¹⁰

Thiolanes presumably originate from the dithio-Claisen rearrangement of bis-1-propenyl thiosulfinate (**3c**) to a dithial *S*-oxide (**21**, Figure 2.4). Compound **3c** is formed by condensation of two molecules of 1-propenesulfenic acid (**2c**), in turn produced by the enzymatic cleavage of *S*-(1-propenyl) cysteine sulfoxide (**1c**, Figure 2.4). Compound **21** can undergo two types of intramolecular cyclizations: a 1,3-dipolar cycloaddition (red), leading to the formation of a bicyclic sultene **10**, or a [2+2]-cycloaddition (blue), leading to zwiebelane (**9**).¹¹ This process is unique to *S*-(1-propenyl) cysteine sulfoxide (**1c**), since no thio-Claisen rearrangement is possible for the other alk(en)yl cysteine sulfoxide enzymatic products. Sultene **10** reacts quickly with nucleophiles as shown in Figure 2.5. This was demonstrated by trapping with thiophenol of the sultene formed from rearrangement of the thiosulfinate of bis-1-propenyl disulfide, a sequence that furnished **22** (Figure 2.5).

A compound with a structure comparable to cepatherolane can be predicted to form in garlic extracts, where allyl alcohol would act as the nucleophile (Figure 2.6). Mislow-Evans rearrangement (or sulfoxide-sulfenate rearrangement) would then lead to sulfoxide **20**. We named this predicted structure *ajothiolane* to describe both its origin (*ajo* means garlic in Spanish) and structure (*thiolane*).

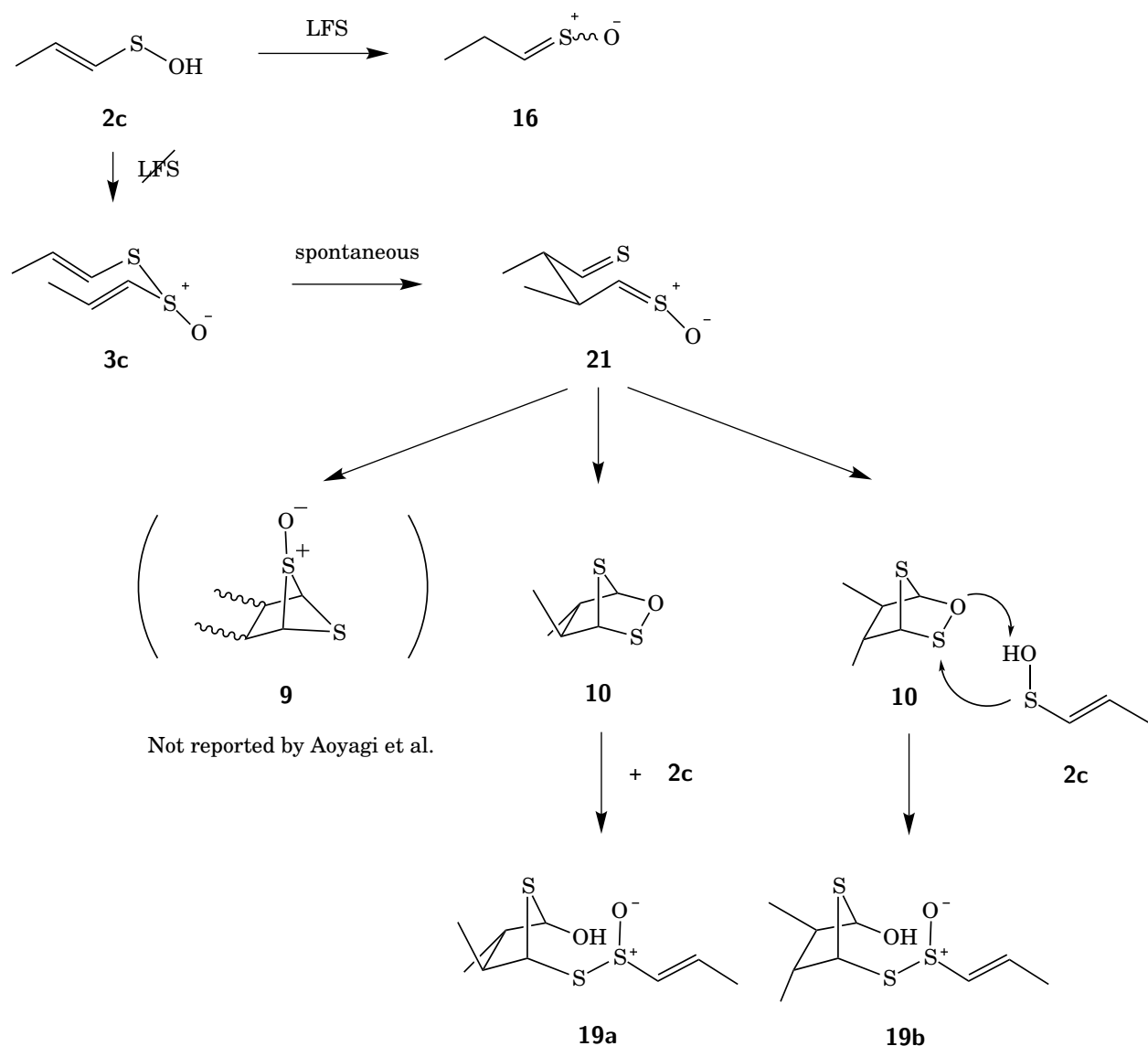


Figure 2.3: Formation of cepathiolanes (**19**) in the absence of lachrymatory factor synthase (LFS) in onion. Two molecules of 1-propenesulfenic acid (**2c**) condense in the absence of LFS to form thiosulfinate **3c**. The latter rearranges into **21**, which in turns forms bicyclic sultenes **10** and zwiebelane (**9**, not reported in Aoyagi's work). Nucleophilic attack by **2c** leads to cepathiolane (**19a** and **19b**). Figure adapted from Aoyagi et al.⁸

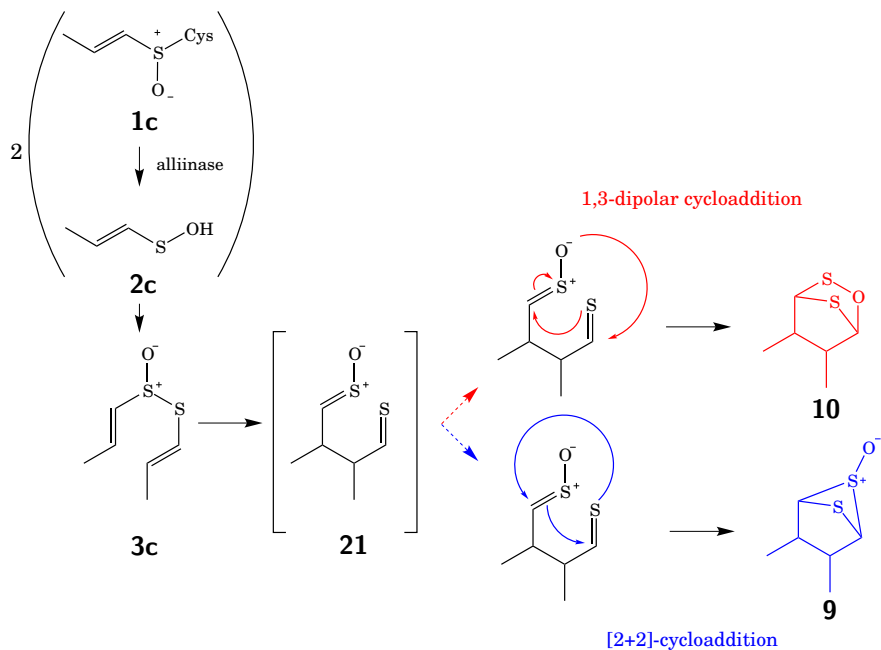


Figure 2.4: Biosynthesis of bicyclic sultene **10** and zwiebelanes (**9**) by rearrangement of bis-1-propenyl thiosulfinate (**3c**). The stereochemistry of the the double bonds defines which product is formed.¹¹ Methyl groups stereochemistry in **9** and (**10**) is not shown.

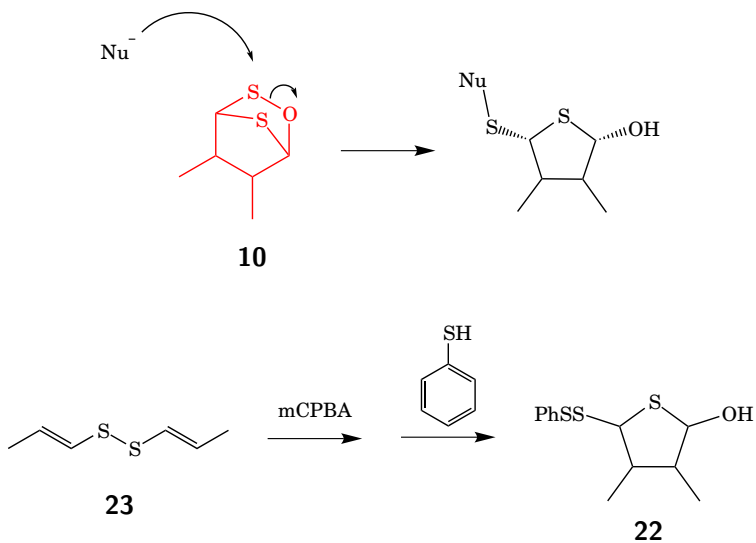
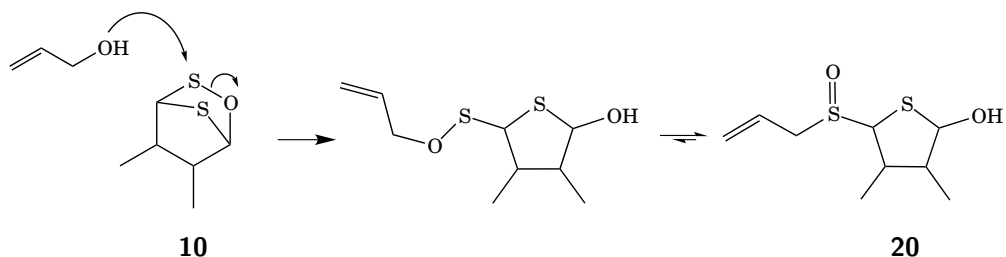


Figure 2.5: Ring-opening of the bicyclic sultene **10** is achieved by nucleophilic addition. The product is a 2-hydroxythiolane. This mechanism has been demonstrated by the Block group as follows: the sultene **10** formed from the rearrangement of the thiosulfinate **3c** of bis-1-propenyl disulfide (**23**) was trapped by thiophenol, a reaction that produced **22**. The rearrangement of **3c** is presented in Figure 2.4. Methyl groups stereochemistry in **22** was not determined.



Mislow-Evans rearrangement:

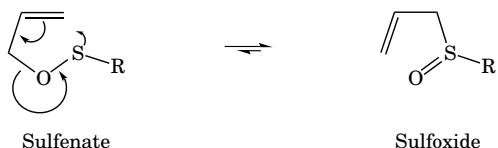


Figure 2.6: Ajothiolane (**20**) is predicted to be formed in garlic from **10** in the same way cepathiolane is formed. Allyl alcohol opens the 6-membered ring, and the allyl sulfenate rearranges (Mislow-Evans rearrangement) to form an allyl sulfoxide. Stereochemistry in **20** is not shown.

On the other hand, a series of dimethylthiolanes have been reported in garlic and onion extracts and named garlicinins (**17**) and onionin (**18**), respectively, by Nohara's research group (Figure 2.7).^{12–16} These compounds have a higher molecular weight than previously reported garlic derivatives. Garlicinin A and C in particular, with formula C₁₂H₂₀O₂S₄, have a molecular weight of 324. Garlicinin B (**17b**) has the same formula as the postulated ajothiolane (**20**, C₉H₁₆O₂S₂).

The structures of compounds **17** and **18** do not follow the same biosynthetic logic as cepathiolane or ajothiolane. Other discrepancies with what is known about *Allium* chemistry are also observed: the persistence of sulfenic acids and presence of chains longer than six carbons, for example, are not known in garlic chemistry. These issues will be discussed in Chapter 3. In this context, a rigorous structural assignment is important to settle the apparent conflicts between the structure of ajothiolane (**20**) and garlicinin B (**17b**). The aim of the work reported in this chapter is to discuss the extraction of thiolane-containing compounds from garlic and establish their structure to resolve this controversy.

The extraction was challenging, and a quick study with DART-MS was performed to inform the extraction steps. The purification process was optimized to obtain pure ajothiolane for spectroscopic studies. However, routine structure elucidation methods did not enable structure determination. Nuclear magnetic resonance (NMR) multiple-bond correlation experiments (COSY, HMBC) showed long-range coupling data that were difficult to interpret. Mass spectrometry (MS) fragmentation and infrared spectroscopy (IR) did not allow

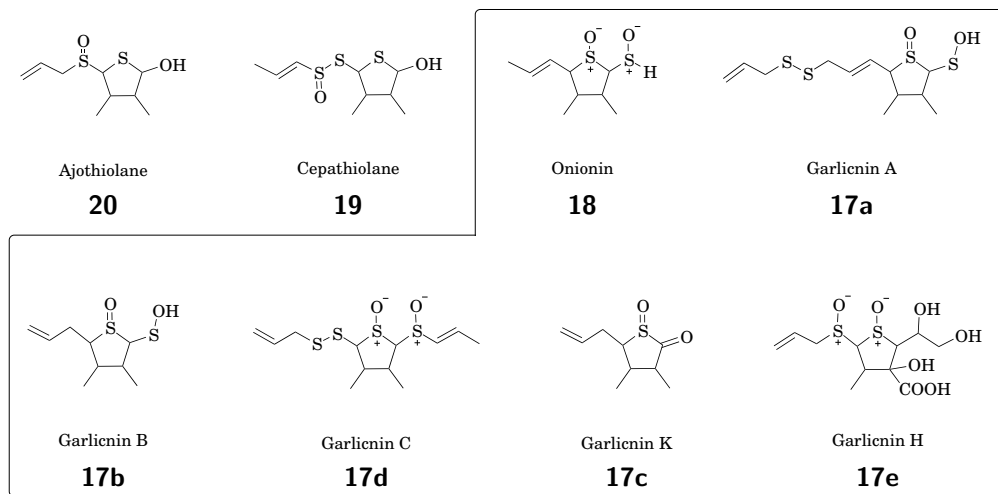


Figure 2.7: Proposed structures of thiolane compounds isolated from *Allium* extracts: cepathiolane (**19**),^{7,8} onionin (**18**)^{12–16} and garlicnins (**17**).^{12–16} Besides the common thiolane core, functional groups in these compounds are different. It is proposed that some of the functional groups featured in **17a,b**, **18** and **17c** are unlikely because they contain highly reactive functionalities which typically cannot be isolated (Section 3.1.1). Boxed and unboxed molecules show contrasting structures, some of which corresponding to the same molecular formula (**20** and **17b** for instance).

clear assignment of the functional groups and atom connectivity. Thus, additional techniques were employed, such as INADEQUATE NMR (^{13}C – ^{13}C correlation) and reduction/oxidation or derivatization studies. The correct structure was proven to be ajothiolane (**20**), ignoring stereochemistry.

A second compound was purified and found to be methylisoajoene (**8**) published by Yoshida et al.,¹⁷ an isomer of methylajoene (**7b**)¹⁸ also present in garlic extracts (Figure 2.8). The spectroscopic data matched a second compound wrongly identified by Nohara et al. as a novel compound, garlicnin D (**24**).¹⁴ Its chemistry and characteristics will be explained in the second part of this chapter.

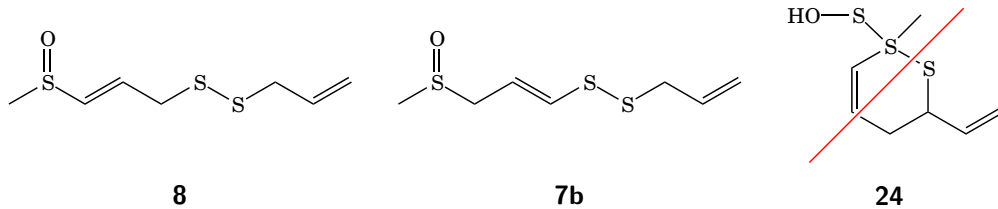


Figure 2.8: Proposed structures for compound with molecular formula $\text{C}_7\text{H}_{12}\text{OS}_3$ isolated from garlic extracts. Compound **8** was purified from a garlic extract and shown to be the correct structure of the previously reported compound **24** (garlicnin D).¹⁴

2.2 DART-MS as a semi-quantitative tool

The literature presented two different approaches to isolate thiolane compounds. On the one hand, Aoyagi et al. used LFS-suppressed onion extracts for analytical purposes, then *S*-1-propenyl cysteine sulfoxide (**1c**) and alliinase extracted from plants for the preparative study.⁸ However, the biosynthesis postulated for ajothiolane involves not only *S*-1-propenyl cysteine sulfoxide, the main cysteine sulfoxide in onion, but also *S*-allyl cysteine sulfoxide (alliin, **1a**) and other metabolites specific to garlic. This approach was therefore not ideal for us. On the other hand, Nohara et al.¹² isolated the compounds they called garlicnins after a 3-day extraction of crushed garlic cloves in acetone. This is the approach we first adopted.

This procedure leads to a complex mixture in which all types of metabolites are present. A suitable analytical method was required to follow the progression of the purification and to assess the presence of the compounds in the different fractions. Nohara's group used a macrophage activation bioassay, which was not available to us. Among other techniques, NMR and DART-MS were suitable for the type of mixtures being analyzed. This section reviews the advantages and specificities of the two, and our attempts to quantify the formation of the target compounds as a function of the extraction conditions.

NMR is, in general, the most informative characterization technique. It is quantitative, allows diastereomer identification, and provides a great amount of structural information. However, its low sensitivity, inability to resolve mixtures and tedious sample preparation made it a poor choice in our case. Acetone garlic extracts were not fully soluble in suitable solvents. Even after preliminary purification steps, the complexity of the mixture lead to NMR peak overlap and did not allow conclusions about its composition to be drawn.

Direct Analysis in Real Time mass spectrometry (DART-MS) provided a good alternative analytical technique in the first stages of the purification. The main advantage of DART is the ease of sampling: the analysis is performed simply by dipping a capillary tube into the sample, neat or in solution, and presenting it to the open air space between the ion-source and mass spectrometer inlet. DART ionization occurs under soft conditions at atmospheric pressure under ambient conditions. In positive mode DART-MS, helium gas is exposed to a glow discharge which results in formation of excited-state metastable He species. The interaction of the metastables with atmospheric vaporized water ultimately yields protonated water clusters ((Equation 2.1) to (Equation 2.3)). Analytes *S* are ionized by proton transfer from the water clusters (Equation 2.4).

In negative mode, O_2^- is a common intermediate anion that later deprotonates the analyte to produce $[M - H]^-$.¹⁹ Other ions such as $[M + NH_4]^+$, $[M]^+$, $[M]^-$, etc., are also formed, especially if a dopant such as ammonia is present.²⁰



The millimass unit resolution of the Time of Flight (TOF) detector allows determination of the chemical formula. Complex samples can be analyzed in a few seconds, in a wide range of solvents, making this method extremely useful in the analysis of garlic extracts. However, response factors depend on the ionization conditions. Therefore, without the use of an internal standard, relative peak heights cannot be used to infer analyte amounts. Furthermore, as with most other mass spectrometric techniques, isomers and stereoisomers are not differentiated by DART-MS. The method is therefore useful as a preliminary screening tool.

2.2.1 Critical aspects of DART-MS

Even though ions formed by DART have low internal energy, the ionization method is not as soft as electrospray in ESI,²¹ and fragments can form. Some of our purified samples, despite a clean NMR spectrum, displayed several ions in addition to that of the protonated molecule $[M + H]^+$ in their DART spectra. Two techniques allowed us to formally identify the additional peaks as being representative of fragment ions (Figure 2.9):

- The sample was analyzed with ammonia as a dopant: a solution of diluted ammonium hydroxide was placed at the ion source, and ammoniated ions $[M + NH_4]^+$ were produced. The relative abundances of $[M + H]^+$ and $[M + NH_4]^+$ increased at the expense of the relative abundance of fragments.

- Low energy analysis conditions were used: the ion source temperature was decreased to room temperature and the orifice voltage was set to 10 V. Under these conditions, the relative abundance of the $[M + H]^+$ peak increased compared to the fragments.

The fragment composition supports the proposed structure of ajothiolane (Figure 2.10).

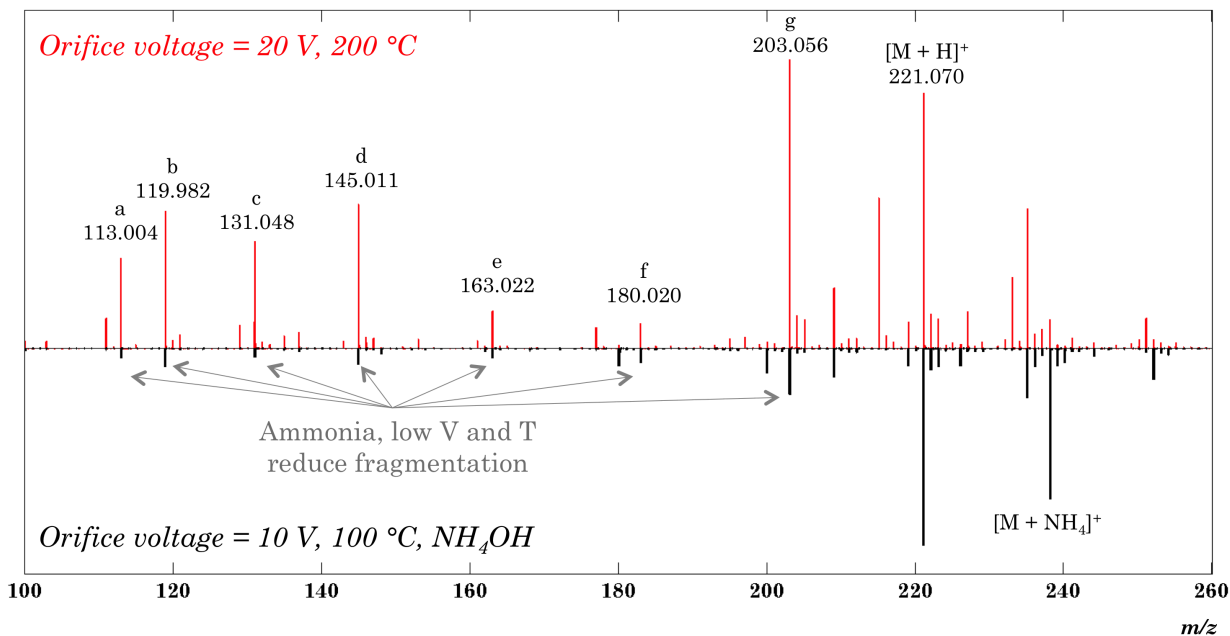
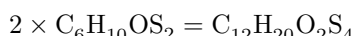


Figure 2.9: Comparison of the fragmentation of ajothiolane by DART-MS under different conditions. Softer ionizing conditions (10 V, 100 °C) and addition of a dopant (bottom spectrum) reduced the fragmentation of ajothiolane (**20**) compared to the standard conditions (20 V, 200 °C, top spectrum). Assignment of fragments a to g have been made based on the mass and isotope distribution and are detailed on Figure 2.10.

Another problem encountered when using DART-MS is the confusion between actual compounds and their dimers. The formula of higher mass thiolanes (**25** and **26**) and dimers of known molecules such as allicin (**3a**) are identical. This led to an inaccurate assessment of the presence and amount of higher molecular weight compounds such as garlicnin A or C by DART-MS.



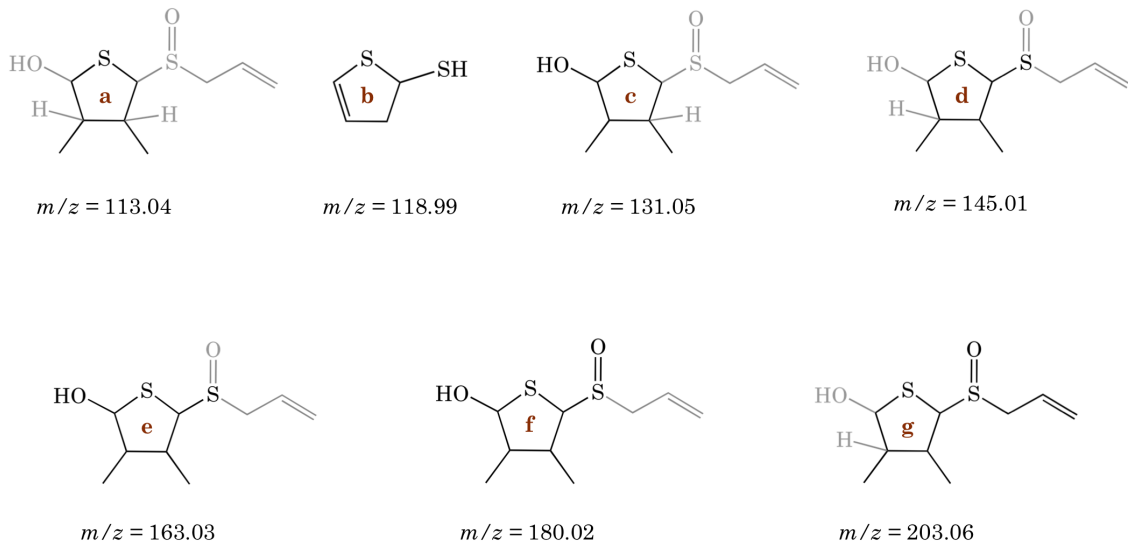
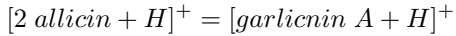


Figure 2.10: The fragments of ajothiolane (**20**) observed by DART-MS are consistent with the proposed structure. Fragments are pictured in black, and neutral losses in gray. Letters refer to the ions on the spectra to which the fragments correspond in Figure 2.9.



This issue was tackled in part by increasing the energy in the ion source (increasing the voltage of the second orifice during the run, also called function switching). Under 90 V or even 60 V, no dimers were observed, but fragmentation was dominant. A compromise between a low voltage (to avoid fragmentation) and high voltage (to avoid dimer formation) was found at 20 V. A second experiment is sometimes done at 10 V with ammonia to distinguish fragment peaks from precursor ion peaks.

2.2.2 Validation of the method

Despite these problems, DART-MS remains superior in early purification stages. But can it be used for quantitation? An internal standard (IS) is usually employed by analytical chemists. The IS needs to be as similar in structure to the analyte as possible to give a similar response to ionization. A deuterated version of the analyte is recommended. This was not an option because standards of ajothiolane are not available. However, what we wanted to measure was not the concentration of one compound, or even the relative amount of each component in the mixture. Rather, we needed to assess the evolution of the concentration of a few key

compounds over time. In principle, this could be done simply by using the response of molecules to DART ionization, as long as the results were reproducible. The analysis of one particular sample should always lead to the same value in order to be able to compare this value over time. The nature of typical sampling by DART-MS (manually exposing a capillary tube coated with the sample of interest in front of the ion source) does not yield reproducible results. To improve the reproducibility of the DART-MS results, semi-automated sampling was employed. Special capillary tubes (DIP-it tips[®]) dipped in the analyte solution were placed on a linear rail (Figure 2.11). The support moves along the rail at a defined speed, exposing each of the samples to the ion source for the same amount of time.

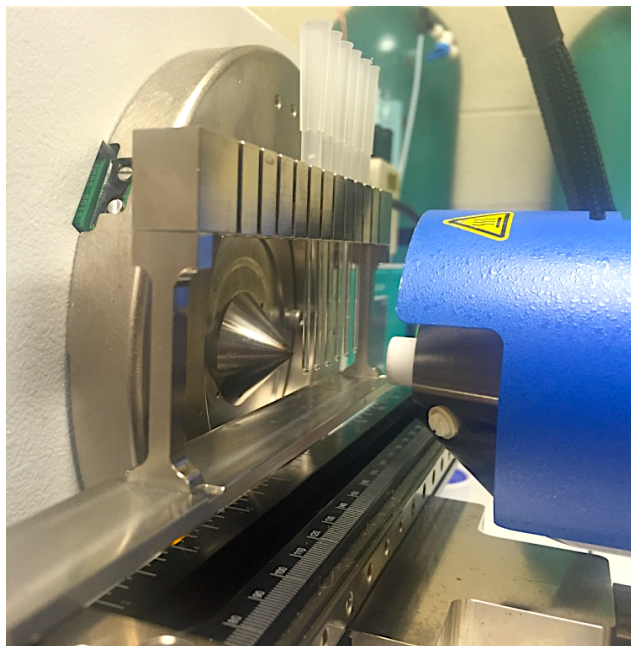


Figure 2.11: The linear rail that holds the capillary tubes allows semi-quantitative analysis. The rack moves at a controlled speed and exposes the samples to the ion source in a reproducible fashion.

The experimental approach to roughly validate DART-MS as an analytical method for the monitoring of analytes over time is presented in Figure 2.12. The reproducibility of the linear rail system results was assessed by measuring the coefficient of variation (CV) of six replicates derived from the same flask (①, Figure 2.12). Then, three sets of the same analysis (six replicates) were compared (②). Samples prepared at different times from one source of garlic were analyzed (③), as well as samples from two different sources of garlic (one in the Fall, one in the Spring, both using garlic from a local market, Figure 2.12, ④). The

solutions exposed to the DART source represented the supernatant of the extract; no further treatment was applied.

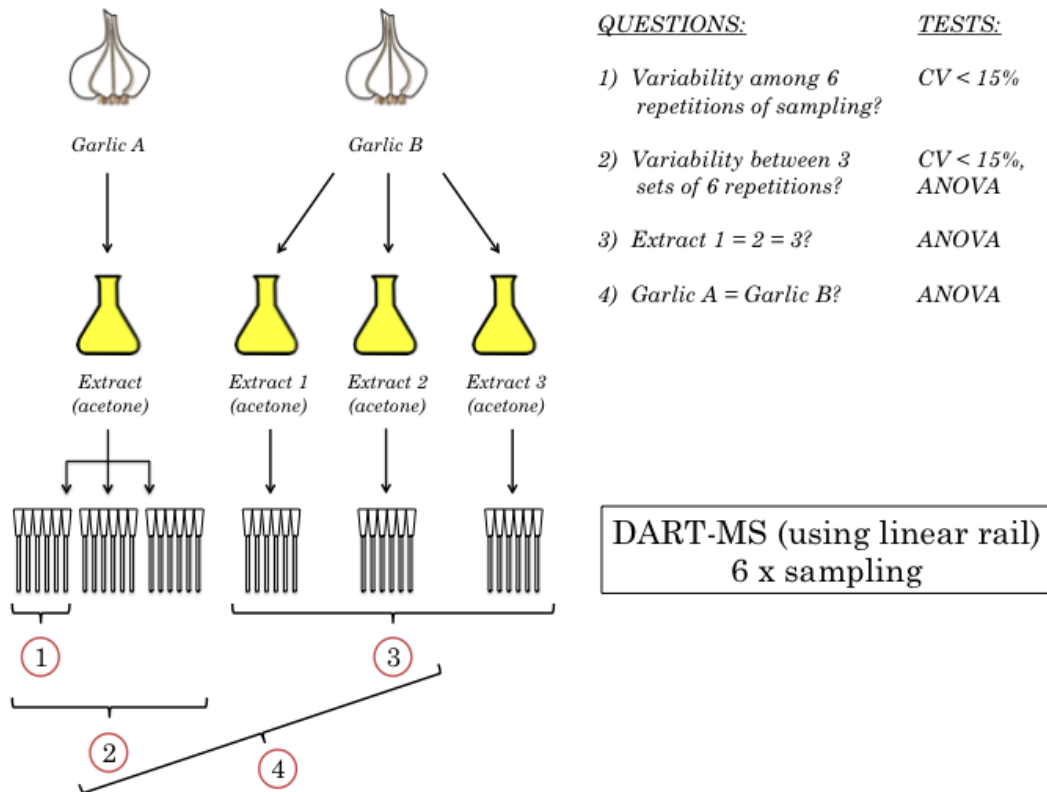


Figure 2.12: Experiments run to assess the reproducibility of the DART-MS. Intra-sample variability (variability between six replicates of the same sample (①), and between three sets of replicates of the same sample (②)) was assessed by using the coefficient of variation (CV). Coefficients of variation smaller than 15% are recommended for validation of bioanalytical methods by the Food and Drug Administration (FDA). Inter-extract variability (for extracts prepared from the same (③) or different garlic cloves (④)) was assessed by an analysis of variance (ANOVA).

Variations between six identical samples on one rack (intra-sample variability) and between samples from three different extraction flasks (inter-extract variability) were assessed using the coefficient of variation (CV), which is calculated as follows:

$$CV = [\sigma]/[\mu] \quad (\text{Equation 2.5})$$

where σ is the standard deviation and μ the mean of the relative abundances. The FDA accepts CVs of up to 15% for the validation of bioanalytical methods,²² while 20% is accepted for the limits of quantification.

For this experiment, peaks corresponding to the following compounds were used:

1. Allicin, (**3a**), $m/z = 163.025$ [$\text{C}_6\text{H}_{10}\text{OS}_2 + \text{H}^+$]
2. Ajoenes (**7**), $m/z = 235.029$ [$\text{C}_9\text{H}_{14}\text{OS}_3 + \text{H}^+$]
3. Ajothiolane (**20**), $m/z = 221.067$ [$\text{C}_9\text{H}_{16}\text{O}_2\text{S}_2 + \text{H}^+$]

CVs have been calculated for the sum of the normalized abundances of the $[\text{M}+\text{H}]^+$ peak over 18 scans after the beginning of the peak on the chromatogram (Figure 2.13). The beginning of a peak on the chromatogram was arbitrarily chosen as a sequence of three scans with an abundance above 10,000 a.u. on the chromatogram of ajoenes (the most reproducible, as shown later). The sum of abundances was normalized to the sum of the abundances of the total ion chromatogram (TIC) for the same scans to increase reproducibility.

The results are presented in Figure 2.14. Each repetition R1 to R3 consists in exposing 6 capillary tubes on the linear rail to the DART source (①, Figure 2.12). The last column corresponds to the CV of the whole data set, i.e. 18 exposures of the sample to the ion source (②, Figure 2.12).

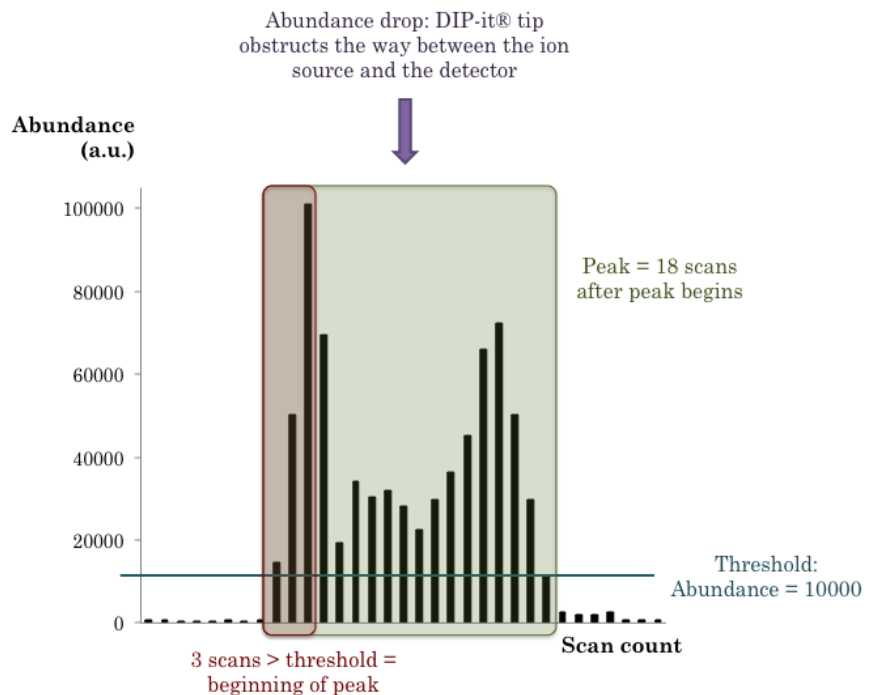


Figure 2.13: Utilization of the DART-MS signal for quantification: example of the peak detection on the chromatogram of peak 235.03 (ajoene). A peak is detected if three consecutive scans exhibit values above the threshold (arbitrarily set at 10,000), and the peak value consists of the sum of the signals of the 18 scans after detection of the beginning of a peak.

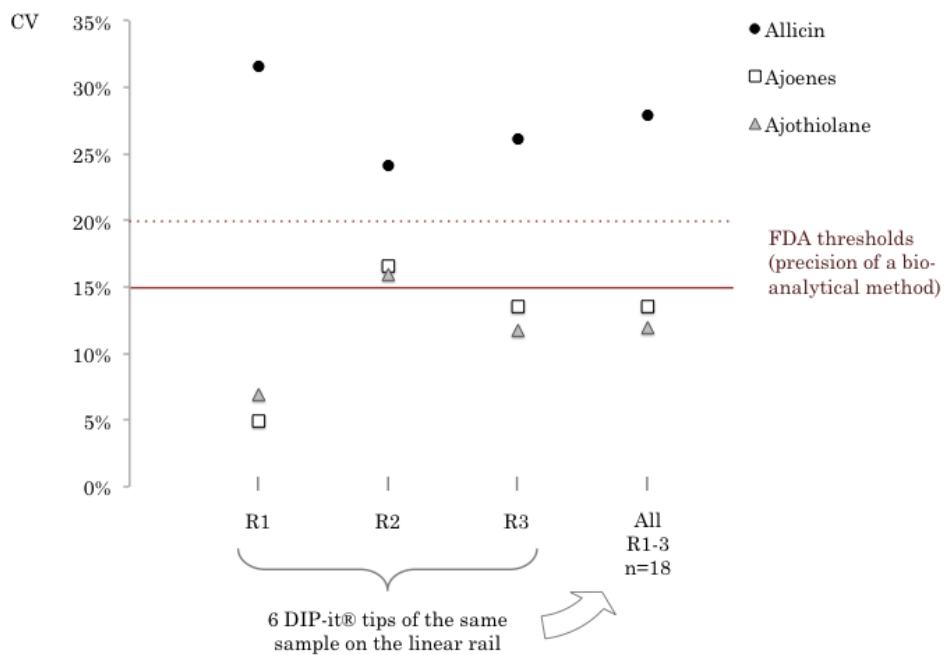


Figure 2.14: Coefficients of variation for three repetitions of a 6-tube DART experiment. A threshold of 15% is accepted by the FDA (20% at the LOQ). Ajoenes and ajothiolane are within these limits, but allicin is not. Increasing the number of replicates to 18 did not improve the CV (right).

The method is satisfactory for ajoenes and ajothiolane, since the CVs are within acceptable values. Increasing the number of analyses from 6 to 18 did not improve the reproducibility (the CV was not lower when calculated from 18 repetitions instead of 6). The amount of allicin could not be measured by DART-MS in a reliable fashion. This is a consequence of its instability (the time between sampling and analysis is sufficient to observe degradation), as well as its tendency to form dimers. As the most abundant compound in the mixture, it is more likely to form dimers to the detriment of the parent peak. The results show that the DART response is reliable for the analysis of ajoenes and ajothiolane, but not for allicin.

Analysis of variance (One-way ANOVA) was performed on different groups to assess equality of means for the same three compounds, allicin, ajoenes and ajothiolane. The equality of means is a concept in statistics in which the null hypothesis, the equality of means between the populations considered, is assessed by a F-test. One would reject the null hypothesis, concluding that there is strong evidence that the expected values in the three groups differ, if the p-value for the test is less than or equal to the significance level (0.002 in this work). The software used for statistical analysis were StatPlus and Excel.

First, the response of the DART was compared for three repetitions of the linear rail experiment (three repetitions of six replicates of the sample, ②). The results indicated the equality of means (Table 2.1), which was desired to confirm the reliability of the DART-MS response (one sample is expected to give the same response at every run). The linear rail improved the reproducibility to a point where the signals for three repetitions of an analysis were not significantly different. The response of the DART for two of the three compounds of interest, ajoene and ajothiolane, is sufficiently reproducible in the context of this study. Other metabolites will be considered in the next section without having been statistically validated. However, the principle of the method, using the linear rail to allow us to quantify the compounds, is still reasonable.

A second experiment using the equality of means was performed, not to validate the method but to assess the variability in the formation of the compounds of interest. An ANOVA was performed on three different samples prepared from the same garlic (③) on the one hand, and samples prepared from two different garlic sources, one purchased in the Fall and one in the Spring (④) on the other hand (Table 2.1). Significant differences were found between the sets of population, indicating the variability in the extraction process and the biological material. The amount of ajothiolane extracted varies between samples, and the amount of other organosulfur compounds varies depending on the garlic they have been extracted from.

Table 2.1: Test of equality of means for the abundance of three garlic compounds analyzed by DART-MS (One-way ANOVA).

	② R1 = R2 = R3	③ E1 = E2 = E3	④ Garlic A = Garlic B
Allicin	No evidence against equality of means		Evidence against equality of means
Ajoenes			
Ajothiolane			Evidence against equality of means

2.2.3 Improving the yield: starting from an enriched extract

Starting from material with a higher concentration in thiolane-containing compounds (e.g., by adding in synthetic isoalliin before activating the garlic) as well as a higher purity would ease the purification process. The parameters that can be optimized in the extraction have been identified as follows (Figure 2.15):

1. Rest time: time for the enzyme to work, after crushing the cloves and before denaturing it with acetone
2. Extraction time: time for the mixture to stand at room temperature once the garlic pulp is soaked in acetone

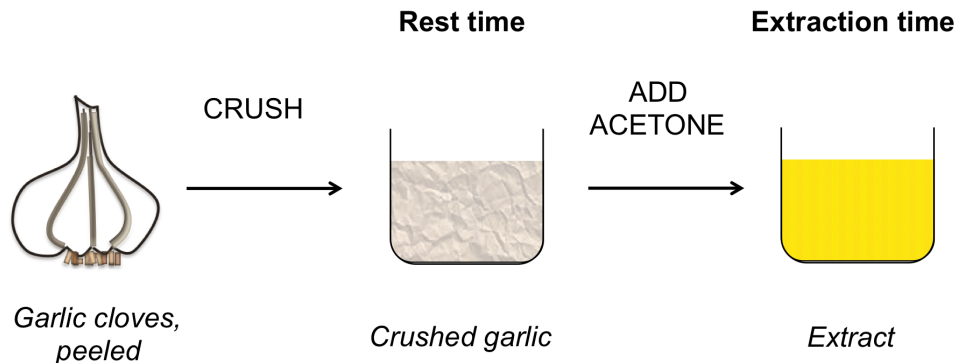


Figure 2.15: Parameters in the extraction of ajothiolane are the rest time and the extraction time.

In addition to allicin, ajoenes and ajothiolane, a fourth compound is analyzed. A peak corresponding to $[\text{C}_7\text{H}_{12}\text{OS}_3 + \text{H}]^+$ is observed in the DART spectra. This formula has been associated with methylajoene (**7b**)¹⁸ but also methylisoajoene (**8**)¹⁷ and garlicin D (**24**)¹⁴ in garlic extracts. This compound is not the

focus of this extraction, but since it is present as a by-product, we sought to identify which of the three mentioned structure(s) are formed during the extraction. The amount of vinyldithiins is also measured.

Optimization of the rest time A short rest time reduces the time allocated for the enzymatic reaction, because the enzyme is likely denatured by acetone. On the other hand, some reactions could only occur in a solvent, or the compounds of interest could be more stable in a solvent than exposed to air. To address this question, garlic extracts have been allowed to stand for a few seconds, 20 min or 120 min before acetone was added, then the composition of the extracts was measured by DART-MS. These results are presented Figure 2.16. According to these, ajothiolane is produced in higher amount with a short rest time. The enzymatic reaction seems to proceed rapidly, and allowing more time for alliinase to react does not improve the yield in target compounds. On the contrary, exposure to air seems to reduce the formation of ajothiolane, possibly in favor of vinyldithiins and ajoenes.

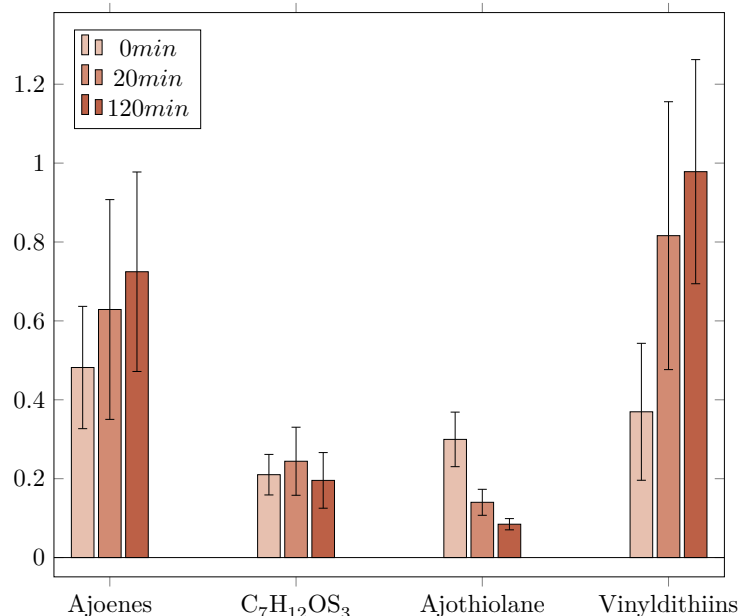


Figure 2.16: Amount of each metabolite depending on the rest time as determined by DART-MS, in % of total ion count (see Section 2.2.2 for quantification methodology). The rest time corresponds to the time between crushing the cloves and adding acetone. More ajothiolane (**20**) is produced if acetone is added immediately, while vinyldithiins and ajoenes are produced if more time passes before denaturing the enzyme. Error bars represent standard deviation, n = 6.

Optimization of the extraction time The evolution of the composition of the extract is presented in Figure 2.17. The amount of allicin decreases quickly, which is expected. The amount of other components also decreases, but at a slower rate. Only $C_7H_{12}OS_3$ seems to be formed over time. In the light of these results, processing the extract soon after blending is recommended to avoid loosing material. A short extraction time is consistent with the work of Aoyagi et al.,⁸ where the samples are extracted after only 30 s.

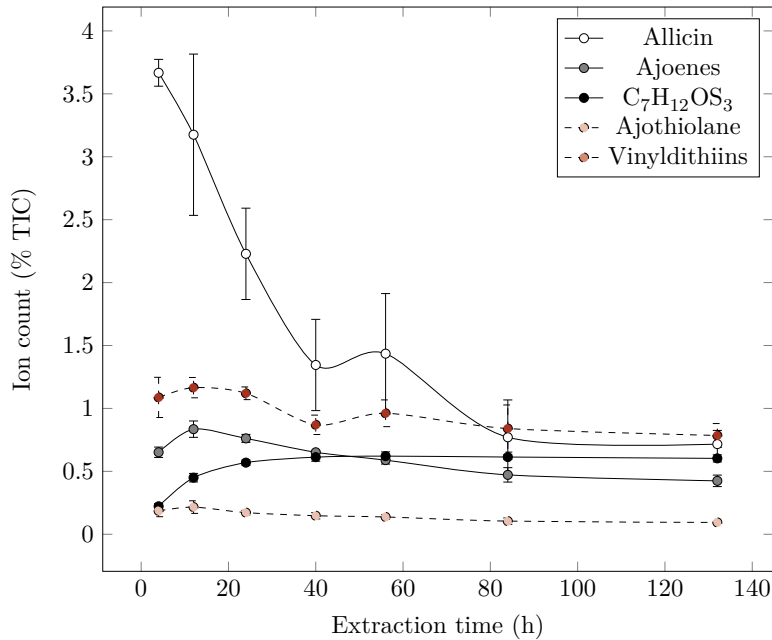


Figure 2.17: Amount of metabolites measured over time as determined by DART-MS, in % of the total ion count (see Section 2.2.2 for quantification methodology). The extraction time corresponds to the time the garlic pulp was standing soaked in acetone. The concentration of all compounds except $C_7H_{12}OS_3$ decreases over time. Quick extraction is therefore recommended to avoid loss of target compound. Error bars represent standard deviation, three repetitions and six replicates/repetition.

After this screening of the garlic extract, we are able to use DART-MS as our analytical tool for the next step: the production and purification of ajothiolane.

2.3 Purification of thiolane-containing compounds from garlic extracts

Challenges in the isolation of the target compound were to recover a minor component of the extract (about 0.02% of the mass of garlic), and to resolve it from a variety of other similar compounds. The target is polar

due to sulfoxide and hydroxyl groups, and chromatography of the mixture led to coelution. To overcome this obstacle, preparative thin-layer chromatography (TLC) was employed. The low R_f (0.1) was compensated by repeated elutions (four or five), until the resolution was sufficient to reach an NMR purity of 85% in the target compound. The main advantage of preparative TLC over column chromatography is the ability to recover weakly eluted compounds.

The extraction and purification of ajothiolanes (**20**) was performed as follows (Figure 2.18 and Figure 2.19):

1. Garlic cloves are peeled and crushed in a blender. The elapsed time once garlic is crushed and before adding acetone is called *rest time* (see Section 2.2.1). *Typical mass: 3 kg of peeled garlic.*
2. Acetone is added in the proportion of 1 mL/g of garlic, and the mixture is homogenized (still in the blender). The acetone had been freshly distilled to remove all plasticizers from caps and bottles. The time garlic extract is allowed to stand before filtration is called *extraction time* (see Section 2.2.1). All samples are stored in the dark until the next step. The supernatant of this mixture was used for the DART experiments (see Section 2.2.1). *Typical volume of acetone: 3 L, volume of the mixture 5 L.*
3. The mixture is filtered through Celite in a Büchner funnel. The garlic pulp is discarded, and the filtrate (larger in volume than the added acetone due to the water released from the plant) is kept for the following step. *Typical volume of filtrate: 4 L.*
4. Acetone is evaporated under vacuum, and the aqueous suspension is extracted three times with DCM. If acetone is present, the layers don't separate properly. Emulsions can form, in which case NaCl was added to salt out the compounds. DART-MS confirmed the transfer of the organosulfur compounds of interest in the organic layers, which were combined, dried and concentrated. *Typical mass of concentrate: 15 g of brown sticky paste.*
5. An initial column chromatography is performed on the extract based on a procedure by El-Aasr et al.¹² Two solvent systems are used: first DCM/MeOH (99:1), then pentane/acetone (4:1). Interestingly, the polarity index of the first system is higher than the second (3.12 and 1.02, respectively). Other phenomena such as solubility must be at play in this separation. Vinyldithiins and allicin were the first compounds eluted. No ajothiolane (**20**) was detected by DART-MS in the fractions of the first solvent system. After five column volumes (CVs), visual examination indicated that the elution was

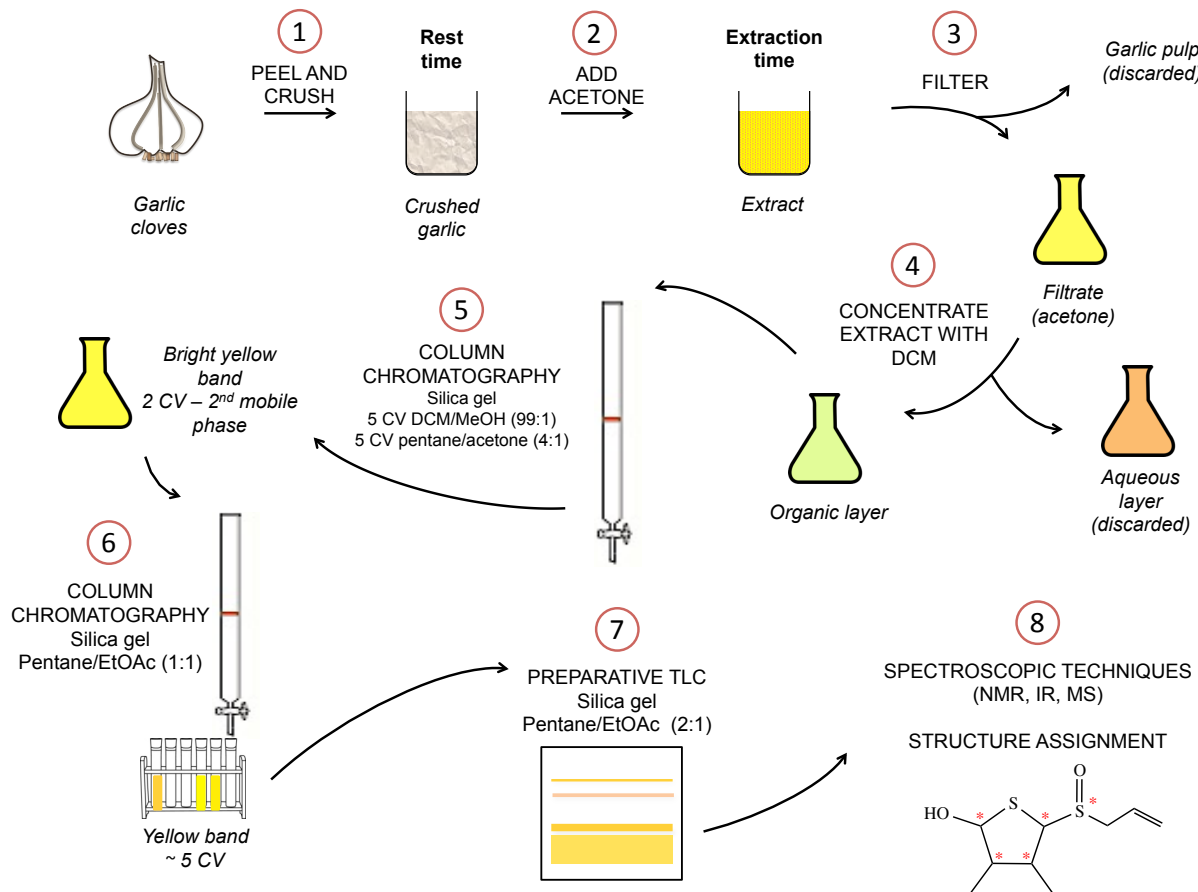


Figure 2.18: Optimized purification of ajothiolane from garlic cloves.

not progressing, and the second solvent system was used. A yellow band quickly emerged from the top of the column and was eluted after three to five CVs of the new solvent. DART-MS confirmed the high concentration of **20** in the final fractions (see graph, Figure 2.19), which were combined and concentrated. Some ajoenes, allyl methyl thiosulfinate and $C_7H_{12}OS_3$, later identified as methylisoajoene, coeluted. *Typical mass of fraction of interest: 2-4 g.*

6. A second column is then performed with pentane/EtOAc (1:1). Ajothiolane is the third compound to be eluted. The combined fractions are still impure: the above mentioned organosulfur compounds and some grease from the solvents and glassware are eluting with the target compound. *Typical mass of fraction of interest: 700 mg.*

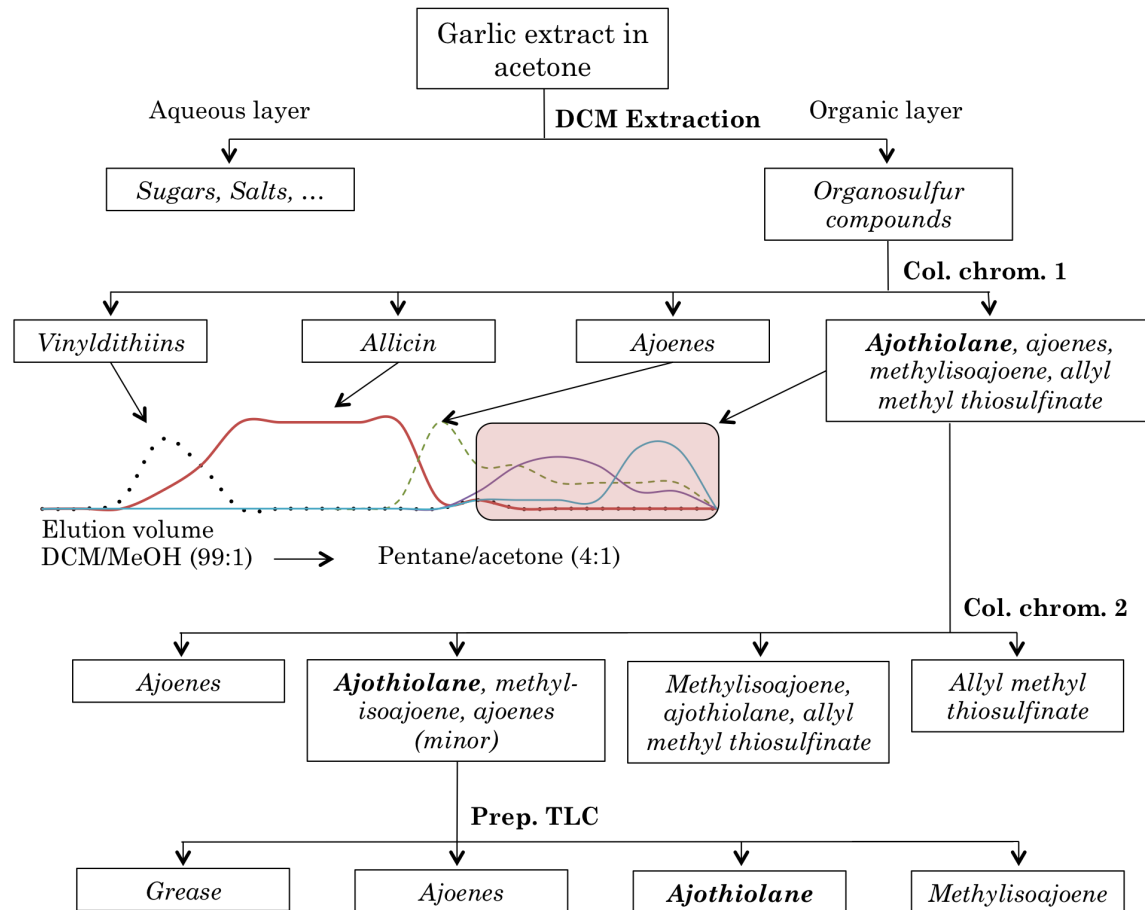


Figure 2.19: Purification of ajothiolane: separation scheme.

7. Finally, the mixture is eluted on a preparative TLC plate with pentane/EtOAc (2:1). Bands revealed by UV light are scraped, and compounds are dissolved in EtOAc by sonication of the silica gel, then tested by DART-MS. The band corresponding to ajothiolane is concentrated to a yellow oil. *Typical mass of ajothiolane: 100 mg.*

The minute amount of ajothiolane recovered compared to the amount of solvent used makes the quality of these solvents a major concern. A small amount of impurity would be concentrated in each step. Furthermore, contact with rubber or plastic should be completely avoided since they can leach out and lead to the same problem. Carbonyl bands from phthalates (such as bis(2-ethylhexyl)phthalate) were found by IR, and impurities in the methyl region were present on the NMR spectra despite extreme care in handling the samples.

A cryogenic grinder was also used to achieve a better control over the enzymatic reaction. The garlic cloves are placed in a vessel with a piston, and this vessel is immersed in liquid nitrogen. After the plant material has frozen, the system is shaken, and the cloves are ground to a fine powder by the mechanical action of the piston. The powder can be kept at -80 °C with no alliinase activity. The composition of the mixture analyzed by DART-MS after warming and addition of acetone did not appear different from the garlic extract prepared with a standard blender.

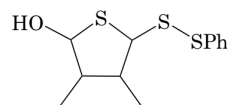
In a separate experiment, a sample enriched in ajothiolane (after step five of the purification) was injected on a preparative HPLC system in order to separate stereoisomers. Elution with MeOH/H₂O + 0.05% TFA (gradient 16% to 100% MeOH) allowed us to spread the peaks detected by UV at 220 nm over 45 min. Unfortunately, the target compound does not absorb very well at this wavelength. The cutoff absorbance of MeOH is too high to decrease further the detector's wavelength. In this instance again, DART-MS was used to detect the presence of ajothiolane in each collected tube. The fractions of interest were then extracted with DCM for NMR analysis. Two stereoisomers have been identified as major: ajothiolane A (**20a**) and B (**20b**). Other stereoisomers could also be identified, and will be described in the next section.

2.4 Characterization and stereochemistry of ajothiolane

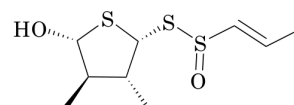
Once pure material was available, the usual spectroscopic experiments were run. However, ¹H, ¹³C, COSY, HSQC and HMBC NMR were not sufficient to unambiguously determine the structure of ajothiolane. To help resolve the case, ¹H NMR data were compared with those from a synthesized compound (the thiophenol

derivative **22**¹¹) and reported cepathiolane (**19**) and garlicnin B (**17b**) ¹H NMR. Chemical shifts of the protons in 2-hydroxy-3,4-dimethyl-5-(phenyldisulfanyl)thiolan-2-ol (**22**), cepathiolane (**19**)⁸ and proposed garlicnin B (**17b**)¹⁴ are summarized (Figure 2.20).

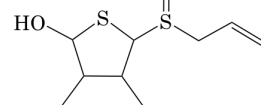
The first conclusion one can draw from these data is the identity between garlicnin B (isomer 1) and the isolated compound. However, the values of the chemical shifts are more consistent with a thiolane ring (not thiolane sulfoxide), a hydroxy group in position 2 (protons **a**) and a sulfur in position 5 (protons **d**) based on chemical shifts of synthetic compound **22** and cepathiolane (**19**). The presence of a carbon in position 5, as suggested for garlicnin B, does not fit the reported highly deshielded proton chemical shift of proton **d**. Nonetheless, a better technique than comparing chemical shifts with those in standard compounds is required.



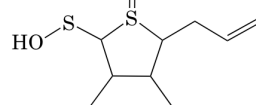
Phenylthiolane
22



Cepathiolane
19



Ajothiolane
20



Garlicnin B
17b

Phenylthiolane				Cepathiolane	Measured	Garlicnin B			
Isomer 1	Isomer 2	Isomer 3				Isomer 1	Isomer 2	Isomer 3	Isomer 4
a 5.29	5.02	5.05	5.2		5.05	5.04	5.07	4.98	5.14
b 2.46	1.97	2.48	1.99-2.06		2.00	1.98	1.92	2.46	2.04
c 2.08	2.08	2.63	2.10-2.19		2.18	2.15	2.35	2.84	2.51
d 4.61	4.42	4.16	4.87		4.09	4.08	4.06	3.94	4.08
e 1.25	1.25	1.05	1.07		1.06	1.04	1.11	0.95	1.10
f 1.13	1.17	0.97	1.15		1.27	1.23	1.35	1.19	1.3

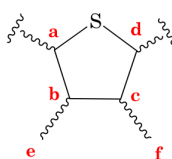


Figure 2.20: ¹H NMR chemical shifts of the thiolane ring of phenylthiolane (2-hydroxy-3,4-dimethyl-5-(phenyldisulfanyl)thiolan-2-ol, **22**),¹¹ cepathiolane (**19**),⁸ proposed ajothiolane (**20**) and the proposed garlicnin B (**17b**).¹⁴ The chemical shift of proton **d** points toward a dithioacetal in **20**, as in **22** and **19**. The compound identified as the first isomer of garlicnin B is likely identical to ajothiolane.

2.4.1 Why is the NMR data so confusing?

The difficulty in interpreting the NMR spectra lies in long-range coupling (4J and more) and the presence of heteroatoms, not detected by NMR, which makes the structure assignment so challenging. Two effects contribute to the 1H - 1H long-range coupling. First, strained and cyclic systems (such as saturated heterocycles) lead to long-range coupling, particularly a W-effect.²³ Second, heteroatoms allow coupling across them: hydrogen-hydrogen coupling through sulfur is reported to be in the range of 0.8 Hz.²⁴ 1H - ^{13}C coupling appears on HMBC spectra, also across heteroatoms, if a W-shape is present.²⁵ Protons on carbons 2, 5 and 2' (Figure 2.21) are all next to heteroatoms. 2D NMR indicates coupling to neighboring atoms as shown by the arrows. For example, the proton on C₅ is correlated to three carbons. Conventional structure assignment would have placed methine C₅H between C₂, C₄ and CH₃-C₄, but its chemical shift (74.9 ppm) could not be explained. We will learn later that C₅ is actually only connected to one of these carbons.

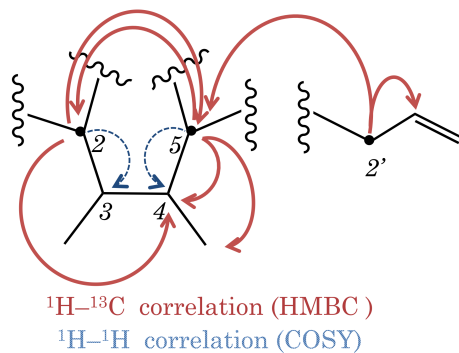


Figure 2.21: Spin-spin correlation experiments lead to confusion in the determination of the structure of the isolated ajothiolane. The ring imposes a W-arrangement to the protons, resulting in long-range coupling.

To overcome this problem, another 2D NMR experiment was run to highlight one-bond length correlation for the only atom combination not tested yet: carbon. ^{13}C - ^{13}C correlation experiments are rarely performed, since the low natural abundance of carbon-13, the NMR-active isotope, considerably lowers the sensitivity of the experiment. Incredible Natural Abundance Double QUAntum Transfer Experiment (INADEQUATE) requires large amount of material and NMR time. Two parameters have been tuned in this INADEQUATE experiment to increase the sensitivity:

- The coupling constant used in the pulse sequence was set at 40 Hz (sp^3 carbons). Correlation with sp^2 carbon might not be visible.

- The evolution period after the pulse sequence was doubled, following Turner's method.²⁶ This tweak avoided collecting data points that would not contain signal and be wasted (about half of the data points in a classical INADEQUATE experiment), increasing the sensitivity by a factor 4. A second consequence of this change is the presence of signals on the diagonal, usually not present on INADEQUATE.

After these changes, 24 h of accumulation time were needed to obtain a spectrum from 45 mg of sample (0.2 mol in 0.5 mL CDCl_3).

Despite these difficulties, the experiment was successfully used to confirm the absence of correlation between C_2 and C_5 , as well as between C_5 and $\text{C}_{2'}$ (Figure 2.22 and Figure 2.23). This confirms the implausibility of the structure of garlicnin B, in which C_5 and $\text{C}_{2'}$ would be connected. Full NMR results are presented in Figure 2.24.

2.4.2 Functional groups confirmation

IR was used to distinguish the sulfenic acid proposed by Nohara et al.¹⁴ and an alcohol and sulfoxide proposed in **20**. A broad absorption band is present at 3200 cm^{-1} even when proton NMR does not show any traces of water, confirming the presence of a hydroxy group. Furthermore, a strong band absorbing at 1027 cm^{-1} indicates unquestionably that there is a sulfoxide in the molecule. However, to remove doubts on the identity of the functional groups, compound **20** was oxidized. In the case of the sulfoxide/alcohol hypothesis, the oxidation products should be a thiolactone (-OH oxidized to carbonyl) and/or a sulfone (SO oxidized to SO_2). Oxidation of a sulfenic acid could lead to a sulfinic or sulfonic acid. The difference in chemical shifts by NMR and in band wavenumbers by IR should provide sufficient evidence. The exact position of the sulfoxide, whether on the ring or the side-chain, should also be confirmed by the change in chemical shift of the nearby protons when oxidized to sulfone. Finally, this operation should remove a stereocenter and possibly simplify the NMR spectra (Figure 2.25).

Oxidation with KMnO_4 (2:1 ratio in acetone) was followed by DART. Two new peaks were observed after 2 h of reaction. High-resolution MS indicates m/z corresponding to $[\mathbf{20} + \text{O} + \text{H}]^+$ (+ O) (**27**) and $[\mathbf{20} + \text{O} - \text{H}]^+$ (+ O, - H_2 , alcohol to ketone, **28**). Unfortunately, the small amount of material recovered did not allow us to verify this by NMR or IR.

Derivatization of the hydroxyl with 2,4-dinitrobenzoyl chloride was attempted. We sought to enhance HPLC detection and separation, and to grow crystals for stereochemistry assignment. Unfortunately, attempts on an analogue, 2-hydroxythiolane (**29**, prepared in Chapter 3), failed; the compound decomposed

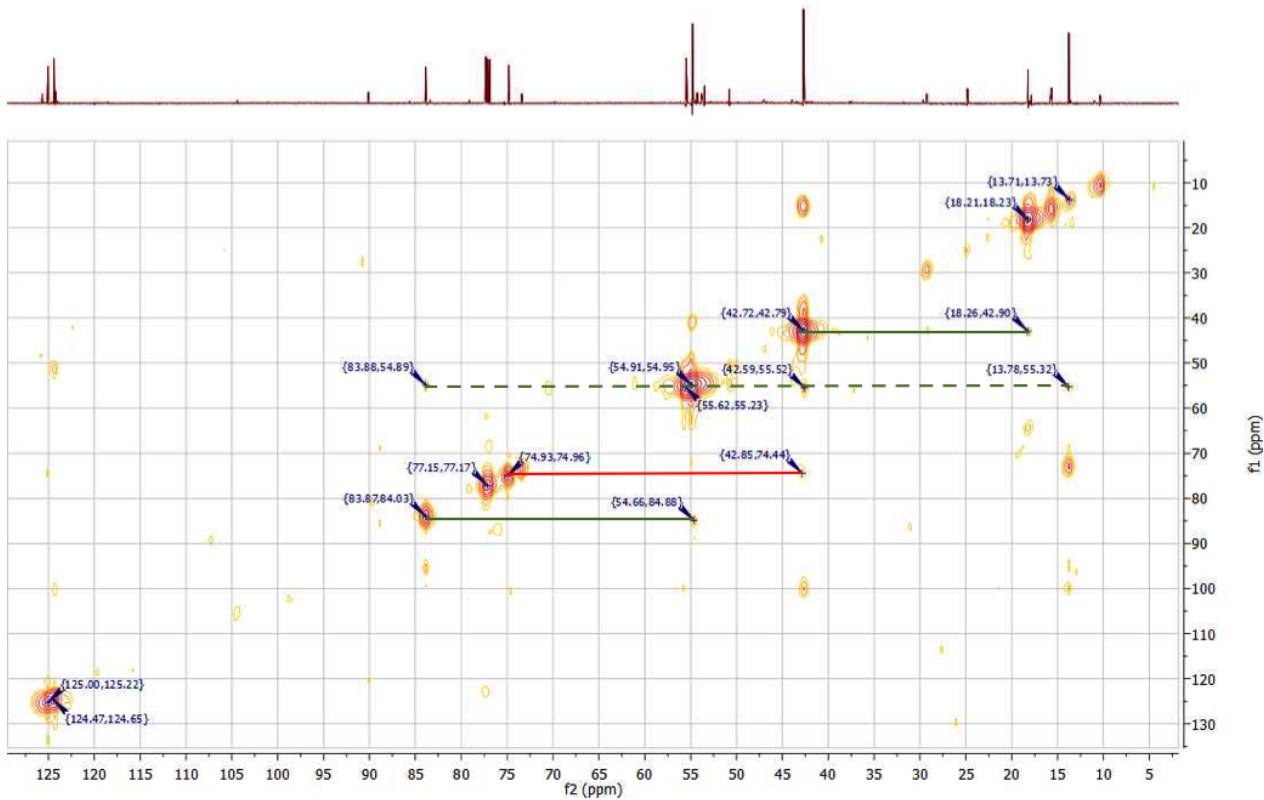


Figure 2.22: INADEQUATE (Incredible Natural Abundance DoublE QUAntum Transfer Experiment) allows the determination of neighboring carbons by displaying correlation between them. The experiment is very insensitive, since only one out of 10,000 carbon-carbon bonds links ^{13}C nuclei at natural abundance. Peaks projecting at the same y-coordinate (cross-peaks) indicate one-bond correlations between the carbons. For example, the carbon at 54.9 ppm is bonded to carbons at 83.9, 42.6 and 13.7 ppm (green dashed line). Carbon at 74.9 ppm is not connected to carbon at 55.6 ppm (red line). Vertical bands are known artifacts in these type of spectra.

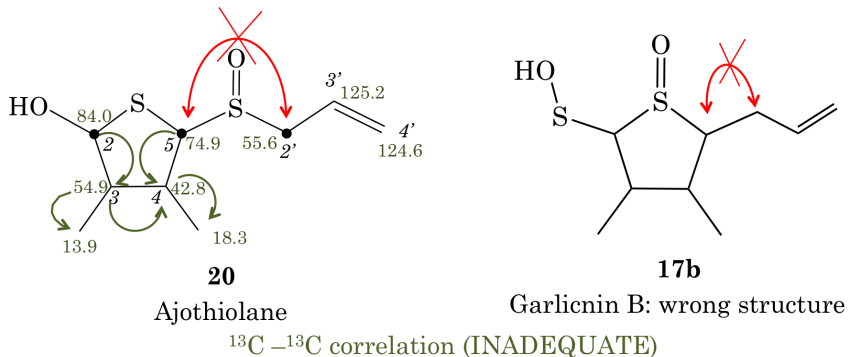


Figure 2.23: INADEQUATE (Incredible Natural Abundance DoublE QUAntum Transfer Experiment) allows the determination of neighboring carbons by displaying correlation between them. Green arrows represent correlations on spectrum Figure 2.22. Carbon at 74.9 ppm is not connected to carbon at 55.6 ppm (red arrow). The proposed structure (**17b**) of garlicnin is therefore invalidated.

under basic conditions. Other attempts using neutral conditions also failed, possibly because the dinitrobenzoate is a good leaving group and the carbocation is stabilized by the adjacent sulfur (glycosylation reactivity).

2.4.3 Mass spectrometry

In addition to the DART-MS fragmentation, ajothiolane was fragmented by LC-MS/MS on an SCIEX TripleTOF. The calculated mass for $C_9H_{16}O_2S_2$ is 220.05917, the proton adduct has an expected m/z of 221.06700 (for $[C_9H_{16}O_2S_2 + H]^+$). The fragmentation pattern is similar to that using DART, however peaks from other compounds are not present: only ions with $m/z = 221.1$ are selected and fragmented (Figure 2.26). A formula was deduced from the exact mass and the isotope distribution of each fragment, then parts of the proposed structures of ajothiolane (**20**) and garlicnin B (**17b**) were matched with the fragments (Figure 2.27). Fragments with $m/z = 131.055$ and 113.044 are inconsistent with the structure of **17b**. The major fragments formed, however, are consistent with the proposed structure for ajothiolane (**20**). Furthermore, with a higher collision energy, more fragments are formed, including a fragment with $m/z = 89.006$, which corresponds to $[C_3H_5OS]^+$ (Figure 2.27, in blue). This fragment is not consistent with the structure of **17b**.

The electrospray ionisation (ESI) ion source was replaced then by an atmospheric pressure chemical ionization (APCI) ion source. Under these conditions, no sodium adduct was observed. This likely occurs to the benefit of the proton adduct, which increases the sensitivity of the method. Fragmentation and screening

	δ ^{13}C (ppm)	δ ^1H (ppm)	Multiplicity and integration ^1H	HMBC (^1H correlated to ^{13}C)	INADEQUATE (^{13}C – ^{13}C corr.)	COSY (^1H – ^1H corr.)
-OH		4.34	d, $J = 11.0$ Hz, 1H			/
2	83.98	5.05	dd, $J = 10.9, 3.4$ Hz, 1H	5.05 to 42.8 and 74.9	84.0 to 54.9	5.05 to 2.00
3	54.90	2.00	ddq, $J = 13.5, 6.8, 3.4$ Hz, 1H	2.0 to 13.9 and 18.3	54.9 to 13.9, 42.8 and 84.0	2.00 to 1.06
CH ₃ -3	13.89	1.06	d, $J = 6.7$ Hz, 3H	1.06 to 42.78, 55 and 84.0		1.06 to 2.0
4	42.78	2.18	m*, 1H	2.18 to 18.3, 54.9 and 74.9	42.8 to 18.3	2.18 to 1.27
CH ₃ -4	18.32	1.27	d, $J = 6.7$ Hz, 3H	1.27 to 42.78, 54.9 and 74.9		1.27 to 2.18
5	74.87	4.09	d, $J = 5.8$ Hz, 1H	4.09 to 18.3, 42.9 and 84	74.9 to 42.8	4.1 to 2.2
2'	55.57	3.61	dd, $J = 12.5, 6.5$ Hz, 1H	3.61 to 74.9 and 125.1		3.61 to 3.35
		3.34	dd, $J = 12.6, 8.5$ Hz, 1H	3.34 to 74.9 and 125.1	/	3.35 to 3.61
3'	125.08	5.74	dddd, $J = 16.9, 10.6,$ 8.5, 6.6 Hz 1H			5.74 to 5.4
4'	124.56	5.41	m, 1H	5.4 to 55 and 125.1		5.4 to 5.38
		5.37	m, 1H			and 5.71

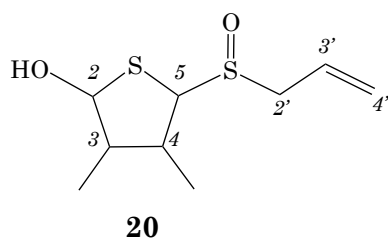


Figure 2.24: Summary of the NMR data of the major stereoisomer of ajothiolane (**20**), including 2D NMR. INADEQUATE was required to confirm the connectivity of carbons 2, 2' and 5, which is unclear when using only proton correlation (COSY, HMBC and HSQC).

*Multiplicity of the signal at 2.18 ppm is undefined due to the interference of an impurity.

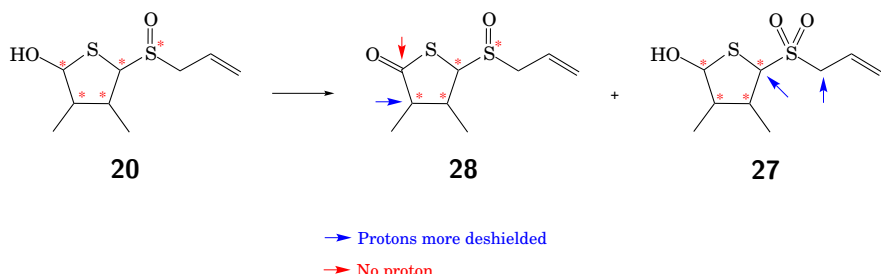
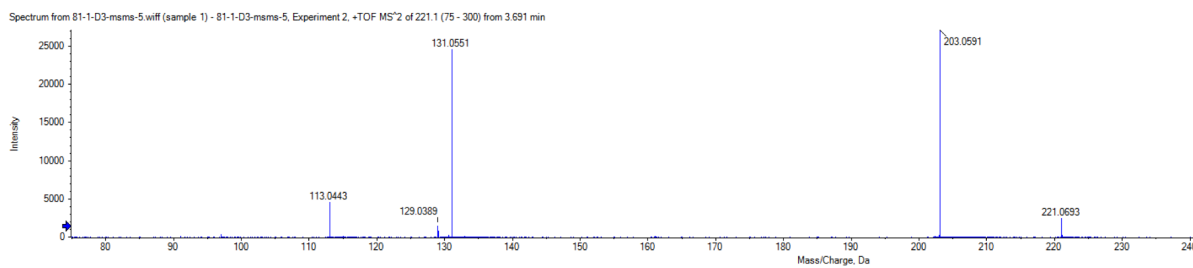


Figure 2.25: Tentative products of the oxidation of ajothiolane. Oxidation at the hydroxyl group (**28**) or the sulfoxide group (**27**) would lead to changes in the chemical shifts of the neighboring atoms, and the loss of one stereocenter. Products **28** and **27** have been tentatively identified by HR-MS.

of the lower masses indicated the presence of a fragment with $m/z = 73.0138$, which confirms again the correct structure: the loss of everything but $[\text{C}_3\text{H}_5\text{S}]^+$ is not easily justified for structure **17b**.

Whether ESI or APCI was used, a peak corresponding to the ion with $m/z = 203.056$ ($[\text{C}_9\text{H}_{14}\text{OS}_2 + \text{H}]^+$) is present on the spectrum. Facile loss of H_2O is plausible for a thiohemiacetal such as **20**. This peak could be the precursor ion of a different specie that would by chance coelute by UPLC. To eliminate this ambiguity, parameters of the APCI source have been modified. Under standard conditions, the temperature in the source is $650\text{ }^\circ\text{C}$. By lowering this temperature up to $200\text{ }^\circ\text{C}$, we were able to see less of the suspected elimination peak. However, the ionization and therefore the sensitivity also decrease, and low temperatures are not suitable for routine analyses.

Collision energy = 10 V



Collision energy = 43 V

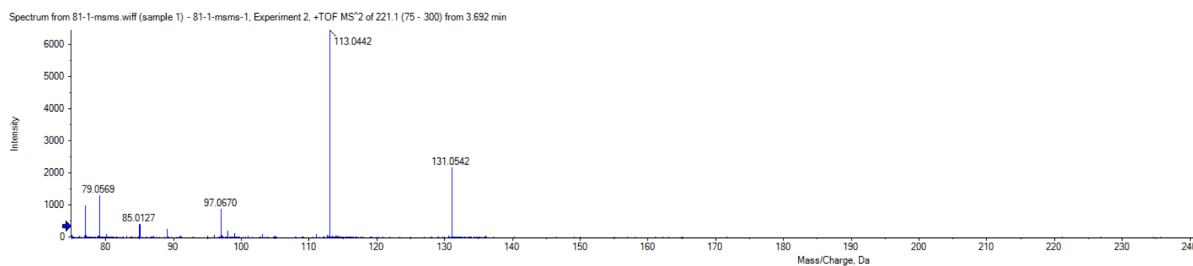


Figure 2.26: MS/MS analysis of ion $m/z = 221.1$ ($[\text{C}_9\text{H}_{16}\text{O}_2\text{S}_2]^+$), collision energy = 10 V (top) and 43 V (bottom). These fragments are explained in Figure 2.27.

2.4.4 Characterization of stereoisomers

Preparative HPLC was used to separate the stereoisomers of ajothiolane. The ^1H NMR spectrum of the crude product indicates many doublets in the methyl region. Reverse phase HPLC (C18 column) successfully separated some of the stereoisomers, with two limitations. Firstly, the compounds absorb weakly in UV. Fifty fractions of a defined volume were therefore collected, with no regards to the actual distribution of

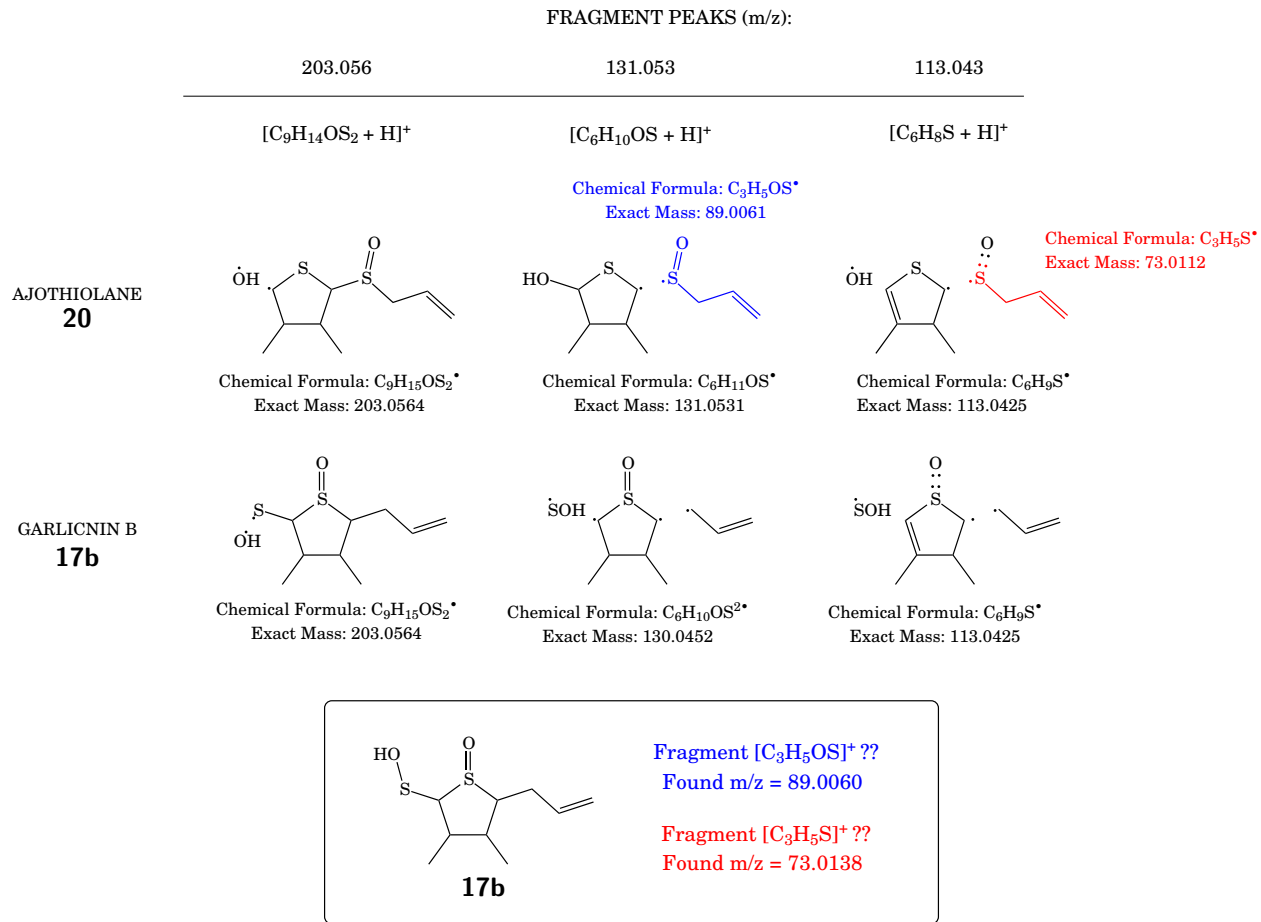


Figure 2.27: Fragment assignment of the MS/MS analysis of ion $m/z = 221.1$ (mass spectrum Figure 2.26). Fragmentation confirms the structure of ajothiolane (**20**), since no plausible explanations were found for fragment peaks with a m/z of 89.006 and 73.0138 ($[\text{C}_3\text{H}_5\text{OS}]^+$ and $[\text{C}_3\text{H}_5\text{S}]^+$, respectively).

compounds. Second, each of these fractions had to be extracted with distilled DCM in order to be dried prior to NMR. Unfortunately, following this treatment, grease and plasticizers were found in most of the samples. Each fraction contained less than 5 mg of material, rendering further purification impracticable. This technique could be repeated on more sample in future work. Despite the impurities, up to 22 different doublets were observed for the methyl groups, indicating the presence of as many as 11 stereoisomers. One stereoisomer is major (methyls at 1.08 and 1.29 ppm), and a second one is abundant (methyls at 1.15 and 1.36 ppm, Figure 4.3). The other compounds are minor.

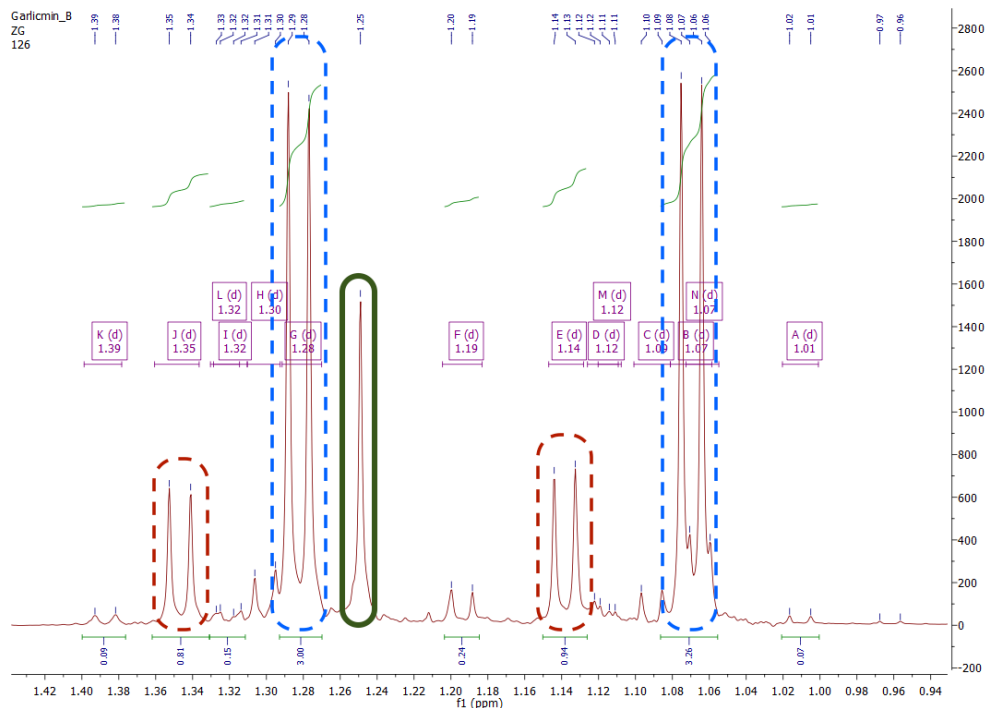


Figure 2.28: Representative example of a mixture of stereoisomers of ajothiolane (**20**) showing the methyl region of the ^1H NMR spectrum. Each isomer has two doublets in the methyl region, with coupling constants between 5 and 7 Hz.

Characterization of the stereoisomers by NMR was challenging on a mixture with peak overlap. Separation by HPLC and identification by MS was used to solve this problem. Samples were brought to Robert Sheridan of the New York State Department of Agricultural and Markets Laboratory for analysis. Their laboratory is equipped with state-of-the-art UPLC-QTOF and UPLC-Orbitrap. UPLC (Ultra Performance Liquid Chromatography) methods can resolve mixtures of compounds in a few minutes. The excellent resolution of the method was important to characterize the stereoisomers of **20**. The Eksigent UltraLC100 system was

equipped with a reverse phase column. Furthermore, the sensitivity of the mass spectrometer is sufficient to detect trace compounds and the MS/MS system facilitates structure determination.

The chromatograms obtained for ajothiolane ($m/z = 221.06$ and 234.04 , $[\text{C}_9\text{H}_{16}\text{O}_2\text{S}_2 + \text{H}]^+$ and $[\text{C}_9\text{H}_{16}\text{O}_2\text{S}_2 + \text{Na}]^+$, respectively) indicated the presence of at least seven stereoisomers in the mixture, which is consistent with the NMR analysis (Figure 2.29).

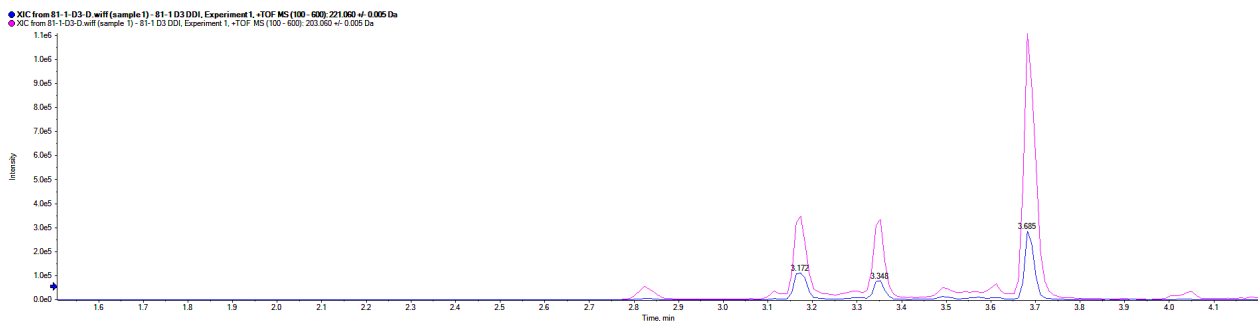


Figure 2.29: Chromatogram of the LC-MS separation of a garlic extract (ion source = ESI). Selected ion chromatograms of ajothiolane: $[\text{C}_9\text{H}_{16}\text{O}_2\text{S}_2 + \text{H}]^+$ in blue ($m/z = 221.06$), and $[\text{C}_9\text{H}_{16}\text{O}_2\text{S}_2 + \text{Na}]^+$ in pink ($m/z = 234.04$).

Other Group members are exploring the capabilities of these instruments in a broader project aiming at the characterization of aged-garlic extract components. This work follows GC-MS and LC-MS characterization of garlic and onion extracts,^{27,28} and DART-MS analysis of the first seconds after the plant is crushed.²⁹ Some minor, novel compounds have not been characterized because their concentration was too low. Identification of these trace compounds may now be possible these new instruments.

2.5 Identification of methylisoajoene

Another compound, which was identified by DART-MS as one of the proposed compound of Nohara's research group, was eluted with ajothiolane. After further purification, an NMR spectrum was obtained with spectral data identical to that published for garlicin D (**24**, Figure 2.30). This proposed structure, with a tetravalent sulfur and a chain of S-S-S-OH seemed implausible, and no similar functional groups has been reported in the literature to our knowledge. Spectral data recorded in our laboratory indicated a different ratio of proton integration than reported by Nohara, and the lack of one hydrogen compared to the formula obtained by high-resolution MS. Changing the NMR solvent to benzene-d₆ allowed us to identify the structure *E*-2,6,7-trithiadeca-4,8-diene 2-oxide, or methylisoajoene (Figure 2.31). Compound **8** had been previously identified,¹⁷

also thanks to ^1H NMR spectroscopy in benzene. The use of CDCl_3 may have misled Nohara et al. Benzene is known to affect the chemical shift of polar compounds by partial orientation of the solvent by the dipole moment of the molecule. In particular, the positive end of the dipole would complex weakly with the electron rich π -cloud of benzene.^{30,31}

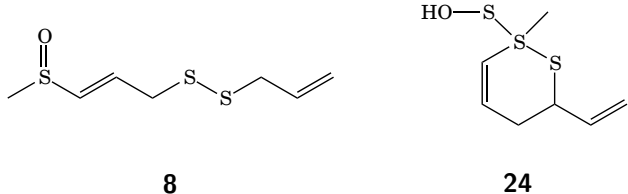
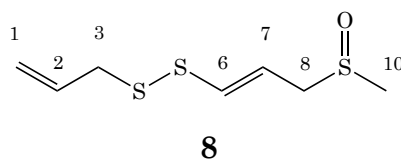


Figure 2.30: Proposed structures of methylisoajoene (**8**) and garlicin D (**24**).



Atom	1H NMR			13C NMR	
	CDCl ₃	C ₆ D ₆		CDCl ₃	C ₆ D ₆
1 CH ₂ =	5.21 (dd, <i>J</i> = 17.0, 1.2 Hz, 1H)	5.03 (d, <i>J</i> = 16.9 Hz, 1H)		118	118.9
	5.16 (d, <i>J</i> = 9.9 Hz, 1H)	4.95 (d, <i>J</i> = 10.4 Hz, 1H)			
2 =CH	5.82 (ddt, <i>J</i> = 17.2, 9.9, 7.3 Hz, 1H)	5.60 (dt, <i>J</i> = 17.1, 7.3 Hz, 1H)		132	133.12
3 CH ₂	3.33 (d, <i>J</i> = 7.3 Hz, 2H)	3.00 (d, <i>J</i> = 7.4 Hz, 2H)		42	42.87
6 CH ₂	3.45 (d, <i>J</i> = 6.2 Hz, 2H)	2.86 (d, <i>J</i> = 7.6 Hz, 2H)		39.4	38.8
7 CH=		6.38 (dt, <i>J</i> = 14.9, 7.5 Hz, 1H)		134	131.4
8 =CH	6.46 – 6.44 (m, <i>1H</i>)		5.74 (d, <i>J</i> = 14.7 Hz, 1H)	137	137.9
10 CH ₃	2.65 (s, 3H)	1.87 (s, 3H)		41	39.8

Figure 2.31: Comparison of the spectral data of methylisoajoene (**8**) in CDCl_3 and C_6D_6 . Olefinic signals of protons on carbons 7 and 8 were not separated in CDCl_3 and benzene- d_6 helped to resolve them.

These findings disprove the structure of garlicnin D. Methylajoene, also previously discovered by Sendl et al.,¹⁸ has been relabeled garlicnin L-2 by Nohara's group. We recommend care when considering the other structures proposed by this group.

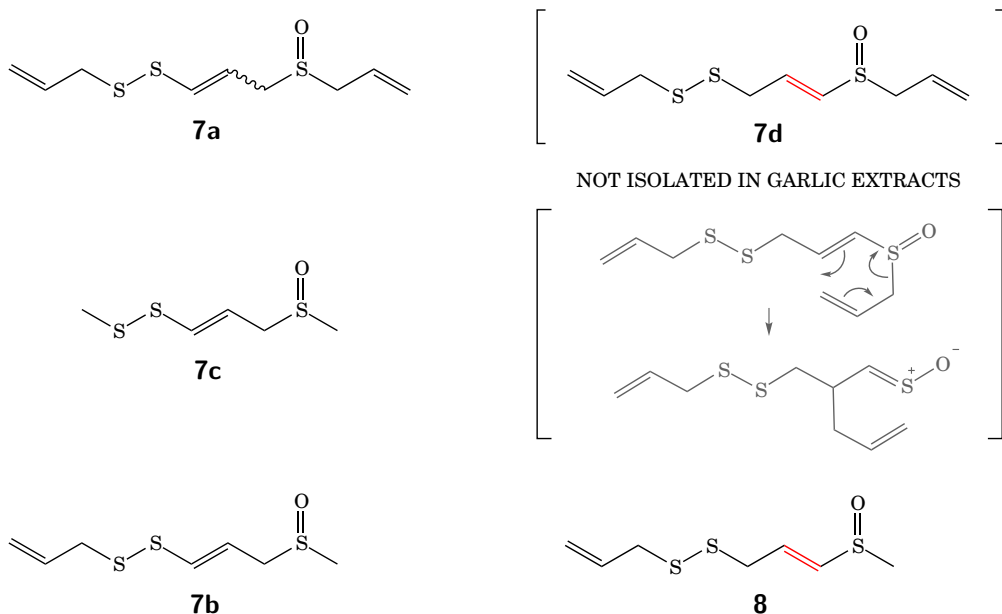


Figure 2.32: Overview of the ajoene-like compounds. Ajoene (**7a**), dimethylajoene (**7c**) and methylajoene (**7b**) are formed by the mechanism presented Figure 2.33. Methylisoajoene had been wrongly labeled garlicin D, which structure is now disproved. Methylajoene (**7b**) had also been renamed garlicin L-2 by Nohara's research group.³² Isoajoene has not been identified in a garlic extract, likely due to the rearrangement presented.

Methylajoene (**7b**) and dimethylajoene (**7c**, Figure 2.32) were first isolated from wild garlic (*Allium ursinum*) in which the proportion in alliin and methiin is almost 1:1. Garlic contains far more alliin than other alk(en)yl groups, up to 70%, and therefore two to three times less methylajoenes.¹⁸ An important question comes to mind when looking at the structure: why is this compound not present in the allyl form, allyl being the most abundant alk(en)yl group in garlic? Clues to answer the second question can be found in previous results by our team. Investigations on allyl 1-propenyl sulfoxide reveal formation of a sulfine by a thio-Claisen rearrangement,³³ which could explain the absence of isoajoene (**7d**, Figure 2.32). Ajoenes **7** are formed by the mechanism proposed in Figure 2.33.

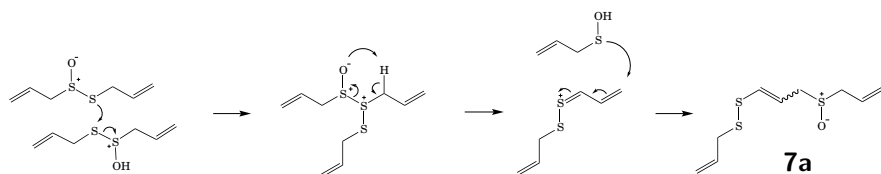


Figure 2.33: Mechanism of formation of (E,Z)-ajoene (**7a**), one of the most abundant compounds in garlic extracts. The position of the internal double bond is shifted in methylisoajoene (**8**), perhaps as a result of an acid-catalyzed rearrangement.

2.6 Conclusions

Ajothiolane was isolated, and its structure confirmed by spectroscopic methods. A second compound identified by Nohara's group as cyclic garlicin D was found to match the NMR data of previously reported acyclic methylisoajoene (**8**). Both topics are discussed further in the next chapter, in which the reactivity of some functional groups is presented and efforts were made to synthesize the compounds.

2.7 Experimental

NMR spectra were recorded in CDCl_3 , unless otherwise indicated, on a Bruker 400 Ultrashield operating at 400 MHz for proton and 100 MHz for carbon, or a 600 MHz Bruker Avance III HD operating at 600 MHz for proton and 125 MHz for carbon. The chemical shifts (δ) are indicated in ppm downfield from tetramethylsilane, with the internal standard being the residual CHCl_3 (7.27 ppm). Infrared spectra of the neat compounds were recorded on a Perkin Elmer UATR 2 FTIR. Mass spectra were obtained using the Hewlett Packard 6890 GC and a 5972A selective mass detector. A DART-AccuTOF mass spectrometer operating in positive or negative ion mode was employed with a polyethylene glycol spectrum as reference standard for exact mass measurements (PEG average molecular weight: 600). The atmospheric pressure interface was typically operated at the following potentials: orifice 1 = 15 V; orifice 2 = 5 V; ring lens = 3 V. The RF ion guide voltage was generally set to 800 V to allow detection of ions greater than m/z 80. The DART ion source was operated with helium gas at 200°C, and a grid voltage = 530. Diethyl ether and THF were distilled from sodium-benzophenone ketyl. Ethyl acetate was purchased from Pharmaco-Aaper and used without further purification. Throughout the study pure *m*-chloroperbenzoic acid (*m*CPBA) was employed. The reagent was obtained by washing a dichloromethane solution of the commercial sample, purchased from Sigma-Aldrich as a 70% mixture with *m*-chloroperbenzoic acid (*m*CPBA), with pH 7.5 phosphate buffer followed by drying and evaporation of the solvent (activity assessed by iodometric titration: 96%). The drying agent employed was anhydrous magnesium sulfate unless indicated otherwise. Analytical TLC was performed on precoated silica gel plates (Merck) with a 254 nm fluorescent indicator and was visualized under a UV lamp and by staining with a KMnO_4 solution. Preparative TLC plates (Analtech) were 1 or 2 mm thick and were visualized under UV light. Because of the very low levels of the compounds found in the garlic extracts, exposure to plastic and rubber was rigorously avoided to prevent contamination of samples by plasticizers.

Semi-quantitation of ajothiolane (20) concentration by DART-MS. Garlic extracts were prepared by chopping peeled cloves obtained from a local market in a blender, then adding acetone in a 1:1 w/v ratio and homogenizing the mixture. The extracts were kept away from light for the extraction. Six DIP-it ®tips were dipped in crude garlic extracts and positioned on the linear rail holder. The rail was moved at 0.5 mm/s in front of the ion source in the conditions described above (Orifice 2 = 20 V, temperature = 200 °C).

Translated files were processed as follows:

1. Chromatograms of the ions of interest were saved, then opened in an Excel document
2. Beginnings of peaks were identified as a sequence of at least three scans with an abundance superior to 10,000 on the 235.04 chromatogram (ajoenes, found to be the most robust component of the mixture). Peak areas were calculated as the sum of the abundances of the eighteen scans following the beginning of the peak (see example Figure 2.13). These surface areas were then normalized to the peak area of the TIC for the same scan range.

$$\text{Peak Area}(x) = \frac{\sum_{i=\text{scan1}}^{i+18} \text{Abundance}(x)}{\sum_{i=\text{scan1}}^{i+18} \text{Abundance(TIC)}}$$

3. Peak areas of each of the six repetitions were compiled, their mean, standard deviation and coefficient of variation were calculated.
4. One-way analyses of variance were conducted on some of the data using StatPlus software combined with Excel.

This procedure was repeated on three separate extracts, then on a fourth extract prepared with garlic cloves purchased in the winter.

Optimization of the rest time and extraction for the formation ajothiolane (20). Garlic cloves were peeled and chopped in a blender. Acetone was added in a 1:1 w/v ratio after different rest times (immediately, after 20 min or after 120 min). After addition of acetone, the mixture was homogenized with the blender for one min, three times. An extract prepared with a 20 min rest time was then analyzed regularly by DART-MS by the method described above.

Extraction of ajothiolanes. *ALL SOLVENTS FOR THE EXTRACTION AND ISOLATION OF AJOTHIOLANE NEEDED TO BE FRESHLY DISTILLED, AND CONTACT WITH PLASTIC AND RUBBER*

STRICTLY AVOIDED! Garlic cloves are peeled manually, and the material is chopped in a food processor. After the rest time, distilled acetone (1 v/w) is added and the mixture is blended for one min, three times. The homogeneous mixture is then left at room temperature for the determined extraction time in a large flask in the dark. After standing, the mixture is filtered on Celite with a Büchner funnel. The filtrate is concentrated under vacuum in a rotary evaporator at 45 °C, affording a brown, sticky paste. Two procedures have been tested to separate polar compounds from the target: polymer resin chromatography or liquid-liquid extraction. *Styrene resin chromatography*¹² The material is dissolved in acetone and purified by chromatography on a styrene polymer adsorbant DIAIONTMHP20. Elution by H₂O, MeOH then acetone affords 3 fractions. NMR spectra of the methanol and acetone fractions present the characteristic doublets of methyl groups in position 3 and 4 at δ 0.8–1.2 ppm. DART-MS indicate signals corresponding to the *m/z* of garlicins A, C and B in the methanol fraction mainly, and some in the acetone. *Liquid-liquid extraction* The concentrated filtrate is extracted three times by CH₂Cl₂ after NaCl was added to salt out the surfactant compounds. The organic layers are combined, dried over MgSO₄ and concentrated, yielding a sticky brown oil.

Typical extraction A total of 6 kg of peeled garlic cloves are chopped in a blender as follows: small batches of about 500 g of garlic are blended, then 500 mL acetone are immediately added and the mixture is homogenized (total acetone: 6 L). The batches are combined in two 2 L flasks and the mixture is allowed to stand for 12 h in the dark. The garlic pulp is separated from the liquid by Büchner filtration on Celite, and the filtrate is concentrated down to a volume of about 2 L. This mixture is saturated with NaCl then extracted three times by CH₂Cl₂. Organic layers are combined, dried over MgSO₄ and concentrated, yielding 17 g of sticky brown oil.

Optimized procedure. Peeled garlic cloves (6 kg) are crushed in a blender, then blended with acetone (1:1 v/w). The mixture is allowed to stand for 12 h, then the garlic pulp is filtered off. The filtrate is concentrated and extracted with 3 \times its volume of CH₂Cl₂ after NaCl was added to salt out the surfactant compounds. The organic layers are combined, dried over MgSO₄ and concentrated, yielding 17 g of sticky brown oil.

Purification of ajothiolane and methylisoajoene by flash chromatography. Elution of the brown oil by five column volumes of CH₂Cl₂/MeOH (99:1) then hexanes/acetone (4:1) leads to a fraction enriched in ajothiolanes¹⁶ (yellow band after 2 CV of the second mobile phase). After drying and concentrating, 2.5 g of yellow oil (**30**) are recovered. DART-MS and NMR indicate the presence of the target compounds, methylisoajoene, ajoenes and higher mass compounds. A second column chromatography is performed on

silica gel, elution with pentane/EtOAc (1:1). Fractions enriched in ajothiolane are collected after 4-5 volumes of column, combined and concentrated, yielding 750 mg of a yellow liquid. Methylisoajoene eluted right after ajothiolane.

Preparative TLC. The material (200 mg) is then loaded on a preparative TLC plate (thickness: 1 mm) and repeatedly eluted with pentane/EtOAc (2:1). The yellow, second-to-last band ($R_f = 0.102$) contains 40 mg of ajothiolane (**20**) about 85% pure. ^1H NMR (600 MHz, CDCl_3) δ 5.74 (dd, 1H, $J = 16.9, 10.6, 8.5, 6.6$ Hz), 5.41 (m, 1H), 5.37 (m, 1H), 5.05 (dd, 1H, $J = 10.9, 3.4$ Hz), 4.34 (d, 1H, $J = 11.0$ Hz), 4.09 (d, 1H, $J = 5.8$ Hz), 3.61 (dd, 1H, $J = 12.5, 6.5$ Hz), 3.34 (dd, 1H, $J = 12.6, 8.5$ Hz), 2.18 (m (impurity), 1H), 2.00 (ddq, 1H, $J = 13.5, 6.8, 3.4$ Hz), 1.27 (d, 3H, $J = 6.7$ Hz), 1.06 (d, 3H, $J = 6.7$ Hz) ppm.

Separation of stereoisomers of ajothiolane **20 by preparative HPLC.** Mixture **30** (50 mg) is diluted in MeOH and injected on a preparative HPLC column (RP-C18 column, 2.5 x 40 cm). A gradient of MeOH and $\text{H}_2\text{O} + 0.05\%$ formic acid is applied at 10 mL/min, the proportion of MeOH varying as follows (%MeOH (time in minutes)): 15 (0 min), 15 (10 min), 25 (30 min), 25 (55 min), 40 (65 min), 40 (70 min), 80 (75 min), 80 (100 min). UV detection is not sensitive for ajothiolanes (limited absorption of UV light), therefore fractions are collected and the presence of **20** is assessed by DART-MS. The fractions containing **20** are salted with NaCl then extracted by distilled CH_2Cl_2 . Organic layers are dried over MgSO_4 , concentrated and dissolved in CDCl_3 for NMR analysis. A total of 22 different methyl doublets have been identified by NMR (11 stereoisomers) from these fractions. Unfortunately, grease and other pollutants from the HPLC system led to poor quality spectra. Two stereoisomers are consistently major in the mixture: ajothiolane 1 (methyls at 1.08 and 1.29 ppm) and ajothiolane 2 (methyls at 1.15 and 1.35 ppm).

Analysis of the stereoisomers of ajothiolane **20 by UPLC-MS.** A UPLC Eksigent UltraLC100 system was used. A water-acetonitrile gradient was used on a XBridge C18 2.5 μm column (2.1 x 50 mm) at a flow rate of 0.5 mL/min. Water (mobile phase A) is acidified with 0.1% formic acid. The gradient program was set as follows : time(min)/%ACN(v/v): 0/5, 2/5, 6/80, 8/80, 8.02/5, 12/5. Detection was performed by a TOF mass spectrometer with different collision energies (standard collision energy = 15 V) after ionization either by electrospray or atmospheric pressure chemical ionization (declustering potential/energy of ionization = 40 V).

References

- (1) Wratten, S. J.; Faulkner, D. J. Cyclic polysulfides from the red alga *Chondria californica*. *J. Org. Chem.* **1976**, *41*, 2465–2467.
- (2) Damsté, J. S.; De Leeuw, J. W.; Kock-Van Dalen, A.; De Zeeuw, M. A.; Lange, F. D.; Irene, W.; Rijpstra, C.; Schenck, P. The occurrence and identification of series of organic sulphur compounds in oils and sediment extracts. I. A study of Rozel Point Oil (U.S.A.) *Geochim. Cosmochim. Acta* **1987**, *51*, 2369–2391.
- (3) Richard, L. Calculation of the standard molal thermodynamic properties as a function of temperature and pressure of some geochemically important organic sulfur compounds. *Geochim. Cosmochim. Acta* **2001**, *65*, 3827–3877.
- (4) Xavier, F.; De Las Heras, C.; Grimalt, J. O.; Lopez, J. F.; Albaigés, J.; Damste, J. S. S.; Schouten, S.; De Leeuw, J. W. Free and sulphurized hopanoids and highly branched isoprenoids in immature lacustrine oil shales. *Org. Geochem.* **1997**, *27*, 41–63.
- (5) Amrani, A.; Aizenshtat, Z. Photosensitized oxidation of naturally occurring isoprenoid allyl alcohols as a possible pathway for their transformation to thiophenes in sulfur rich depositional environments. *Org. Geochem.* **2004**, *35*, 693–712.
- (6) Peng, P.; Morales-Izquierdo, A.; Fu, J.; Sheng, G.; Jiang, J.; Hogg, A.; Strausz, O. P. Lanostane sulfides in an immature crude oil. *Org. Geochem.* **1998**, *28*, 125–134.
- (7) Yoshida, M.; Kameyama, M.; Hosoda, H.; Shimizu, Y.; Sakagami, K.; Washino, K.; Iwata, J.; Omoto, M. New thiolane compound and use thereof; JP143866 , 2010.
- (8) Aoyagi, M.; Kamoi, T.; Kato, M.; Sasako, H.; Tsuge, N.; Imai, S. Structure and bioactivity of thiosulfinates resulting from suppression of lachrymatory factor synthase in onion. *J. Agric. Food Chem.* **2011**, *59*, 10893–10900.
- (9) Block, E. The organosulfur chemistry of the genus *Allium* - Implications for the organic chemistry of sulfur. *Angew. Chem. Int. Ed.* **1992**, *31*, 1135–1178.
- (10) Naganathan, S. Organosulfur Chemistry of *Allium* Species , Ph.D. Thesis, State University of New York at Albany, 1992, p 175.

(11) Block, E.; Bayer, T.; Naganathan, S.; Zhao, S.-H. *Allium* chemistry: synthesis and sigmatropic rearrangements of alk(en)yl 1-propenyl disulfide *S*-oxides from cut onion and garlic. *J. Am. Chem. Soc.* **1996**, *118*, 2799–2810.

(12) El-Aasr, M.; Fujiwara, Y.; Takeya, M.; Ono, M.; Nakano, D.; Okawa, M.; Kinjo, J.; Ikeda, T.; Miyashita, H.; Yoshimitsu, H.; Nohara, T. Garlicnin A from the fraction regulating macrophage activation of *Allium sativum*. *Chem. Pharm. Bull.* **2011**, *59*, 1340–1343.

(13) El-Aasr, M.; Fujiwara, Y.; Takeya, M.; Ikeda, T.; Tsukamoto, S.; Ono, M.; Nakano, D.; Okawa, M.; Kinjo, J.; Yoshimitsu, H.; Nohara, T. Onionin A from *Allium cepa* inhibits macrophage activation. *J. Nat. Prod.* **2010**, *73*, 1306–1308.

(14) Nohara, T.; Kiyota, Y.; Sakamoto, T.; Manabe, H.; Ono, M.; Ikeda, T.; Fujiwara, Y.; Nakano, D.; Kinjo, J. Garlicnins B1, C1, and D, from the fraction regulating macrophage activation of *Allium sativum*. *Chem. Pharm. Bull.* **2012**, *60*, 747–751.

(15) Nohara, T.; Fujiwara, Y.; Ikeda, T.; Murakami, K.; Ono, M.; Nakano, D.; Kinjo, J. Cyclic sulfoxides garlicnins B2, B3, B4, C2, and C3 from *Allium sativum*. *Chem. Pharm. Bull.* **2013**, *61*, 695–699.

(16) Nohara, T.; Fujiwara, Y.; Komota, Y.; Kondo, Y.; Saku, T.; Yamaguchi, K.; Komohara, Y.; Takeya, M. Cyclic sulfoxides-garlicnins K 1, K 2, and H 1-extracted from *Allium sativum*. *Chem. Pharm. Bull.* **2015**, *63*, 117–121.

(17) Yoshida, H.; Katsuzaki, H.; Ohta, R.; Ishikawa, K.; Fukuda, H.; Fujino, T.; Suzuki, A. An organosulfur compound isolated from oil-macerated garlic extract, and its antimicrobial effect. *Biosci. Biotechnol. Biochem.* **1999**, *63*, 588–590.

(18) Sendl, A.; Wagner, H. Isolation and identification of homologues of ajoene and alliin from bulb-extracts of *Allium ursinum*. *Planta Med.* **1991**, *57*, 361–362.

(19) Cody, R. B.; Dane, A. J. Soft ionization of saturated hydrocarbons, alcohols and nonpolar compounds by negative-ion direct analysis in real-time mass spectrometry. *J. Am. Soc. Mass Spectrom.* **2013**, *24*, 329–334.

(20) Domin, M.; Cody, R., *Ambient Ionization Mass Spectrometry; New Developments in Mass Spectrometry*; The Royal Society of Chemistry: London, 2015, p 508.

(21) Harris, G. A.; Hostetler, D. M.; Hampton, C. Y.; Fernández, F. M. Comparison of the internal energy deposition of direct analysis in real time and electrospray ionization time-of-flight mass spectrometry. *J. Am. Soc. Mass Spectrom.* **2010**, *21*, 855–863.

(22) U.S. Department of Health and Human Services - Food and Drug Administration *Guidance for industry bioanalytical method validation*; tech. rep.; 2001, p 25.

(23) Balci, M., *Basic 1H- and 13C-NMR Spectroscopy*; Elsevier Science: Amsterdam, 2005.

(24) Chamberlain, N., *The Practice of NMR Spectroscopy: with Spectra-Structure Correlations for Hydrogen-1*; Springer US: New York, 2013.

(25) Hansen, P. E. Carbon-hydrogen spin-spin coupling constants. *Prog. Nucl. Magn. Reson. Spectrosc.* **1981**, *14*, 175–295.

(26) Turner, D. L. Carbon-13 autocorrelation NMR using double-quantum coherence. *J. Magn. Reson.* **1982**, *49*, 175–178.

(27) Block, E.; Putman, D.; Zhao, S. H. *Allium* chemistry: GC-MS analysis of thiosulfinates and related compounds from onion, leek, scallion, shallot, chive, and Chinese chive. *J. Agric. Food Chem.* **1992**, *40*, 2431–2438.

(28) Block, E.; Naganathan, S.; Putman, D.; Zhao, S.-H. *Allium* chemistry: HPLC analysis of thiosulfinates from onion, garlic, wild garlic (Ramsons), leek, scallion, shallot, elephant (great-headed) garlic, chive and chinese chive. Uniquely high allyl to methyl ratios in some garlic samples. *J. Agric. Food Chem.* **1992**, *40*, 2418–2430.

(29) Block, E.; Dane, A. J.; Thomas, S.; Cody, R. B. Applications of direct analysis in real time mass spectrometry (DART-MS) in *Allium* chemistry. 2-Propenesulfenic and 2-propenesulfinic acids, diallyl trisulfane S-oxide, and other reactive sulfur compounds from crushed garlic and other alliums. *J. Agric. Food Chem.* **2010**, *58*, 4617–4625.

(30) Reich, H. J. Structure Determination Using NMR. Chem 605 Lecture notes, University of Wisconsin. Retrieved from <http://www.chem.wisc.edu/areas/reich/nmr/>, 2010.

(31) Richards, S. A.; Hollerton, J. C., *Essential Practical NMR for Organic Chemistry*; Wiley: Hoboken, 2010.

(32) Nohara, T.; Fujiwara, Y.; Ikeda, T.; Yamaguchi, K.; Manabe, H.; Murakami, K.; Ono, M.; Nakano, D.; Kinjo, J. Acyclic sulfides, garlicnins L-1 - L-4, E, and F, from *Allium sativum*. *Chem. Pharm. Bull.* **2014**, *62*, 477–482.

(33) Block, E.; Ahmad, S. Unusually facile thio-Claisen rearrangement of 1-alkenyl 2-alkenyl sulfoxides: a new sulfine synthesis. *J. Am. Chem. Soc.* **1985**, *107*, 6731–6732.

Chapter 3

Chemistry of thiolane-containing natural products from processed plants of the genus *Allium*

3.1 Introduction

Chapter 2 reviews published structures of thiolane-containing *Allium* compounds (Figure 3.1). The structural differences between these compounds on the one hand and the predicted structures of ajothiolane (**20**) and cepathiolane (**19**) on the other hand, as well as the unusual functional groups they contain, led us to examine garlicnins further. The structure we propose for the compound we purified from garlic extracts corresponds to **20**. This chapter discusses the reasons why the structures of some garlicnins (**17**) seemed wrong in the context of *Allium* chemistry, and our attempts to prove the identity of **20** by chemical synthesis. Other garlicnins with structures we considered to be incorrect are also investigated.

One concern is the high anticipated reactivity of some functional groups in the proposed structures. Thiolactone sulfoxides (as in garlicnin K, **17c**, Figure 3.1) have not been isolated, and are suggested to be very reactive intermediates. Furthermore, sulfenic acids are known to be highly reactive as well, especially in protic solvents. Finally, the biosynthetic route is inconsistent with known pathways, and the introduction

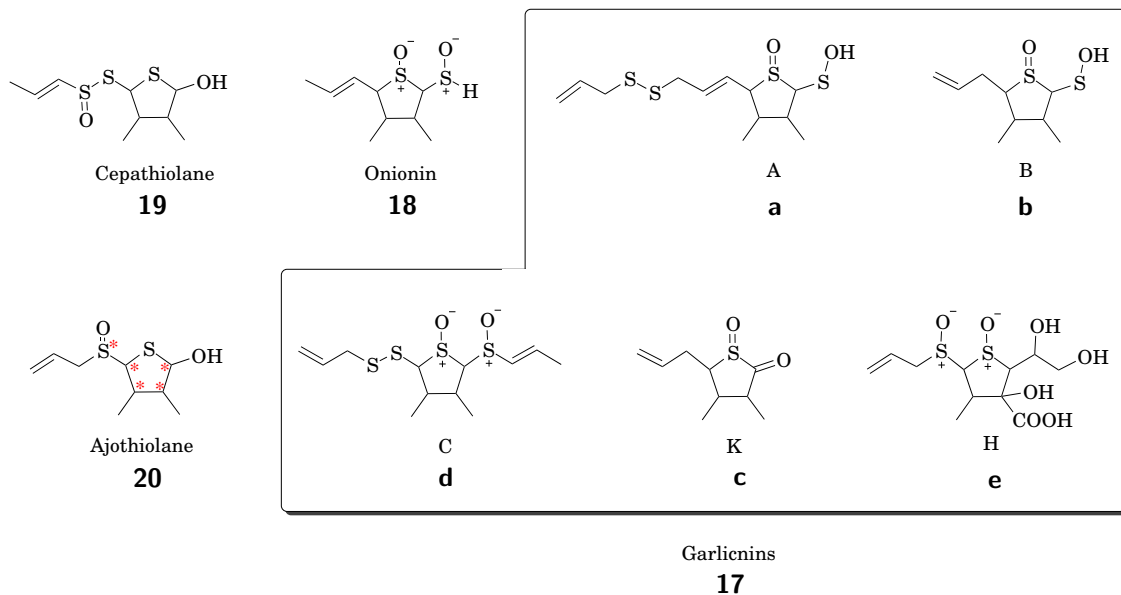


Figure 3.1: Reported thiolanes in *Allium* extracts: cepathiolane (**19**) reported by Yoshida et al.¹ and Aoyagi et al.,² onionin (**18**) and garlicinins (**17**) by Nohara et al.^{3–7} We demonstrated in Chapter 2 that the structure of garlicin B is incorrect. Ajothiolane (**20**) is the alternative structure to garlicin B (**17b**) matching the spectral data and consistent with the known biosynthetic routes in the genus *Allium*. Stereocenters are marked with an asterisk.

of certain intermediates is questionable. We sought to synthesize similar structures to assess their existence as isolable compounds, and to propose and synthesize alternative structures as the case may be.

After a review of the literature on these issues, this work presents our efforts directed toward the synthesis of analogues to garlicin B (**17b**) and ajothiolane (**20**) as a proof of concept for our hypothesis. A synthesis based on the probable biosynthetic route will then be proposed for ajothiolane (**20**). Our efforts toward the synthesis of methylisoajoene (**8**) are also presented. Later, the alleged structure of garlicin K (**17c**), a thiolactone sulfoxide, is investigated.

The stereochemistry of ajothiolanes is a complex topic. Nohara *et al.* isolated multiple diastereomers of the garlicinins on silica gel: four garlicinins B (B1 to B4), three garlicinins C (C1 to C3) and two garlicinins K (K1 and K2). Ajothiolane has five stereocenters, giving rise to 32 potential stereoisomers ($2^5 = 32$). The stereochemistry was briefly addressed in the previous chapter. In this chapter, most structures will be represented without stereochemistry until the stereochemistry is considered (Section 3.3.2).

To clarify cases, the name *garlicinins* (**17**) will be used for the structures published by Nohara's group,^{3,5–7} and *ajothiolane* for the alternative structure we proposed in Chapter 2 (**20**).

3.1.1 Sulfenic acids

Sulfenic acids are well known for their key role in *Allium* chemistry, but also their high reactivity. Isolation and characterization has been a challenge for small, non-hindered sulfenic acids, because they rapidly condense with a second sulfenic acid in solution (Figure 3.2 and Figure 3.3, reaction 1).

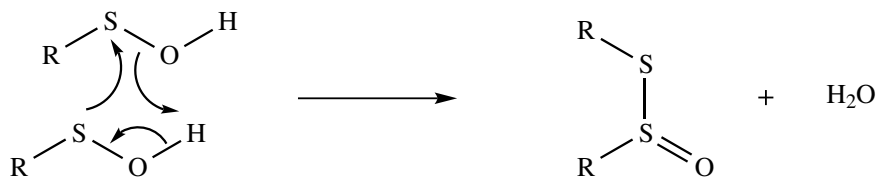


Figure 3.2: Sulfenic acids tend to condense to form thiosulfinates.

In 1978, the preferred form of sulfenic acids was found to be S–O–H (and not S(=O)–H) in the gas phase.⁸ A few sulfenic acids have been isolated in solution. In these cases the reactivity was diminished by stabilization through hydrogen bonding (as in the case of the first isolated sulfenic acid derived from anthraquinone, Figure 3.4⁹) or steric effects.^{10–12} Other examples include photocaged sulfenic acid¹³ and stabilization in a cavity.^{14–16}

A recent review by Gupta and Carroll¹⁷ emphasizes the importance of sulfenic acids in biological processes (as an intermediate in drug metabolism or enzymatic reactions), but also points out their strong reactivity both as a nucleophile (condensation reaction, Figure 3.2) or an electrophile (summary in Figure 3.3). The isolation of a non-sterically stabilized sulfenic acid in solution is therefore unlikely. Hydrogen bonding could stabilize the sulfenic acid in garlicin, but this hypothesis needs to be verified.

3.1.2 Biosynthetic routes of secondary metabolites of *Allium*

Most organosulfur compounds from garlic, onion and other alliums originate from the enzymatic reaction of an alk(en)ylcysteine sulfoxide and alliinase.¹⁹ The known alk(en)ylcysteine sulfoxides are *S*-allylcysteine sulfoxide (alliin, **1a**), *S*-methylcysteine sulfoxide (methiin, **1b**), *S*-propylcysteine sulfoxide (propiin, **1d**) and *S*-1-propenylcysteine sulfoxide (isoalliin, **1c**, Figure 3.5). As a consequence, all secondary metabolites are made of building blocks of one or three carbons (see Figure 3.6).¹⁹ Chains of six carbons are found only if Diels-Alder reactions or [3,3]-sigmatropic rearrangements occur, as in vinylidithiin chemistry. However, the formation of compounds made of chains of nine contiguous carbons is hard to explain from a biosynthetic point of view.

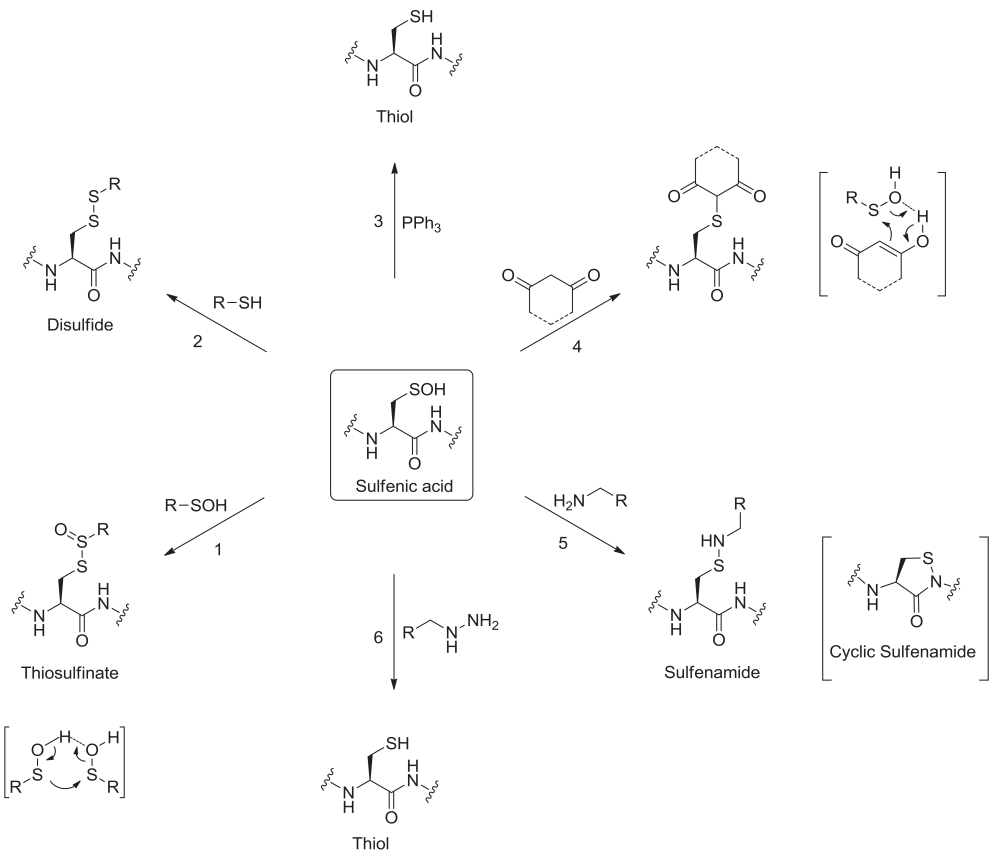
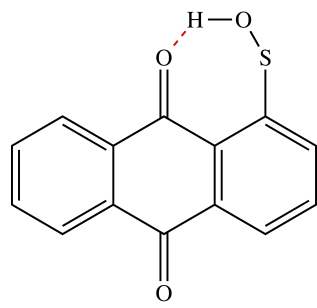


Figure 3.3: Sulfenic acids acting as electrophiles undergo a wide range of reactions. From Gupta and Carroll.¹⁷



1-Anthraquinonesulfenic acid

Figure 3.4: Sulfenic acids stabilized by hydrogen bonds can be isolated, like 1-anthraquinonesulfenic acid.¹⁸

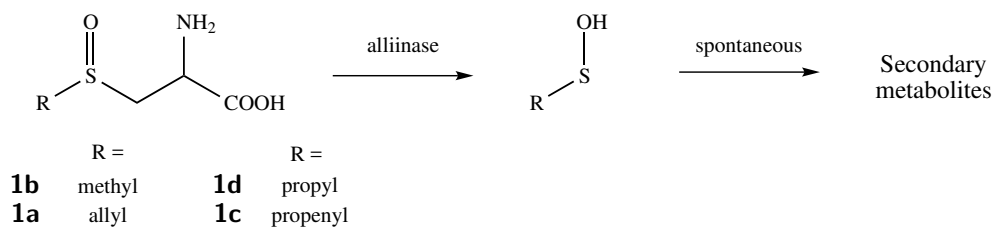


Figure 3.5: Origin of the secondary metabolites in the *Allium* species.

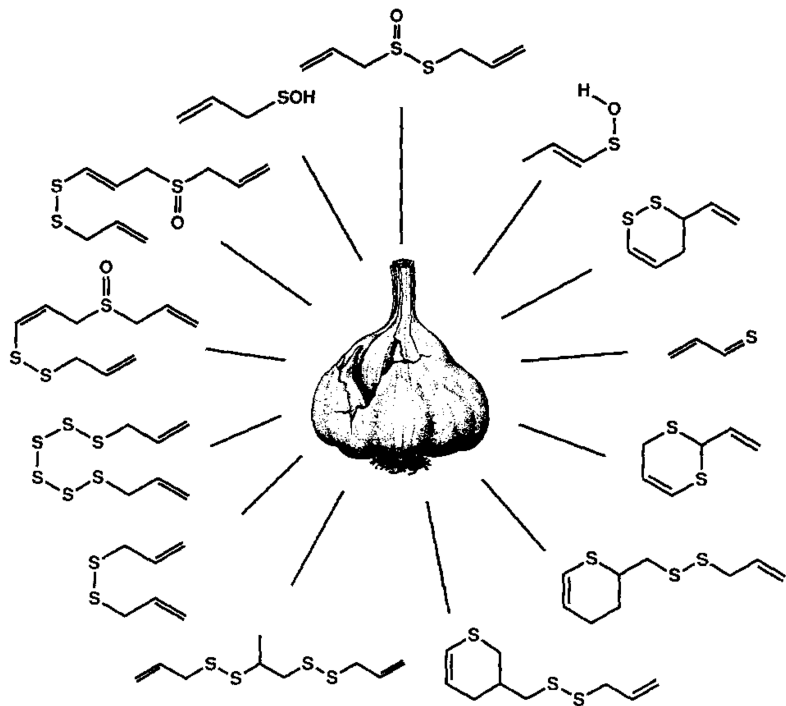


Figure 3.6: Summary of the secondary metabolites extracted from garlic. From Block.²⁰

3.2 Synthesis of thiolane analogues

Our first attempts were made on thiolane (**31**) and thiolane sulfoxide (**32**), which were both commercially available. We wanted to explore the reactivity of these two species. Introduction of substituents on carbons 2 and 5 was the goal discussed in this section.

3.2.1 Insertion of functional groups in the α -position of thiolanes

α -Alkylation of thiolanes

A carbanion is formed by treatment of thiolane sulfoxide (**32**) with *n*-butyllithium (*n*-BuLi), which is then quenched by an alkyl halide (Figure 3.7). 2-Methylthiolane sulfoxide (**33a**) and 2-allylthiolane sulfoxide (**33b**) have been synthesized in this way with yields of 14% and 19%, respectively. Two stereoisomers of (**33b**) are identified by GC-MS and NMR in a 1:10 ratio. Thiolane (**31**) is unreactive under these conditions, the protons being not sufficiently acidic.

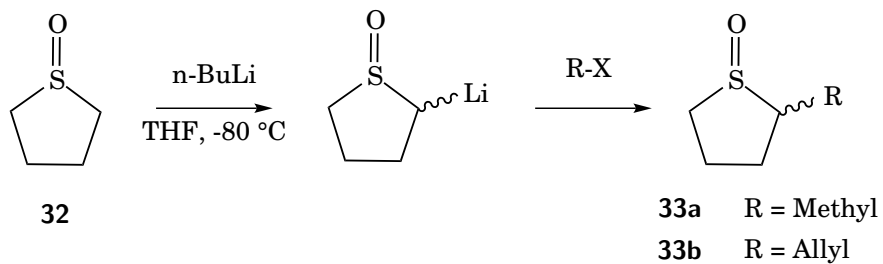


Figure 3.7: Alkylation of thiolane sulfoxide (**32**) by treatment with *n*-butyllithium (*n*-BuLi) followed by treatment with an alkyl halide in THF at -80°C ; $\text{X}_a = \text{I}$, $\text{X}_b = \text{Br}$. Yields: **33a** = 14%, **33b** = 19%.

Introduction of chalcogen functional groups

Via a Pummerer reaction A well-known reaction to introduce oxygen on the α -position to a sulfur atom is the Pummerer reaction, performed on sulfoxides and leading to α -acyloxythioethers (Figure 3.8, left). Thiolane sulfoxide (**32**) reacted quickly and violently with trifluoroacetic anhydride (TFAA), even at low temperature, and no product could be recovered. Reaction with acetic anhydride (AA), on the other hand, led to the Pummerer product **34** in good yield (74%, Figure 3.8). The addition of an organic base (pyridine, lutidine, triethylamine) did not improve the formation of product (on the contrary, TFAA and AA reacted with the base).

2-Acetoxythiolane can be oxidized to the sulfoxide by *m*CPBA, yielding 2-acetoxythiolane sulfoxide (**35**, 63%, Figure 3.8, right). Two diastereoisomers, *cis*- (**35a**) and *trans*-2-acetoxythiolane sulfoxide (**35b**) are separated by GC-MS and distinguished by NMR in a 1:2 ratio. The *trans* isomer is theoretically favored by thermodynamics, but we did not identify the isomers.

Compound **34** has also been hydrolyzed by sodium methoxide to give 2-hydroxythiolane in 65% yield (**29**, Figure 3.9). 2-Acetoxythiolane had been previously synthesized by Cox and Owen in 1967 in the context of

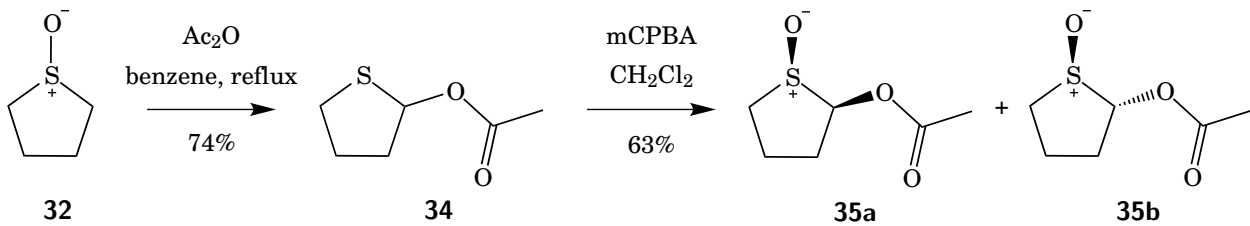
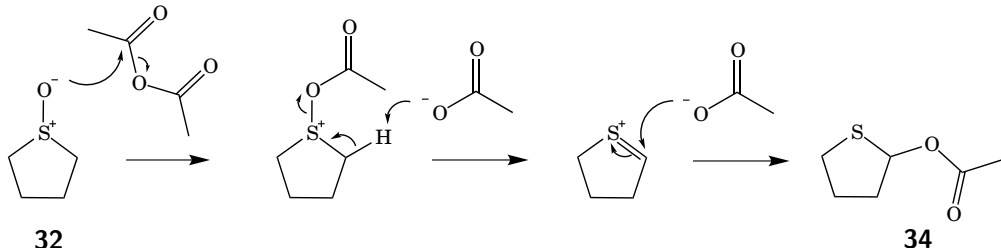
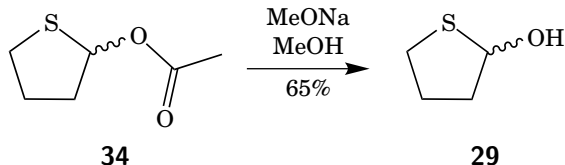


Figure 3.8: Introduction of an oxygen in position 2 of the thiolane ring via the Pummerer reaction (yield = 74%), followed by oxidation of 2-acetoxythiolane by *m*CPBA (yield = 63%). Two diastereoisomers of **35** are separated on the GC-MS and distinguished by NMR in a 1:2 ratio. The *trans* isomer (**35b**) should be thermodynamically favored but we did not identify the isomers. Acetic anhydride and trifluoroacetic anhydride were tested in the Pummerer reaction, the latter being too reactive.

sugar chemistry by treating thiolane with *t*-butylperacetate and cuprous chloride.²¹ 2-Hydroxythiolane had then been obtained by treating a methanol solution of 2-acetoxythiolane with sodium. The yields they report are similar to ours.



If the thiolane sulfoxide is already α -substituted, the Pummerer reaction with acetic anhydride (AA) is more difficult. The substituents tested in this work were chlorine, methyl, allyl, thioallyl, hydroxyl and acetoxy groups. Among these α -substituted thiolane *S*-oxides, most did not react with acetic anhydride, even after three days of reflux. After 24 h of reflux, about 5% of the 2-methylthiolane *S*-oxide is converted. The reaction proceeds via a thiophenium ion (Figure 3.10), whose formation by proton abstraction might not be favored by a substituent. The higher reactivity of TFAA can be used on substituted thiolane sulfoxides

to perform a Pummerer reaction. For example, 2-acetoxythiolane sulfoxide **35** was successfully converted to product **36** (Figure 3.11), but isolation of the latter was not successful.

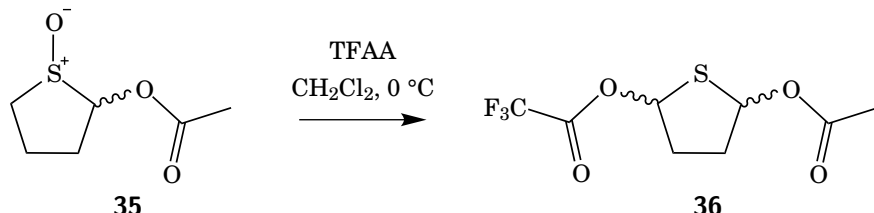


Figure 3.11: Performing a Pummerer reaction on a substituted thiolane sulfoxide was not possible with acetic anhydride (AA), only with trifluoroacetic anhydride (TFAA). The product **36** decomposed rapidly and could not be purified.

A thio-Pummerer reaction was attempted with thioacetic anhydride. However, the major products of this reaction were thiolane (**31**) and the oxidation product of thioacetate (**37**, Figure 3.12). The sulfoxide is likely to oxidize this species, a reaction that cannot happen with the acetate. Even though a small amount of the target product was formed, this procedure is not suitable for our synthesis.

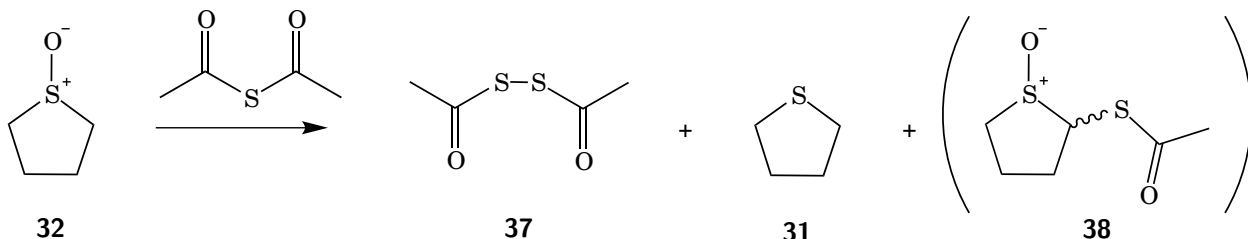


Figure 3.12: Pummerer reaction with thioacetic anhydride led mostly to the formation of **37**, which is formed by oxidation of thioacetate. Only traces of **38** are formed.

Via carbanion chemistry As seen above (Section 3.2.1, "α-Alkylation of thiolanes"), thiolane sulfoxide can be lithiated. The introduction of an electrophilic sulfur is then possible. Elemental sulfur is an option, but the 8-membered ring structure does not ensure the insertion of one single sulfur atom. A preferred option was the use of 2-phenylthiirane (**39**), which would form a lithium thiolate (**40**), as described by Gilman and Woods²² and applied by Block *et al.*²³ The latter was then quenched by allyl bromide, affording 2-allylthiolane sulfoxide with a yield of 17% (**41**, Figure 3.13). The two stereoisomers, present in a 2:5 ratio, could be separated by column chromatography. Despite our attempts to quench **40** with water or D₂O, 2-mercaptopthiolane sulfoxide could not be isolated.

We observed a phenomenon reported by Corey (on silylation):²⁴ after the first proton is exchanged, the geminal proton is highly reactive. As a result, the mixture contained **41**, but also starting material and 2,2-bis(allylthio)thiolane sulfoxide. We believe the lithiated species **40** can deprotonate **41** at position 2. Corey explains this by the dominance of electron withdrawal over steric hinderance.

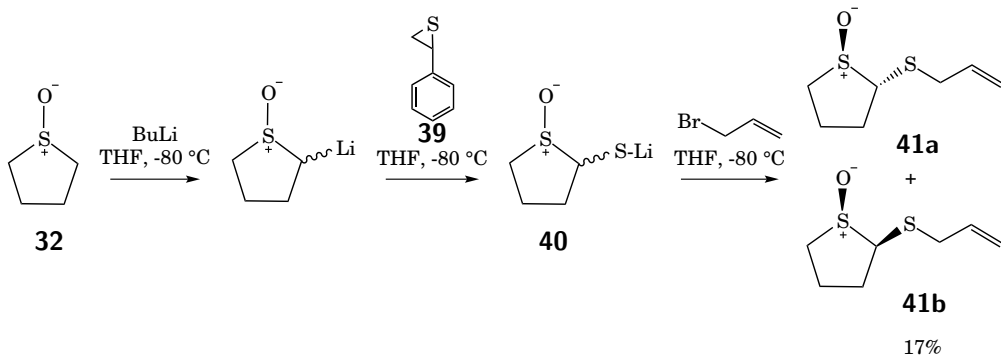


Figure 3.13: Introduction of an allylthio group to the α -position of the thiolane sulfoxide via carbanion chemistry. The yield is low (17%) and compares to the allylation of thiolane sulfoxide (**33**, Figure 3.7). Diastereomers are present in a 2:5 ratio, but have not been identified.

After purification of **41**, attempts to change the oxidation state of the two sulfurs were performed (Figure 3.14). In the ajothiolane structure we propose (**20**), the ring sulfur is a sulfide and the side-chain sulfur a sulfoxide, as in **42**. However, oxidation of the bis sulfide **43** leads back to **41**. From that perspective, this pathway seems unsuitable for our project.

Pummerer reaction of **41** would not be expected to give the 2,5-disubstituted product **41c**. Instead, a geminal Pummerer reaction ($\text{C}_2\text{-H}$ is more acidic), a deprotonation-alkylation or free radical substitution could occur. This reaction has not been attempted.

At this point, the NMR spectra of allylated **33b** and *S*-allylated thiolane sulfoxide (**41**, **43** and **44**) can be compared to spectral data of garlicin B (**17b**, Figure 3.15). In particular, the proton on the carbon bearing the side chain (H_2 in **33b**) is more or less deshielded according to the neighboring atoms: carbons, sulfides then sulfoxides increase the deshielding in that order.

The chemical shift reported for garlicin B (**17b**) for proton H_2 is 5.04 ppm, which is more consistent with an α -sulfide, α' -sulfoxide proton such as in **41**. A simple allyl chain on the thiolane sulfoxide led to a chemical shift of 3.15 ppm for proton H_2 (**33b**, Figure 3.15), which is lower by almost two ppm units. The methyl groups or the sulfenic acid of **17b** are not likely to shift proton H_2 that much. These observations confirm our doubts about the structure proposed for garlicinins.

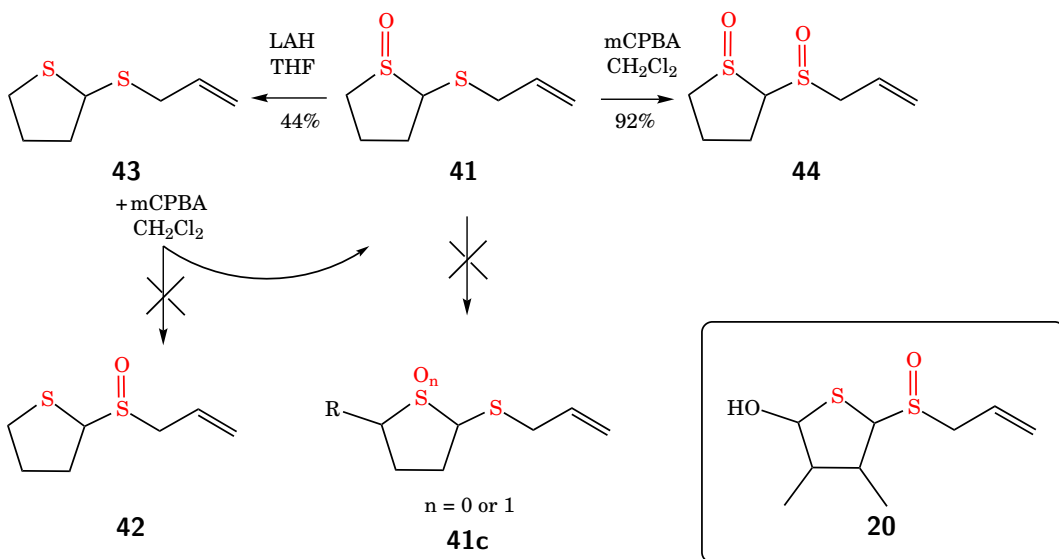


Figure 3.14: Synthesis of 2-allylthiolane sulfoxide (**41**) derivatives with different oxidation level at the sulfurs. The aim is to make **42** (which is similar to **20**, the target), but the thiolane sulfur reacts first upon oxidation to form **41** again. While not attempted, Pummerer reaction of **41** would be expected to give a geminal rather than the 2,5-disubstituted product **41c**.

By nucleophilic substitution of the chlorinated thiolane The chlorination of thiolane can be achieved by treating a CCl_4 solution of thiolane with *N*-chlorosuccinimide (NCS) (Figure 3.16).²⁵ Displacement of 2-chlorothiolane (**45**) by a nucleophile can then be carried out to obtain α -substituted thiolanes: reaction with thiourea followed by hydrolysis leads to 2-mercaptopthiolane (**46**).²⁵

We successfully synthesized **46**. The compound was then treated with Cl_2 in order to form a sulfenyl chloride (**47**), characterized by a bright red color, before treatment with allyl alcohol. The aim was the nucleophilic attack on the electrophilic sulfur by the alcohol. The sulfenate could then rearrange by the well-known Mislow-Evans rearrangement to a sulfoxide (**41**, Figure 3.17). This approach could be used even if **46** had been oxidized to the corresponding disulfide **46a**.

The success of this reaction was limited: a peak corresponding to the product was identified by DART-MS, but in a mixture with chlorinated compounds. Using chlorine gas was inconvenient, despite the color change indication. This approach was not pursued.

3.2.2 Synthesis of 3,4-dimethylthiolane

The formation of *cis*-3,4-dimethylthiolane (**48**) can be performed by displacing two leaving groups on derivatives of *meso*-2,3-dimethylsuccinic acid by sodium sulfide (Figure 3.18).²⁶ The choice of a specific

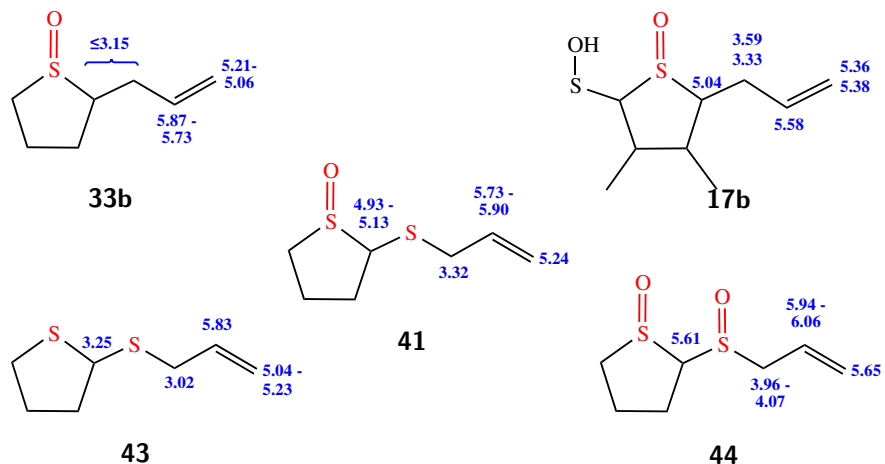


Figure 3.15: Comparison of the chemical shifts of the protons in the synthesized structures **33b** and **41** increase doubts about the correctness of the structure of garlicin B (**17b**). This figure is shown without regard to the stereochemistry.

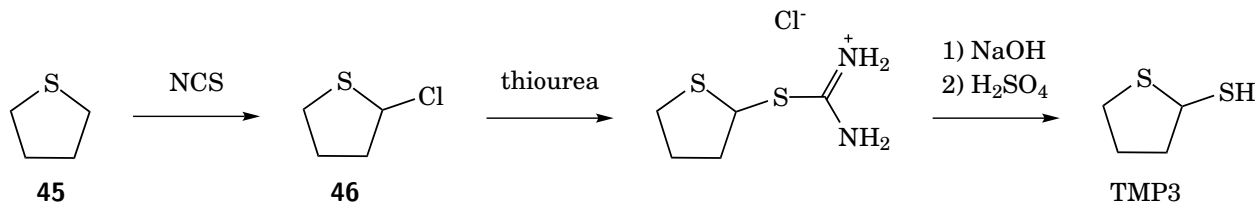


Figure 3.16: Chlorination of thiolane followed by displacement by a sulfur-containing nucleophile yields 2-mercaptopthiolane.²⁵

diastereomer of succinic acid leads to stereospecificity: *meso*-2,3-dimethylsuccinic acid (Figure 3.18) or *dl*-2,3-dimethylsuccinic acid lead to *cis*- or *trans*-3,4-dimethylthiolane, respectively. The high volatility of **48** made this compound difficult to handle, and other strategies were preferred. Oxidation of crude **48** to the corresponding sulfoxide was attempted, and this approach could be pursued to facilitate isolation.

3.3 Attempted syntheses of ajothiolane

A synthesis mimicking the proposed biosynthesis was attempted, based on the successful nucleophilic attack of the sultene **10** leading to a 2-hydroxythiolane in previous work (see Chapter 2). The sultene is obtained by rearrangement of thiosulfinate **3d**, Figure 3.19), which is formed by oxidation of bis-1-propenyl disulfide (**23**). Previous work²³ showed the importance of the stereochemistry of the two double bonds of **23** (Figure 3.19). In the chair-like transition state for the [3,3]-sigmatropic rearrangement of propenyl thiosulfinate (**3d**) to a dithial *S*-oxide (**21**), the oxygen can be in pseudoequatorial or pseudoaxial orientation. This influences the

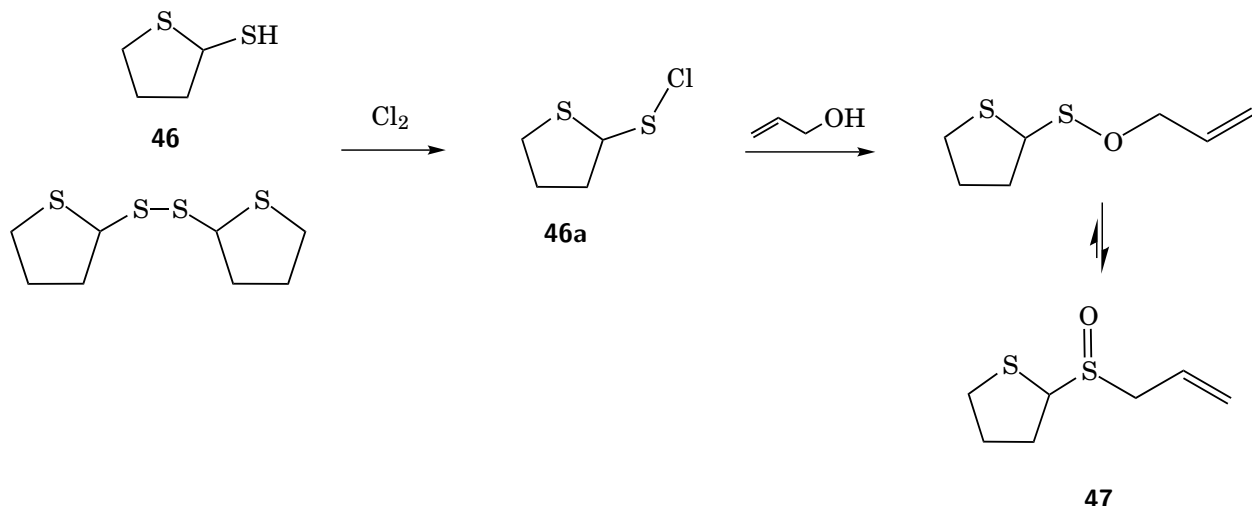


Figure 3.17: Chlorination of 2-mercaptopthiolane affords a sulfenyl chloride, which is susceptible to nucleophilic attack. Allyl alcohol was the chosen nucleophile. This approach was not successful.

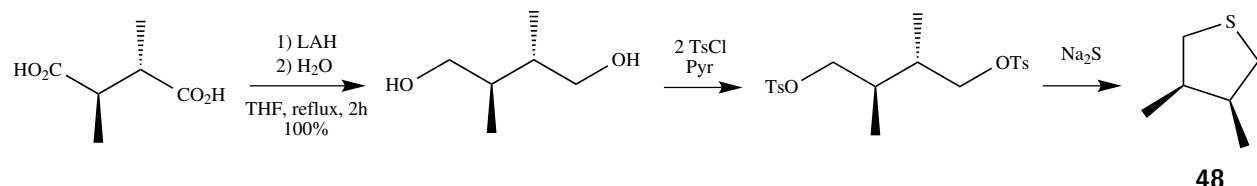
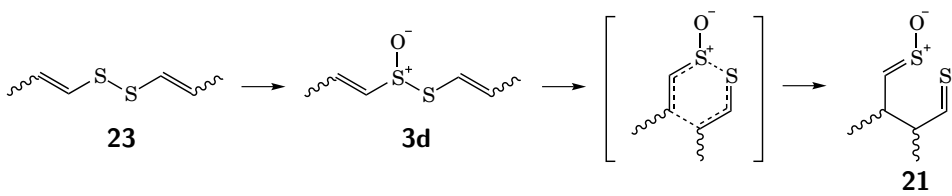


Figure 3.18: Synthesis of 3,4-dimethylthiolane.²⁶

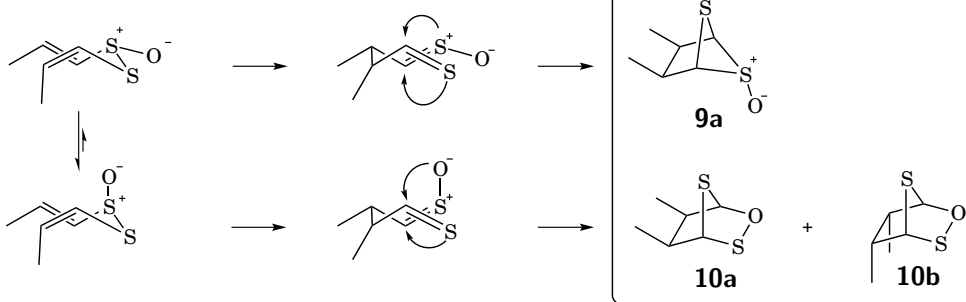
ratio between zwiebelanes (**9**) and sultenes **10**; pseudoequatorial oxygen is in the appropriate configuration to rearrange to zwiebelanes via a [2+2] process, whereas pseudoaxial oxygen leads to the formation of sultenes via 1,3-dipolar cycloaddition (Figure 3.19).

Mixed thiosulfinates (*E,Z*)- and (*Z,E*)-1-propenyl thiosulfinate rearrange to a mixture of *cis*-zwiebelane (**9a**) and *cis*-sultene (**10a** and **10b**) since both pseudoaxial and pseudoequatorial oxygens are found in the transition state. (*E,E*)-Propenyl thiosulfinate rearranges exclusively to *trans*-**10**, because the pseudoaxial orientation is highly favored. Finally, (*Z,Z*)-propenyl thiosulfinate rearranges mostly to form *trans*-zwiebelane (**9b**), likely because the steric repulsion between the oxygen in pseudoequatorial configuration and the methyl group of the thiosulfinate (*Z,Z*)-**3d** favors the other configuration (top configuration, see red arrow, Figure 3.19).

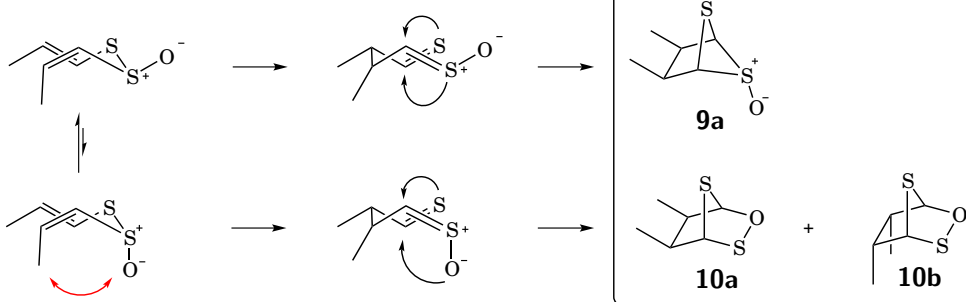
Our goal is to use stereoisomers of **10**, therefore (*E,E*)-bis-1-propenyl disulfide (**23a**) is the preferred starting material. The preparation of bis-1-propenyl disulfide (**23**) is challenging and will be described in the



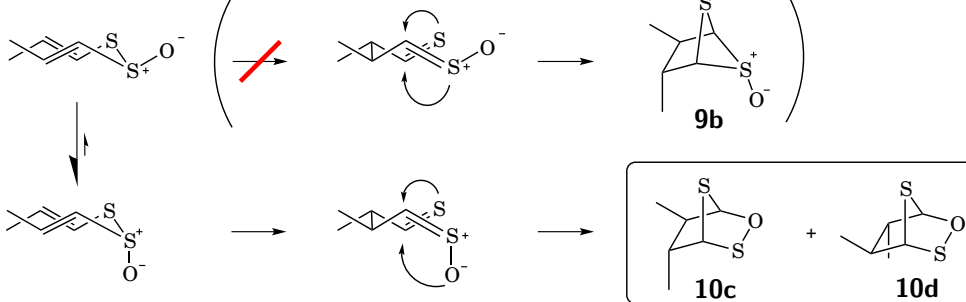
(E,Z)- **3d**



(Z,E)- **3d**



(E,E)- **3d**



(Z,Z)- **3d**

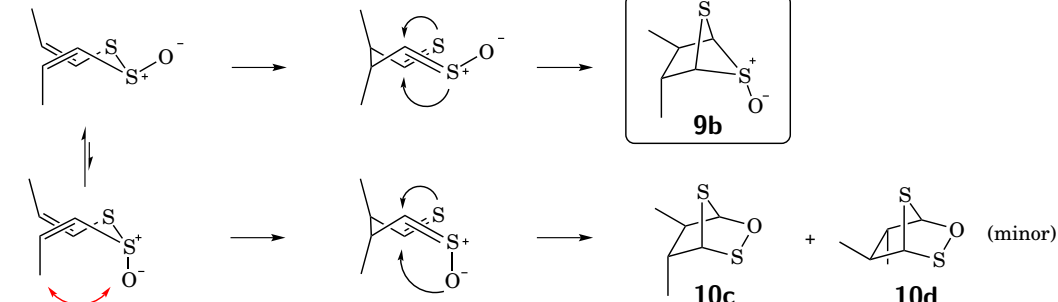


Figure 3.19: The rearrangement of *S*-(1-propenyl)-1-propene thiosulfinate (**3d**) to zwiebelanes (**9**) and/or sultenes (**10**) depends on the stereochemistry of the double bonds.²³

next section. Attempts to make ajothiolane by rearrangement of 1-propenyl thiosulfinate are then described. An alternative rearrangement of bis-1-propenyl disulfide was explored later.

3.3.1 Synthesis of bis-1-propenyl disulfide

The synthesis of **23** leads to relatively reactive intermediates and products. Bis-1-propenyl disulfide rearranges at temperatures above 60 °C - this property will be used later - and therefore cannot be distilled. It is also highly volatile and the only solvents we were able to concentrate it from are pentane and diethyl ether. These features made the synthesis challenging, and improvements were attempted.

An alkyl 1-propenyl sulfide (**49**) is first prepared by isomerization of allyl alkyl sulfide (**50**, Figure 3.20). Allyl methyl sulfide (**50a**) is commercially available; allyl propyl sulfide (**50b**) was prepared by reacting propanethiol with allyl bromide.²³ A similar procedure can be used to prepare (*E*)-**49** (Figure 3.21). Propargyl bromide is used to make propargyl propyl sulfide (**51a**), which is isomerized with sodium methoxide to **51b**. Reduction of the triple bond with lithium aluminium hydride occurred stereospecifically, leading exclusively to (*E*)-**49a**.²⁷

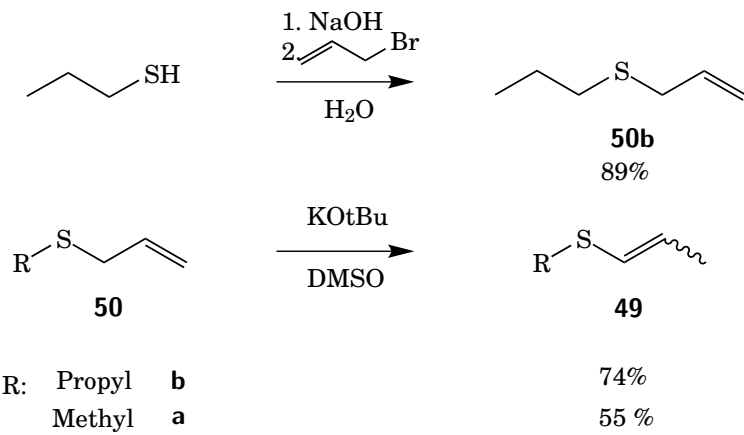


Figure 3.20: Synthesis of alkyl (*E/Z*)-propenyl sulfide (**49**). Alkyl groups: propyl (**b**) and methyl (**a**).

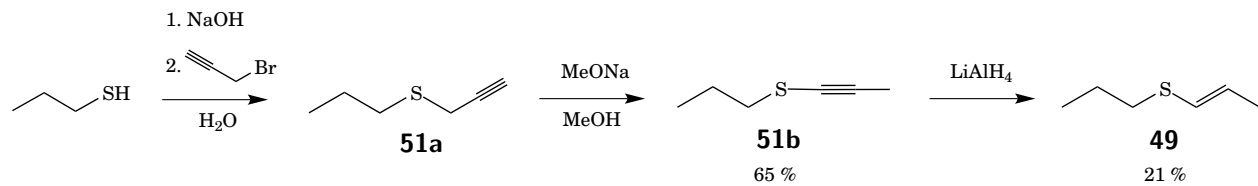


Figure 3.21: Stereospecific synthesis of (*E*)-propenyl propyl sulfide ((*E*)-**49**) with propargyl bromide.

The sulfide is converted to a thiolate (**52**) by Birch reduction; then the disulfide is formed by oxidation of the thiolate. The first step, the reduction, is performed in liquid ammonia by lithium (Figure 3.22). This reaction seemed successful as indicated by the strong thiol smell released and the discoloration of the deep-blue ammonia solution. Oxidation of the thiolate, however, was more problematic. Reagents such as iodine or methanesulfonyl chloride were employed, but they both react with ammonia. Allowing the ammonia to evaporate overnight resulted in very low yields for the bis-1-propenyl disulfide. We suspected other reactions occur when the thiolate is standing at room temperature for an extended period of time, and therefore sought an alternative for the reduction of alkyl propenyl sulfide that would not use ammonia.

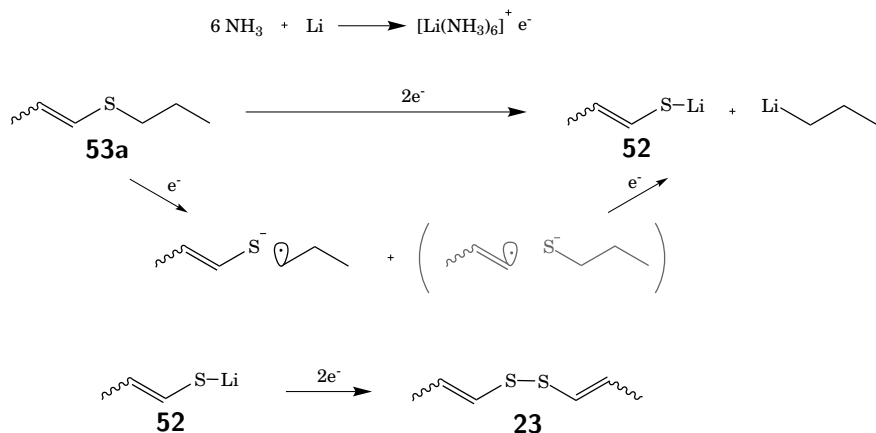


Figure 3.22: Mechanism of the reduction of 1-propenyl propyl disulfide (**49a**) by lithium in NH_3 . This mechanism is similar to that of the Birch reduction.^{23,27}

Two options are proposed in the literature to replace ammonia in the Birch reduction: using another amine,²⁸ or an aromatic electron carrier.^{29–31} The second option seemed promising, especially since the aromatic electron carrier can be added only in catalytic amount (Figure 3.23). The reaction was performed in THF with 4,4'-di-*tert*-butylbiphenyl (DBB, **54**) as electron carrier. Sonication is required to help dissolve the lithium. Addition of sulfide discolored the turquoise solution, and oxidation of 1-propenyl thiolate (**52**) was achieved easily with iodine. Nonetheless, two major problems were encountered. When an equimolar amount of DBB is used, the purification of **23** from **54** is extremely tedious. If a catalytic amount was used instead, the separation was feasible, but the regiospecificity of the reaction was low, leading to as much propyl thiolate as propenyl thiolate. The mixture of disulfides produced was also hard to separate. Despite a promising start, this approach did not facilitate the production of **23**. Other aromatic electron carriers could be explored in future work, however syntheses were carried out in ammonia for the rest of this project.

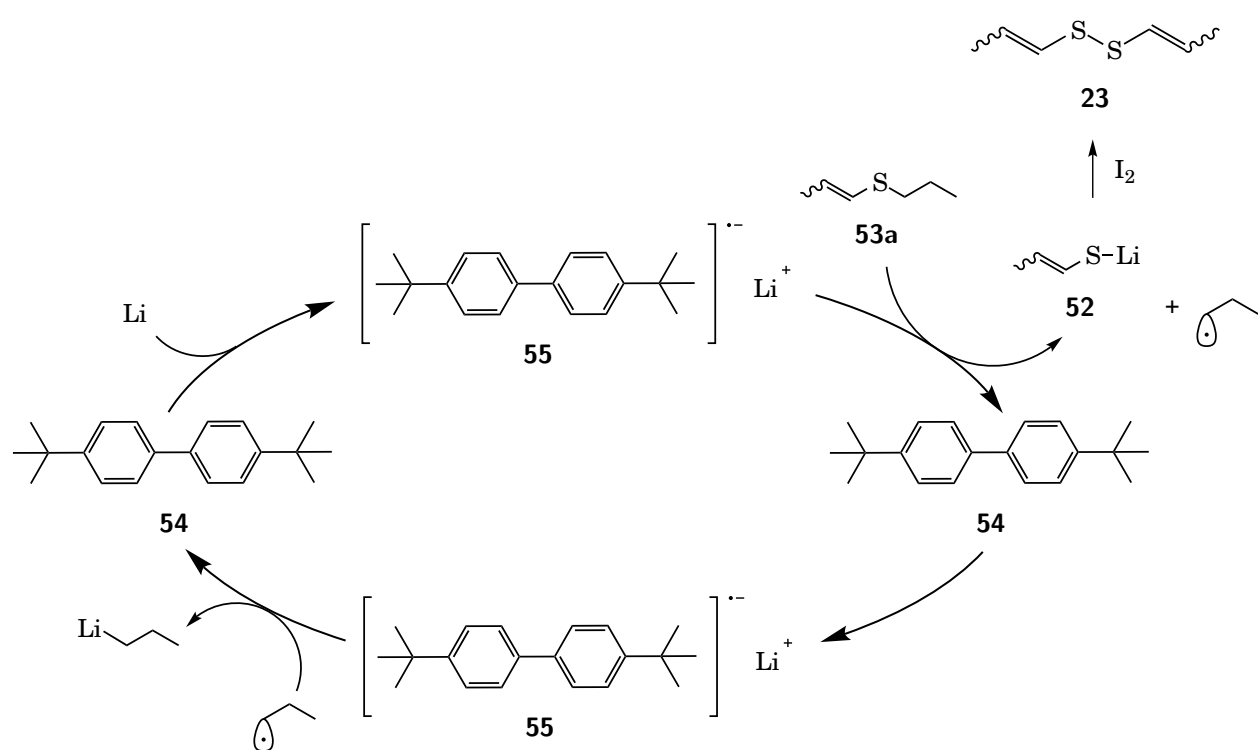


Figure 3.23: Ammonia-free synthesis of bis-1-propenyl disulfide (**23**) in THF. This procedure, inspired by the work of Cohen's research group,^{30,32,33} is safer than the Birch reduction used in previous work (Figure 3.22).^{23,27} However, the regiospecificity is lower (more propyl thiolate is formed) and the purification of **23** from the aromatic electron carrier is too tedious.

The conversion of thiolate **52** into bis-1-propenyl disulfide was attempted with methanesulfonyl chloride and iodine (Figure 3.24). Both reagents could react with ammonia or lithium amide to form hazardous product. The syntheses were performed at low temperature under vigorous stirring. Iodine provided the highest yield (40%). The low yield can possibly be explained by the formation of by-products with iodine. Despite low yields, this procedure was the best option to prepare **23**. A mixture of **23a**, **23b** and **23c** was formed in a 1:2:1 ratio.

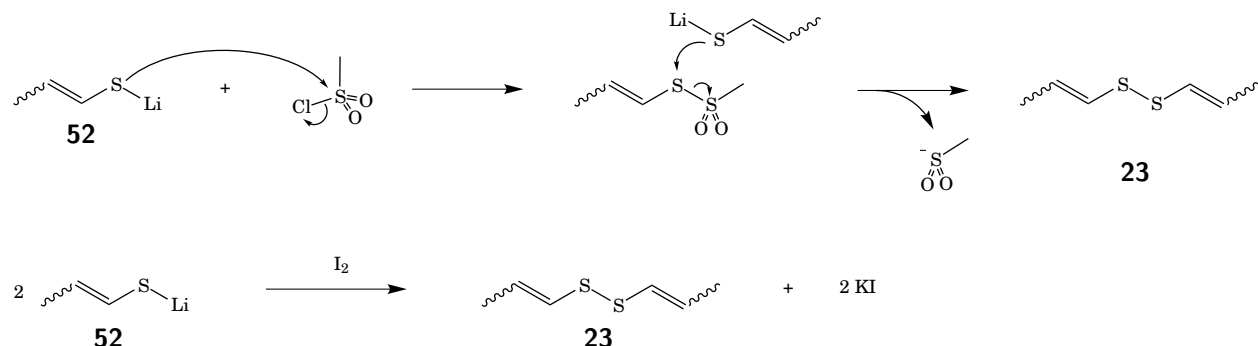


Figure 3.24: Compound **52** is converted by methanesulfonyl chloride (top) or iodine (bottom) to bis-1-propenyl disulfide (**23**). The iodine procedure was preferred for its higher yield.

Our primary interest is (*E,E*)-bis-1-propenyl disulfide. Treating pure (*E*)-**49a** with lithium in ammonia led to isomerization of about 20% of the double bonds, and did not give pure (*E,E*)-**23**. Purification of the mixture of stereoisomers on silica gel by pentane led to fractions enriched in one of the stereoisomer, but not pure compounds. The isomerization of the (*Z*)-double bonds by catalytic iodine was attempted but led to loss of the material. The typical smell of the disulfide was replaced by a sweet, foul odor similar to the smell of the crude oxidation products by iodine.

3.3.2 Synthesis of ajothiolane by oxidation of bis-1-propenyl disulfide

In previous work, Naganathan (working in the Block group) treated a bicyclic sultene obtained by oxidation of bis-1-propenyl disulfide with thiophenol.^{23,27} Among the products, 2-hydroxy-3,4-dimethyl-5-(phenyldisulfanyl)thiolane (**22**, Figure 3.25) was isolated. The acidic conditions could have activated the sultene (oxygen protonated). Stereospecificity was expected, since the opening of the sultene ring implies that the oxygen and sulfur on the thiolane are *cis* to each other, however, *trans* product was also recovered. Additionally, basic conditions can explain the conversion to the other stereoisomer (Figure 3.26).

The same reasoning could be applied to prepare ajothiolane in a partially stereocontrolled fashion (Figure 3.25). The nucleophile would have to be allyl alcohol, and the sulfenate would rearrange to the sulfoxide (Mislow-Evans rearrangement).

Despite numerous attempts, ajothiolanes have yet to be isolated from the mixture. Three oxidizing agents were tested: *m*CPBA, dimethyldioxirane and peracetic acid. Low temperature NMR allows us to follow the formation of sultenes (**10**), in which the temperature is critical. Addition of allyl alcohol, however, did not lead to a sufficient amount of product. A peak corresponding to the formula of ajothiolane was present in the mass spectrum, but only as traces, and the product could not be isolated. The same by-products as in Naganathan's work were present, namely bis-1-propenyl disulfide (**23**) and 1-(prop-1-en-1-yl)-2-((prop-1-en-1-yl)sulfinyl)propyl disulfane (**56**, Figure 3.27). A more powerful nucleophile, allyl Grignard, was also employed. The product would then have been deoxyajothiolane (**57**, Figure 3.27). Allyl Grignard reacted with *meta*-chlorobenzoic acid. When excess allyl Grignard was used to overcome this problem, compounds with multiple allyl groups were formed (according to the mass spectrum). Washing the mixture with aqueous NaHCO_3 to isolate the intermediates is not ideal, although done for NMR analysis: the liquid-liquid extraction exposes the sample to water, which is an issue for the subsequent Grignard reagent addition. Exposure to room temperature during the extraction also leads to decomposition of the sultene. Longer drying would result in more decomposition.

3.3.3 Synthesis of ajothiolane by heating bis-1-propenyl disulfide

Another approach was proposed to make ajothiolane. Heating bis-1-propenyl disulfide promotes a thio-Claisen rearrangement to 3,4-dimethyl-2,3-dihydrothiophene-2-thiol (**58**). Addition of H_2O to the double bond could lead to the anti-Markovnikov product, the secondary carbocation being stabilized by the adjacent sulfide, but an interesting hydroboration of vinyl sulfides reported³⁴ was used instead. Prior to any treatment, the thiol needed to be protected. Oxidation to the disulfide **59** was achieved by deprotonation with *n*-BuLi then oxidation with I_2 in 54% yield. Unfortunately, the hydroboration did not proceed as expected so this approach was abandoned.

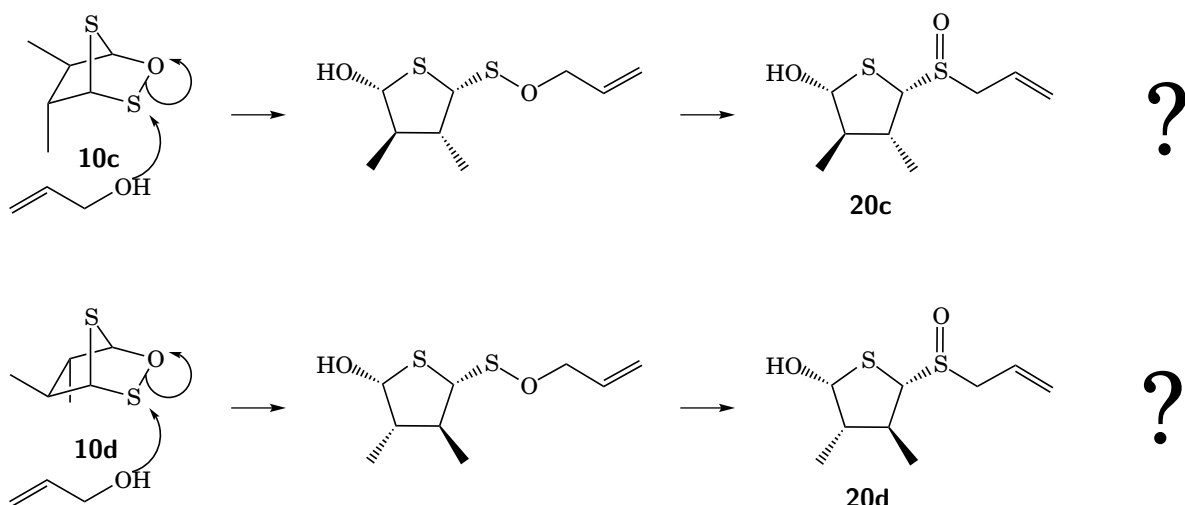
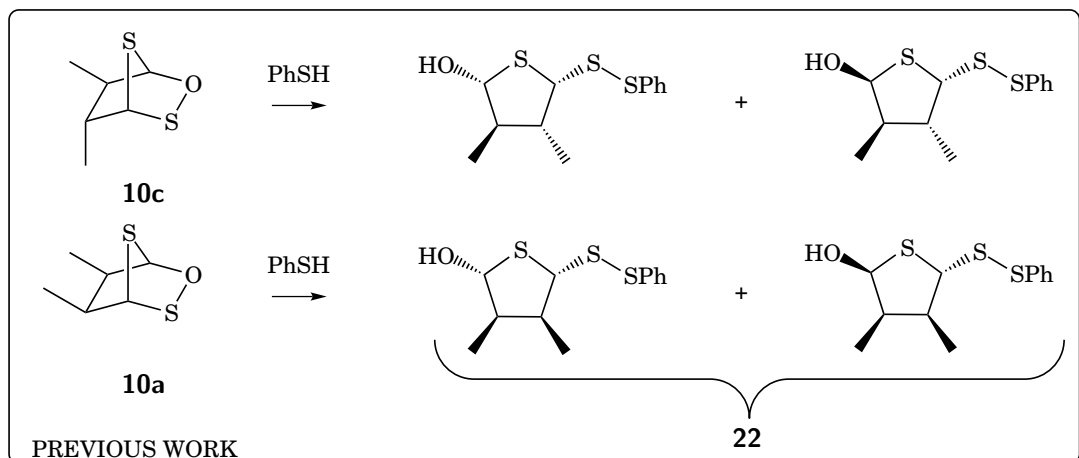
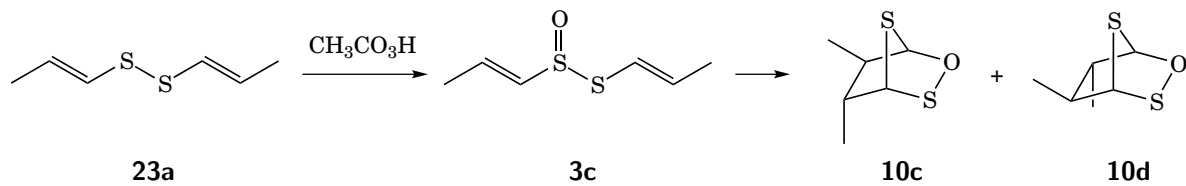


Figure 3.25: Proposed synthesis of two stereochemically pure ajothiolanes (**20c** and **20d**) from bis-1-propenyl disulfide (**23a**) based on previous syntheses of phenyl derivative **22**.²³

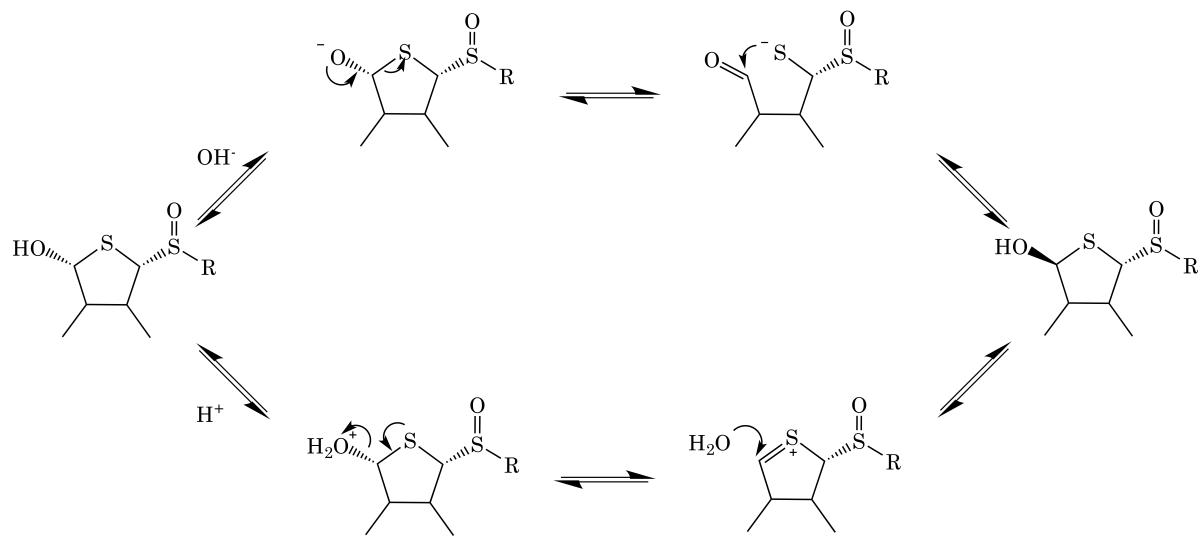


Figure 3.26: Isomerization of ajothiolanes under basic (top) and acidic conditions (bottom).

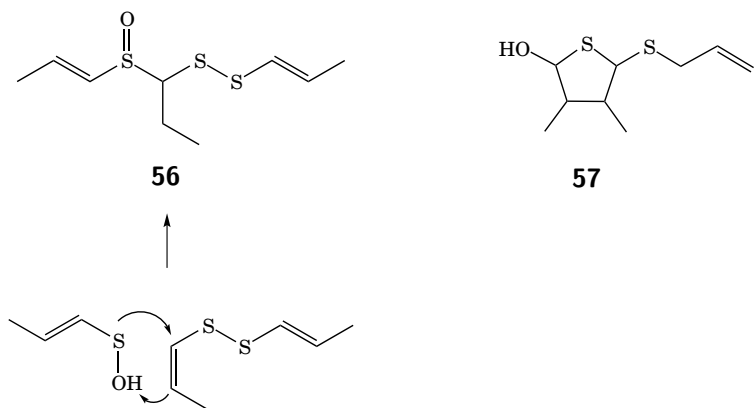


Figure 3.27: Structures of the by-product **56** of the oxidation of bis-1-propenyl disulfide, likely formed by addition of 1-propenesulfenic acid to **23**; and deoxyajothiolane (**57**) which would be obtained if the bicyclic compound were treated with allyl Grignard as a nucleophile.

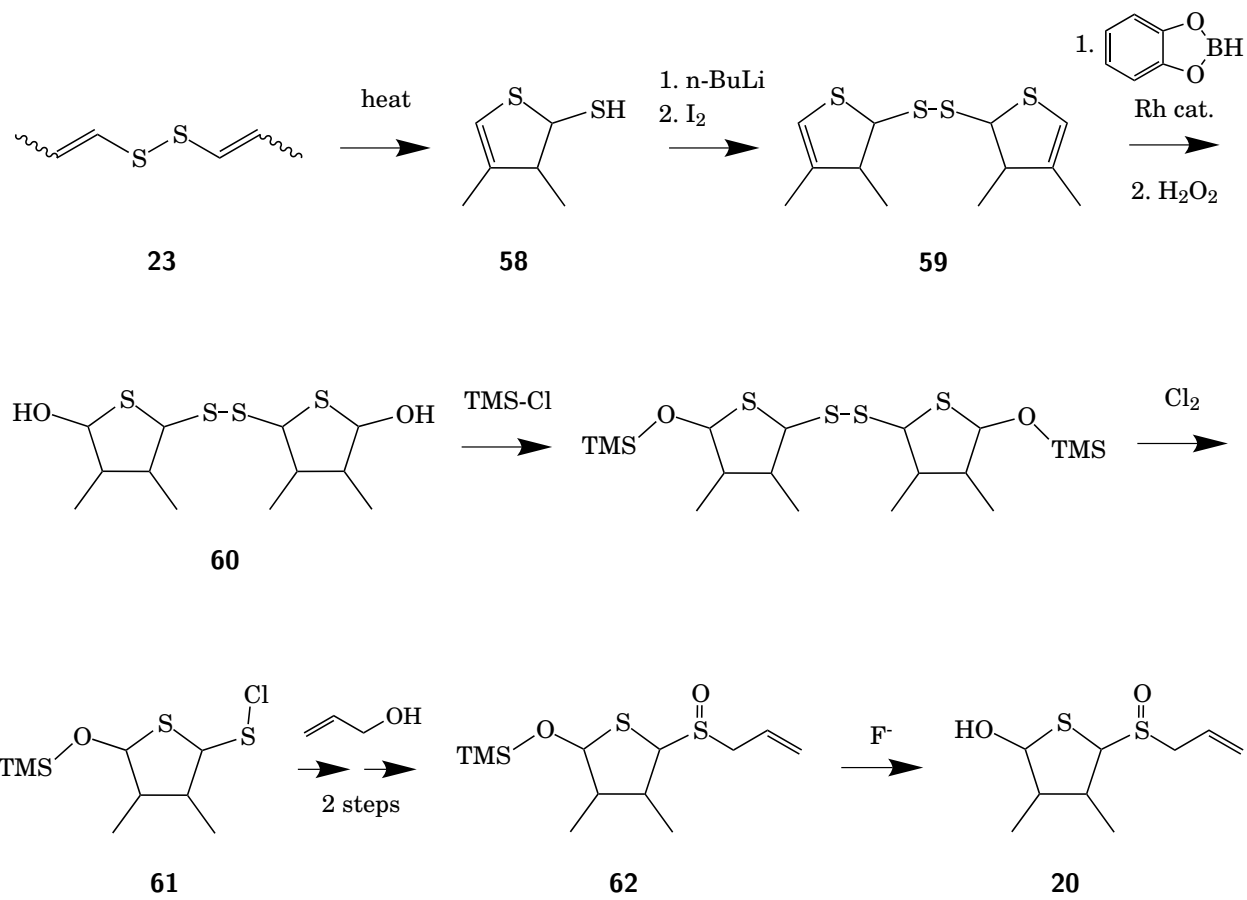


Figure 3.28: Proposed synthesis of ajothiolanes from bis-1-propenyl disulfide (**23**), heated to promote the thio-Claisen rearrangement to a thiol **58**. The latter was then oxidized to the disulfide **59**. Hydroboration of **59** was unsuccessful.

3.3.4 Ideas for future work

A few ideas emerged after summarizing these syntheses. They are represented in gray on the following figures. 2-Chlorothiolane could be treated with a thioacetate, then chlorine gas in acetic acid. Addition of allyl Grignard would then lead to 2-allylsulfinylthiolane (Figure 3.29).

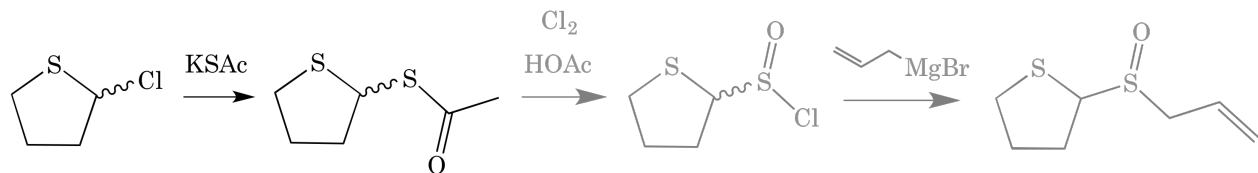


Figure 3.29: Ideas for future work: treatment of 2-thioacetoxythiolane with chlorine to form a sulfinyl chloride.

The product of the second Pummerer reaction (see section 3.2.1) could not be isolated, but was seen by GC-MS. Trapping the reactive intermediate with a thiolate would lead to a potentially useful compound (Figure 3.30).

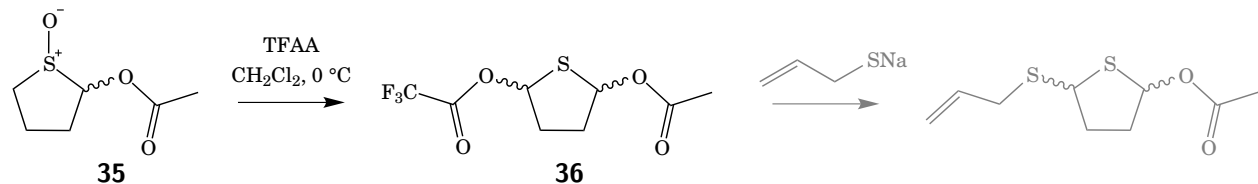


Figure 3.30: Ideas for future work: trap the short-life double Pummerer product **36**.

Other ways could also be investigated, such as a simpler hydration of compound **58**.

3.4 Synthesis of methylisoajoene

An attempted synthesis of methylisoajoene (**8**) involved four steps. Commercially available allyl methyl sulfide (**50a**) was oxidized by H_2O_2 to the sulfoxide **63**. Two different brominations have been tested: the radical path with NBS shown in blue, and the ionic path with Br_2 shown in red in Figure 3.31. The radical mechanism favors the 2-bromo-1-propenyl product **64** by allylic rearrangement. The bromination with bromine leads to a vicinal dibromide (**65**), which requires an elimination step to form monobrominated **64**. The protons on C_1 are more acidic and elimination should be regiospecific. The proposed path included nucleophilic attack by 2-propenethiol to form the product **8**.

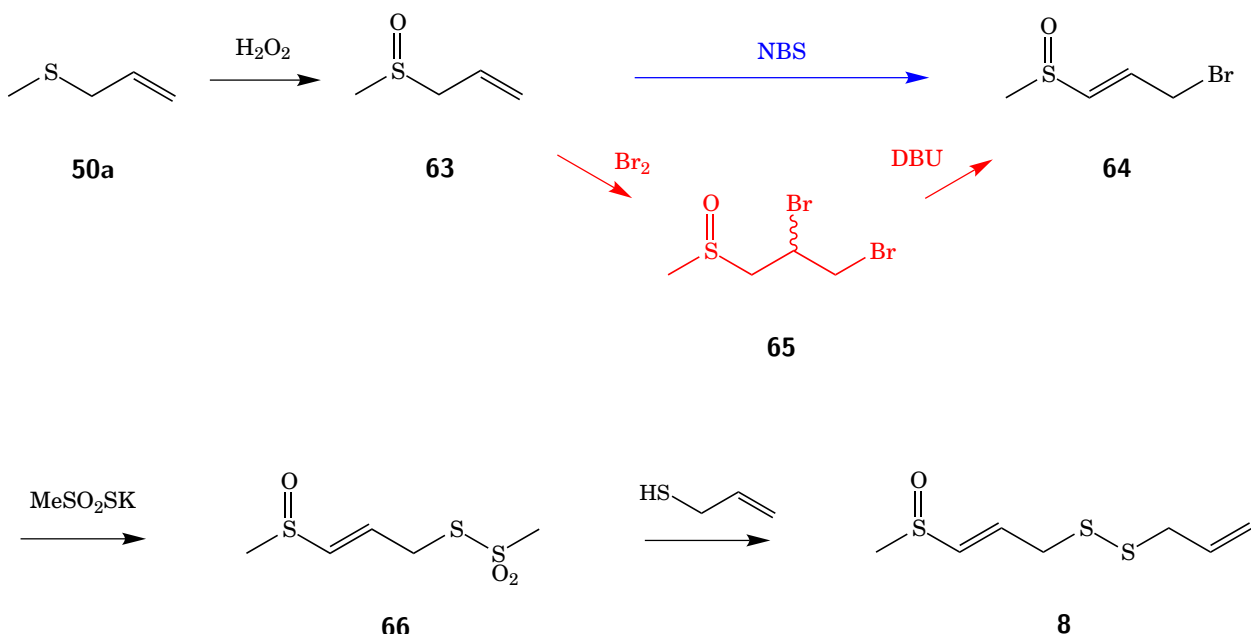


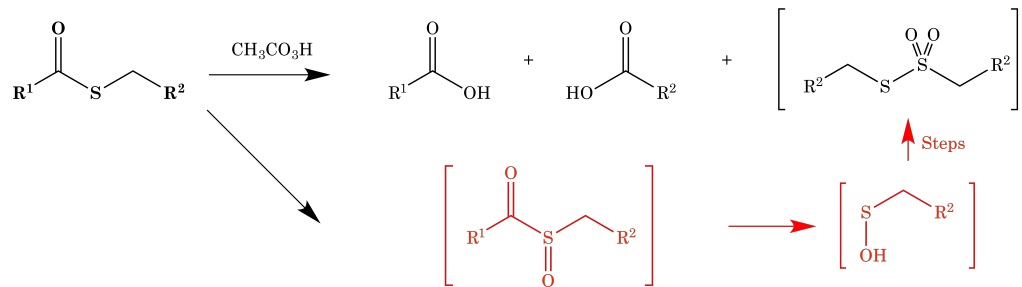
Figure 3.31: Proposed synthesis of methylisoajoene (8).

3.5 Thiolactone sulfoxides

3.5.1 Literature review

An attempt to synthesize α -keto sulfoxide was made in 1949 by oxidizing thioesters with peracetic or perbenzoic acids. Four thioesters were oxidized under different conditions, and none led to the target, but to acid degradation products (Figure 3.32, top).³⁵ Proposed intermediates for the oxidation of aromatic thioesters suggest the formation and rearrangement of an α -keto sulfoxide. A thiosulfonate was found as an intermediate in the oxidation of aliphatic thioesters, possibly formed in several steps from a sulfenic acid produced by the hydrolysis of a thiolactone sulfoxide (Figure 3.32, red). In a paper by Kumamoto *et al.* in 1968,³⁶ the synthesis of esters by oxidizing a thiolactone in the presence of an alcohol suggested the existence of a thiolactone sulfoxide (or α -keto sulfoxides) as the oxidized intermediate. The same reaction was successfully carried on to various thiolactones, and various alcohols were used for the hydrolysis (Figure 3.32, bottom). The oxidation was performed with a mixture of *N*-bromosuccinimide (NBS) and an alcohol or with iodosobenzene (peracids or KMnO_4 as oxidants lead to the formation of carboxylic acids). The NBS procedure is adapted from the oxidation of sulfides to sulfoxides in water by NBS.³⁷

Attempts by Cavallito et al. (1949)



Attempts by Kumamoto et al. (1968)

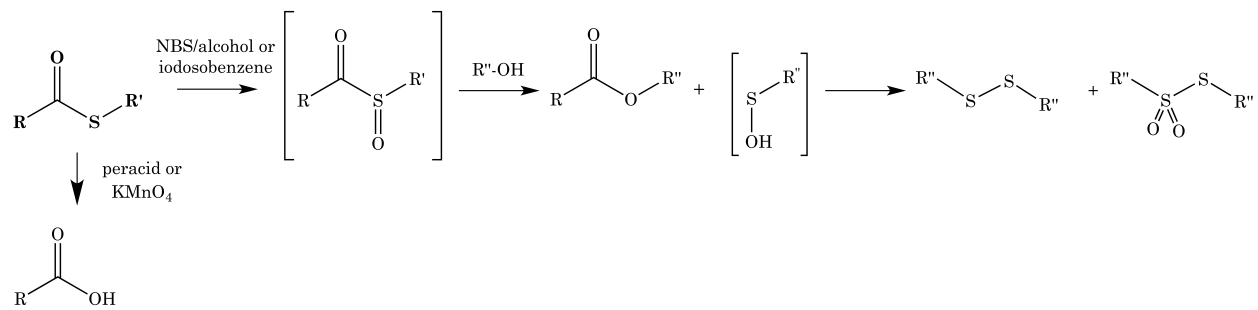


Figure 3.32: Attempts to synthesize thiolactone sulfoxides by Cavallito et al.³⁵ and Kumamoto et al.³⁶

The thiolactone sulfoxide could not be isolated (the reaction with a second equivalent of alcohol directly led to the formation of an ester and presumably a sulfenic acid) but it was identified by a strong sulfoxide band appearing on the IR spectrum at 1180 cm^{-1} during the reaction. This wavenumber is uncommon for sulfoxide bands, generally found in the $1070\text{-}1030\text{ cm}^{-1}$ region.³⁸ Other effects could be involved, but the unusual published value needs to be kept in mind.

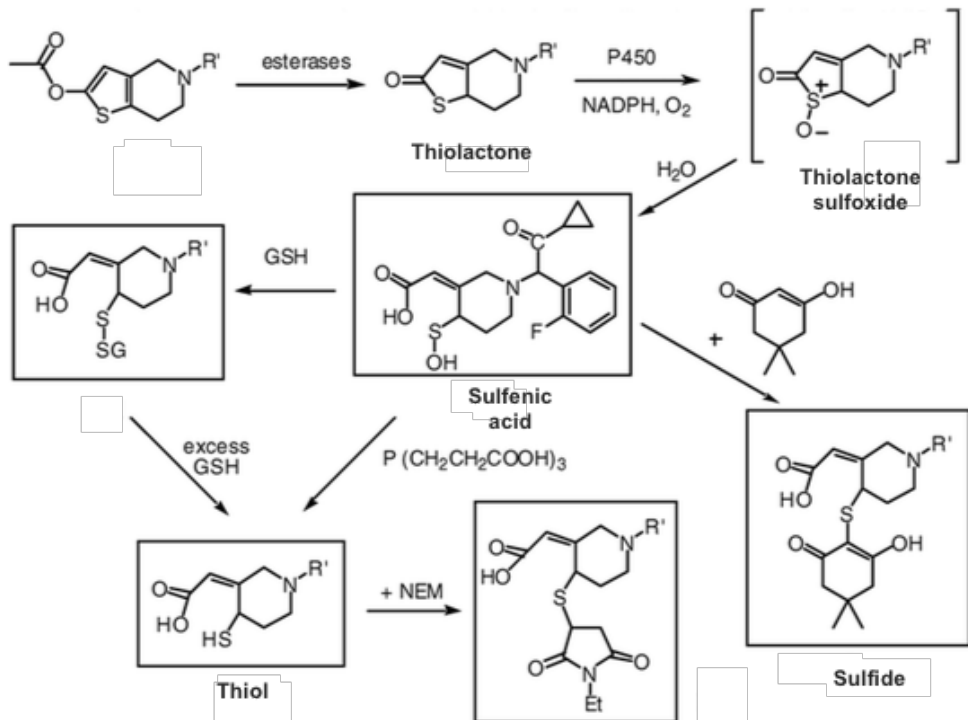


Figure 3.33: Thiolactone sulfoxides react very quickly to form a sulfenic acid in the metabolism of the prodrug Prasugrel[©]. Adapted from Dansette *et al.*³⁹

The unlikelihood of isolating thiolactone sulfoxides because of their reactivity was confirmed by the work of Dansette and co-workers³⁹ on the metabolism of a prodrug, Prasugrel[©]. The enzymatic oxidation of a cyclic, five-member thiolactone led to ring opening and presumed formation of a sulfenic acid and a carboxylic acid (Figure 3.33). The intermediate is, again, a thiolactone sulfoxide that is immediately hydrolyzed. The sulfenic acid itself is quickly reduced in the presence of a nucleophile (S-, P- or C-nucleophiles). This reactivity will be discussed in the next section.

Later, the same group established the presence of the thiolactone sulfoxide intermediate by trapping it using a nucleophile (Figure 3.34⁴⁰). Simultaneously, another group had identified a thiolactone sulfoxide as the intermediate in 2-oxo-clopidogrel metabolism (also presented in Figure 3.34).⁴¹

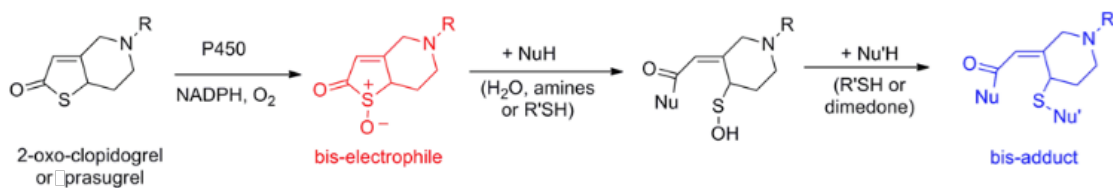


Figure 3.34: Proof of the presence of a thiolactone sulfoxide intermediate by nucleophilic trapping in the metabolism of Prasugrel. From Dansette *et al.*⁴⁰

To our knowledge, only one publication mentions an isolated thiolactone sulfoxide. This entry is also the only recorded α -keto sulfoxide. The oxidation of *N*-acetylhomocysteine thiolactone by periodate was studied for kinetic purposes. Their focus is the disappearance of periodate. The claim that thiolactone sulfoxide is not hydrolyzed (in aqueous solution) by this paper⁴² is however questionable, since the compound was only characterized by MS in negative mode. Our experiments will show that $[M+O]^-$ and $[M+O_2]^-$ are adducts of a thiolactone by DART-MS in negative mode. Therefore, the presence of a thiolactone sulfoxide was likely assumed from an artifact of the mass spectrum.

The plausibility of the isolation of a thiolactone sulfoxide after treatment by a protic solvent like methanol (such as described by Nohara *et al.* in the extraction of garlicin K⁷) is questionable, even unlikely according to three different research groups. The oxidation of a simple cyclic thiolactone, γ -thiobutyrolactone, should be easy to follow by IR or NMR and give a good indication of the likelihood of the persistence of such compounds.

3.5.2 Attempts to synthesize a thiolactone sulfoxide

γ -Thiobutyrolactone (**67**) was synthesized by condensing γ -mecaptobutyric acid (**68**), itself produced by treating γ -butyrolactone (**69**) with a nucleophilic sulfur donor under acidic conditions (Figure 3.35).⁴³

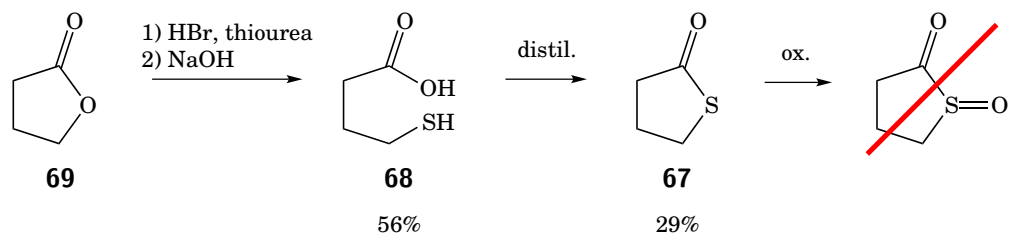


Figure 3.35: Synthesis of γ -thiobutyrolactone (**67**) from γ -butyrolactone (**69**).

Oxidation experiments have been conducted on **67** in organic and aqueous media, with different oxidizing agents. Sodium periodate was used at 0 °C in aqueous and acetone/H₂O, and *m*CPBA in CDCl₃. Both experiments were monitored closely by DART-MS. No oxidation product was seen even for a tenth of a second, but the starting material is consumed by the reaction. Low temperature NMR was used at -40 °C with a *m*CPBA/CDCl₃ system. A precipitate, possibly a polymer is formed in chloroform, but once again, the starting material disappears and no peaks corresponding to a thiolactone sulfoxide appear, confirming the unlikelihood of the formation of this type of compounds, let alone the isolation thereof.

In conclusion, the proposed structure of garlicin K (**17c**) is deemed unlikely, since even the simplest thiobutyrolactone sulfoxide could not be isolated. No compound with the formula of garlicin K has been identified in our garlic extract from the previous chapter, precluding spectroscopic experiments as in the case of ajothiolane. The absence of this metabolite in the extracts likely occurred because our extraction time was significantly shorter, our primary goal being to work on ajothiolane. We suggest that the compound with formula C₉H₁₄O₂S is formed later when the extract is standing. Based on the spectroscopic data provided as well as our knowledge of thiolanes in *Allium* chemistry, we suggest the structure 5-(allyloxy)-3,4-dimethyldihydrothiophen-2(3H)-one (**70**, Figure 3.36). This compound has heteroatoms on C₂ and C₅. The proposed thiolactone could be an oxidation product of a 2-hydroxythiolane formed in aged garlic extract.

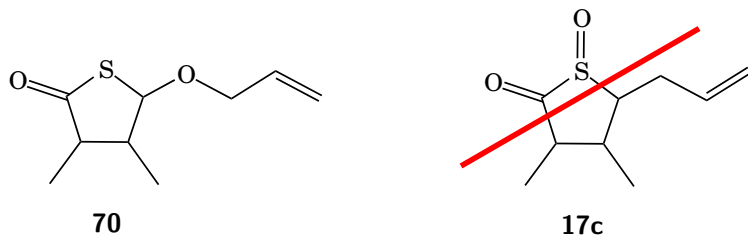


Figure 3.36: Alternative structure for compound C₉H₁₄O₂S. The structure of garlicin K (**17c**) is considered to be implausible.

3.6 Conclusions

The research project was initiated by publications on thiolanes extracted from alliums both by Aoyagi's group² and by Nohara's group.^{3-7,44,45} Some of the structures proposed by Nohara's group were problematic for two reasons: the biosynthesis was inconsistent with garlic and onion building blocks, and some functional groups reported were known to be too reactive to be isolated (sulfenic acid, thiolactone sulfoxide). Some of

these papers contain structures we believe are incorrect; unfortunately, they are now being cited in the literature^{46–48} and in literature reviews.^{49,50} It was therefore important to tackle the issue. Typically, a structure is proposed based on the spectroscopic data of the natural product, then the identity of the compound is confirmed by synthesis.

The extraction was challenging because the target compounds were minor components in the garlic extracts. Only a few milligrams were isolated from several kilograms of fresh garlic. Because of this, extreme care was required when handling the samples. All solvents needed to be distilled, and contact with rubber or plastic strictly avoided, since plasticizers can leach out. A small amount of impurities in the solvents would ultimately be concentrated and impact strongly the few milligrams of product recovered.

We faced a second challenge once the compound had been isolated. Structure assignment based on the traditional techniques were ambiguous. The position of the heteroatoms and the oxidation level of each individual sulfur atom was impossible to determine based on ¹H, ¹³C, HSQC and HMBC NMR, MS and IR. INADEQUATE NMR was therefore employed and corroborated the structure of ajothiolane, which we had suggested based on the biosynthesis.

The next step was the synthesis of the compound to prove its identity. Despite promising ideas, our attempts to synthesize ajothiolane remained unsuccessful. The compounds we have been working on are of low molecular weight and may appear simple at first glance, but their chemistry is not trivial. The two substituents on position 2 and 5 are both chalcogens and therefore present similar reactivity toward nucleophiles. The hemithioacetal easily opens up under basic conditions. Selective functionalization of the thiolane core turned out to be very challenging. We were only able to prepare analogues to prove the structure. Attempted derivatization did not work. We then tried to modify the natural product and remove one stereocenter by selectively oxidizing the sulfoxide of ajothiolane to the sulfone. Tentative results indicate that both a sulfur and the hydroxyl were oxidized under these conditions, but the characterization of the products was incomplete.

If the synthesis of analogues, INADEQUATE NMR and comparison of the spectral data with previously published molecules are good indications to prove the structure of ajothiolane, a total synthesis would have concluded this project. Future work could include some of the ideas proposed above.

Our lack of success in the synthesis should not overshadow our contribution to the field of garlic chemistry. Two of the structures proposed by Nohara's group (garlicnin B and garlicnin K) have been invalidated, and we recommend caution with respect to accepting the structures proposed for several of the other compounds,

especially the thiolanes. Thiolanes are confirmed as compounds found in garlic extracts, and their origin can be traced back to *S*-1-propenyl cysteine sulfoxide (**1c**). The general scheme presented in the introduction (Chapter 1) can therefore be completed as presented in Figure 3.37. This demanding project underscores the reactivity of low molecular weight organosulfur compounds and the richness of garlic-related chemistry.

3.7 Experimental

NMR spectra were recorded in CDCl_3 , unless otherwise indicated, on a Bruker 400 UltrashieldTM, operating at 400 MHz for proton and 100 MHz for carbon. The chemical shifts (δ) are indicated in ppm downfield from tetramethylsilane, with the internal standard being the residual CHCl_3 (7.27 ppm). Infrared spectra of the neat compounds were recorded on a Perkin Elmer UATR 2 FTIR. Mass spectra were obtained using the Hewlett Packard 6890 GC and a 5972A selective mass detector. A DART-AccuTOF mass spectrometer operating in positive or negative ion mode was employed with a polyethylene glycol (average molecular weight 600) spectrum a reference standard for exact mass measurements. The atmospheric pressure interface was typically operated at the following potentials: orifice 1 = 15 V; orifice 2 = 5 V; ring lens = 3 V. The RF ion guide voltage was generally set to 800 V to allow detection of ions greater than m/z 80. The DART ion source was operated with helium gas at 200°C, and a grid voltage = 530. Diethyl ether and THF were distilled from sodium-benzophenone ketyl. Ethyl acetate was purchased from Pharmaco-Aaper and used without further purification. Throughout the study 100% *m*CPBA was employed. The reagent was obtained by washing a dichloromethane solution of the commercial sample, purchased from Sigma-Aldrich as a 70% mixture with *m*-chloroperbenzoic acid (*m*CPBA), with pH 7.5 phosphate buffer followed by drying and evaporation of the solvent. The drying agent employed was anhydrous magnesium sulfate unless indicated otherwise. Analytical TLC was performed on precoated silica gel plates (Merck) with a 254 nm fluorescent indicator and was visualized under a UV lamp and by staining with a KMnO_4 solution.

2-Methylthiolane sulfoxide (33a). To a THF solution (15 mL) of thiolane sulfoxide (0.5 mL, 5.6 mmol) at -80 °C under argon are added 2.5 mL of a *n*-butyllithium (*n*-BuLi) solution in hexane (2.5 M, 6.25 mmol). After 30 min of stirring at low temperature, the mixture is stirred at RT for 30 min then cooled down again. Methyl iodide (0.4 mL, 6.25 mmol) is added at - 80 °C, and the mixture is stirred at this temperature for 30 min. After dilution in EtOAc , the mixture is washed with NH_4Cl (aq sat), then brine, the organic layer is dried and concentrated under vacuum. GC-MS indicates the presence of the desired product together with

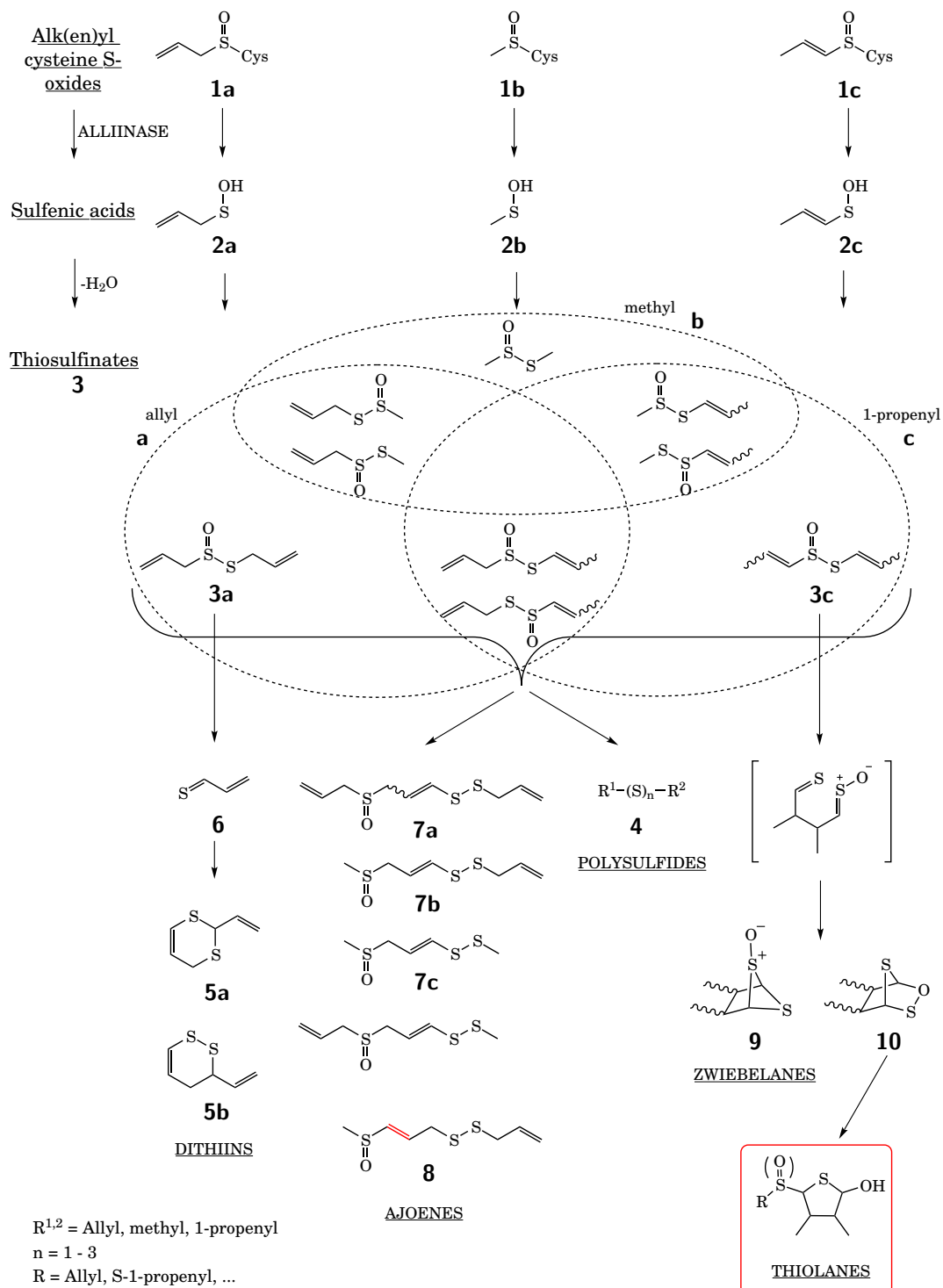


Figure 3.37: A new class of compounds derived from isoalliin (**1c**) was found in garlic extracts. They are characterized by a thiolane core substituted with a hydroxyl, two methyl groups and a sulfur in positions 2, 3, 4 and 5, respectively. The sulfur in position 5 can be oxidized, and two R chains have been reported so far: allyl in ajothiolane (**20**) and S-1-propenyl in cepathiolane (**19**).

starting material and dimethylthiolane sulfoxide. Chromatography on silica gel with a mixture of EtOAc and methanol (98:2) affords 90 mg of a light yellow liquid (yield = 14%). The yield could be improved by a second purification, two products being co-eluted during chromatography. NMR indicates the presence of one stereoisomer (about 20% of the main product). The by-product, 2,2-dimethylthiolane sulfoxide, is also isolated as 30 mg of a colorless liquid (yield = 4%). Sulfoxides are highly soluble in water; the aqueous layer could be reextracted to improve the yield. *Isomer 1 (80%)*: ^1H NMR (400 MHz, CDCl_3) δ 3.22–3.10 (m, 1H), 2.87–2.76 (m, 1H), 2.76–2.61 (m, 1H), 2.40 (ddd, J = 17.0, 11.1, 6.9 Hz, 1H), 2.22–2.06 (m, 2H), 1.97–1.82 (m, 1H), 1.42 (d, J = 6.9 Hz, 3H) ppm. *Isomer 2 (20%)*: ^1H NMR (400 MHz, CDCl_3) δ 3.06 (dd, J = 14.8, 7.4 Hz, 1H), 2.94–2.87 (m, 1H), 2.57 (td, J = 13.0, 6.7 Hz, 1H), 2.50–2.44 (m, 1H), 1.79–1.69 (m, 1H), 1.64 (dt, J = 19.3, 6.5 Hz, 2H), 1.38 (d, J = 6.9 Hz, 3H) ppm.

2-Allylthiolane sulfoxide (33b). To a THF solution (20 mL) of thiolane sulfoxide (0.47 mL, 4.8 mmol) at -80 °C under argon are added 2.2 mL of a *n*-BuLi solution in hexane (2.5 M, 5.5 mmol). After 30 min of stirring at low temperature, the mixture is stirred at RT for 30 min then cooled down again. Allyl bromide (5 mL, 51 mmol) is added at -80 °C, and the mixture is stirred at this temperature for 30 min. After dilution in CH_2Cl_2 , the mixture is washed with NH_4Cl (aq sat), then brine, and the organic layer is dried and concentrated under vacuum, yielding 420 mg of crude product. GC-MS indicates the presence of the desired product together with starting material and 2,2-diallylthiolane sulfoxide. Column chromatography on silica gel with a mixture of EtOAc and methanol (95:5) affords 130 mg of a light yellow liquid (yield = 19%). The yield could have been improved by a second purification because two products are being co-eluted during chromatography. Both NMR and GC-MS indicate the presence of a second stereoisomer (about 10% of the main product). The by-product is isolated as 110 mg of a yellow liquid (yield = 12%) and identified as 2,2-diallylthiolane sulfoxide. Sulfoxides are highly soluble in water, the aqueous layer could be reextracted to improve the yield. *2-Allylthiolane sulfoxide, stereoisomer 1*: ^1H NMR (400 MHz, CDCl_3) δ 5.87–5.73 (m, 1H), 5.21–5.06 (m, 2H), 3.15–3.03 (m, 1H), 2.95–2.85 (m, 1H), 2.76 (ddd, J = 14.2, 9.4, 7.3 Hz, 1H), 2.54–2.35 (m, 3H), 2.29–2.19 (m, 1H), 2.19–2.08 (m, 1H), 1.70–1.54 (m, 1H) ppm. The second stereoisomer has not been purified. *2,2-Diallylthiolane sulfoxide*: ^1H NMR (400 MHz, CDCl_3) δ 5.96–5.72 (m, 2H), 5.25–5.05 (m, 4H), 3.11–2.99 (m, 1H), 2.74–2.46 (m, 3H), 2.46–2.23 (m, 3H), 2.23–2.08 (m, 1H), 1.86–1.67 (m, 2H), 1.57–1.40 (m, 1H) ppm. GC-MS: 67 (100), 79 (70), 127 (62, $[\text{M}-\text{OH}]^+$), 95 (47), 103 (16, $[\text{M}-\text{allyl}]^+$), 144 (15, $[\text{M}]^+$).

2-Acetoxythiolane (34). To a benzene (12 mL) solution of thiolane sulfoxide (4 g, 39 mmol) is added freshly distilled acetic anhydride (5 mL, 51 mmol). The mixture is refluxed for 4h (GC-MS: starting material

and product, ratio 1:5), then 0.5 eq of acetic anhydride (2.5 mL, 26 mmol) is added and the mixture is refluxed for two more hours (GC-MS: no starting material). After dilution by dichloromethane, the mixture is washed by NaHCO_3 (aq. sat) then brine. The organic layer is dried over MgSO_4 and concentrated under vacuum, then chromatographed on silica gel with a mixture of EtOAc and hexane (2:1 to 6:1), affording 4.3 g of a colorless, acetic acid smelling liquid. Yield = 74%. ^1H NMR (400 MHz, CDCl_3) δ 6.16 (dd, J = 4.8, 1.3 Hz, 1H), 3.06–2.98 (m, 1H), 2.81 (td, J = 10.3, 6.2 Hz, 1H), 2.30–2.24 (m, 1H), 2.23–2.16 (m, 2H), 2.11–1.97 (m, 1H), 2.04 (s, 3H), 1.97–1.86 (m, 1H) ppm. ^{13}C NMR (100 MHz, CDCl_3) δ 170.71, 82.98, 37.39, 32.52, 28.35, 21.45 ppm. GC-MS: 86 (100, $[\text{M}-\text{AcO}-\text{H}]^+$), 58 (26 $[\text{AcO}-\text{H}]^+$), 103 (20, $[\text{M}-\text{Ac}]^+$), 146 (19, $[\text{M}]^+$).

2-Acetoxythiolane sulfoxide (35). To a dichloromethane (25 mL) solution of 2-acetoxythiolane (**34**) (300 mg, 2.05 mmol) is added recrystallized *m*CPBA (390 mg, 2.26 mmol). The mixture is stirred at RT overnight, then 0.25 eq of *m*CPBA is added and the mixture is stirred for 5 h (GC-MS: product and traces of sulfone, addition of *m*CPBA increased the oxidation to the sulfone). The mixture is extracted by NaHCO_3 (aq sat). The aqueous layer is then saturated with NaCl and reextracted with dichloromethane five times (sulfoxide soluble in the aqueous layer). The organic layers are combined, dried over MgSO_4 and concentrated under vacuum, affording 209 mg of a pale yellow liquid. Yield = 63%. ^1H NMR (400 MHz, CDCl_3) δ 5.79 (dd, J = 5.4, 2.9 Hz, 1H), 2.98 (dt, J = 14.1, 8.0 Hz, 1H), 2.86 (ddd, J = 13.4, 6.6, 5.5 Hz, 1H), 2.73–2.59 (m, 1H), 2.53 (ddd, J = 15.2, 7.4, 5.4 Hz, 1H), 2.22 (d, J = 14.2 Hz, 1H), 2.11 (d, J = 20.5 Hz, 4H) ppm. ^{13}C NMR (100 MHz, CDCl_3) δ 169.3, 169.1, 93.64, 82.54, 51.98, 49.96, 30.45, 28.17, 24.52, 20.70, 20.50, 19.19 ppm (double signal probably due to the two stereoisomers). IR: 1747 cm^{-1} (carbonyl), 1039 cm^{-1} (sulfoxide). GC-MS: 102 (100, $[\text{M}-\text{AcO}-\text{H}]^+$), 120 (68, $[\text{M}-\text{Ac}+\text{H}]^+$), 63 (57), 57 (50), 76 (40), 162 (18, $[\text{M}]^+$).

2-Hydroxythiolane (29). 2-Acetoxythiolane (**34**) (950 mg, 6.5 mmol) is dissolved in 13 mL of a sodium methoxide solution in methanol (0.5 M, 1 eq) at room temperature. The mixture is stirred for 20 h at RT (until TLC and GC-MS indicate that only the product is present), then quenched with dry ice. Methanol is evaporated and the crude product is dissolved in Et_2O , dried over MgSO_4 and concentrated, affording 440 mg of a pale yellow liquid. Yield = 65%. ^1H NMR (400 MHz, CDCl_3) δ 5.59–5.53 (m, 1H), 3.10 (ddd, J = 9.8, 7.2, 2.4 Hz, 1H), 2.81 (td, J = 10.4, 6.2 Hz, 1H), 2.18 (qdd, J = 5.5, 4.1, 2.1 Hz, 2H), 2.11–1.99 (m, 1H), 1.96 (s, 1H), 1.83 (tdd, J = 12.9, 5.9, 4.6 Hz, 1H) ppm. ^{13}C NMR (100 MHz, CDCl_3) δ 81.84, 40.69, 32.79, 27.78 ppm. IR: 3407 cm^{-1} (hydroxy), 1043 cm^{-1} (sulfoxide). GC-MS: 57 (100), 104 (84), 60 (81), 85 (18).

2-Phenylthiirane (39)⁵¹. To 40 mL of a mixture of dioxane and H_2O (1:1) are added 11.4 mL of styrene oxide (11.97 g, 0.1 mol) and 12 g of KSCN. The mixture is stirred at $60\text{ }^\circ\text{C}$ for 2 h, then 6 g of KSCN are

added. After 1 h of stirring, the GC-MS purity is 87%. After cool down, 80 mL of H₂O and about 40 g of ice are added, then the mixture is extracted by Et₂O. The combined organic layers are washed with H₂O, then brine, and finally dried over MgSO₄ and concentrated. Yield = 93% of crude product. The impurities are remaining starting material (styrene oxide) and styrene. Attempts to purify were unsuccessful (distillation leads to polymerization of styrene upon heating, chromatography leads to loss of 50% of the material without a big impact on purity) so the material was used as such. GC-MS: 135 (100, [M-H]⁺), 91 (27, [tropylium]⁺), 77 (12, [C₆H₅]⁺), 103 (11, [styrene]⁺).

Lithium 2-mercaptopthiolane sulfoxide (40). To a THF solution (20 mL) of thiolane sulfoxide (0.47 mL, 4.8 mmol) at -80 °C under argon is added 2.2 mL of a *n*-butyllithium (*n*-BuLi) solution in hexane (2.5 M, 5.5 mmol). After 30 min of stirring at low temperature, the mixture is stirred at RT for 30 min then cooled down again. 1.6 mL of 2-phenylthiirane (**39**, 6.4 mmol) is then added dropwise. The solution turns cloudy as stirring goes on for 30 min. Attempts to isolate the thiol were not successful, and this solution needs to be immediately used in the next step.

2-Allylthiolane sulfoxide (41). To the previous solution is added allyl bromide (0.5 mL, 5.4 mmol). The mixture is stirred at -80 °C for 1 h, then slowly brought to RT. After dilution in ethyl acetate (EtOAc), the mixture is washed by NH₄Cl (aq. sat), then brine. The aqueous layer is extracted again by EtOAc, and the combined organic layers are dried then concentrated under vacuum. Crude yield: 690 mg (82%), contains styrene according to GC-MS. Chromatography on silica gel with a mixture of EtOAc and hexane (2:1 to 5:1 to EtOAc only) affords 140 mg of a colorless liquid (yield = 17%). Only one of the two stereoisomers is present in this fraction. ¹H NMR (400 MHz, CDCl₃) δ 5.90–5.73 (m, 1H), 5.24 (m, 2H), 4.10 (m, 1H), 3.37 and 3.25 (2H in ABX system, *J*_{AB} = 13.8, *J*_{AX} = 7.2, *J*_{BX} = 8.5 Hz), 3.15 (dt, *J* = 14.1, 8.2 Hz, 1H), 2.85 (m, 2H), 2.50 (ddd, *J* = 13.1, 7.7, 5.3 Hz, 1H), 2.14 (tt, *J* = 12.8, 7.5 Hz, 1H), 2.05–1.94 (m, 1H) ppm. ¹³C NMR (100 MHz, CDCl₃) δ 132.37, 119.33, 68.31, 51.98, 35.88, 31.73, 25.18 ppm. IR: 1028 cm⁻¹ (sulfoxide), 989 and 922 cm⁻¹ (sp² C–H), 1634 cm⁻¹ (C=H). GC-MS: 103 (100, [M-thioallyl]⁺), 85 (63, [M-thioallyl-H₂O]⁺), 135 (45, [M-allyl]⁺), 79 (36), 176 (19, [M]⁺), 159 (7, [M-OH]⁺).

2-Allylthiolane (43). To a 12 mL THF solution of 2-allylthiolane sulfoxide (**41**, 100 mg, 0.57 mmol) at 0 °C is added a solution of lithium aluminium hydride (LAH) 1 M in THF (0.6 mL, 0.6 mmol). The mixture is stirred at 0 °C for 1 h, then brought to RT. GC-MS indicates the reduction of the starting material. After dilution in EtOAc, the mixture is washed by H₂O, then brine. The combined organic layers are dried then concentrated under vacuum. Crude yield: 70 mg (78%). Chromatography on silica gel with a

mixture of EtOAc and hexane (2:1) affords 30 mg of a colorless liquid (yield = 44%). ^1H NMR (400 MHz, CDCl_3) δ 5.85 (ddt, J = 17.0, 9.8, 7.1 Hz, 1H), 5.23–5.04 (m, 2H), 3.25 (d, J = 7.2 Hz, 1H), 3.02 (ddd, J = 29.0, 16.1, 7.9 Hz, 1H), 2.95–2.75 (m, 2H), 2.24–1.97 (m, 4H) ppm. IR: no sulfoxide band. GC-MS: 87 (100, [M-thioallyl] $^+$), 160 (20, [M] $^+$), 119 (19, [M-allyl] $^+$).

2-Allylthioliolane bissulfoxide (44). To a 10 mL CH_2Cl_2 solution of 2-allylthioliolane sulfoxide (**41**, 30 mg, 0.17 mmol) at RT is added *m*CPBA (33 mg, 0.19 mmol). The mixture is stirred at RT for 20 h. GC-MS indicates the formation of the bissulfoxide and absence of starting material. After dilution in CH_2Cl_2 , the mixture is washed by Na_2CO_3 aq. sat., then brine. The combined organic layers are dried then concentrated under vacuum. Crude yield: 30 mg (92%). No purification was performed. ^1H NMR (400 MHz, CDCl_3) δ 6.06–5.94 (m, 1H), 5.65 (s, 1H), 5.61 (d, J = 5.9 Hz, 1H), 5.29 (s, 1H), 4.07 and 3.96 (2H in ABX system, J_{AB} = 14.2, J_{AX} = 8.2, J_{BX} = 6.6 Hz), 3.18 (d, J = 12.7 Hz, 1H), 2.90–2.80 (m, 1H), 2.75–2.62 (m, 2H), 2.59–2.50 (m, 1H), 2.42 (ddd, J = 10.3, 9.2, 4.8 Hz, 1H) ppm. GC-MS: 87 (100, [thioliolane core] $^+$), 103 (15, [M-thioallyl S-oxide] $^+$).

2-Mercaptothioliolane (46)⁵². Thiolane (6 g, 0.068 mol) is dissolved in 60 mL of toluene, then 6 g of NCS (0.045 mol) is added in portions (in 15 min) at RT (kept at RT, the reaction is exothermic). After 1h of stirring, the floating succinimide is filtered out, and 3.4 g of thiourea (0.045 mol, 1 eq) suspended in 10 mL of acetone is added. The mixture is stirred at RT for 2 h, then the brown solid is filtered and washed with cold acetone. After dissolution of the solid in H_2O , 1.8 g of NaOH (0.045 mol, 1 eq) dissolved in 5 mL of H_2O is added. The yellow suspension turns white and cloudy, then brown. After 1 h of stirring, the mixture is acidified to pH < 7 with H_2SO_4 1 M. The clear solution has a strong smell of thiol. The aqueous mixture is extracted with DCM. Combined organic layers are washed with NaHCO_3 aq. sat. and brine, then are dried and concentrated. A yellow liquid is recovered (1.02 g), GC-MS indicates the presence of 2-mercaptothioliolane and its disulfide. ^1H NMR (400 MHz, CDCl_3) δ 4.65 (m, 1H), 3.17–3.08 (m, 1H), 3.09–2.98 (m, 1H), 2.87 (m, 1H), 2.35–2.18 (m, 2H), 2.19–1.92 (m, 2H) ppm.

2,3-Dimethylbutane-1,4-diol⁵³. A 1 M solution of LiAlH_4 in THF (10 mL, 10 mmol) is refluxed under argon. A solution of meso-2,3-dimethylsuccinic acid (150 mg, 1 mmol) in 15 mL of THF is added dropwise to the mixture, and the reaction is carried out for 30 min under reflux conditions, until TLC indicates formation of the product. The mixture is cooled in an ice bath and carefully quenched with H_2O . Rochelle's salt (sodium potassium tartrate) is added to break the aluminium emulsion (mixture stirred overnight). The aqueous layer is separated and extracted with Et_2O . Combined organic layers are dried and concentrated,

yielding 100 mg of yellow oil (yield = 77%). GC-MS confirmed the reduction of the starting material to a diol (m/z = 118).

2,3-Dimethyl-1,4-ditosylbutane⁵³. 2,3-Dimethylbutane-1,4-diol (100 mg, 0.85 mmol) is dissolved in 1.5 mL of pyridine. Tosyl chloride (390 mg, 2.04 mmol) is then added at 0 °C, and the solution is stirred for 0 °C to RT for two days. Water (1 mL) is added, followed by H₂SO₄ (25 mL of a 1 N solution). The suspension is extracted three times with EtOAc, the organic layers are combined and washed with CuSO₄ aq. to remove pyridine, dried and concentrated. White-gray crystals are recovered (180 mg, yield = 50%). Two recrystallizations in EtOH lead to 105 mg of gray crystals. ¹H NMR (400 MHz, CDCl₃) δ 7.76 (d, J = 8.4, 4H, tosyl), 7.35 (d, J = 8.0, 4H, tosyl), 3.89 (d, J = 5.0, 4H, CH₂-O), 2.46 (s, 6H, tosyl CH₃), 1.83 (m, 2H, CH), 0.84 (d, J = 6.56, 6H, CH₃-CH) ppm.

3,4-Dimethylthiolane (48)⁵³. 2,3-Dimethyl-1,4-ditosylbutane (100 mg) is refluxed in 15 mL of EtOH with 100 mg of Na₂S for 2 h. GC-MS indicates the presence of one peak with a m/z of 116 ([M]⁺). Attempts to purify the compound were unsuccessful: emulsions form when extracellular with DCM, compound evaporates when EtOH is pumped. GC-MS: 116 (67, [M]⁺), 69 (67), 74 (80), 41 (100).

Allyl propyl sulfide (50b). Propanethiol (15.2 g, 0.2 mol) is added to a solution of NaOH (9 g in 200 mL H₂O) at 0 °C. After 1 h of stirring, the organic layer is dissolved, and 24.2 g of allyl bromide (0.2 mol, 1 eq) is added. The mixture is stirred at 0 °C for another hour. The organic layer is separated, and the aqueous layer is extracted three times with 150 mL of pentane. Organic layers are combined, dried over MgSO₄ and concentrated, yielding 20.6 g of a colorless liquid. NMR and GC-MS confirm the formation of **50b** in 89% yield. ¹H NMR (400 MHz, CDCl₃) δ 5.79 (ddd, J = 14.5, 13.4, 7.2 Hz, 2H, 1H, C-CH=), 5.10 (d, J = 6.5 Hz, 1H, CH=CH_a), 5.06 (d, J = 0.7 Hz, 1H, CH=CH_b), 3.13 (d, J = 7.0 Hz, 2H, S-CH₂-C=), 2.44 (t, J = 7.3 Hz, 2H, S-CH₂), 1.58 (dt, J = 14.5, 7.2 Hz, 2H, -CH₂-CH₃), 0.98 (t, J = 7.4 Hz, 3H, -CH₃) ppm. GC-MS: 116 (46, [M]⁺), 41 (100, [M-(S-propyl)]⁺), 74 (89, [M-propyl]⁺).

Alkyl E,Z-1-propenyl sulfide (49).⁵⁴

Methyl E,Z-1-propenyl sulfide (49b). To 14.4 g of potassium *tert*-butoxide (0.129 mol) in DMSO (50 mL) is added dropwise 28.4 g of allyl methyl sulfide (**50a**, 0.323 mol) in DMSO (15 mL) under argon. The brown mixture is stirred at 45 °C for 1 h, then at RT overnight. The mixture is then poured into 100 mL iced water. The organic layer is separated, and the aqueous layer is extracted with two times 50 mL of pentane. The organic layers are combined, dried over MgSO₄, and concentrated. Distillation of the resulting mixture separates the title compound **49b**, boiling at 110 °C, from water and DMSO (yield = 55%). *trans*-Isomer:

¹H NMR (400 MHz, CDCl₃) δ 5.98 (d, *J* = 14.9 Hz, 1H, S-CH=), 5.60 (dq, *J* = 13.5, 6.5 Hz, 1H, -CH=), 2.23 (s, 3H, S-CH₃), 1.77 (d, *J* = 6.6 Hz, 3H, C-CH₃) ppm. *cis*-Isomer: ¹H NMR (400 MHz, CDCl₃) δ 5.90 (d, *J* = 9.3 Hz, 1H, S-CH=), 5.48 (dq, *J* = 14.0, 7.0 Hz, 1H, -CH=), 2.28 (s, 3H, S-CH₃), 1.72 (d, *J* = 6.8 Hz, 3H, C-CH₃) ppm. GC-MS: 88 (100, [M]⁺), 45 (84), 73 (93, [M-methyl]⁺).

E,Z-1-Propenyl propyl sulfide (49a). The same reaction was performed on allyl propyl sulfide (**50b**). To 9 g of potassium *tert*-butoxide (0.08 mol) in DMSO (50 mL) is added dropwise 13.55 g of allyl methyl sulfide (**50a**, 0.117 mol) in DMSO (15 mL) under argon. The brown mixture is stirred at 45 °C for 1 h, then at RT overnight. The mixture is then poured into 100 mL iced water. The organic layer is separated, and the aqueous layer is extracted with two times 50 mL of pentane. The organic layers are combined, dried over MgSO₄, and concentrated. Compound **49a** is distilled from water and DMSO at 140 °C as a clear liquid (m = 10.03 g, yield = 74%). *trans*-Isomer: ¹H NMR (400 MHz, CDCl₃) δ 5.92–5.89 (m, 1H, S-CH=), 5.66 (d, *J* = 6.6 Hz, 1H, -CH=), 2.67–2.58 (m, 2H, S-CH₂), 1.74 (dd, *J* = 6.6, 1.5 Hz, 3H, =C-CH₃), 1.68–1.60 (m, 2H, -CH₂), 0.99 (t, *J* = 7.3 Hz, 3H, -CH₃) ppm. *cis*-Isomer: ¹H NMR (400 MHz, CDCl₃) δ 5.93 (d, *J* = 1.4 Hz, 1H, S-CH=), 5.62–5.56 (m, 1H, -CH=), 2.67–2.58 (m, 2H, S-CH₂), 1.71 (dd, *J* = 6.8, 1.5 Hz, 3H, =C-CH₃), 1.68–1.60 (m, 2H, -CH₂), 0.99 (t, *J* = 7.3 Hz, 3H, -CH₃) ppm. GC-MS: 116 (70, [M]⁺), 45 (64), 74 (100, [M-propyl]⁺).

Propargyl propyl sulfide (51a). Propanethiol (15.2 g, 0.2 mol) are added to a a solution of NaOH (9 g in 200 mL H₂O) at 0 °C. After 1 h of stirring, the organic layer is dissolved, and 23.8 g of propargyl bromide (0.2 mol, 1 eq, 80% w:w in toluene) is added. The mixture is stirred at 0 °C for another hour. The organic layer is separated, and the aqueous layer is extracted three times with 150 mL of pentane. Organic layers are combined, dried over MgSO₄ and concentrated. A colorless liquid is recovered. GC-MS indicates the presence of **51a** and toluene.

1-Propynyl propyl sulfide (51b). Sodium (6 g, 0.26 mol) is dissolved in 200 mL cold MeOH by addition of small pieces of solid to a flask over ice. The sodium methoxide solution formed is refluxed and all the propargyl propyl sulfide is added to it. The mixture is refluxed for two days, then cooled down and poured into a mixture of pentane and ice (200 mL of each). The organic layer was separated and the aqueous layer was extracted two times with pentane. The organic layers were combined, washed with brine, dried and concentrated. The titled compound is distilled at 150 °C (14.9 g of a colorless liquid, yield = 65%).

E-1-Propenyl propyl sulfide ((E)-49a) 1-Propynyl propyl sulfide (**51b**, 14.9 g, 0.13 mol) is added to 140 mL of a LiAlH₄ solution in THF (1 M, 0.14 mol) at 0 °C. The mixture is stirred at RT overnight, then

refluxed for three days (until GC-MS of an aliquot indicates disappearance of the starting material). The aluminum salts are quenched by the Fieser procedure: at 0 °C, addition of 5.32 g of H₂O, 5.32 g of NaOH 15%, then 16 g of H₂O followed by filtration. Distillation at 140 °C gives 3.2 g of a yellow liquid (yield = 21.2 %). ¹H NMR (400 MHz, CDCl₃) δ 5.92 (dd, *J* = 15.0, 1.4 Hz, 1H, S-CH=), 5.65 (dd, *J* = 14.9, 6.7 Hz, 1H, -CH=), 2.61 (t, *J* = 7.3 Hz, 2H, S-CH₂), 1.7 (dd, *J* = 6.6, 1.4 Hz, 3H, =C-CH₃), 1.64 (dd, *J* = 14.6, 7.3 Hz, 2H, -CH₂), 1.00 (t, *J* = 7.4 Hz, 3H, -CH₃) ppm.

Bis-1-propenyl disulfide (23). Lithium (1.12 g cut in small pieces, 0.16 mol) is dissolved in about 100 mL of NH₃ condensed with a cold trap at -78 °C. (*E,Z*)-1-Propenyl propyl sulfide (**49a**, 10.5 g, 0.09 mol) is dissolved in 25 mL of dry Et₂O, and this solution is added dropwise to the deep blue lithium solution. The blue color is discharged in about 30 min. Ammonia is evaporated overnight. The milky residual liquid is diluted with 150 mL Et₂O. *Oxidation with I₂.* A solution of iodine is prepared in water (20 g of I₂ and 5 g of KI to help dissolve in 250 mL H₂O) and added slowly to the previous mixture under vigorous stirring. Two layers are separated, and the aqueous layer is extracted with Et₂O. Combined organic layers are washed with aqueous Na₂S₂O₃, dried and concentrated. The crude material is chromatographed on silica gel with pentane. Product is recovered as 2.6 g of a smelly, colorless liquid (yield = 26%). *Oxidation with methanesulfonyl chloride.* Methanesulfonyl chloride (15.6 mL, 0.2 mol) is added to the previous solution under vigorous stirring at 0 °C (exothermic reaction!). After 30 min, the mixture is quenched with H₂O. The mixture is then extracted and purified as in the iodine procedure (yield = 10%). ¹H NMR (400 MHz, CDCl₃) δ 6.10 (m, 2H), 6.02–5.87 (m, 1H), 5.75 (m, 1H), 1.78 (m, 6H) ppm.

Oxidation of bis-1-propenyl disulfide (23) to form sultenes 10. *Low temperature NMR - oxidation with mCPBA.* Bis-1-propenyl disulfide (9 mg, 0.06 mmol) is dissolved in 0.5 mL of CDCl₃ in an NMR tube. The NMR probe is cooled to -40 °C, then a solution of *m*CPBA (11 mg, 0.06 mmol in 0.5 mL of CDCl₃) is added. Spectra are recorded every five minutes. Thiosulfinate is observed on the spectrum after 5 min. After 30 min, since no changes were observed, the temperature is slowly brought up to -30 °C then -15 °C, when rearrangement products **10** and **9** start being formed (peaks at 4.91, 4.84, 4.60, 4.56, 4.24 and 4.12 ppm, as reported in the literature²³). The experiment was reproduced on a bench scale, where the mixture was extracted by ice-cold NaHCO₃. NMR indicates the presence of the same products. DART-MS indicates the presence of starting material, target product and C₉H₁₄OS₃. *Oxidation with dimethyldioxirane.* Dimethyldioxirane is prepared according to Adam et al.⁵⁵ A mixture of acetone (192 mL), water (254 mL) and NaHCO₃ (58 g) is placed in a 5-L flask equipped with a mechanical stirrer and connected via a U tube to

receiving flask cooled at -78 °C. Oxone (120 g) is added by portions to the flask (kept at 0–5 °C). Once the addition is complete, the cooling bath is removed from under the main flask, the receiving flask is placed under vacuum, and dimethyldioxirane starts distilling. The collected solution is titrated with thioanisole by NMR (0.075 M). Oxidation of **23** is performed in acetone at -20 °C by mixing 183 mg of bis-1-propenyl disulfide (1.25 mmol) with 20 mL of dimethyldioxirane solution (1.5 mmol). DART-MS indicates the formation of oxidation products and C₉H₁₄OS₃ a few seconds after the oxidant is added. *Oxidation with peracetic acid.* 1-Propenyl disulfide (100 mg, 0.68 mmol) is dissolved in DCM at -40 °C. One equivalent of solid Na₂CO₃ (72 mg) is added, then 5.2 mg of peracetic acid (35% wt., 0.68 mmol). The solution warms up to -20 °C in about 2 h, then is extracted with cold NaHCO₃. NMR of the organic layer indicates the same signals as the *m*CPBA procedure.

Attempted synthesis of ajothiolane (20). Addition of nucleophiles (allyl alcohol or allyl Grignard) to the crude or extracted mixture of oxidized **23** by each of the three oxidation procedures did not lead to a sufficient amount of ajothiolane (**20**) or deoxyajothiolane (**57**) to allow us to isolate them. A mixture of products separated by TLC analyzed by DART-MS indicates the presence of 3,4-dimethylthiophene as a fragment in all of bands, but no **20** could be isolated.

3,4-Dimethyl-2,3-dihydrothiophene-2-thiol (58). Bis-1-propenyl disulfide (**23**, 636 mg, 4.4 mmol) are dissolved in 50 g of benzene and refluxed for 4 h. The solution is analyzed by GC-MS and NMR. *trans*-*Isomer*: ¹H NMR (400 MHz, CDCl₃) δ 5.68 (s, 1H, CH=C), 4.33 (dd, *J* = 7.4, 3.9 Hz, 1H, S-CH-), 2.75 (dd, *J* = 6.9, 4.0 Hz, 1H, CH-CH₃), 2.40 (d, 1H, *J* = 7.5 Hz, -SH), 1.79 (m, 3H, =C-CH₃), 1.21 (d, *J* = 7.1 Hz, 3H, -CH₃) ppm. *cis*-*Isomer*: ¹H NMR (400 MHz, CDCl₃) δ 5.80 (s, 1H, CH=C), 4.90 (dd, *J* = 8.2, 7.0 Hz, 1H, S-CH-), 2.98–2.86 (m, 1H, CH-CH₃), 2.03 (d, 1H, *J* = 8.3 Hz, -SH), 1.79 (m, 3H, =C-CH₃), 1.13 (d, *J* = 7.0 Hz, 3H, -CH₃) ppm. *trans*-*Isomer*: ¹³C NMR (100 MHz, CDCl₃) δ 128.45, 115.54, 58.00, 54.57, 16.10 or 16.00, 12.41 ppm. *cis*-*Isomer*: ¹³C NMR (100 MHz, CDCl₃) δ 128.45, 117.61, 53.93, 49.75, 16.10 or 16.00, 15.98 ppm.

1,2-Bis(3,4-dimethyl-2,3-dihydrothiophene-2-yl)disulfane (59). Diethyl ether (25 mL) is added to the previous solution cooled at 0 °C, then 2 mL of a 2.25 M BuLi solution (4.5 mmol). After 15 min of stirring, iodine in Et₂O is added (560 mg, 2.2 mmol). The mixture is quenched with H₂O and extracted with Et₂O. Preparative TLC leads to the isolation of 340 mg of the titled compound (yield = 54%).

Attempted hydroboration of 59³⁴. Compound **59** (50 mg, 0.17 mmol) is dissolved in 1 mL of C₆D₆ with 0.4 mL of a 1 M THF solution of catecholborane (0.4 mmol) and 8 mg of RhCl(PPh₃)₃ (0.011 mmol). The

reaction is followed by NMR. No change is recorded after three days, and the mixture is heated at 60 °C for 2 h. NMR reveals decomposition of the catalyst and no change in the olefinic proton chemical shift or abundance.

Allyl methyl sulfoxide (63). Allyl methyl sulfide (5.3 g, 60 mmol) is dissolved in acetone. Hydrogen peroxide 30% (7 mL, 68 mmol) is added and the mixture is stirred at RT for 3 h. DART-MS indicates the formation of product **63** and the corresponding sulfone. Excess H₂O₂ is quenched by solid MnO₂. When no O₂ release is observed, the suspension is filtered and extracted by EtOAc. Combined organic layers are dried and concentrated. ¹H NMR (400 MHz, CDCl₃) δ 5.89 (ddt, *J* = 17.7, 10.2, 7.5 Hz, 1H), 5.47 (ddd, *J* = 10.2, 0.7 Hz, 1H), 5.41 (ddd, *J* = 17.1, 1.2 Hz, 1H), 3.50 (dd, *J* = 10.3, 7.7 Hz, 1H), 2.58 (s, 3H) ppm.

γ-Mercaptobutyric acid (68)⁴³. A mixture of γ-butyrolactone, (**69**, 43 g, 0.5 mol), thiourea (38 g, 0.5 mol) and HBr 48% (100 g, 0.6 mol) is refluxed for 5 h. The liquid turns golden yellow. After cool down, a solution of NaOH (63 g in 65 mL H₂O) is added slowly. A precipitate and foam form. The mixture is refluxed for 2 h, during which time the precipitate disappears. Upon cool down, a solid is formed. The mixture is washed by Et₂O, then the aqueous layer is acidified to pH 1. A yellow layer separates. The product is extracted by Et₂O. Combined organic layers are dried then concentrated under vacuum, affording about 55 g of a colorless oil. Distillation of the crude under high vacuum (fractions collected: 90 - 100 °C) affords 33.5 g of yellow oil. Yield = 56%. ¹H NMR (400 MHz, CDCl₃) δ 10.27 (s, 1H, C₁OOH), 2.59 (dt, *J* = 8.1, 7.0 Hz, 2H, C₄), 2.54–2.46 (m, 2H, C₂), 1.93 (p, *J* = 7.2 Hz, 2H, C₃), 1.35 (t, *J* = 8.1 Hz, 1H, -SH) ppm. DART-MS: 121.034 (100, [M+H]⁺), 103.023 (82, M-OH)⁺, 87.045 (52, [γ-butyrolactone+H]⁺).

γ-Thiobutyrolactone (67). γ-Mercaptobutyric acid (**68**) is brought to a boil in a distillation apparatus. Two fractions are collected: a fraction distilling at 100-110 °C (H₂O), and a colorless liquid distilling at 190-195 °C. A yellow liquid remains in the flask. Fraction 2 is then distilled under vacuum to yield 7.3 g of a colorless liquid. Yield = 29%. NMR indicates the presence of γ-butyrolactone, confirmed by GC-MS. ¹H NMR (400 MHz, CDCl₃) δ 3.40 (t, *J* = 6.5 Hz, 2H, C₄), 2.51 (t, *J* = 7.4 Hz, 2H, C₂), 2.26 (p, *J* = 6.9 Hz, 2H, C₃) ppm. GC-MS: 102 (100, [M]⁺), 54.9 (43), 103.9 (5, [M+2]⁺). DART-MS: 103.022 (100) [M+H]⁺, 120.051 (10). IR: 2930 (S-H) and 1700 (carbonyl) cm⁻¹.

Oxidation of γ-thiobutyrolactone (67). *In organic solvent.* γ-Thiobutyrolactone (17 mg, 0.17 mmol) is dissolved in 0.5 mL of CDCl₃. *m*CPBA (13 mg, 0.085 mmol) is also dissolved in 0.5 mL of CDCl₃. The two solutions are mixed in an NMR tube at 0 °C, and NMR spectrum is collected right away. Some starting

material is gone, and a precipitate forms. The experiment is repeated at - 40 °C and in front of the DART-MS with the same results. The precipitate is not soluble in D₂O, only in acetone.

In water. γ -Thiobutyrolactone (0.1 g, 1 mmol) is dissolved in 10 mL of H₂O. Potassium periodate (0.21 g, 1 mmol) is also dissolved in 10 mL of H₂O. The two solutions are mixed in front of the DART-MS in positive and negative mode. No traces of the oxidation product are observed. An infrared spectrum of the product lacks a strong band between 1500–1000 cm⁻¹.

References

- (1) Yoshida, M.; Kameyama, M.; Hosoda, H.; Shimizu, Y.; Sakagami, K.; Washino, K.; Iwata, J.; Omoto, M. New thiolane compound and use thereof; JP143866 , 2010.
- (2) Aoyagi, M.; Kamoi, T.; Kato, M.; Sasako, H.; Tsuge, N.; Imai, S. Structure and bioactivity of thiosulfinates resulting from suppression of lachrymatory factor synthase in onion. *J. Agric. Food Chem.* **2011**, *59*, 10893–10900.
- (3) El-Aasr, M.; Fujiwara, Y.; Takeya, M.; Ono, M.; Nakano, D.; Okawa, M.; Kinjo, J.; Ikeda, T.; Miyashita, H.; Yoshimitsu, H.; Nohara, T. Garlicnin A from the fraction regulating macrophage activation of *Allium sativum*. *Chem. Pharm. Bull.* **2011**, *59*, 1340–1343.
- (4) El-Aasr, M.; Fujiwara, Y.; Takeya, M.; Ikeda, T.; Tsukamoto, S.; Ono, M.; Nakano, D.; Okawa, M.; Kinjo, J.; Yoshimitsu, H.; Nohara, T. Onionin A from *Allium cepa* inhibits macrophage activation. *J. Nat. Prod.* **2010**, *73*, 1306–1308.
- (5) Nohara, T.; Kiyota, Y.; Sakamoto, T.; Manabe, H.; Ono, M.; Ikeda, T.; Fujiwara, Y.; Nakano, D.; Kinjo, J. Garlicnins B1, C1, and D, from the fraction regulating macrophage activation of *Allium sativum*. *Chem. Pharm. Bull.* **2012**, *60*, 747–751.
- (6) Nohara, T.; Fujiwara, Y.; Ikeda, T.; Murakami, K.; Ono, M.; Nakano, D.; Kinjo, J. Cyclic sulfoxides garlicnins B2, B3, B4, C2, and C3 from *Allium sativum*. *Chem. Pharm. Bull.* **2013**, *61*, 695–699.
- (7) Nohara, T.; Fujiwara, Y.; Komota, Y.; Kondo, Y.; Saku, T.; Yamaguchi, K.; Komohara, Y.; Takeya, M. Cyclic sulfoxides-garlicnins K 1, K 2, and H 1-extracted from *Allium sativum*. *Chem. Pharm. Bull.* **2015**, *63*, 117–121.
- (8) Penn, R. E.; Block, E.; Revelle, L. K. Flash vacuum pyrolysis studies. 5. Methanesulfenic acid. *J. Am. Chem. Soc.* **1978**, *100*, 3622–3623.
- (9) Fries, K. Über α -Anthrachinon-sulfensäure. *Berichte der Dtsch. Chem. Gesellschaft* **1912**, *45*, 2965–2973.
- (10) Shelton, J. R.; Davis, K. E. Decomposition of sulfoxides. II. Formation of sulfenic acids. *Int. J. Sulfur Chem.* **1973**, *8*, 205–216.
- (11) Nakamura, N. A stable sulfenic acid, 9-triptycenesulfenic acid: its isolation and characterization. *J. Am. Chem. Soc.* **1983**, *105*, 7172–7173.

(12) Ishihara, M.; Abe, N.; Sase, S.; Goto, K. Synthesis, structure, and reactivities of a stable primary-alkyl-substituted sulfenic acid. *Chem. Lett.* **2015**, *44*, 615–617.

(13) Pan, J.; Carroll, K. S. Light-mediated sulfenic acid generation from photocaged cysteine sulfoxide. *Org. Lett.* **2015**, *17*, 6014–6017.

(14) Goto, K.; Tokitoh, N.; Okazaki, R. Synthesis of a stable arenesulfenic acid bearing a bowl-shaped macrobicyclic cyclophane skeleton. *Angew. Chem. Int. Ed.* **1995**, *34*, 1124–1126.

(15) Goto, K.; Holler, M.; Okazaki, R. Synthesis, structure, and reactions of a sulfenic acid bearing a novel bowl-type substituent: the first synthesis of a stable sulfenic acid by direct oxidation of a thiol. *J. Am. Chem. Soc.* **1997**, *119*, 1460–1461.

(16) Saiki, T.; Goto, K.; Tokitoh, N.; Goto, M.; Okazaki, R. Syntheses and structures of novel *m*-xylylene-bridged calix[6]arenes: stabilization of a sulfenic acid in the cavity of calix[6]arene. *J. Organomet. Chem.* **2000**, *611*, 146–157.

(17) Gupta, V.; Carroll, K. S. Sulfenic acid chemistry, detection and cellular lifetime. *Biochim. Biophys. Acta (BBA)-General Subj.* **2014**, *1840*, 847–875.

(18) Freidinger, R. M. Chiral, *N*-protected, *N*-substituted alpha-amino acids., US 4535167, 1985.

(19) Block, E., *Garlic and Other Alliums: the Lore and the Science*; Royal Society of Chemistry: Cambridge, UK, 2010.

(20) Block, E. The organosulfur chemistry of the genus *Allium* - Implications for the organic chemistry of sulfur. *Angew. Chem. Int. Ed.* **1992**, *31*, 1135–1178.

(21) Cox, J. M.; Owen, L. N. Cyclic hemithioacetals: analogues of thiosugars with sulphur in the ring. *J. Chem. Soc. C Org.* **1967**, 1130–1134.

(22) Gilman, H.; Woods, L. A. Some 6-methoxy-8-quinolylamino sulfides. *J. Am. Chem. Soc.* **1945**, *67*, 1843–1845.

(23) Block, E.; Bayer, T.; Naganathan, S.; Zhao, S.-H. *Allium* chemistry: synthesis and sigmatropic rearrangements of alk(en)yl 1-propenyl disulfide *S*-oxides from cut onion and garlic. *J. Am. Chem. Soc.* **1996**, *118*, 2799–2810.

(24) Han, Y.; Ma, Y.; Keresztes, I.; Collum, D. B.; Corey, E. J. Preferential geminal bis-silylation of 3,4-benzothiophane is caused by the dominance of electron withdrawal by R_3Si over steric shielding effects. *Org. Lett.* **2014**, *16*, 4678–4679.

(25) Gais, H.-J. Cyclic dithiohemiacetals - synthesis and properties. *Angew. Chem. Int. Ed. English* **1977**, *16*, 196–197.

(26) Barbarella, G.; Garbesi, A.; Fava, A. Conformational analysis of the thiolane ring system. II. Proton magnetic resonance spectra and base-catalyzed hydrogen-deuterium exchange of sulfonium cations and sulfoxides derived from 3,3-dimethylthiolane and trans-2-thiahhydrindan. *J. Am. Chem. Soc.* **1975**, *97*, 5883–5889.

(27) Naganathan, S. Organosulfur Chemistry of *Allium* Species , Ph.D. Thesis, State University of New York at Albany, 1992, p 175.

(28) Garst, M. E.; Dolby, L. J.; Esfandiari, S.; Fedoruk, N. A.; Chamberlain, N. C.; Avey, A. A. Reductions with lithium in low molecular weight amines and ethylenediamine. *J. Org. Chem.* **2000**, *65*, 7098–7104.

(29) Cohen, T.; Doubleday, M. D. A simple method for producing cycloalkenyllithiums from cycloalkanones via reductive lithiation of enol phenyl thioethers. *J. Org. Chem.* **1990**, *55*, 4784–4786.

(30) Cohen, T.; Kreethadumrongdat, T.; Liu, X.; Kulkarni, V. Use of aromatic radical-anions in the absence of THF. Tandem formation and cyclization of benzyllithiums derived from the attack of homo- and bishomoallyllithiums on α -methylstyrenes: two-pot synthesis of cuparene. *J. Am. Chem. Soc.* **2001**, *123*, 3478–3483.

(31) Yang, A.; Butela, H.; Deng, K.; Doubleday, M. D.; Cohen, T. Organolithiums by reductive lithiation: the catalytic aromatic method versus the use of preformed aromatic radical-anions. Naphthalene can behave as a catalyst or an inhibitor. *Tetrahedron* **2006**, *62*, 6526–6535.

(32) Kennedy, N.; Lu, G.; Liu, P.; Cohen, T. Reductive lithiation in the absence of aromatic electron carriers. A steric effect manifested on the surface of lithium metal leads to a difference in relative reactivity depending on whether the aromatic electron carrier is present or absent. *J. Org. Chem.* **2015**, *80*, 8571–8582.

(33) Kennedy, N.; Liu, P.; Cohen, T. Fundamental difference in reductive lithiations with preformed radical anions versus catalytic aromatic electron-transfer agents: *N,N*-dimethylaniline as an advantageous catalyst. *Angew. Chem. Int. Ed.* **2016**, *55*, 383–386.

(34) Webb, J. D.; Harrison, D. J.; Norman, D. W.; Blacquiere, J. M.; Vogels, C. M.; Decken, A.; Bates, C. G.; Venkataraman, D.; Baker, R. T.; Westcott, S. A. Metal catalysed hydroboration of vinyl sulfides, sulfoxides, sulfones, and sulfonates. *J. Mol. Catal. A Chem.* **2007**, *275*, 91–100.

(35) Cavallito, C. J.; Fruehauf, D. M. Peracetic acid oxidation of thiol esters. *J. Am. Chem. Soc.* **1949**, *71*, 2248–2249.

(36) Kumamoto, T.; Mukaiyama, T. The formation and reactions of alpha-keto sulfoxide. *Bull. Chem. Soc. Jpn.* **1968**, *41*, 2111–2114.

(37) Tagaki, W.; Kikukawa, K.; Ando, K.; Oae, S. The reaction of sulphides with *N*-bromosuccinimide. Oxidation of sulphide to sulphoxide. *Chem. Ind.* **1964**, *38*, 1624.

(38) Silverstein, R. M.; Webster, F. X., *Spectrometric Identification of Organic Compounds*; Wiley: Hoboken, 1998.

(39) Dansette, P. M.; Thébault, S.; Bertho, G.; Mansuy, D. Formation and fate of a sulfenic acid intermediate in the metabolic activation of the antithrombotic prodrug Prasugrel. *Chem. Res. Toxicol.* **2010**, *23*, 1268–1274.

(40) Dansette, P. M.; Levent, D.; Hessani, A.; Bertho, G.; Mansuy, D. Thiolactone sulfoxides as new reactive metabolites acting as bis-electrophiles: implication in clopidogrel and Prasugrel bioactivation. *Chem. Res. Toxicol.* **2013**, *26*, 794–802.

(41) Zhu, Y.; Zhou, J. In vitro biotransformation studies of 2-oxo-clopidogrel: multiple thiolactone ring-opening pathways further attenuate prodrug activation. *Chem. Res. Toxicol.* **2013**, *26*, 179–190.

(42) Sexton, A.; Mbiya, W.; Morakinyo, M. K.; Simoyi, R. H. Kinetics and mechanism of the oxidation of *N*-acetyl homocysteine thiolactone with aqueous iodine and iodate. *J. Phys. Chem. A* **2013**, *117*, 12693–12702.

(43) Kharasch, N.; Langford, R. B. Derivatives of sulfenic acids. XLII. 3-chloroformylpropanesulfenyl Chloride and 1,2-thiazan-3-one. *J. Org. Chem.* **1963**, *28*, 1901–1903.

(44) Nohara, T.; Fujiwara, Y.; Ikeda, T.; Yamaguchi, K.; Manabe, H.; Murakami, K.; Ono, M.; Nakano, D.; Kinjo, J. Acyclic sulfides, garlicins L-1 - L-4, E, and F, from *Allium sativum*. *Chem. Pharm. Bull.* **2014**, *62*, 477–482.

(45) Nohara, T.; Fujiwara, Y.; Ikeda, T.; Murakami, K.; Ono, M.; El-Aasr, M.; Nakano, D.; Kinjo, J. Two new bicyclic sulfoxides from Welsh onion. *J. Nat. Med.* **2016**, *70*, 260–265.

(46) Kotoulas, S. S.; Kojić, V. V.; Bogdanović, G. M.; Koumbis, A. E. Synthesis of novel pyrimidine apiothionucleosides and in vitro evaluation of their cytotoxicity. *Tetrahedron* **2015**, *71*, 3396–3403.

(47) Hu, Y.-J.; Wang, X.-B.; Li, S.-Y.; Xie, S.-S.; Wang, K. D. G.; Kong, L.-Y. Facile synthesis of spiro chromanone-tetrahydrothiophenes with three contiguous stereocenters via sulfa-Michael/aldol cascade reactions. *Tetrahedron Lett.* **2015**, *56*, 105–108.

(48) Zeng, X.-M.; Meng, C.-Y.; Bao, J.-X.; Xu, D.-C.; Xie, J.-W.; Zhu, W.-D. Enantioselective construction of polyfunctionalized spiroannulated dihydrothiophenes via a formal thio [3+2] cyclization. *J. Org. Chem.* **2015**, *80*, 11521–11528.

(49) Majewski, M. *Allium sativum*: facts and myths regarding human health. *Roczn. Państwowego Zakładu Hig.* **2014**, *65*.

(50) Upadhyay, R. K. Garlic: a potential source of pharmaceuticals and pesticides: a review. *Int. J. Green Pharm.* **2016**, *10*.

(51) Guss, C. O.; Chamberlain, D. L. Styrene sulfide. *J. Am. Chem. Soc.* **1952**, *74*, 1342–1343.

(52) Delaney, P. A.; Johnstone, R. A. W. Solvent effects in the chlorination of tetrahydrothiophens with *N*-chlorosuccinimide. *Tetrahedron* **1985**, *41*, 3845–3851.

(53) Barbarella, G.; Dembech, P. ¹³C chemical shifts and conformational analysis of methyl substituted thiacyclopentanes. *Org. Magn. Reson.* **1980**, *13*, 282–286.

(54) Block, E.; Thiruvazhi, M.; Toscano, P. J.; Bayer, T.; Grisoni, S.; Zhao, S.-H. *Allium* chemistry: structure, synthesis, natural occurrence in onion (*Allium cepa*), and reactions of 2,3-dimethyl-5,6-dithiabicyclo[2.1.1]hexane S-oxides. *J. Am. Chem. Soc.* **1996**, *118*, 2790–2798.

(55) Adam, W.; Bialas, J.; Hadjiarapoglou, L. A convenient preparation of acetone solutions of dimethyl-dioxirane. *Chem. Ber.* **1991**, *124*, 2377–2377.

Chapter 4

Alliin, the precursor: analytical and preparative study

4.1 Alliin: origin and interest

Among the compounds that can be extracted from garlic cloves, alliin attracted our attention. Alliin undergoes an enzymatic reaction to produce allicin (Figure 4.1), which is the precursor of novel, biologically active organosulfur compounds, such as ajoene and vinyldithiins (1).

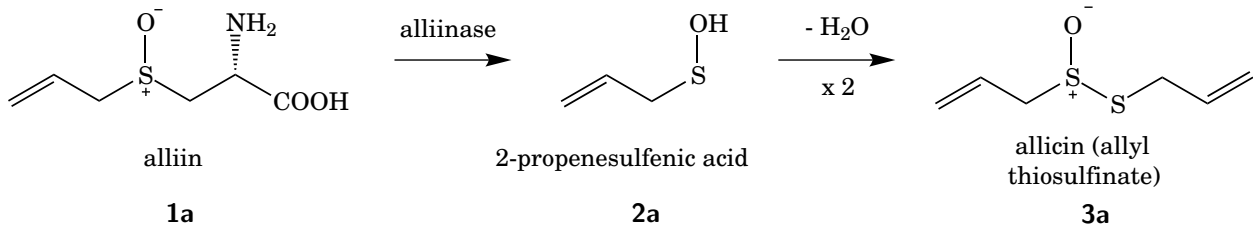


Figure 4.1: The C–S bond of alliin (**1a**) is cleaved by the enzyme alliinase, producing 2-propenesulfenic acid (**2a**). Two molecules of the latter condense to form allicin (**3a**).

Alliin is chemically synthesized in two steps (Figure 4.2). Deoxyalliin (**71**) is produced by the reaction of L-cysteine with allyl bromide, and oxidation leads to alliin (**1a**). The synthesis produces two diastereoisomers: L-(+)- and L-(-)-alliin ((+)- and (-)-**1a**, respectively, Figure 4.3).

The configuration of stereocenters is significant in organic chemistry. The bioavailability of drugs can be enhanced for one enantiomer. For example, Nexium, the USA's second largest-selling drug in 2013,¹, contains a sulfoxide stereocenter. Alliin (**1a**), the main flavor precursor in garlic, exists mainly as one single isomer, (+)-alliin or (*S*)-*S*-allyl-L-cysteine sulfoxide ((+)-**1a**). The analytical separation and quantification of these stereoisomers by high-performance liquid chromatography (HPLC) was the first aim of this study.

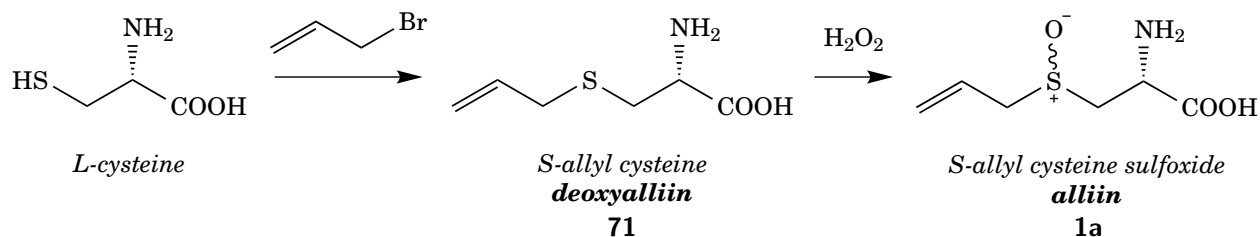


Figure 4.2: Alliin (**1a**) is synthesized in two steps from L-cysteine. Cysteine reacts with allyl bromide (nucleophilic substitution) to form deoxyalliin (**71**) that is then oxidized by hydrogen peroxide.

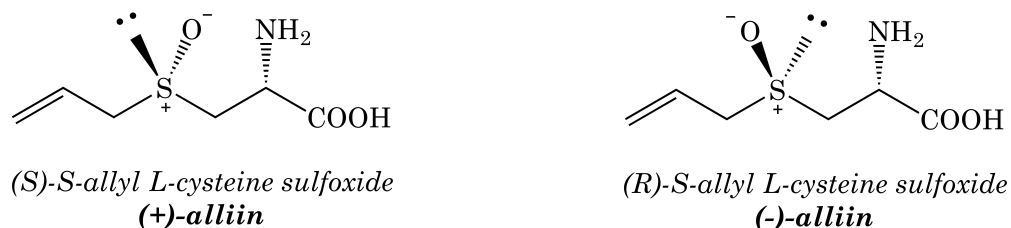


Figure 4.3: Alliin (**1a**) has two stereocenters. Starting from L-cysteine, chemical synthesis leads to a mixture of (+)- and (-)-alliin. Compound (+)-**1a** is the natural isomer.

In the second part, methods to produce pure stereoisomers of alliin are explored. Extraction from garlic and chemical synthesis of (\pm)-alliin followed by separation and stereospecific synthesis are compared. Finally, work on alliinase and vinyldithiins is proposed.

4.2 Analytical separation of the diastereoisomers of alliin

The following material has been published in Talanta¹ (Dethier, B.; Laloux, M.; Hanon, E.; Nott, K.; Heuskin, S.; Wathelet, J. P. Analysis of the Diastereoisomers of Alliin by HPLC. Talanta 2012, 101, 447–452). The content of this section draws heavily on the article.

The study of alliin (**1a**) required a tool to quantify the two stereoisomers. An HPLC method was developed on a special stationary phase, porous graphitic carbon. This section describes the set up, optimization and

¹ According to <http://www.drugs.com/stats/top100/2013/sales>, updated in February 2014

validation of this method by the accuracy profile approach, also published in *Talanta*.¹ A validated way to analyze (+)- and (-)-alliin in less than 25 min was developed. The concentration range, between 0.5 and 3 mg/mL, meets our requirements for further experiments. This useful tool can be applied to other chiral garlic non-volatile compounds as well, and may open the way to analyses of other structurally similar molecules.

The analysis of garlic extracts and measure of its alliin content is frequently proposed in the literature. Methods reported employ spectrophotometry,² capillary electrophoresis,³ biosensors,⁴ micellar electrokinetic chromatography,⁵ GC-MS⁶ or TLC,⁷ but most of them use HPLC.⁸⁻¹⁷ HPLC methods have been developed for the analysis of L-(+)-alliin and other cysteine sulfoxides, but none of them sought to separate and quantify each diastereoisomer. Most of these methods involve the formation of a derivative to improve retention or allow UV, visible or fluorimetric detection.⁸⁻¹⁴ Generation of a derivative presents disadvantages: it requires time, reagents, and could cause a bias in quantification if the reaction is not complete. Methods avoiding derivatives have been developed for garlic-derived molecules.^{10,15-17} In particular, Ichikawa et al.¹⁶ proposed a methodology using an amino stationary phase (UV detection at 210 nm), and Kubec and Musah¹⁴ developed a method for aromatic cysteine sulfoxides. However, none of them was designed for the separation of L-(\pm)-alliin.

On the other hand, Chaimbault et al.¹⁸ separated twenty protein amino acids on a PGC stationary phase. This material, composed of a crystalline array of hexagonally disposed carbons, forms planar sheets. No residual functional groups are present. PGC shows interesting retention properties because it is more hydrophobic than classical reversed-phases.^{19,20} The delocalized electrons of the graphite allow the separation of polar compounds. Structurally similar molecules have different retention properties as they interact differently with the PGC planar structure.²⁰ Furthermore, PGC is resistant to extreme temperature and pH ranges. For all of these reasons, PGC was selected as a good candidate for the separation of L-(\pm)-alliin. After optimization of the HPLC separation of the two diastereoisomers, performance was compared to the separations using amino HPLC column (work by Ichikawa et al.¹⁶). Finally, the method was validated by the accuracy profile methodology.

4.2.1 Method development on porous graphitic carbon (PGC)

The interpretation of the quality of the separation is based on the following parameters: resolution between the peaks, symmetry and number of theoretical plates. The retention factor was also considered during temperature optimization.

Mobile phase: acidification and gradient

Solvents used, H_2O and acetonitrile (ACN), are common on reverse phase HPLC. Acidification of the mobile phase is often suggested in HPLC as the compound protonation state affects its retention. The most common acids used in HPLC are formic, phosphoric and trifluoroacetic acid (TFA). All three were tested. No separation of the diastereoisomers was obtained without acidifying the mobile phase. The use of phosphoric acid does not result in any separation: only one broad peak was observed. Formic acid leads to encouraging results, but the second peak shows tailing. Only TFA provided good resolution and peak symmetry. The improvement in the separation obtained with TFA did not seem to be due only to acidification of the medium. TFA seemed to play the role of an ion-pairing agent for cationic compounds as is often the case with the perfluorocarboxylic acids used in chromatography.²¹ Examples of good separations have been reported for selenoamino acids with heavier perfluorinated carboxylic acids as ion-pairing agents.^{22,23} At pH lower than the pKa of alliin, the compound is protonated (carboxylic acid $-\text{COOH}$ and ammonium $-\text{NH}_3^+$). The pKa of alliin was found to be 3.67. Solution of formic, phosphoric and trifluoroacetic acid (0.1% in water) have a pH of 2.88, 2.33 and 1.98 respectively, which were all under the pKa value. 0.1% TFA provided maximal resolution and satisfactory number of theoretical plates and symmetry of the peaks. A deviation of the baseline is observed when the TFA concentration exceeds 0.1% (TFA UV absorbance becomes significant).

A gradient was necessary to separate the diastereoisomers. A ten minute gradient seemed to be well-adapted for the separation. Indeed, a shorter gradient decreased peak resolution, symmetry and number of theoretical plates, and lengthening it was unnecessary and solvent consuming. The final program (including the reconditioning of the column) was set as follows: ACN = 0% (0 min), 16% (10 min), 100% (12 min), 100% (13 min), 0% (15 min), 100% (22 min).

The optimal flow rate for the separation is determined by a Van Deemter plot (Figure 4.4). The efficiency was higher for (+)-**1a**. Optimal flow rate was found to be 0.1 mL/min, but 0.3 mL/min was selected as a compromise of efficiency and short analysis time.

Temperature

The effects of temperature on the separation on PGC column was studied. Contradictory results can be found in the literature. Investigations have been conducted on PGC between 13 and 250 °C (see West et al.²⁴ for a review), high temperature liquid chromatography (HT-HPLC) being achievable on PGC as the phase is resistant to extreme conditions (up to 200 °C).²⁵ Optimal temperatures of 160 and 150 °C

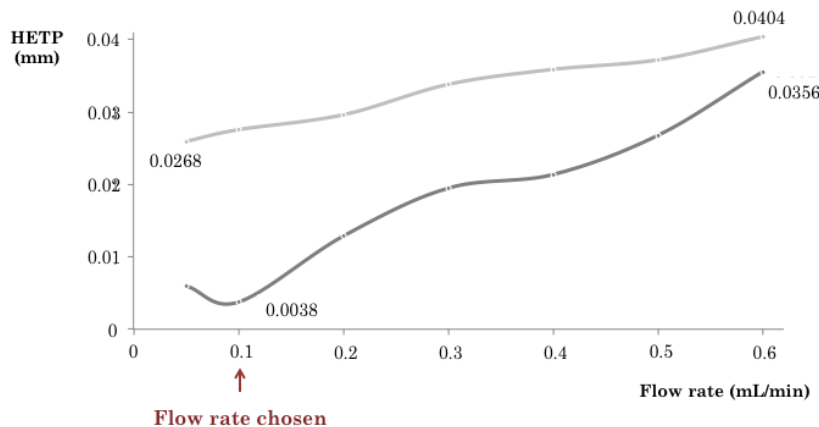


Figure 4.4: Van Deemter plot. The optimal flow rate is 0.1 mL/min, but 0.3 mL/min was selected to shorten the analysis time.

have been reported, respectively, for the separation of polymers and lipid molecular species,^{26,27} as well as temperature of 80 °C for the separation of small anions.²⁸ Furthermore, PGC appears to provide good resolution for amino alcohol enantiomers below 0 °C,²⁹ and the best separation of the 20 amino acids was achieved at 10 °C.¹⁸ The prediction of the effect of temperature is thus complex and an optimization of the temperature during the separation of alliin appeared mandatory. Temperatures between 10 and 60 °C were investigated. Higher temperatures had to be avoided because they required stainless steel tubing instead of PEEK (polyether ether ketone), strong mobile phase preheating and post column cooling.³⁰ Water in the mobile phase restricted lower temperatures. The resolution, the number of theoretical plates and the symmetry have been processed. Resolution was satisfactory over the whole range of temperatures even if a maximum was observed at 30 °C. On the other hand, the number of theoretical plates increased rapidly when the temperature decreased, especially for (+)-alliin. Symmetry of the (+)-alliin peak is maximal at 10 and 30 °C. The aforementioned results led to the selection of a temperature of 30 °C for the analysis. Although 10 °C give the best efficiency (*i.e.*, number of theoretical plates, N) with a correct resolution, this temperature is harder to reach and maintain by the system. A compromise was found at 30 °C since retention time decreases when the temperature is increased. Furthermore, the retention factors of each diastereoisomer tend to equalize at the extreme temperatures, which is consistent with the evolution of the resolution. Retention factors at 30 °C show a greater separation.

Final program

The chromatogram obtained for the separation of L-(+)- and L-(-)-alliin with the optimized method is shown Figure 4.5. After the gradient, the following items were implemented: the water in the mobile phase was acidified with 0.1% of TFA, the column temperature was set at 30 °C and the flow rate was 0.3 mL/min. The major peak (6.7 min) was identified as (-)-alliin ((-)-**1a**) by means of a garlic extract, and the second peak (8.1 min) as (+)-alliin, the natural form of alliin. Two other peaks were identified as by-products of the synthesis: remaining L-cysteine was detected at 4.3 min and deoxyalliin after 11.5 min. The final impurity at 13.1 min is alliin overoxidized to sulfone. LC-MS analysis confirmed this hypothesis. Tests on methiin showed that the method also succeeds in the separation of other diastereoisomers of cysteine sulfoxides: the resolution between (+) and (-)-methiin is 1.08. Finally, the method provided a good separation of other organosulfur compounds in an aqueous garlic extract (Figure 4.6). Peaks were identified as methiin, cycloalliin, and isoalliin by comparing the retention times and UV spectra with those of reference compounds (synthesized standards and/or molecules identified by the HPLC method developed by Ichikawa et al.¹⁶). The final peaks were identified as most likely being γ -glutamyl cysteine derivatives.

The reported separation on an amino HPLC column¹⁶ was then compared to our method. The "amino" stationary phase consists of propyl-amino silane bonded to silica. This method separates the two forms of alliin in 12 min. The resolution between (+) and (-)-alliin is 1.08 (with 0.05% of phosphoric acid in the mobile phase). The PGC method leads to a resolution > 3 . Furthermore, the flow rate (1 mL/min compared to 0.3 mL/min) on the amino column led to a smaller response factor, therefore less sensitivity.

4.2.2 Method validation by the accuracy profiles

The optimized HPLC method was validated according to the accuracy profile procedure.^{31,32} Calibration standards were used to establish the response function, while validation standards were used as samples of unknown concentrations to validate the analytical method. Three replicates of four calibration standards (concentrations: 0.1, 0.5, 1.0 and 4.0 mg/mL of L-(\pm)-alliin in water) were prepared and analyzed. This manipulation was repeated on three different days by three different operators (three series). The same concept was applied to the validation standards: five standards (0.1, 0.5, 1.0, 1.5, 3.0 mg/mL) underwent the same process. In a first step of the method validation, the accuracy criteria (trueness and precision) were checked for concentrations between 0.1 and 4.0 mg/mL. The second step allowed representing the accuracy of the method through its accuracy profile. After injection, data were processed as follows (Figure 4.7):

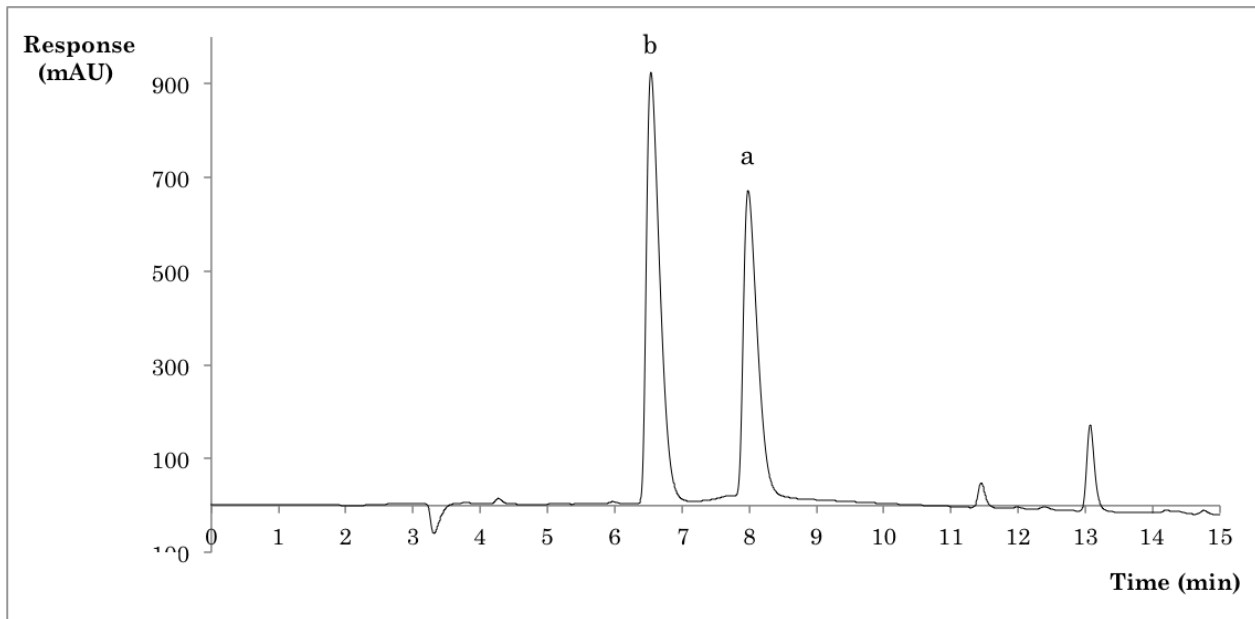


Figure 4.5: Optimized separation of (+)- and (-)-alliin on PGC column (flow: 0.3 mL/min, gradient ACN 0%–16% in 10 min, temperature: 30 °C, acidification of the mobile phase: 0.1% TFA). Peaks: a, (+)-alliin ((+)-**1a**); b, (-)-alliin ((-)-**1a**)

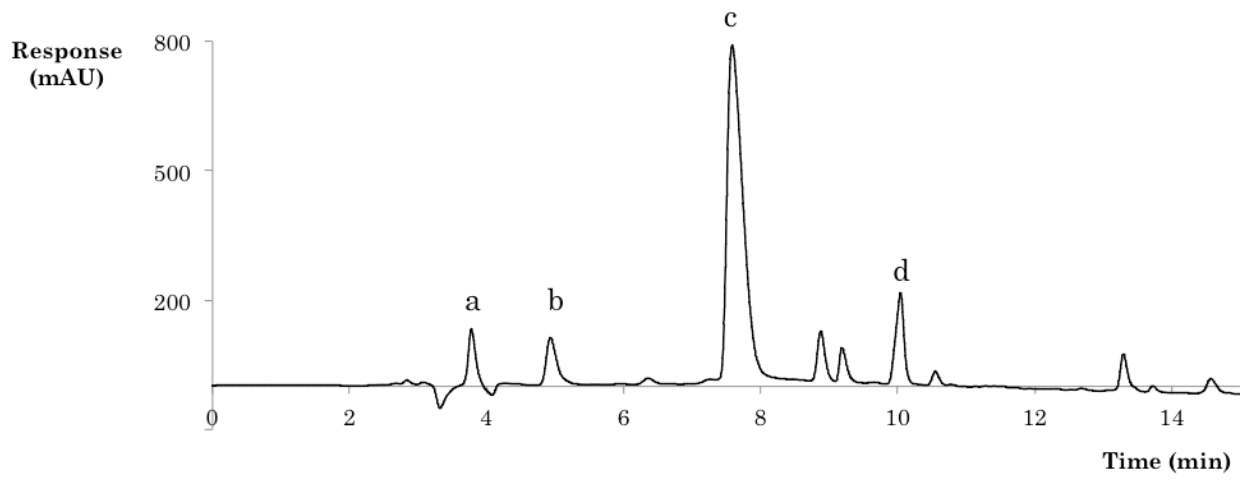


Figure 4.6: Typical PGC-phase chromatogram of garlic aqueous extract. Peaks: a, methiin (**1b**); b, cycloalliin; c, alliin (**1a**); d, isoalliin.

1. The three series of calibration standards were injected, the peaks integrated and the calibration curves plotted. The best fitting regression model was selected. Then, the response function (relationship between the peak area and the concentration) was established through the chosen regression model.
2. The validation standards were then injected, and the peaks areas were measured.
3. The concentrations of the validation standards were determined thanks to the response function chosen in step 1.
4. The trueness (the mean bias) was estimated for each concentration level of the validation standards, as well as the precision.
5. The accuracy profile was drawn according to the regression model chosen in step 1.

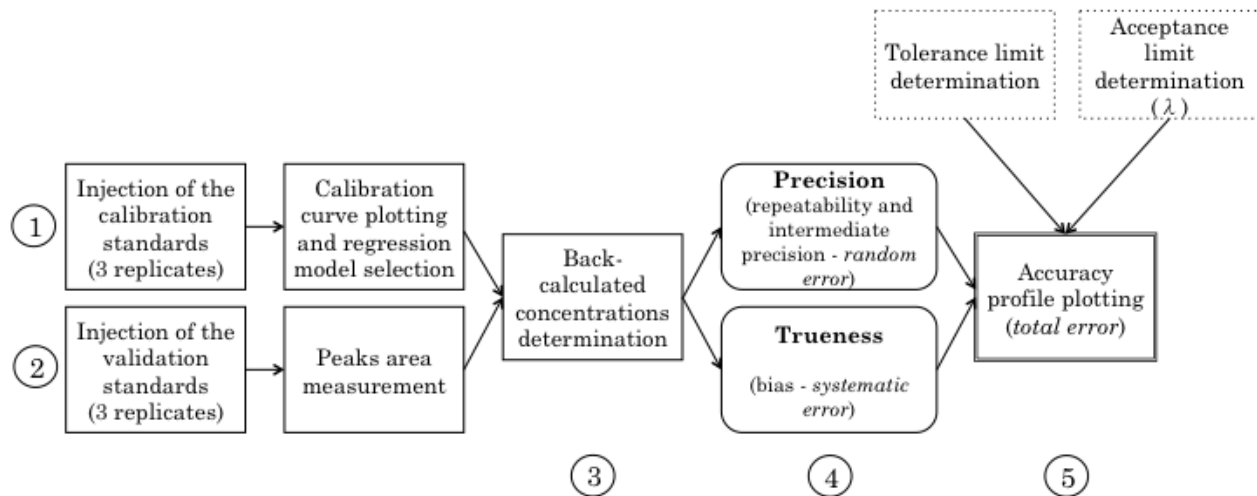


Figure 4.7: Accuracy profile methodology.

Response function and linearity

The response function is the mathematical relationship between the concentration and the response (the signal) within a concentration range. It is determined using a calibration curve and is often linear (even if exceptions exist, *e.g.*, with particular detectors or wide concentration ranges).³¹ UV-detectors should provide a linear response according to Beer-Lambert's law. The calibration curve is sometimes confused

with linearity, which actually describes the relationship between the concentrations injected and the back-calculated concentrations (even if the curve is not a straight line).³² It is important to check the suitability of the model but also the linearity of the response function. The curve was drawn and the linear model for the response function fit with a mean correlation factor (R^2) for the three curves of 0.9999. The choice of the model can also be corroborated with the linearity profile (Figure 4.8). The regression line of the relation between the introduced concentrations and the back-calculated concentrations fits, because the β -expectation limits (with $\beta=95\%$ in the Student's t-test) are fully included in the acceptance limits (set at 10%).

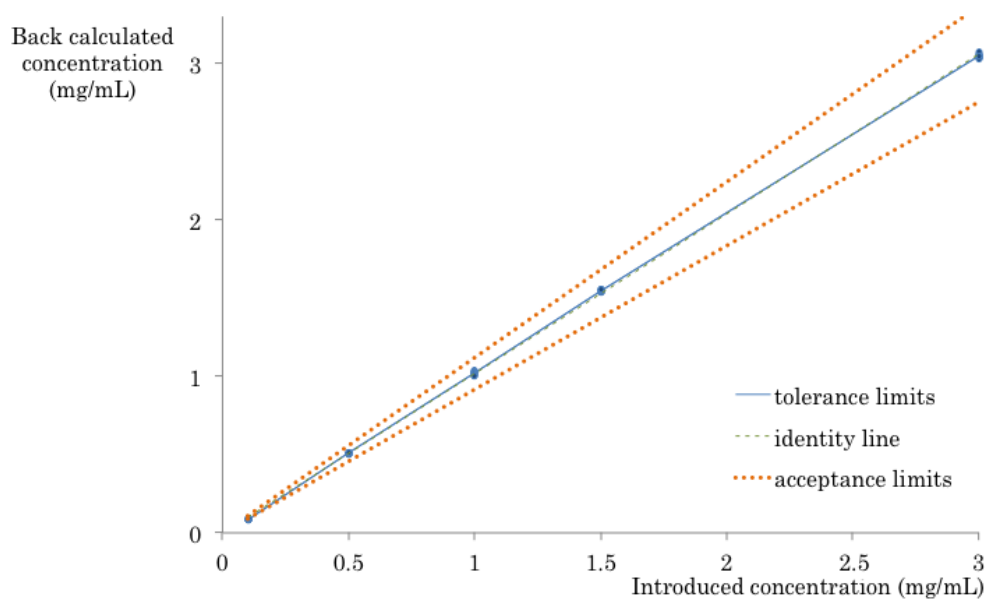


Figure 4.8: Linearity profile. The linearity of the chosen response function is satisfactory: β -expectation or tolerance limits (blue lines) are within the acceptance limits (10%, orange dotted lines).

Accuracy of the method

The accuracy of an analytical method depicts the closeness between the observed value and the true value (fixed by another tool, here with scales). The performance criteria calculated are the trueness (systematic error) and the precision (random error), the latter including the repeatability and the intermediate precision. The *trueness* represents the systematic error (or relative bias) and depicts the closeness between the theo-

retical value (accepted as the true value) and the mean value within series of measurements. It is expressed in absolute or relative value. Differences smaller than 5% are usually considered as acceptable.³⁰ It is the case for the four highest concentrations tested (Table 4.1). The *precision* expresses the closeness between series of measurements obtained from multiple analysis of one sample. Measurements done the same day by the same operator give the repeatability, while those on different days by different operators give the intermediate precision. The repeatability expresses the random error and should be less than 2%. Our analyses are excellent for all the tested concentrations. Finally, the intermediate precision, that illustrates the intra-laboratory variation and is supposed to be less than 2.5%, is acceptable except, once again, for the lowest concentration (Table 4.1). This approach to assess the method would exclude the theoretical concentration of 0.100 mg/mL, but the accuracy profile, which combines all the information, is a better tool to make a decision and may lead to a different conclusion.

Table 4.1: Performance criteria at five concentrations. The lowest concentration has to be excluded; its trueness and intermediate precision are not satisfactory.

Theoretical concentration (mg/mL)	Accuracy		
	Trueness (relative bias, %)	Repeatability (%RSD)	Precision Intermediate precision (%RSD)
0.100	13.9	1.66	9.47
0.500	1.6	0.54	0.57
1.000	2.0	0.43	1.48
1.500	3.2	0.62	0.49
3.000	1.6	0.41	0.45
Limit	5	2	2.5

Accuracy profile

Contrary to the one-by-one factor validation, the accuracy profile takes the global error into account. It shows the ability of the method to give a result within acceptance limits. The acceptance limits are arbitrarily set at 10%. The usual value for biological samples is 15%, and for pharmaceuticals 5%.³³ The trueness and the precision are assessed simultaneously: the trueness via the relative bias, and the precision through the β -expectation tolerance limits. The latter were set via a Student's t-test ($\beta=95\%$). Accuracy profile (Figure 4.9) gives the final information to decide if the method can be validated in the concentration range. The lowest concentration did not fulfill the fixed criteria: the low tolerance limit exceeded the acceptance limit. The method is therefore only validated for concentrations between 0.5 and 3 mg/mL. This concentration range is

satisfactory for the present analysis. The two ways to validate, accuracy profile and validation criteria, are consistent and show that the HPLC method is fully validated for concentrations between 0.5 and 3 mg/mL.

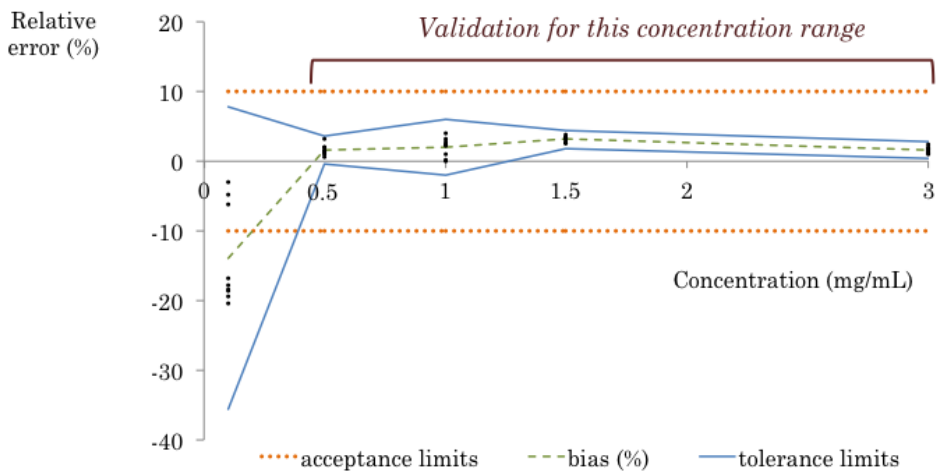


Figure 4.9: Accuracy profile: the relative error is within the 10% acceptance limits (orange dotted line), except for the lowest concentration. The method can therefore be validated between 0.5 and 3 mg/mL.

4.2.3 Conclusions

The porous graphitic carbon (PGC) column gave excellent results for the separation of structurally similar molecules such as diastereoisomers. Compared to the amino column, the resolution was up to four times higher. Furthermore, the quality of the developed method is clearly demonstrated. Parameters such as the resolution, symmetry of the peaks, or the number of theoretical plates have been optimized and are excellent. Furthermore, the method has been fully validated for concentrations between 0.5 and 3 mg/mL and was already applied in the laboratory. This range is suitable for our next experiments. The presented method is also versatile: the separation of other diastereoisomers such as (+) and (-)-methiin was achieved, as well as the analysis of the main organosulfur compounds in garlic aqueous extracts. This original method will allow further investigation on alliin, its synthesis, and its transformation into the high value-added biologically active molecules of garlic. Better knowledge of the formation of garlic organosulfur molecules could help in providing natural ways to improve health or fight diseases.

4.3 Preparation of pure stereoisomers of alliin

Alliin (**1a**) was discovered and extracted by Stoll and Seebeck in 1948,³⁴ and the first synthesis was achieved two years later by the same team.³⁵ The conformation of natural **1a** was found to be (2R,S_S), which corresponds to (+)-alliin. A mixture of stereoisomers (2R,S_S) and (2R,R_S) is easily obtained by the reaction between allyl bromide and L-cysteine followed by oxidation (Figure 4.2). Since then, little improvement has been proposed: Kubec et al.¹⁴ separated the diastereoisomers by recrystallization and a stereospecific synthesis was developed by Koch and Keusgen.³⁶ Aversa et al. proposed a stereospecific synthesis of analogues by reacting a sulfenic acid with a Michael acceptor.³⁷ A review was published in 2015 on the synthesis of alliin, isoalliin and selenoalliin.³⁸ The purification of the diastereoisomers (+)-**1a** and (-)-**1a** is reportedly achieved by recrystallization and HPLC. This section attempts to improve the production of pure (+)-**1a** for further studies. Factors such as the price, waste generation and toxicity were taken into account to choose the best method.

The Mislow-Evans rearrangement is a known rearrangement interconverting allyl sulfenates and sulfoxides. Furthermore, allyl alcohol is the main product of the thermal decomposition of alliin, suggesting that the rearrangement to a sulfenate takes place at high temperatures.³⁹ If the equilibrium leads to a racemic mixture, there is no point in trying to make pure **1a** (Figure 4.10). Before any work was done, we needed to assess the stability of a pure stereoisomer. A sample of (+)-alliin (purified from a synthetic mixture) was allowed to stand at room temperature for three weeks. The stereoisomer ratio was measured by HPLC and did not change (*i.e.* no (-)-**1a** was observed). Racemization at room temperature does not seem to occur, probably because a higher temperature is required for the rearrangement to take place. Our own experiments on the thermal degradation of alliin at 100 °C indicated no degradation at 80 °C, but at 100 °C. Once this was settled, we could move on to the different ways to prepare (+)-alliin. Extraction from garlic cloves, synthesis followed by separation of the stereoisomers and stereospecific synthesis have been investigated.

4.3.1 Extraction and purification of (+)-alliin from garlic cloves

In order to extract alliin from garlic cloves, the enzyme that would convert it needs to be deactivated. Phenol was used,⁴⁰ as well as extracts from cloves boiled in water¹⁵ or in methanol/water.^{17,41} We have extracted alliin from garlic cloves under different conditions to compare the efficiency of temperature, pH and solvent

Mislow-Evans rearrangement:

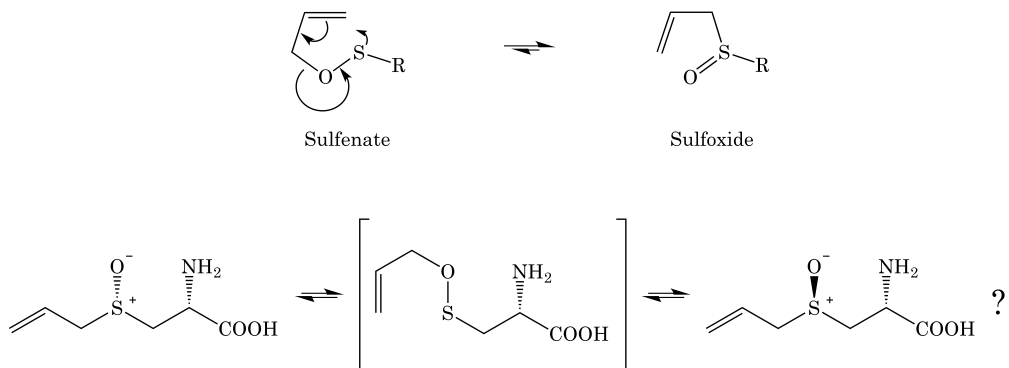


Figure 4.10: If (+)-alliin easily racemizes via Mislow-Evans rearrangement, the relevance of making pure diastereoisomers would have been questioned. After 3 weeks, no signs of racemization are observed.

in inactivating alliinase. Yield was assessed by calculating the alliin content with our HPLC method. The highest yield we obtained was 49.8 mg/g of dry matter.

We first verified the thermal stability of alliin by regularly sampling a solution of synthetic (\pm)-alliin in water at two temperatures, 80 °C and reflux, for 4 h. HPLC analysis revealed no concentration change at 80 °C but a degradation at 100 °C after 1 h.

Water and MeOH/water mixtures were tested. Extraction of (+)-alliin in water without cosolvent called for a minimum temperature of 80 °C (to deactivate alliinase). Addition of methanol (fMeOH:H₂O proportion 9:1) led to deactivation of the enzyme at temperatures as low as 20 °C. Addition of HCl as denaturing agent was also investigated, but did not give superior results. All of these solvent systems were applied to classical extracts (crushed cloves in solvent), Soxhlet and ultrasound assisted extractions (Figure 4.11, left). A mixture of MeOH/H₂O 9:1 at 60 °C is recommended to deactivate the enzyme.

Once the optimal solvent system had been determined, three substrates were tested: fresh cloves, home-made garlic powder (cloves in liquid N₂, ground and lyophilized) and commercial garlic powder (Figure 4.11, right). The amount of alliin extracted from freshly prepared powder is higher than the amount extracted from fresh cloves, probably because the size of particles allows a better diffusion of alliin, and commercial powder, in which alliin may have been degraded over time. Assisted extractions (ultrasound, microwave) did not improve the yield of this extraction. Cysteine sulfoxides (CSOs) are thought to make up 1 to 5% of the dry matter of garlic cloves, and our extraction represented 5% of the dry matter for alliin only. Alliin constitutes 83% of the ACSOs in garlic,⁴² but variability among garlic bulbs is known.¹⁰

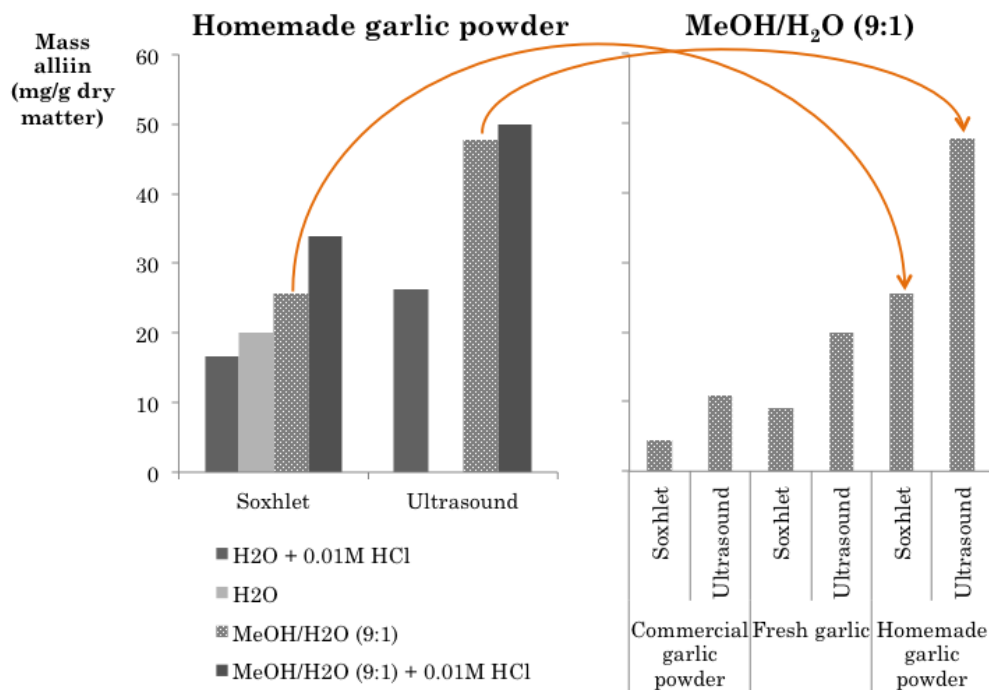


Figure 4.11: Conditions for the extraction of alliin from garlic cloves. Ultrasound assisted extraction in MeOH/H₂O is recommended with homemade garlic powder as a substrate.

Jiang et al. reported yields of 15.0 to 20.4 mg/g of garlic powder in an optimized alliin extraction⁴³ after we completed our experiments. The two step procedure uses (NH₄)₂SO₄, 1-propanol and NaCl in an aqueous two-phase extraction at 30 °C. Our methanol procedure gives superior results.

Purification of alliin from these extracts was done on silica gel, eluting with BuOH/MeOH/H₂O (3:1:1). Compound (+)-**1a** was isolated in over 90% purity and 80% yield. Reverse phase chromatography didn't provide a good separation. Jiang's research group developed a purification method on ion-exchange resin leading to an alliin purity of 80%.⁴³ A drawback of ion-exchange chromatography is the presence of salts in the purified fractions.

Production of (+)-**1a** by extraction and purification takes about a week. A mass of 64.2 mg of alliin was purified from 30 g of cloves (between 36% and 64% of the alliin initially present, based on the literature¹⁶) using MeOH, BuOH and common laboratory supplies.

4.3.2 Chemical synthesis followed by separation

A second option for the preparation of pure (+)-**1a** would be to synthesize a mixture of **1a**, then separate the stereoisomers. The separation could be achieved enzymatically (enzymatic resolution) or by chromatography. The synthesis is easily achieved in acceptable yield (60%). The (+)-**1a**:(-)-**1a** ratio is 4:6. Titration of alliin was performed to determine its pKa. pK_C and pK_N were found to be 3.7 and 9.75, respectively. The pI was calculated to be 6.7.

Enzymatic kinetic resolution

Alliinase has been reported to cleave (+)-alliin at a higher rate due to the better docking in the enzyme's active site (Figure 4.12).⁴⁴ The activity of alliinase varies among species and even brand or source of garlic.⁴⁴ For example, K_M of 1.6 mM and 2.8 mM are reported for L-(+)- and L-(-)-alliin, respectively, with alliinase from garlic powder.⁴⁵ Other sources mention a K_M value of 2.9 mM⁴⁴ and 2.2 mM⁴⁶ on racemic alliin. This difference in activity could be applied to resolve a mixture of diastereoisomers, since the products of the enzymatic reaction are easy to separate from unreacted amino acid (Figure 4.13). If we use alliinase from garlic, the non-natural stereoisomer (-)-**1a** would be isolated. However, reports of bacterial alliinase cleaving (-)-**1a** more selectively than (+)-**1a** (K_M (**1a**) = 2.3 mM and K_M ((+)-**1a**) = 5.7 mM, so K_M ((-)-**1a**)⁴⁷ probably around 1 mM or less) may provide a method to resolve the other diastereoisomer. Alliinase purification is described in the next section (4.4).

The concept was first tested on an analytical scale (0.03 mmol of alliin). A mixture of (\pm)-alliin was mixed with purified alliinase under optimized conditions (37 °C, pH, cofactor, etc.) and the reaction was followed by HPLC. In particular, the starting material disappearance was measured by the PGC HPLC method described earlier. A first assay aimed to narrow down the time frame for this reaction (Figure 4.14), the second allowed a more accurate determination of the optimal parameters. Under these conditions, after 2.5 min, (-)-alliin represented 97% of the alliin sample, and little of the initial starting material has been lost (84% yield, Figure 4.15).

Despite these promising results, attempts to scale up the process (25 times, production of 150 mg of (-)-alliin) were unsuccessful. If the amount of enzyme is kept constant or even tripled when the substrate concentration is increased, no change in the concentration of (+)-alliin is observed in over 2 h. The turnover of the enzyme is not maintained under these conditions. A proportional scale-up is out of question, since

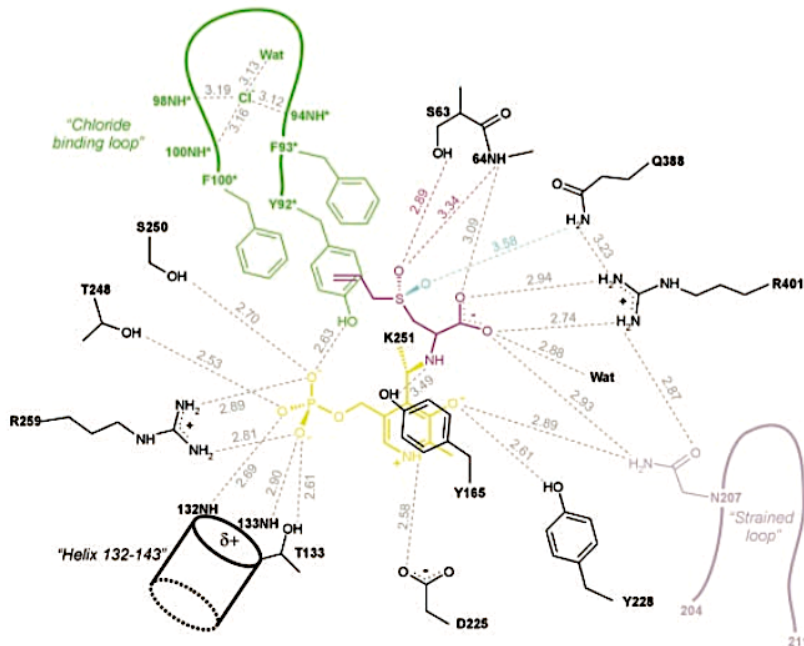


Figure 4.12: (+)-Alliin (magenta) and (-)-alliin (cyan) bind differently in the active site of alliinase (Figure from Keusgen et al.⁴⁴).

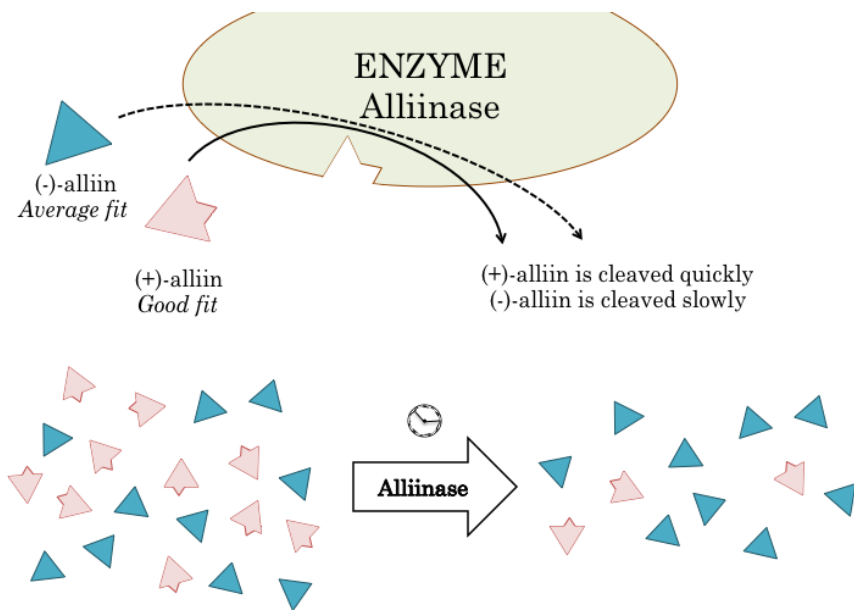


Figure 4.13: (+)-Alliin (magenta) and (-)-alliin (cyan) react with alliinase at different rates thanks to their difference in affinity (see Figure 4.12). This phenomenon could be used to resolve a mixture of **1a**.

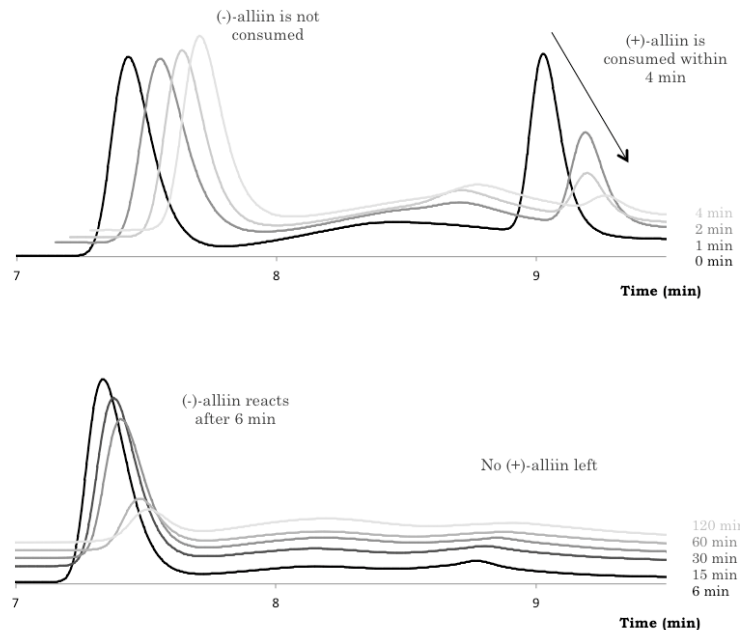


Figure 4.14: Enzymatic resolution of (\pm) -alliin by alliinase: HPLC chromatograms of the samples (from 0 to 120 min).

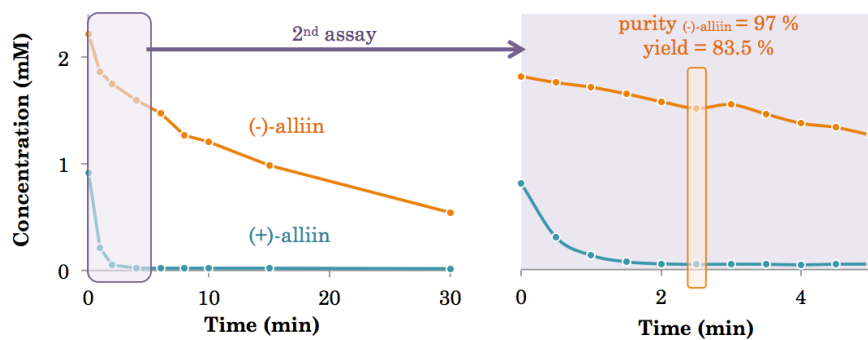


Figure 4.15: $(+)$ -Alliin and $(-)$ -alliin are resolved in 2.5 min by alliinase under optimal conditions for the enzymatic reaction (37 °C, pH, concentrations and cofactor optimized).

the amount of resources to invest in the extraction of alliinase (garlic and reagents) and in the reaction itself (PLP) would not be economically feasible.

Chromatography

The literature reports a separation of (+)- and (-)-**1a** on silica gel TLC with Rf of 0.58 and 0.49 when eluted by 1-butanol/acetic acid/water (2:1:1).³⁹ This mobile phase is close to what was used for the purification of the natural product, and can probably also be applied on the synthetic mixture. A different stationary phase was tried: amino-modified silica gel, like the HPLC method by Ichikawa et al.¹⁶ The mobile phase selected was ACN/H₂O (3:2). After elution, fractions were identified by TLC. Compounds (+)-**1a** and (-)-**1a** were recovered and their purity assessed by NMR and HPLC. A purity of 95 and 92% was found for (+)- and (-)-**1a**, respectively. The yield of (+)-**1a** is low, with only 40% of the material being recovered, while all the (-)-alliin is recovered. This can be explained by the fact that (+)-**1a** is tailing on the column and TLC. The synthesis has a yield of 60%, but only 40% of the product is (+)-alliin. The overall yield is 10%, with a two-step synthesis and a separation by column chromatography.

Despite numerous attempts to separate the diastereoisomers of alliin on carbon graphite (by analogy to the HPLC method), the separation was not good enough with a self-packed column. Preparative columns are prohibitively expensive, and this approach was abandoned.

Recrystallization

Stoll et al.⁴⁸ and then Kubec et al.¹⁴ reported recrystallization as a way to purify the stereoisomers of ACSOs. Attempts to use Stoll's technique in acetone/water failed. Recrystallization in ethanol/water was more successful, leading to up to 60% of (+)-**1a**. The yield was low (5%, as reported), but the material is not lost. With some improvement, it can be a good way to purify (+)-alliin. After our experiments were finished, Gupta et al. reported a successful isolation of (+)-alliin in 13% yield by recrystallization in aqueous ethanol.³⁸

4.3.3 Stereospecific synthesis

Two stereospecific oxidations have been attempted: enzymatic oxidation, and oxidation with a chiral ligand. Enzymatic oxidation by mono-oxygenases or oxidases showed good stereoselectivity (review by Faber⁴⁹). Mono-oxygenases require nicotinamide cofactors that can be expensive. Cyclohexanone mono-oxygenase has

been tested by Koch et al.³⁶ and leads to a diastereoisomer ratio of 82:18 of (+)-**1a**/(-)-**1a**. However a garlic smell was noticed during oxidation, indicating unexpected side reaction(s). We decided to add deoxyalliin to a culture of *Acinetobacter calcoaceticus*, known to produce a mono-oxygenase,⁵⁰ and see if any alliin was recovered. The following questions needed to be addressed:

1. Is oxidation occurring, *i.e.* is the enzyme extracellular? If not, the work required to extract and purify the enzyme may not be worth the result.
2. Is the enzyme stereospecific, ideally affording a better ratio than previous reports?
3. Is the yield sufficient?

Analysis of the crude cell culture showed oxidation to alliin when the cells were in a stationary phase (as opposed to the log phase). This result is consistent with the microorganism metabolism.⁵⁰ The diastereoisomer ratio was inverted compared to the oxidation by H_2O_2 , *i.e.* 63:37 ((+)-**1a**/(-)-**1a**). However, only a small portion of deoxyalliin had reacted. Purification from the culture medium is too tedious with low yield and poor diastereoisomeric purity.

A stereospecific synthesis using diethyl tartrate and $\text{Ti}(\text{O}i\text{-Pr})_4$ similar to Sharpless' epoxidation was proposed by Koch et al.³⁶ The diastereoisomeric excess in (+)-alliin was 74%. The amino and carboxy groups of deoxyalliin had been protected by *tert*-butoxycarbonyl and 9-fluorenylmethyl, respectively. The oxidation was performed with cumene hydroperoxide (CHP).

Protection of the amine and carboxylic acid of deoxyalliin (**71**) was performed in two steps to lower its hydrophilicity (Figure 4.16). A similar result was obtained in the synthesis of (*S*)-tenatoprazole, a proton pump inhibitor, with another Kagan system.⁵¹ The stereospecific oxidation of the sulfur was attempted with a chiral ligand (*cis*-1-amino-2-indanol), a catalyst (titanium isopropoxide) and CHP (oxidant) on N-BOC deoxyalliin (Figure 4.17, top). The first results were encouraging, and the crude NMR seemed to indicate stereospecificity. However, product was recovered. Other ideas included oxidation with Davis' chiral oxaziridines (Figure 4.17, middle) or cyclization to a oxazolidinone (**72**) with pivalaldehyde to promote oxidation on one side (Figure 4.17, bottom).⁵² Unfortunately, none of these efforts were successful and the project was discontinued.

4.3.4 Conclusions

The results for the production of pure (+)-alliin are summarized on Figure 4.18.

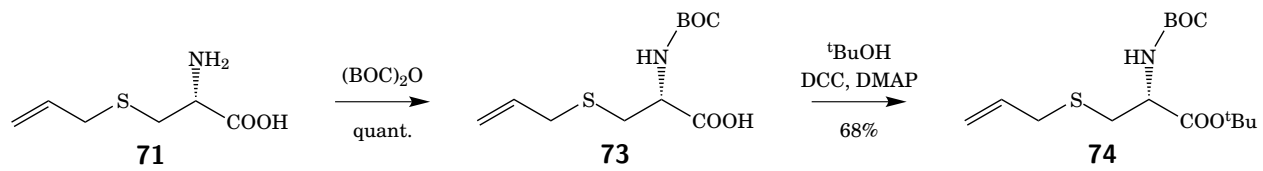


Figure 4.16: Protection of the amine and carboxylic acid functions of deoxyalliin (**71**).

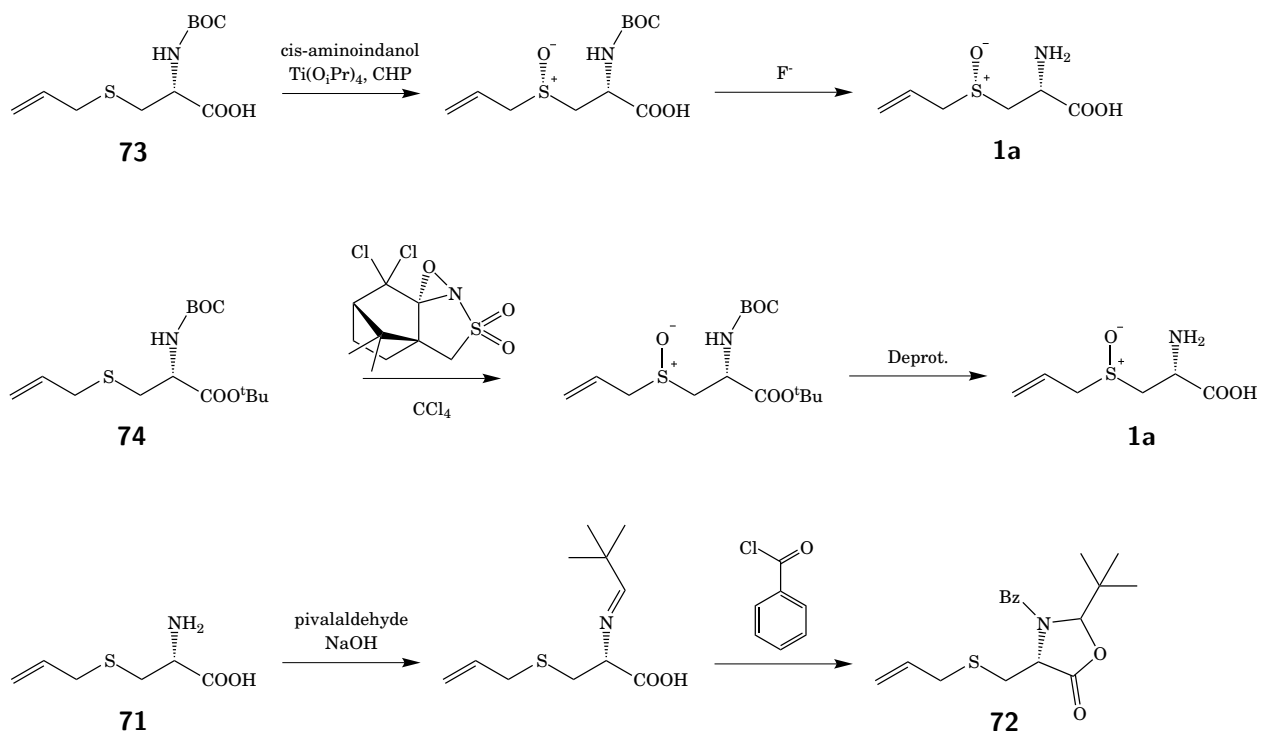


Figure 4.17: Proposed stereospecific synthesis of alliin (**1a**) from protected deoxyalliin (**73** and **74**) or deoxyalliin (**71**). Oxidation with chiral ligand *cis*-aminoindanol (top)⁵¹ or chiral oxaziridine oxidant (middle), as well as cyclization to an oxazolidinone (**72**, bottom)⁵² to promote oxidation on one face were tested. Despite promising results, these syntheses were not pursued.

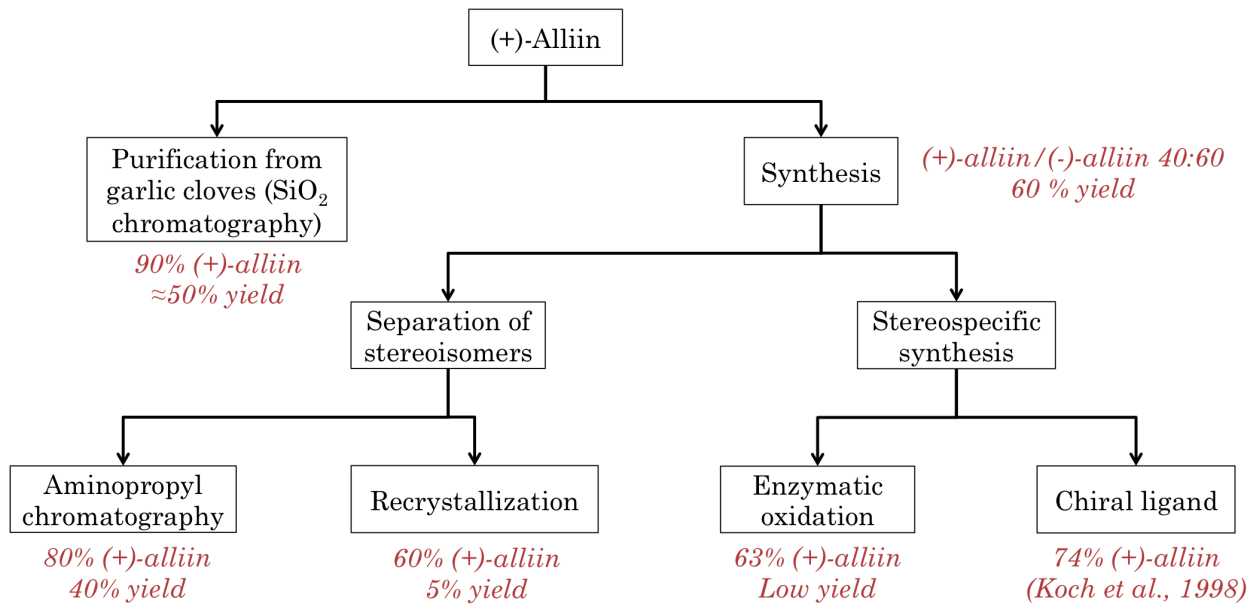


Figure 4.18: Summary of the different approaches in the production of pure (+)-alliin. Purification from garlic cloves is recommended as the most economic and ecological path.

In the light of the above results, we can conclude that the most economic way to produce pure (+)-**1a**, both in terms of time and resources, is by synthesis followed by purification on amino modified silica gel. In fact, the synthesis is straightforward with only two steps, the work-up is very simple, and the separation leads to good purity in a satisfactory yield. The second best option is the extraction from garlic cloves. This option also makes sense ecologically, since the solvents used, methanol and butanol, are the only by-products besides garlic pulp.

4.4 Alliinase purification

Alliinase was used in the previous chapter. Improvements to its extraction are described in this section. Two extraction procedures were compared: protein precipitation by ammonium sulfate, or by polyethylene glycol (PEG) 8000. Purity of the alliinase was assessed by SDS-PAGE and the specific activity of the enzyme. After precipitation, each extract was purified by affinity chromatography (Concanavalin A on Sepharose, ConA) or size exclusion chromatography. The purity and activity of crude alliinase is compared to that for purified alliinase in Figure 4.19.

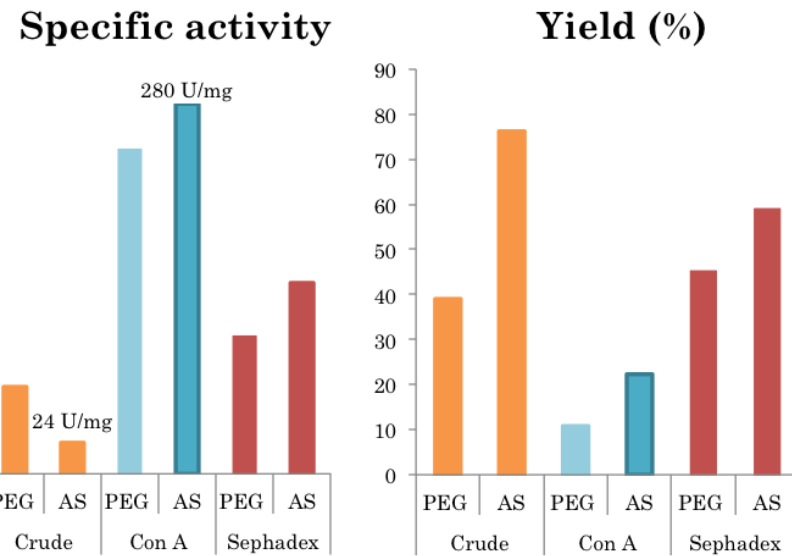


Figure 4.19: Yield of extraction is superior with ammonium sulfate (AS). The purification on ConA-Sepharose is superior than the size-exclusion chromatography in terms of purity of the recovered enzyme. Ammonium sulfate precipitation followed by ConA purification is the recommended procedure. (Yield based on the reported values for alliinase in garlic cloves, specific activity normalized to the maximal specific activity, 285 U/mg of alliinase, of the $(\text{NH}_4)_2\text{SO}_4$ -ConA product).

The yield of ammonium sulfate extraction is always higher, almost twice the yield of PEG 8000. The purity after affinity chromatography is superior, as indicated by the higher specific activity. The specific activity of 285 U/mg is comparable to the activity reported in the literature (228-660 U/mg depending on the garlic).⁵³ The purity of each sample as assessed by SDS-PAGE matches the specific activity, even if it is not easy to quantify the intensity of the stained bands.

We recommend using ammonium sulfate for the extraction. As a matter of fact, even if the procedure is more tedious because it requires a dialysis step, the amount of material collected is worth the work. Another option would be to purify on Sephadex first, then on ConA-Sepharose. This would avoid the use of a methyl α -D-mannopyranoside gradient to elute alliinase from ConA.

4.5 Extraction of vinyldithiins from garlic

The following material has been published in European Food Research and Technology (Dethier, B.; Hanon, E.; Maayoufi, S.; Nott, K.; Fauconnier, M.-L. Optimization of the Formation of Vinyldithiins, Therapeutic

*Compounds from Garlic. Eur. Food Res. Technol. 2013, 237, 83–88.*⁵⁴ The content of this section draws heavily on the article.

As explained in 1, vinyldithiins (**5**) are one of the main products of the rearrangement of allicin. Two different vinyldithiins have been discovered by Brodnitz⁵⁵ (one structure has been corrected by Block et al.⁵⁶): the 3-vinyl-4*H*-1,2-dithiin or 1,2-vinyldithiin (**5b**), and the 2-vinyl-4*H*-1,3-dithiin or 1,3-vinyldithiin (**5a**, Figure 4.20). A study by Keophiphath et al.⁵⁷ highlights the capacity of 3-vinyl-4*H*-1,2-dithiin to inhibit the differentiation of preadipocytes by reducing the gene expression of adipogenesis transcription factors. Obesity is an important factor contributing to the increase in chronic diseases, such as diabetes, cardiovascular diseases or musculoskeletal disorders.⁵⁸ Adipocytes are cells which form the adipose tissue. Their size can reach up to fifty times the size of their precursors, the preadipocytes, by the storage of fat during the differentiation process. The control of adipose tissue expansion could be an answer to fight obesity. Numerous studies have been undertaken to investigate the health benefits of compounds extracted from garlic.^{59,60}

Both vinyldithiins have shown cholesterol lowering⁶¹ and antioxidant activities.⁶² Pharmacokinetic assays of vinyldithiins show that they were found in the serum, kidney and fat tissues of rats 24 h after oral ingestion.⁶³ 1,2-Vinyldithiin was degraded in whole blood in 15 min, while the amount of 1,3-vinyldithiin did not change after 2 h,⁶⁴ confirming that the first compound is more lipophilic and tends to accumulate more in the fat tissue than the 1,3-vinyldithiin.⁶³ This property corroborates the fact that only the 1,2-vinyldithiin has an influence on the adipogenesis.

Figure 4.20 shows the biosynthetic route to 3-vinyl-4*H*-1,2-dithiin (or 1,2-vinyldithiin, **5b**) and 2-vinyl-4*H*-1,3-dithiin (or 1,3-vinyldithiin, **5a**). When garlic is crushed, enzyme alliinase acts on its substrate, alliin, forming sulfenic acid **2a**. Allicin (**3a**) is formed by condensation of two molecules of **2a**, and can rearrange to **2a** and thioacrolein (**6**). The suggested mechanism for the formation of vinyldithiins is a Diels-Alder addition of two thioacrolein molecules.⁵⁶ Garlic extracts and synthetic allicin preparation in oil and solvents both contain a higher amount of 1,3-vinyldithiin than the corresponding 1,2-vinyldithiin.^{56,59,65} The aim of this work is to optimize the extraction and purification of vinyldithiins from fresh garlic as a key step for further studies on the therapeutic effect of these interesting organosulfur compounds.

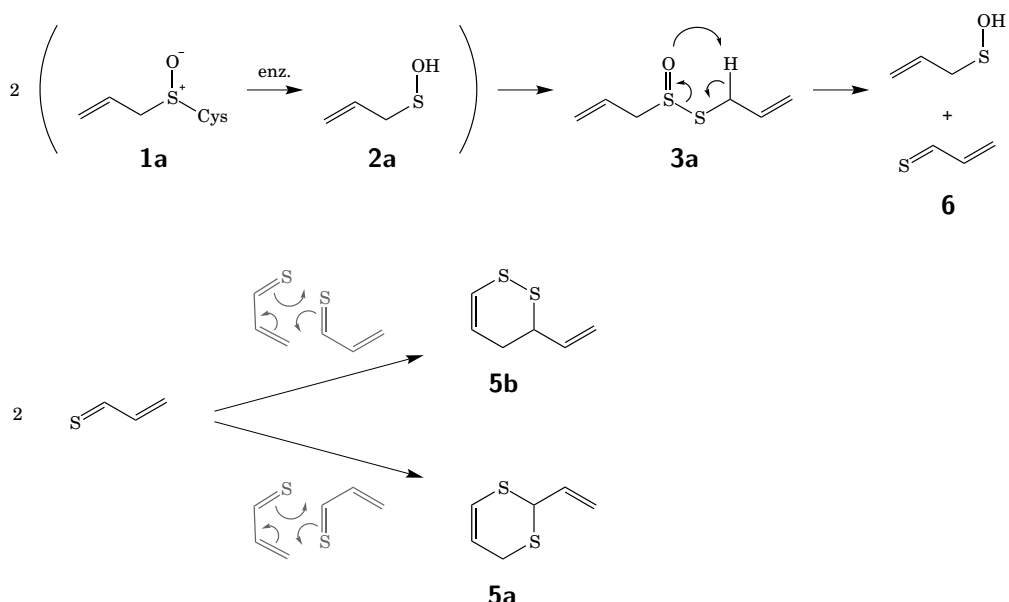


Figure 4.20: Alliin (**1a**) is cleaved by alliinase and forms 2-propenesulfenic acid (**2a**) then allicin (**3a**). The latter can decompose and thioacrolein (**6**) is formed. Two molecules of thioacrolein undergo a Diels-Alder reaction to form vinyldithiins **5b** and **5a** (predominant form).

4.5.1 Extraction optimization

Best garlic and oil for the extraction

Garlic of different origins was used for extraction in sunflower oil. The highest quantity of both 1,2- and 1,3-vinyldithiin were obtained with Spanish garlic (Figure 4.21, top). Eight oil types were compared for extraction of vinyldithiins from Spanish garlic. The formation of vinyldithiins was the highest in olive oil, but the result was similar with sunflower oil. The latter would be the best choice for scaling up considering that it is much cheaper than olive oil. For the eight oils tested, the iodine value, the acid value and the fatty acid composition were determined but no correlation could be found between the amount of vinyldithiins obtained and any of these parameters. Other physico-chemical parameters of the oils could be involved. Finally, the influence of the garlic/oil weight ratio on the extraction of vinyldithiins from Spanish garlic in olive oil was studied (Figure 4.21, bottom). The 1:2 and 1:3 ratios provided similar amounts of vinyldithiins. The 1:2 proportion is therefore the most economical choice.

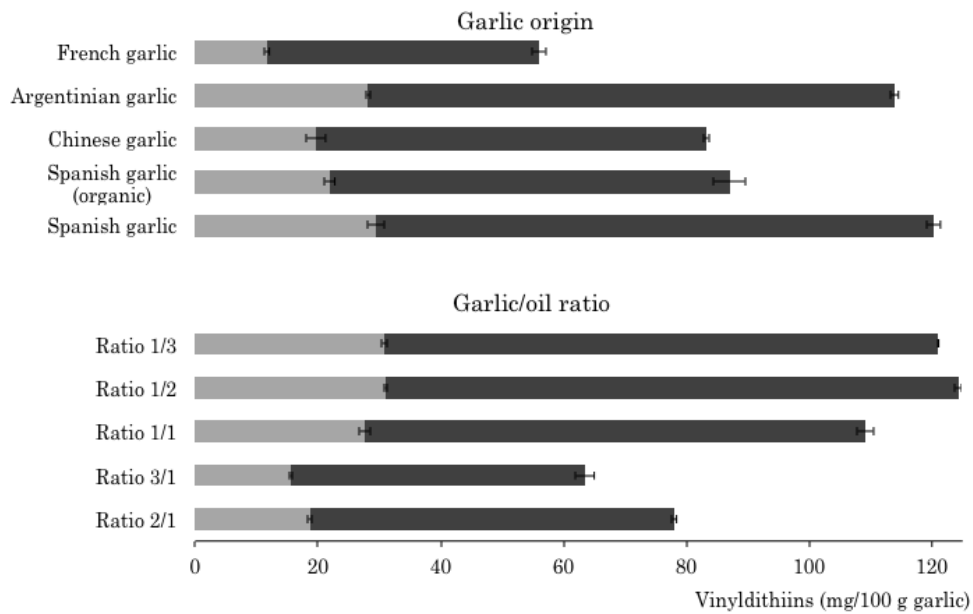


Figure 4.21: Extraction optimization, influence of the garlic origin and the garlic/oil ratio. Spanish garlic in a 1/2 weight ratio provided the highest amount of 1,2- and 1,3-vinyldithiin.

Extraction conditions

Extraction conditions (temperature, with or without stirring) of the vinyldithiins from Spanish garlic in olive oil in a 1:2 garlic/oil ratio (w/w) during 24 h were optimized. A temperature of 37 °C provided the highest quantity of vinyldithiins Figure 4.22, top). This value can be linked to alliinase optimal activity temperature (between 30 °C⁶⁶ and 40 °C¹³). At 37 °C, the amount of vinyldithiins decreased 3.5 fold when magnetic stirring was used (Figure 4.22, bottom). Stirring is therefore a key parameter. The kinetic assay done under optimal conditions (Spanish garlic, olive oil, 1/2 ratio, 37 °C and no stirring) showed a rapid increase in amounts of vinyldithiins during the initial 6 h. However, yields decreased after about 10 h (data not shown). This may be due to volatilization of the compounds or to degradation by oxidation, temperature or other reactive compounds present in the macerate. Oxidation is also possibly enhanced with stirring. The impact of oxidation on the extraction and degradation of the products was assessed by comparing the results obtained when bubbling argon or air during the extraction. No significant differences were found between the amounts of vinyldithiins after the two processes, even if the appearance of the oils were different. This result indicates that the oil was oxidized, but it did not influence the amount of vinyldithiins in the final

extract. Finally, a second and third extraction performed on the same, extracted, garlic pulp did not release additional vinyldithiins.

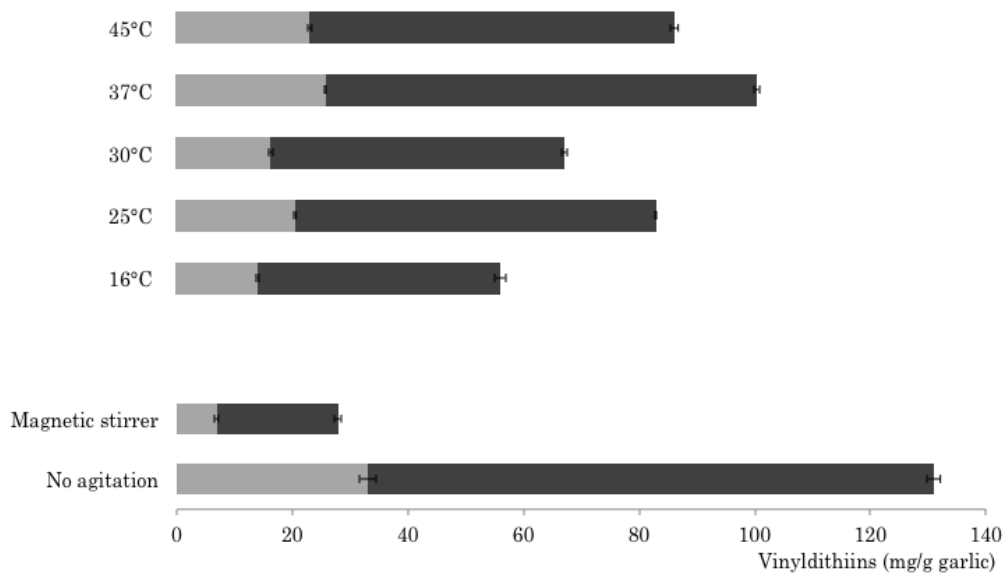


Figure 4.22: Extraction optimization, influence of temperature (no stirring) and stirring. Extraction at 37 °C with no stirring provided the highest amount of 1,2- and 1,3-vinylidithiin.

Assisted extractions

The application of microwave or ultrasound increased the extraction yields (Figure 4.23), especially microwave (quantity up to 3.6-fold compared to the classical extraction process). This result might be linked to rupture of the cell walls under the pressure developed by the heating of cells water under microwave,⁶⁷ and the development of over-heated zones in the sample that could improve this effect.⁶⁸ The instantaneity of the heating in the core of the sample could also explain the performance of the microwave assisted extraction,⁶⁹ as well as the homogeneous distribution of the pulp in the vessel. To our knowledge, no mention of microwave-assisted extraction using edible oil as solvent is reported in the recent literature on natural product isolation. The complexity of the edible oil composition and its interactions with the sample matrix does not allow us to draw conclusions regarding the oil extractive performances. However, this solvent meets the requirements for microwave-assisted extraction:⁷⁰ the solubility of vinyldithiins in oil is suitable and oil absorbs microwave, ensuring rapid heating of the sample and improving the extraction. Furthermore, the microwave-assisted extraction is easier to set up than the extraction using an ultrasound bath.

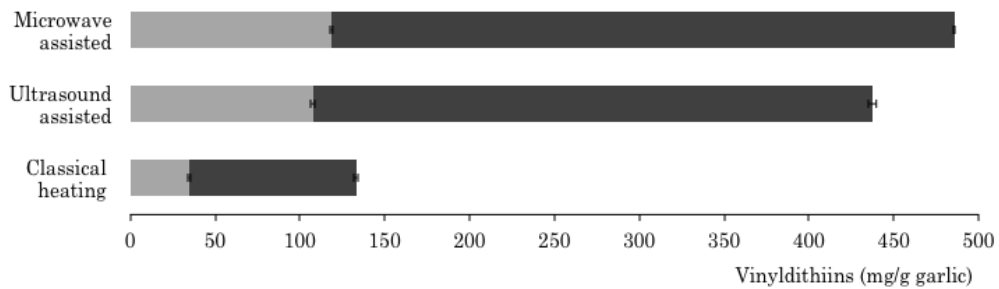


Figure 4.23: Assisted extractions (microwave or ultrasound) induced a better extraction of both vinyldithiins (up to 3.6-fold in microwave oven).

4.5.2 Conclusions

After having selected the best garlic and oil type for vinyldithiins production, the extraction conditions (temperature with or without stirring, garlic/oil ratio) were optimized. The best yield was achieved with Spanish garlic in sunflower or olive oil in a 1:2 weight ratio at 37 °C in 6 h. Under these conditions, 500 mg of vinyldithiins (1,2- and 1,3-vinyldithiin) was obtained from 100 g of fresh garlic (4-fold increase compared to the initial conditions). Stirring diminished the yield, and microwave-assisted extraction led to a further increase in the amount of vinyldithiins (3.6 fold compared to the non assisted optimized process). For quantification purposes, the 1,2- and 1,3-vinyldithiins were purified by preparative HPLC from garlic oil macerates with high purity. The results obtained in this study can be applied for the production of vinyldithiins with a high yield in edible oil. The extract could be incorporated in food preparations in order to prevent obesity. Furthermore, other studies on the effects of vinyldithiins as therapeutic agents can be tested with pure compounds obtained with high yield.

4.6 Conclusion

An HPLC method was successfully developed to quantify the diastereoisomers of alliin. This work was published in *Talanta*.¹ Investigations on alliin highlighted the most economical way to prepare pure (+)-alliin, by synthesis followed by separation of the stereoisomers. Finally, the preparation of alliinase and vinyldithiins have been optimized, and the latter was published in *European Food Research and Technology*.⁵⁴

Garlic and the compounds derived from garlic have been extensively studied, and providing original work is challenging in this respect. Despite this context, our work presents important aspects of *Allium*

chemistry. Firstly, it provides hands-on information on how to analyse and prepare alliin, alliinase and vinyldithiins that can be useful for production in future research or for the industry. The work on the preparation of stereoisomers of alliin can be seen as a more theoretical study on the different ways to make a stereochemically pure natural product. Finally, comparing these ways while taking into account factors such as the environment and costs is in line with a contemporary approach of atom efficiency and solvent economy.

4.7 Experimental

NMR spectra were recorded in D_2O , unless otherwise indicated, on a Varian Unity 600TM, operating at 600 MHz for proton and 150.87 MHz for carbon. The chemical shifts (δ) are indicated in ppm downfield from tetramethylsilane, with the internal standard being the residual H_2O (4.72 ppm). Infrared spectra of the neat compounds were recorded on a Bruker IFS 48. KBr pellets were prepared (1 mg/100 mg KBr). Mass spectra were obtained using a Bruker Esquire HCT electrospray combined with an ion trap. Nitrogen is generated by a Nitrox system (UHPLCMS 18). Solutions of 5 $\mu\text{m}/\text{mL}$ in miili-Q water are analyzed by infusion mode. Analytical TLC was performed on precoated silica gel plates (Merck) with a 254 nm fluorescent indicator and was visualized under a UV lamp and by staining with a phosphomolybdic acid solution.

The HPLC system used for the study consisted of a Hewlett-Packard 1100 series (Agilent Technologies), with the following specifications: a quaternary pump, an online degasser, an autosampler, a column heater and a diode-array detector. The data treatment was performed on the ChemStation software (Agilent Technologies). Two different columns were tested: an amino-bonded silica gel column Nucleosil 100-NH2 RP (125x3 mm, particle size 5 μm) provided by Macherey-Nagel and a porous graphitic carbon column (PGC, Hypercarb 150x3 mm, particle size 3 μm , Thermo scientific). All reagents were of analytical grade. Acetonitrile provided by Scharlab was HPLC grade (>99.85%). Pure water was obtained from an Elix system Millipore.

Garlic extracts. Plant extract were prepared from fresh cloves bought at the local market: 20 g of cloves were carefully peeled and boiled in 200 mL of deionized water during 15 min, then crushed and boiled for 15 more minutes. The preparation was then filtered.

L-S-Allyl cysteine or deoxyalliin (71). L-Cysteine (24.2 g, 0.2 mol) is dissolved in a mixture of 240 mL of a 1M aqueous solution of NaOH and 400 mL of ethanol. The mixture is stirred at RT until complete

dissolution, then 20 mL of allyl bromide (0.216 mol, 1.16 eq) is added dropwise in 15 min. After stirring overnight at RT, the mixture is acidified by formic acid to pH 5.5. White crystals precipitate. The mixture is cooled to 4 °C then filtered. The filtrate is concentrated under vacuum, cooled down and newly formed solid is recovered by filtration. The white powder is dried under vacuum. Yield: 94 %. ^1H NMR (600 MHz, D_2O) δ 5.68 (m, 1H, $\text{CH}=\text{CH}_2$), 5.07 (d, J = 9.6, 1H, $\text{CH}=\text{CH}_2$ cis), 5.04 (d, J = 16.8, 1H, $\text{CH}=\text{CH}_2$ trans), 3.72 (dd, J = 7.8, 4.8 Hz, 1H, C_2), 3.06 (dd, J = 7.2, 3.6 Hz, 2H, $\text{CH}_2\text{CH}=\text{CH}_2$), 2.8 and 2.92 (ABX system: J_{AB} = 15, J_{AX} = 4.8, J_{BX} = 7.8 Hz, 2H, S- C_3) ppm. ^{13}C NMR (150 MHz, D_2O) δ 172.66 (C_1 , carboxylic acid), 133.36 (olefinic CH), 118.16 (olefinic CH_2), 53.37 (C_2 , α -amino acid), 33.75 (allylic CH_2), 30.57 (S- C_3) ppm. MS: 162 ([$\text{M}+\text{H}]^+$), 184 ([$\text{M}+\text{Na}]^+$), 145 ([$\text{M}-\text{NH}_2]^+$). IR: 3300-2500 cm^{-1} (O-H), 1587 cm^{-1} (COO), 1305 cm^{-1} (COO).

L-(\pm)-S-Allylcysteine sulfoxide or alliin (1a). Crude **71** is suspended in H_2O (0.1 mol in 200 mL). Hydrogen peroxide (1.27 eq) is added dropwise, and the mixture is stirred at RT overnight. Excess H_2O_2 decomposes after addition of a spatula tip full of MnO_2 . Once the oxygen release is over, charcoal is added and the suspension is filtered. The filtrate is then lyophilized, leading to a white powder. Yield: 78%. MS: 162 ([$\text{M}+\text{H}]^+$), 184 ([$\text{M}+\text{Na}]^+$), 145 ([$\text{M}-\text{NH}_2]^+$). IR: 3300-2500 cm^{-1} (O-H), 1585 cm^{-1} (COO), 1316 cm^{-1} (COO), 1021 cm^{-1} (S=O). *L*-($+$)-*S*-allylcysteine sulfoxide, *(+)*-**1a** ^1H NMR (600 MHz, D_2O) δ 5.78 (m, 1H, $\text{CH}=\text{CH}_2$), 5.43 (dd, J = 10.1, 1H, $\text{CH}=\text{CH}_2$ cis), 5.37 (d, J = 16.8, 1H, $\text{CH}=\text{CH}_2$ trans), 4.08 (dd, J = 7.8, 4.8 Hz, 1H, C_2), 3.72 (dd, J = 7.2, 3.6 Hz, 2H, $\text{CH}_a\text{CH}=\text{CH}_2$), 3.52 (dd, J = 7.2, 3.6 Hz, 2H, $\text{CH}_b\text{CH}=\text{CH}_2$), 3.32 and 3.09 (ABX system: J_{AB} = 15, J_{AX} = 4.8, J_{BX} = 7.8 Hz, 2H, S- C_3) ppm. ^{13}C NMR (150 MHz, D_2O) δ 171.1 (C_1 , carboxylic acid), 125.4 (olefinic CH_2), 124.3 (olefinic CH), 55.1 (C_2 , α -amino acid), 50.7 (allylic CH_2), 49.3 (S- C_3) ppm. *L*-($-$)-*S*-allylcysteine sulfoxide (*-*)-**75** ^1H NMR (600 MHz, D_2O) δ 5.91 (m, 1H, $\text{CH}=\text{CH}_2$), 5.53 (d, J = 10.8, 1H, $\text{CH}=\text{CH}_2$ cis), 5.48 (d, J = 16.8, 1H, $\text{CH}=\text{CH}_2$ trans), 3.99 (dd, J = 9.0, 3.0 Hz, 1H, C_2), 3.80 and 3.64 (2H in ABX system: J_{AB} = 13.2, J_{AX} = 6.6, J_{BX} = 7.8 Hz, $\text{CH}_2\text{CH}=$), 3.31 and 3.20 (2H in ABX system: J_{AB} = 13.8, J_{AX} = 3.0, J_{BX} = 9.0 Hz, S- C_3) ppm. ^{13}C NMR (150 MHz, D_2O) δ 171.1 (C_1 , carboxylic acid), 125.3 (olefinic CH_2), 124.3 (olefinic CH), 54.5 (C_2 , α -amino acid), 50.1 (allylic CH_2), 49.6 (S- C_3) ppm.

L-(\pm)-S-methyl cysteine S-oxide or methiin (1b)) as described by Stoll and Seebeck.³⁴

HPLC method optimization L-(\pm)-alliin standard was purchased from LKT Laboratories (Saint Paul, USA) and the solutions were prepared in water (0.1, 0.5, 1.0, 1.5, 3.0 and 4.0 mg/mL), then synthesized as above. L-(\pm)-methiin was synthesized as described above. Times between 5 and 13 min are tested for the

gradient (0 to 16% ACN). Acid concentrations from 0 to 0.5% are tested. Trifluoroacetic acid (TFA), formic acid and phosphoric acid were screened, but only TFA impacted the separation. Flow rate is optimized via a Van Deemter plot (flow rates between 0.025 and 0.6 mL/min), and the effect of the mobile phase temperature is studied between 10 and 60 °C.

(+)-Alliin racemization tests. A vial containing (+)-alliin purified from (\pm)-mixture was kept on the bench top for three weeks. An aqueous solution of the yellow powder was prepared and analyzed by HPLC. The peak areas had not changed, indicating that the diastereoisomer ratio had not changed.

Extraction of (+)-alliin. The inactivation of alliinase is performed by heating, denaturation by methanol (mixture MeOH/H₂O, 9:1) and/or acidification (by HCl, pH \downarrow 3.6). Thermal stability of alliin was assessed by refluxing synthesized alliin in water for up to 4 h and follow its decomposition by HPLC. Dry weight of the garlic cloves has been calculated to be 23% (6 repetitions) by lyophilization until no variation in mass is observed for several days. Three sources of alliin are used: fresh garlic cloves, commercial powder and freshly made powder. The latter is prepared as follows: peeled cloves are submerged in liquid N₂, then ground in a Grindomix at 10000 rpm for 1 min, and finally the powder is lyophilized. 1 g (powder) or 4 g of substrate are stirred for 15 min in 50 mL of solvent (H₂O or MeOH/H₂O), then the mixture is ground in an IKA grinder. Solutions are filtered and the volume the filtrate is adjusted to 100 mL. This procedure is performed at 20, 40, 60 and 80 °C (100 °C for H₂O extraction). Ultrasound-assisted and microwave-assisted extractions are performed under the same conditions at 60 °C and 80 °C, respectively. Silica gel column: 500 mg of the garlic extract is loaded on a column filled with silica gel (30 g) equilibrated by BuOH/MeOH/H₂O (3:1:1). Fractions of 20 mL are collected. Tubes containing alliin (as determined by TLC then HPLC) are combined and lyophilized. 64.2 mg of (+)-alliin are recovered with a purity of 90%. Flash chromatography led to a purity of 80%.

Enzymatic resolution. Solutions of (\pm)-alliin (9 mM) and pyridoxal phosphate (PLP, 0.025 mM) are prepared in phosphate buffer. Alliin solution (3 mL) and PLP solution (3 mL) are mixed and brought to 37 °C in a test tube. Alliinase extract (3 mL, activity = 393 U/mL) is added, and 0.5 mL aliquots are pipetted at given times then denatured in HCl 10% prior to HPLC analysis. These kinetics are performed over 30 min and 2h30. HPLC analyses and calibration curves are performed as described above. Scale-up (substrate \times 25, enzyme \times 3) did not give encouraging results.

Separation of (+)- and (-)-1a by column chromatography. Synthetic mixture of **1a** (200 mg) is loaded on a column filled with amino-modified silica gel (30 g) equilibrated by ACN/H₂O + 0.1% H₃PO₄ (3:2).

Fractions of 20 mL are collected. Fractions containing >95% of each isomer are combined and lyophilized. 32.3 mg of (+)-alliin are recovered with a purity of 95% (yield = 40%) and 124.8 mg of (-)-alliin (purity = 92%, quantitative).

Enzymatic oxidation of deoxyalliin (71). An *Acinetobacter calcoaceticus* strain was kept at -80°C in the Unit of Bioindustries collection. The microorganism is inoculated on a Petri dish on enriching culture media and incubated for two days at 35 °C. A colony is transferred to a sterile flask containing aqueous glucose (20 g/L), yeast extract (10 g/L) and peptone (10 g/L). The flask is incubated at 25 °C until absorbance at 590 nm is adequate. Bacteria are then observed microscopically to confirm identity and absence of contamination. The content of the flask is then divided in two flasks containing 400 mL of medium A. Medium A contains monosodium glutamate (30 g/L), $(\text{NH}_4)_2\text{SO}_4$ (6 g/L), Na_2HPO_4 (4 g/L), KH_2PO_4 (2 g/L), cyclohexanol (1 g/L) and 1 mL of trace element solution (HCl 37%, 200 g/L; $\text{MgSO}_4 \cdot 7\text{H}_2\text{O}$, 56 g/L; $\text{FeSO}_4 \cdot 7\text{H}_2\text{O}$, 22 g/L; CaCO_3 , 8 g/L; $\text{ZnSO}_4 \cdot 7\text{H}_2\text{O}$, 6 g/L; $\text{MnCl}_2 \cdot 4\text{H}_2\text{O}$, 4 g/L; CuSO_4 , 1 g/L; CoCl_2 , 1 g/L; H_3BrO_4 , 2 g/L). The last two components are added after autoclave and are sterilized by filtration on sterile 0.2 μ filters. The two flasks are then incubated under stirring at 25 °C. Bacterial concentration is monitored by absorbance measurement. After 48 h, the absorbance value is between 1 and 2, the content of one flask is transferred to a new sterile flask of medium A (bacteria in exponential phase). Deoxyalliin (for a concentration of 1 g/L in the solution) is added to both the culture in exponential and stationary phase. A garlicky smell is released, indicating side reactions. After four days, the mixtures are centrifuged, proteins in the supernatant are precipitated with methanol, and the filtrates are analyzed by HPLC. Oxidation only occurred in the culture in stationary phase, and there is a lot of unreacted starting material. The proportion in diastereoisomers determined by HPLC indicates an inversion of the ratio compared to chemical oxidation: (+)-alliin/(-)-alliin (6/4).

Attempted stereospecific synthesis.

N-BOC-S-allyl L-cysteine (73). Deoxyalliin (71, 4 g, 24.8 mmol) is dissolved in 50 mL of 1,4-dioxane and 25 mL of H_2O . Aqueous 1 M Na_2CO_3 (25 mL, 25 mmol) are added, and the mixture is cooled to 0 °C. Di-tert-butyl dicarbonate (6 g, 27.3 mmol) is added, and the suspension is stirred at 0 °C for 1.5 h, then at RT for 15 h. When no 71 is observed by TLC, the pH of the mixture is adjusted to 10 with aq. 1 M Na_2CO_3 , then washed by Et_2O . The aqueous layer is then acidified to pH 2 by HCl (6 M) at 0 °C. An organic layer forms, and is extracted by 3 \times 80 mL CHCl_3 . Organic layers are combined, dried and concentrated, yielding 7.45 g of colorless oil (106% yield, traces of dioxane by NMR). The product is then purified by trituration in

hexanes. ^1H NMR (600 MHz, CDCl_3) δ 5.68 (1H, m, -CH=), 5.05 (2H, m, $\text{CH}_2=\text{C}$), 4.45 (1H, m, NH), 3.08 (2H, d, J = 7.2, vinyl- $\text{CH}_2\text{-S}$), 2.90 and 2.81 (2H in ABX system, J_{AB} = 13.2, J_{AX} = 4.2, J_{BX} = 5.4 Hz, $\text{CH}_2\text{-CH}=$), 1.38 (9H, tert-butyl) ppm.

N-BOC-S-allyl L-cysteine tert-butyl ester (74). A procedure from the literature is adapted.⁷¹ Compound **73** (1.02 g, 3.6 mmol) is mixed with 4-dimethylaminopyridine (DMAP, 143 mg, 1.17 mmol) and $^t\text{BuOH}$ (348 mg, 4.38 mmol) in 6 mL of DCM. After cooling to 0 °C, 900 mg (4.38 mmol) of N,N'-dicyclohexylcarbodiimide (DCC) is added. The mixture is stirred at 0 °C then RT overnight. When TLC indicates the absence of starting material **73**, the suspension is filtered through Celite and concentrated under vacuum. The crude material is dissolved in 25 mL EtOAc, then washed successively with 5% NaHSO_4 , H_2O and brine. Organic layer is then dried and concentrated, but the formation of a solid indicates remaining dicyclohexyl urea. Dissolution in hexane, filtration and concentration of the filtrate yields 781 mg of pure product (yield = 68%). ^1H NMR (400 MHz, CDCl_3) δ 5.75 (1H, m, -CH=), 5.13 (1H, d, J = 5.6, $\text{CH}_a=\text{C}$), 5.01 (1H, s, $\text{CH}_b=\text{C}$), 4.38 (1H, m, NH), 3.15 (2H, d, J = 6.0, vinyl- $\text{CH}_2\text{-S}$), 2.91 and 2.81 (2H in ABX system, J_{AB} = 13.2, J_{AX} = 4.4, J_{BX} = 5.6 Hz, - $\text{CH}_2\text{-S}$), 1.44 (9H, tert-butyl), 1.42 (9H, tert-butyl) ppm.

Oxidation of N-BOC-S-allyl L-cysteine (73). In a flask under argon, compound **73** (1.2 g, 4.6 mmol) and (+)-(1*R*,2*S*)-cis-1-amido-2-indanol (0.69 g, 4.6 mmol) are dissolved in 20 mL NMP. $\text{Ti}(\text{O}i\text{Pr})_4$ is added (0.7 mL, 2.3 mmol), then the flask is cooled to 0°C. Cumene hydroperoxide (1.4 mL, 10.6 mmol) is then added, and the mixture is stirred overnight.

Alliinase extraction. Buffer A contains the following: Hepes (0.05 M, pH 7.2); PMSF (1mM) ; glycerol (10% v/v); pyridoxal phosphate (PLP, 0.02 mM), CaCl_2 , MgCl_2 and MnCl_2 (all 1 mM) and NaN_3 (3mM). The entire procedure is performed at 4 °C. 120 g of garlic cloves are carefully peeled and ground in a Grindomix system. Buffer A (180 mL) is added and the mixture is homogenized for 2 min at 10000 rpm. The material is filtered with a nylon filter sock. Filtrate is centrifuged for 30 min at 20000 rpm. Supernatant is kept for the next step. Two different precipitations are then performed: with polyethylene glycol (PEG) 8000 or ammonium sulfate.

*With polyethylene glycol.*⁷² Solid PEG 8000 is added to the supernatant in 25% w/v proportion. The mixture is slowly stirred for 20 min, still at 4 °C. A second centrifugation is performed at 20000 rpm for 15 min. Pellet is collected and suspended in 240 mL of buffer A. A third centrifugation is then performed (15 min, 20000 rpm). The supernatant is collected and filtered on 0.45 μm syringe filter. This extract (**76a**) will be used in the next purification step.

With ammonium sulfate. Buffer B is prepared as follows: Hepes (0.15 M at pH 7) ; saccharose (10% w/v) ; NaCl (1% w/v). Proteins are precipitated from the supernatant by adding $(\text{NH}_4)_2\text{SO}_4$ in 45% w/v proportion. Centrifugation at 20000 rpm for 15 min leaves a pellet that is resuspended in 15 mL of buffer B. The solution is desalted by dialysis, H_2O is replaced every hour for 4 h. Desalting solution is then centrifuged at 8000 rpm for 5 min. The supernatant is collected and filtered with a 0.45 μm syringe filter. This extract (**76b**) will be used in the next purification step.

Alliinase purification Buffer C contains buffer A without PMSF but with NaCl (0.5 mM): Hepes (0.05 M, pH 7.2) ; glycerol (10% v/v) ; PLP (0.02 mM), CaCl_2 , MgCl_2 and MnCl_2 (all 1 mM) ; NaN_3 (3mM) and NaCl (0.5 mM). Buffers D are prepared by adding methyl α -D-mannopyranoside to buffer C in the following concentrations: 0.02, 0.04, 0.06, 0.08, 0.1 and 0.15 M. Regeneration solution is made of potassium acetate buffer (0.1M) with NaCl 0.5 M), pH 8.5 and 4.5. Storage solution is a potassium acetate buffer (0.1M pH 6) containing NaCl (1 M), CaCl_2 , MgCl_2 and MnCl_2 (all 1 mM).

*With Concanavaline A - Sepharose (Con A-Sepharose).*⁷² Pharmacia column is filled with about 15 mL Con A-Sepharose stationary phase and equilibrated with buffer C. 50 mL of protein extract **76** is then loaded and eluted with 5 mL volumes of increasing concentration of buffer D. 5 mL fractions are collected. Stationary phase is regenerated with 2-3 column volumes of pH 8.5 then 2-3 column volumes of pH 4.5 regeneration solutions. This procedure (alternating regeneration solutions) is repeated three times, then Con A-Sepharose can be stored in storage solution at 4 °C.

Size exclusion chromatography. Buffer E contains potassium phosphate (60 mM, pH 7), NaCl (1% w/v) and PLP (0.025 mM). Solid Sephadex 200 is stirred in buffer E for 72 h at room temperature to let it expand. 50 mL of protein extract **76** is loaded and eluted with buffer E, 5 mL fractions are collected.

Folin-Lowry's protein assay⁷³ Solution A contains Na_2CO_3 (250 mg/L) and NaOH (4 g/L), solution B contains CuSO_4 (20 g/L), solution C potassium sodium tartrate (20 g/L). Solution D is a 3-fold dilution of Folin's reagent in DI water. Solution E prepared by mixing solutions A, B and C in 100:1:1 proportion.

Calibration. Bovine serum albumine (BSA) is used for calibration of the spectrophotometer. 2, 4, 6, 8 and 10 mg/mL protein solutions are prepared by diluting BSA in pH 7.4 TRIS-HCl buffer (the first data point will be pure buffer, concentration 0 mg/mL). Solution D and BSA are prepared extemporaneously. Solution E (5 mL) is added to 0.5 mL of each solution of BSA. After 10 min, 0.5 mL of solution D is added and the standards are kept away from light for 30 min. After the elapsed time, the absorbance of each solution is measured at 660 nm. A calibration curve then prepared.

Sample. Protein extracts are diluted by buffer A in 10-fold increments. Aliquots (0.5 mL) of these solutions are treated like the standards for calibration: addition of 5 mL solution E, 10 min wait time, addition of 0.5 mL solution D, 30 min wait time away from light, spectrophotometer.

SDS-PAGE protein gel electrophoresis Gels are run in a HOEFFER SE600 Ruby Amersham Gel Electrophoresis System with Pharmacia Electrophoresis Power Supply 3500 XL.

Casting the gels. Polyacrylamid gels are prepared in a Amersham cassette. An acrylamide solution containing 30% acrylamide and 0.8% bisacrylamide is prepared. Running buffer contains 0.025 M Tris, 0.0192 M glycine, 0.1 % sodium dodecylsulfate (SDS) and is at pH 8.3. Separating gel mixture is composed of 15 mL acrylamide solution, 0.15 mL 10% SDS solution, 6 mL H₂O, 75 μ L 10% ammonium persulfate (AP) solution, 5 μ L N, N, N', N'-tetramethylethylenediamine (TEMED) and 3.8 mL of resolving Tris-HCl buffer (1.5 M, pH 8.8). Stacking gel contain 1.33 mL acrylamide solution, 0.1 mL 10% SDS solution, 6 mL H₂O, 50 μ L 10% ammonium persulfate (AP) solution, 5 μ L N, N, N', N'-tetramethylethylenediamine (TEMED) and 2.5 mL of stacking Tris-HCl buffer (0.5 M, pH 6.8). Gels are casted as follows: the space between the glass plates is filled up to an inch from the edge with separating gel mixture, then a small amount of water is added to smooth the surface. After 30 min, the water is absorbed by a filter paper and stacking gel is casted. The comb is placed in the gel before polymerization. Once solidified, carefully remove the comb and fill the wells with running buffer.

Sample preparation. Denaturing solution contains 0.125 M Tris, 4% SDS, 20% glycerol v/v, bromophenol blue 0.02% and 200 μ M 2-mercaptoethanol (pH 6.8). Protein extracts (about 2 mg protein/mL) are denatured by adding 0.5 mL of denaturing solution to 0.5 mL of sample. Samples are then heated at 100 °C for 2 min. A drop of glycerol is added if needed (not dense enough to go to the bottom of the wells).

Loading, running and staining the gels. Sample (15 μ L) is loaded in the wells. Standard for MW determination (6.5 to 200 kDa) is loaded in the middle and right well. The compartment of the apparatus is filled with running buffer, and migration is achieved when the power supply is set up on 500 V, 140 mA and 50 W for 3 h. The gel is placed in a fixation bath (EtOH/HAc/H₂O 4:1:5) for 30 min, then in a staining bath (0.29 g Coomassie blue + 250 mL EtOH 25% HAc 8%) for 10 min at 60 °C. Destaining is achieved by about 10 washes of 200 mL destaining solution (EtOH 25%, HAc 8%) for 2h.

Specific enzyme activity⁷⁴ SEMR solution is made of NaHPO₄ buffer (2M, pH 6.5), LDH (200U for 10 mL) and PLP (0.5 mM). The following volumes of solutions are mixed in a 1 mL spectrophotometer quartz cuvette at 37 °C: 0.5 mL SEMR, 0.1 mL NADH (2 mM) and 0.15 mL alliin (0.1 M). Finally, 0.25 mL of

alliinase is added (concentration of alliinase determined by Folin-Lowry's assay = 1440 ng/mL). Diminution of absorbance at 340 nm (NADH) is followed for 5 min, one scan/2 s. A calibration curve of NADH is prepared to transform absorbance in concentration of NADH, then concentration of pyruvate. Enzyme activity (EA) is calculated from the linear part of the absorbance curve (the slope of moles of pyruvate formed). Specific activity (SA) is found by dividing EA by the protein concentration.

$$SA = EA/C$$

Extraction of vinyldithiins Garlic (from Spain, Argentina, France and China) and vegetable edible oils (linseed, colza, soybean, olive, sunflower, grape seed, corn, peanut) were bought at the local market. Acetonitrile (ACN), hexane, octane and dichloromethane (HPLC grade) were obtained from Scharlau. Wijs reagent was purchased from VWR. Pure water was obtained from an Elix system Millipore. 1,2- and 1,3-Vinyldithiin extraction from garlic was undertaken according to Yoshida et al.⁷⁵ Garlic cloves were peeled and 20 g were crushed in a blender (20 s at 6000 rpm). Variable volumes of edible oil were then added and the mixture was allowed to macerate during set times. An oil bath was used for temperature control. The initial parameters for the maceration were: sunflower oil / Spanish garlic in a 1/3 weight ratio, 24 h, RT. The pulp was then filtered, and vinyldithiins were extracted from the oil by adding an equal volume of ACN and shaking during 2 min. The solvent layer was recovered after centrifugation (2 min, 1250 g). Filtration on 0.2 μ m PTFE membranes allowed direct injection into the HPLC system for quantification of each vinyldithiin by external calibration.

Optimization of the extraction of vinyldithiins A one-by-one factor study was applied for the following parameters (in parenthesis, the number of levels tested): garlic origin (5), oil type (8), garlic/oil proportion (5), extraction T° (5), multi-step extractions (3 re-extraction of the pulp), stirring (on or off) and assisted extractions (either by sonication in a Bandelin Sonorex (at 45 kHz) or using a Milestone Start Synth microwave oven at 100 W). Every newly optimized parameter was applied for subsequent extractions. Each experiment was repeated twice. The kinetics of the extraction under the optimized conditions was followed by RP-HPLC. To evaluate the influence of oxidation on the amounts of vinyldithiins obtained, an extraction was performed under air or argon bubbling (Spanish garlic, sunflower oil, 1/2 ratio, 37°C, no stirring, 6h).

Oil characterization Iodine values were measured according to an adaptation of Wijs method:⁷⁶ an oil sample is diluted in dichloromethane, Wijs reagent is added, followed by potassium iodide. The mixture is

then titrated against sodium thiosulfate. Acid values were calculated according to the IUPAC procedure⁷⁷ (titration of the sample by KOH). The fatty acid composition of each oil was determined by GC-FID (Supelco method⁷⁸) on a CP-WAX 52 CB column (0.25 mm x 0.15 μ m x 30 m). A Supelco mix containing 37 fatty acid methyl esters was used as internal standard. The partition coefficient between octane and water was determined by the shake-flask method.

Quantification and purification of vinyldithiins by RP-HPLC Vinyldithiins were analyzed by HPLC on an Agilent 1050 series system. The separation was achieved in 25 min on a reverse phase column (Pursuit XRs C18, 250 x 3 mm, particle size 3 μ m) with a mixture of ACN and water (45/55, isocratic mode) at 0.4 mL/min. The detection was performed at 210 nm. The 1,2- and 1,3-vinylidithiins standards used for calibration were obtained in the lab. Briefly, after extraction, they were purified in two steps, first by atmospheric pressure chromatography on silica gel (mobile phase: hexane/diethyl ether) then by preparative C18 HPLC (mobile phase: ACN/water). The purified fractions showed an HPLC purity (210 nm) of 89% and 99% for 1,2-vinylidithiin (**5b**) and 1,3-vinylidithiin (**5a**) respectively. The structure was confirmed by infrared spectroscopy, mass spectrometry and NMR. The IR spectrum of both **5b** and **5a** showed absorption bands at 980 and 1607 cm^{-1} which corresponds to vinyl groups and alkenes respectively, and at 720 cm^{-1} (C-S bond). The positive mass spectrometry of **5b** and **5a** showed a peak at m/z 144.9 corresponding to [M + H]⁺. 1,2-vinylidithiin: ¹H NMR (600 MHz, CDCl_3) δ 6.27 (1H, d), 5.96 (1H, m), 5.93 (1H, m), 5.36 (1H, d), 5.26 (1H, d), 4.70 (1H, d), 3.36 (1H, ddd), 3.21 (1H, ddd) ppm. ¹³C NMR (150.87 MHz, CDCl_3): δ 134.16, 122.07, 118.42, 117.16, 45.13, 25.09 ppm. 1,3-vinylidithiin: ¹H NMR (600 MHz, CDCl_3) δ 6.27 (1H, d), 5.96 (1H, m), 5.93 (1H, m), 5.36 (1H, d), 5.26 (1H, d), 4.70 (1H, d), 3.36 (1H, ddd), 3.21 (1H, ddd) ppm. ¹³C NMR (150.87 MHz, CDCl_3) δ = 134.16, 122.07, 118.42, 117.16, 45.13, 25.09 ppm.

References

- (1) Dethier, B.; Laloux, M.; Hanon, E.; Nott, K.; Heuskin, S.; Wathelet, J. P. Analysis of the diastereoisomers of alliin by HPLC. *Talanta* **2012**, *101*, 447–452.
- (2) Miron, T.; Shin, I.; Feigenblat, G.; Weiner, L.; Mirelman, D.; Wilchek, M.; Rabinkov, A. A spectrophotometric assay for allicin, alliin, and alliinase (alliin lyase) with a chromogenic thiol: reaction of 4-mercaptopyridine with thiosulfinate. *Anal. Biochem.* **2002**, *307*, 76–83.
- (3) Horie, H.; Yamashita, K.-I. Non-derivatized analysis of methiin and alliin in vegetables by capillary electrophoresis. *J. Chromatogr. A* **2006**, *1132*, 337–339.
- (4) Keusgen, M.; Jünger, M.; Krest, I.; Schöning, M. J. Biosensoric detection of the cysteine sulphoxide alliin. *Sensors and actuators* **2003**, *95*, 297–302.
- (5) Kubec, R.; Dadáková, E. Quantitative determination of *S*-alk(en)ylcysteine-*S*-oxides by micellar electrokinetic capillary chromatography. *J. Chromatogr. A* **2008**, *1212*, 154–157.
- (6) Kubec, R.; Svobodová, M.; Velísek, J. Gas chromatographic determination of *S*-alk(en)ylcysteine sulfoxides. *J. Chromatogr. A* **1999**, *862*, 85–94.
- (7) Kanaki, N. S.; Rajani, M. Development and validation of a thin-layer chromatography-densitometric method for the quantitation of alliin from garlic (*Allium sativum*) and its formulations. *J. AOAC Int.* **2005**, *88*, 1568–1570.
- (8) Ziegler, S. J.; Sticher, O. HPLC of *S*-alk(en)yl-L-cysteine derivatives in garlic including quantitative determination of (+)-*S*-allyl-L-cysteine sulfoxide (alliin). *Planta Med.* **1989**, *55*, 372–378.
- (9) Iberl, B.; Winkler, G.; Müller, B.; Knobloch, K. Quantitative determination of allicin and alliin from garlic by HPLC. *Planta Med.* **1990**, *56*, 320–326.
- (10) Mutsch-Eckner, M.; Sticher, O.; Meier, B. Reversed-phase HPLC of *S*-alk(en)yl-L-cysteine derivatives in *Allium sativum* including the determination of (+)-*S*-allyl-L-cysteine sulphoxide, γ -L-glutamyl-*S*-allyl-L-cysteine and γ -L-glutamyl-*S*-(trans-1-propenyl)-L-cysteine. *J. Chromatogr.* **1992**, *625*, 183–190.
- (11) Auger, J.; Mellouki, F.; Vannereau, A.; Boscher, J.; Cosson, L.; Mandon, N. Analysis of *Allium* sulfur amino acids by HPLC after derivatization. *Chromatographia* **1993**, *36*, 347–350.
- (12) Thomas, D. J.; Parkin, K. L. Quantification of alk(en)yl-L-cysteine sulfoxides and related amino acids in *Allium* by high-performance liquid chromatography. *J. Agric. Food Chem.* **1994**, *42*, 1632–1638.

(13) Krest, I.; Glodek, J.; Keusgen, M. Cysteine sulfoxides and alliinase activity of some *Allium* species. *J. Agric. Food Chem.* **2000**, *48*, 3753–3760.

(14) Kubec, R.; Musah, R. A. Cysteine sulfoxide derivatives in *Petiveria alliacea*. *Phytochemistry* **2001**, *58*, 981–985.

(15) Mochizukia, E.; Nakayama, A.; Kitada, Y.; Saito, K.; Nakazawa, H.; Suzuki, S.; Fujita, M. Liquid chromatographic determination of alliin in garlic and garlic products. *J. Chromatogr.* **1988**, *455*, 271–277.

(16) Ichikawa, M.; Ide, N.; Yoshida, J.; Yamaguchi, H.; Ono, K. Determination of seven organosulfur compounds in garlic by high-performance liquid chromatography. *J. Agric. Food Chem.* **2006**, *54*, 1535–1540.

(17) Arnault, I.; Christidès, J. P.; Mandon, N.; Haffner, T.; Kahane, R.; Auger, J. High-performance ion-pair chromatography method for simultaneous analysis of alliin, deoxyalliin, allicin and dipeptide precursors in garlic products using multiple mass spectrometry and UV detection. *J. Chromatogr. A* **2003**, *991*, 69–75.

(18) Chaimbault, P.; Petritis, K.; Elfakir, C.; Dreux, M. Ion-pair chromatography on a porous graphitic carbon stationary phase for the analysis of twenty underivatized protein amino acids. *J. Chromatogr. A* **2000**, *870*, 245–254.

(19) Kriz, J.; Adamkova, E.; Knox, J. H.; Hora, J. Characterization of adsorbents by high-performance liquid chromatography using aromatic hydrocarbons Porous graphite and its comparison with silica gel, alumina, octadecylsilica and phenylsilica. *J. Chromatogr. A* **1994**, *663*, 151–161.

(20) Tanaka, N.; Tanigawa, T.; Kimata, K.; Hosota, K.; Akari, T. Selectivity of carbon packing materials in comparison with octadecylsilyl-and pyrenylethylsilylsilica gels in reversed-phase liquid chromatography. *J. Chromatogr. A* **1991**, *549*, 29–41.

(21) Aruda, W. O.; Aruda, K. O. Review of volatile perfluorocarboxylic acids as ion pair reagents in LC: Part I. *LC-GC North Am.* **2009**, *27*, 626–632.

(22) Kotrebai, M.; Birringer, M.; Tyson, J. F.; Block, E.; Uden, P. C. Selenium speciation in enriched and natural samples by HPLC-ICP-MS and HPLC-ESI-MS with perfluorinated carboxylic acid ion-pairing agents. *Analyst* **2000**, *125*, 71–78.

(23) Kotrebai, M.; Tyson, J. F.; Block, E.; Uden, P. C. High-performance liquid chromatography of selenium compounds utilizing perfluorinated carboxylic acid ion-pairing agents and inductively coupled plasma- and electrospray ionization-mass spectrometric detection. *J. Chromatogr. A* **2000**, *866*, 51–63.

(24) West, C.; Elfakir, C.; Lafosse, M. Porous graphitic carbon: a versatile stationary phase for liquid chromatography. *J. Chromatogr. A* **2010**, *1217*, 3201–3216.

(25) Teutenberg, T.; Tuerk, J.; Holzhauser, M.; Kiffmeyer, T. K. Evaluation of column bleed by using an ultraviolet and a charged aerosol detector coupled to a high-temperature liquid chromatographic system. *J. Chromatogr. A* **2006**, *1119*, 197–201.

(26) Chitta, R.; Ginzburg, A.; van Doremale, G.; Macko, T.; Brüll, R. Separating ethylene-propylene-diene terpolymers according to the content of diene by HT-HPLC and HT 2D-LC. *Polymer (Guildf.)* **2011**, *52*, 5953–5960.

(27) Hazotte, A.; Libong, D.; Chaminade, P. High-temperature micro liquid chromatography for lipid molecular species analysis with evaporative light scattering detection. *J. Chromatogr. A* **2007**, *1140*, 131–139.

(28) Cummins, J.; Hull, J.; Kitts, K.; Goodpaster, J. V. Separation and identification of anions using porous graphitic carbon and electrospray ionization mass spectrometry: Application to inorganic explosives and their post blast residues. *Anal. Methods* **2011**, *3*, 1682–1687.

(29) Karlsson, A.; Charron, C. Reversed-phase chiral ion-pair chromatography at a column temperature below 0 °C using three generations of Hypercarb as solid-phase. *J. Chromatogr. A* **1996**, *732*, 245–253.

(30) Teutenberg, T. Potential of high temperature liquid chromatography for the improvement of separation efficiency - A review. *Anal. Chim. Acta* **2009**, *643*, 1–12.

(31) Hubert, P.; Chiap, P.; Crommen, J.; Boulanger, B.; Chapuzet, E.; Mercier, N.; Bervoas-Martin, S.; Chevalier, P.; Grandjean, D.; Lagorce, P.; Lallier, M.; Laparra, M. C.; Laurentie, M.; Nivet, J. C. The SFSTP guide on the validation of chromatographic methods for drug bioanalysis: from the Washington Conference to the laboratory. *Anal. Chim. Acta* **1999**, *391*, 135–148.

(32) Rozet, E.; Ceccato, A.; Hubert, C.; Ziemons, E.; Oprean, R.; Rudaz, S.; Boulanger, B.; Hubert, P. Analysis of recent pharmaceutical regulatory documents on analytical method validation. *J. Chromatogr. A* **2007**, *1158*, 111–125.

(33) Beuving, G. In *Valid. Semin. 2001*, 2001.

(34) Stoll, A.; Seebeck, E. Über Alliin, die genuine Muttersubstanz des Knoblauchöls. 1. Mitteilung über *Allium*-Substanzen. *Helv. Chim. Acta* **1948**, *31*, 189–210.

(35) Stoll, A.; Seebeck, E. Die Synthese des natürlichen Alliins und seiner drei optisch aktiven Isomeren. *Helv. Chim. Acta* **1951**, *34*, 481–487.

(36) Koch, I.; Keusgen, M. Diastereoselective synthesis of alliin by an asymmetric sulfur oxidation. *Pharmazie* **1998**, *53*, 668–671.

(37) Aversa, M. C.; Barattucci, A.; Bonaccorsi, P.; Giannetto, P. L-Cysteine, a versatile source of sulfenic acids. synthesis of enantiopure alliin analogues. *J. Org. Chem.* **2005**, *70*, 1986–1992.

(38) Jayathilaka, L.; Gupta, S.; Huang, J.-S.; Lee, J.; Lee, B.-S. Synthesis of diastereomers of alliin, secanoalliin, and isoalliin. *Curr. Org. Chem.* **2015**, *19*, 1428–1435.

(39) Yu, T. H.; Wu, C. M.; Rosen, R. T.; Hartman, T. G.; Ho, C. T. Volatile compounds generated from thermal degradation of alliin and deoxyalliin in an aqueous solution. *J. Agric. Food Chem.* **1994**, *42*, 146–153.

(40) Greenstein, J. P.; Winitz, M., *Chemistry of the Amino Acids, Volume 3*; Wiley, J., Ed., New York, London, 1961, p 2872.

(41) Ichikawa, M.; Ide, N.; Ono, K. Changes in organosulfur compounds in garlic cloves during storage. *J. Agric. Food Chem.* **2006**, *54*, 4849–4854.

(42) Horníčková, J.; Kubec, R.; Cejpek, K.; Velíšek, J.; Ovesná, J.; Stavělíková, H. Profiles of *S*-alk(en)ylcysteine sulfoxides in various garlic genotypes. *Czech J. Food Sci.* **2010**, *28*, 298–308.

(43) Jiang, X.-m.; Lu, Y.-m.; Tan, C.-p.; -Liang, Y.; Cui, B. Combination of aqueous two-phase extraction and cation-exchange chromatography: New strategies for separation and purification of alliin from garlic powder. *J. Chromatogr. B* **2014**, *957*, 60–67.

(44) Kuettner, E. B.; Hilgenfeld, R.; Weiss, M. S. The active principle of garlic at atomic resolution. *J. Biol. Chem.* **2002**, *277*, 46402–46407.

(45) Krest, I.; Keusgen, M. Quality of herbal remedies from *Allium sativum*: differences between alliinase from garlic powder and fresh garlic. *Planta Med.* **1999**, *65*, 139–143.

(46) Jansen, H.; Müller, B.; Knobloch, K. Characterization of an alliin lyase preparation from garlic (*Allium sativum*). *Planta Med.* **1989**, *55*, 434–439.

(47) Yutani, M.; Taniguchi, H.; Borjihan, H.; Ogita, A.; Fujita, K.-i.; Tanaka, T. Alliinase from *Ensifer adhaerens* and its use for generation of fungicidal activity. *AMB Express* **2011**, *1*, 1–8.

(48) Stoll, A.; Seebeck, E. Chemical investigations on alliin, the specific principle of garlic. *Adv. Enzymol.* **1951**, *11*, 377–400.

(49) Faber, K., *Biotransformations in Organic Chemistry: A Textbook*, 6th Editio; Springer Berlin Heidelberg: 2011, 423 pp.

(50) Barclay, S. S.; Woodley, J. M.; Lilly, M. D.; Spargo, P. L.; Pettman, A. J. Production of cyclohexanone monooxygenase from *Acinetobacter calcoaceticus* for large scale Baeyer-Villiger monooxygenase reactions. *Biotechnol. Lett.* **2001**, *23*, 385–388.

(51) Delamare, M.; Belot, S.; Caille, J.-C.; Martinet, F.; Kagan, H. B.; Henryon, V. A new titanate/(+)-(1R,2S)-*cis*-1-amino-2-indanol system for the asymmetric synthesis of (*S*)-tenatoprazole. *Tetrahedron Lett.* **2009**, *50*, 1702–1704.

(52) Seebach, D.; Fadel, A. N,O-Acetals from pivalaldehyde and amino acids for the α -alkylation with self-reproduction of the center of chirality. Enolates of 3-benzoyl-2-(tert-butyl)-1,3-oxazolidin-5-ones. *Helv. Chim. Acta* **1985**, *68*, 1243–1250.

(53) Kuettner, E. B.; Hilgenfeld, R.; Weiss, M. S. Purification, characterization, and crystallization of alliinase from garlic. *Arch. Biochem. Biophys.* **2002**, *402*, 192–200.

(54) Dethier, B.; Hanon, E.; Maayoufi, S.; Nott, K.; Fauconnier, M.-L. Optimization of the formation of vinylidithiins, therapeutic compounds from garlic. *Eur. Food Res. Technol.* **2013**, *237*, 83–88.

(55) Brodnitz, M. H.; Pascale, J. V.; Van Derslice, L. Flavor components of garlic extract. *J. Agric. Food Chem.* **1971**, *19*, 273–275.

(56) Block, E.; Ahmad, S.; Catalfamo, J. L.; Jain, M. K.; Apitz-Castro, R. Antithrombotic organosulfur compounds from garlic: structural, mechanistic, and synthetic studies. *J. Am. Chem. Soc.* **1986**, *108*, 7045–7055.

(57) Keophiphath, M.; Priem, F.; Jacquemond-Collet, I.; Clément, K.; Lacasa, D. 1,2-Vinyldithiin from garlic inhibits differentiation and inflammation of human preadipocytes. *J. Nutr.* **2009**, *139*, 2055–2060.

(58) World Health Organization - WHO Media Centre Obesity and Overweight - fact sheet 311.

(59) Block, E., *Garlic and Other Alliums: the Lore and the Science*; Royal Society of Chemistry: Cambridge, UK, 2010.

(60) Bongiorno, P. B.; Fratellone, P. M.; LoGiudice, P. Potential health benefits of garlic (*Allium sativum*): a narrative review. *J. Complement. Integr. Med.* **2008**, *5*, 1.

(61) Sendl, A.; Schliack, M.; Loser, R.; Stanislaus, F.; Wagner, H. Inhibition of cholesterol synthesis in vitro by extracts and isolated compounds prepared from garlic and wild garlic. *Atherosclerosis* **1992**, *94*, 79–95.

(62) Nishimura, H.; Higuchi, O.; Tateshita, K. Antioxidative activity of sulfur containing compounds in *Allium* species for human LDL oxidation in vitro. *J. Agric. Food Chem.* **2003**, *51*, 7208–7214.

(63) Egen-Schwind, C.; Eckard, R.; Jekat, F. W.; Winterhoff, H. Pharmacokinetics of vinyldithiins, transformation products of allicin. *Planta Med.* **1992**, *58*, 8–13.

(64) Egen-Schwind, C.; Eckard, R.; Kemper, F. H. Metabolism of garlic constituents in the isolated perfused rat liver. *Planta Med.* **1992**, *58*, 301–305.

(65) Iberl, B.; Winkler, G.; Knobloch, K. Products of allicin transformation: ajoenes and dithiins, characterization and their determination by HPLC. *Planta Med.* **1990**, *56*, 202–211.

(66) Zhou, J. Immobilization of alliinase and its application: flow-injection enzymatic analysis for alliin. *African J. Biotechnol.* **2009**, *8*, 1337–1342.

(67) Tatke, P.; Jaiswal, Y. An overview of microwave assisted extraction and its applications in herbal drug research. *Res. J. Med. Plant* **2011**, *5*, 21–31.

(68) Paré, J. R. J.; Bélanger, J. M. R.; Stafford, S. S. Microwave-assisted process (MAP): a new tool for the analytical laboratory. *TrAC Trends Anal. Chem.* **1994**, *13*, 176–184.

(69) Eskilsson, S.; Björklund, E. Analytical-scale microwave-assisted extraction. *J. Chromatogr. A* **2000**, *902*, 227–250.

(70) Delazar, A.; Nahar, L.; Hamedeyazdan, S.; Sarker, S. D., *Microwave-Assisted Extraction in Natural Products Isolation*. Sarker, D. S., Nahar, L., Eds.; Humana Press: Totowa, NJ, 2012; Chapter 5. Pp 89–115.

(71) Ikeuchi, H.; Meyer, M. E.; Ding, Y.; Hiratake, J.; Richards, N. G. J. A critical electrostatic interaction mediates inhibitor recognition by human asparagine synthetase. *Bioorg. Med. Chem.* **2009**, *17*, 6641–6650.

(72) Rabinkov, A.; Wilchek, M.; Mirelman, D. Allinase (alliin lyase) from garlic (*Allium sativum*) is glycosylated at ASN146 and forms a complex with a garlic mannose-specific lectin. *Glycoconj. J.* **1995**, *12*, 690–698.

(73) Lowry, O. H.; Rosebrough, N. J.; Farr, A. L.; Randall, R. J. Protein measurement with the folin phenol reagent. *J. Biol. Chem.* **1951**, *193*, 265–275.

(74) Schwimmer, S.; Mazelis, M. Characterization of alliinase of *Allium cepa* (onion). *Arch. Biochem. Biophys.* **1963**, *100*, 66–73.

(75) Yoshida, H.; Iwata, N.; Katsuzaki, H.; Naganawa, R.; Ishikawa, K.; Fukuda, H.; Fujino, T.; Suzuki, A. Antimicrobial activity of a compound isolated from an oil-macerated garlic extract. *Biosci. Biotechnol. Biochem.* **1998**, *62*, 1014–1017.

(76) Paquot, C.; Press, P.; International Union of Pure and Applied Chemistry. Commission on Oils, F.; Derivatives, *Standard Methods for the Analysis of Oils, Fats and Derivatives*; Pergamon Press: Oxford, 1979.

(77) Dieffenbacher, A.; Pocklington, W. D., *Standard Methods for the Analysis of Oils, Fats and Derivatives: 1st Supplement to the 7th Edition*; IUPAC Chemical Data; Wiley: Hoboken, 1992.

(78) Sigma-Aldrich Comparison of 37 Component FAME Standard on Four Capillary GC Columns. *Supelco Bull.* **1996**, *907*.

Chapter 5

The chemistry of smell

5.1 Introduction

Olfaction plays a crucial role in food and danger detection for animals. Humans are no exception and can distinguish a very large number of different odors¹⁻⁴ even with only about 350 different olfactory receptors (ORs; compared to >1000 receptors for other mammals such as mice⁵). However, as important as this sense is, the way we smell remains incompletely explained. If major contributions have been made to the field since the discovery of the genes coding for the ORs by L. Buck and R. Axel, a finding rewarded by the 2004 Nobel Prize for Physiology and Medicine,⁶ the biochemistry at the receptor level is mostly unknown to date.

A major focus of my doctoral work is the chemistry of organosulfur compounds, which are particularly strong smelling. Because their threshold of perception is as low as a few part in a billion, thiols are added to natural gas to facilitate detection of leaks at an early stage. Thiols and other sulfur-containing compounds are responsible for the smell of garlic and garlic breath, but also the odor of skunk's spray,⁷ human sweat,⁸ and rotten eggs. They also contribute to the more pleasant roasted coffee or grapefruit odor. Thiols and sulfides are sometimes found as semiochemicals, chemicals that convey a message from one organism to the other, impacting the latter's behavior. Onion maggots are attracted by sulfides and disulfides from onion (interspecific semiochemical),⁹ and (methylthio)methanethiol (MTMT) present in male mice urine stimulates female mice (intraspecific semiochemical),¹⁰ to mention only two examples. The instance of the mice is an excellent model, since MTMT contains a thiol and thioether functional groups. One olfactory receptor was found to be particularly responsive to MTMT, and the presence of copper was shown to be crucial for its

detection.¹¹ Further investigations are required to understand the phenomena at play when a compound - containing sulfur or not - reaches the nose.

In this chapter, we contribute the chemistry of olfaction by investigating - and invalidating - the vibration theory of olfaction. According to this theory, what confers an odor to a chemical is the frequency at which the chemical bonds in the compound vibrate. These vibrations absorb in the infrared region of the spectrum. Turin popularized the theory in the past 20 years and claims that compounds with the same IR bands have the same odor.¹² One of his model hypotheses is that the elongation vibration of the sulfur-hydrogen bond (2550 – 2600 cm⁻¹ in the IR spectrum) is responsible for the thiol odor. This work is reviewed in a 2016 paper.¹³

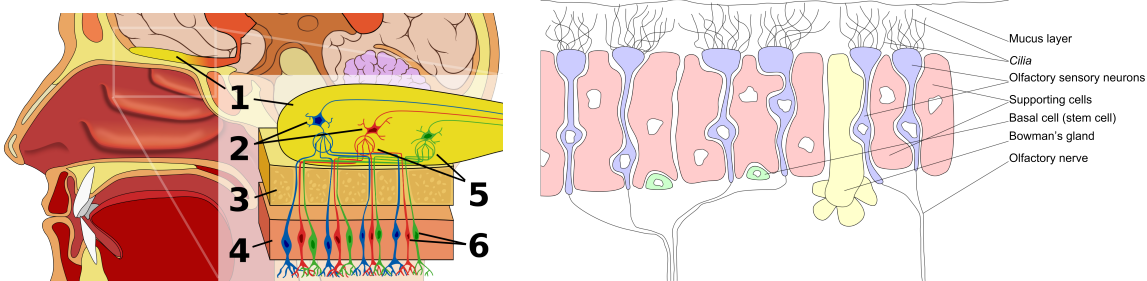
We wanted to work on this thiol model as a continuation of research on garlic sulfur compounds (for example the thiols found in human garlic breath, previously studied by the Block Group¹⁴) but we could not use it in the early stages of our project for two reasons. First, the ORs specific to thiols had yet to be identified. Second, SH protons are highly exchangeable (like OH protons). A deuterated thiol rapidly exchanges the deuterium for hydrogen in water. Since the bioassays are performed in an aqueous environment, no measurement of the effect of deuterium was possible. Instead, we started working on a different model, macrocyclic ketones with nonexchangeable C–D bonds, for which the ORs were identified.

We investigated the interactions between musk odorants and one specific olfactory receptor, OR5AN1. We first performed the synthesis of isotopologues of musk compounds as our model to activate OR5AN1. Then, a bioluminescent assay measures a receptor-luciferase complex's response to the synthesized odorants. The conclusions of this work have recently been published in PNAS,¹⁵ where it generated great interest. After publication, this work has been the topic of a C&EN article,¹⁶ a commentary in PNAS¹⁷ and was highlighted in the “In this issue” section of PNAS.¹⁸ Turin’s response in PNAS through a letter to the Editor¹⁹ was answered in the same journal.²⁰ Finally, the work has been popularized in a *Conversation* article.²¹ After these encouraging findings about the mechanism at the receptor, our research group continues working on thiols and sulfides since the receptors have been identified.

5.1.1 Overview of the olfactory system

The olfaction process can be broken down as follows: a volatile molecule (called odorant) enters the nose, interacts with odorant-binding proteins (OBPs) or enzymes in the nasal mucus, and activates ORs located in the olfactory epithelium (OE). These receptors are covering the *cilia* at the tip of the dendrites of special

neurons called olfactory sensory neurons (OSNs) (Figure 5.1b). OR and odorant interactions are the keys to understand the molecular mechanisms underlying olfaction, because a chemical stimulus becomes an electrical signal by the activation of the OR. This signal is then transmitted to the next neuron, called mitral cell, in the olfactory bulb. At this point, the inputs from several OSNs are combined in a glomerulus. As a matter of fact, each group of unique ORs has their axons converging in one location, enhancing the signal²² and mapping the response to the odorant in different glomeruli.²³ The signal is then carried further to the brain through the nervous system.



(a) Overview. 1: Olfactory bulb, 2: Mitral cells, 3: Bone, 4: Nasal epithelium, 5: Glomerulus, 6: Olfactory receptor cells (image by Patrick J. Lynch under Creative Common license).

(b) Olfactory epithelium (image by Marian Sigler under Creative Common license, modified)

Figure 5.1: Olfactory system

Even in a simple description of the olfaction process, elements need to be emphasized. ORs are present in multiple copies in the nose, and each OSN contains a specific OR type. The number of different OR varies across species, humans having about 350 groups of receptors. In addition to the multiple ORs of the same type in the neuron, each neuron type is also found in several copies (approximately 5000 in total). Thousands of axons from neurons with the same OR converge in 2-4 glomeruli. A model of the signal neuroprocessing in three steps has recently been published.²⁴ The OSNs exhibit a very high replacement rate, uncommon for neurons, and the system is duplicated in the two nostrils. These adaptations and the redundancy serve the purpose of maximizing sensitivity and robustness of the olfactory system.²⁵ The 350 different receptors are not specific to one chemical, or one functional group. Odors are combinations of the activation of different ORs. One particular OR can detect more than one compound, and one particular compound can activate more than one receptor, as illustrated by the work of L. Buck's group²⁶ (Figure 5.2). These concepts will be developed later, but are crucial to understand the complexity of the system.

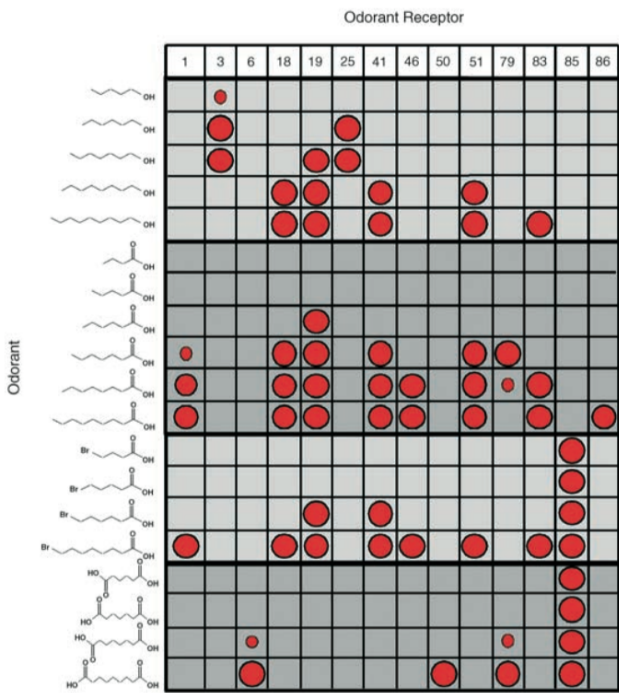


Figure 5.2: Combinations of olfactory receptors are used to detect odorants. Each OR type potentially recognizes multiple odorants, each odorant potentially activates multiple ORs (from Buck²⁷).

The OSNs are the only neurons in direct contact with the outside of the body. They are therefore an easy port of entry for pathogens. One of the roles of nasal mucus is to protect the animal from these pathogens, but other functions are attributed to some of its constituents. Active participation by nasal mucus in olfaction is acknowledged: a study of human adults' mucus proteins²⁸ shows transport, transcription, transduction, cytoskeletal, regulation, binding, and metabolism of odorant molecules functions besides the anti-inflammatory, antimicrobial, protease inhibition, antioxidant functions of the mucus proteins.

Odorants are very diverse, usually hydrophobic small molecules. Their main characteristic is their volatility, and the heaviest odorants are made of about 18 to 20 carbons for a molecular weight limit of about 300 Da. Obviously, odorants also need to be soluble in the nasal mucus to be able to reach the receptors. The OBPs are thought to help carry the hydrophobic odorants through the aqueous mucus, and also to store semiochemicals (the generic word for compounds emitted by an organism which carry a message with the purpose of communication²⁹) for later release.³⁰ Other roles of OBPs include signal attenuation and removal of odorants following detection. Enzymes in the mucus have been isolated and perform a wide range of reactions on odorants such as oxidation, epoxidation, *O*- and *N*-demethylation, and hydroxylation (reviewed

by Schillings *et al.*³¹). The expression of these enzymes by each individual can be different, which can explain why the perception of an odorant can vary somewhat from one person to another.

The ORs are proteins located in the membrane of the OSN, at the interface with the mucus. Their extracellular active sites are where the interactions with odorants take place. The activation of the receptor by a complementary odorant leads to the depolarization of the membrane of the neuron, and this electrical signal is transmitted to the next neuron. Even though the field is only two decades old, the discovery (and Nobel Prize) of Buck and Axel generated great interest in the scientific community, and today almost 15,000 receptors have been identified across the animal kingdom in the Olfactory Receptor Database.³² After identifying the genes coding for the receptors, as noted already, Buck's group found that smell is a combinatorial response of receptors: one odorant stimulates a range of receptors²⁶ and one receptor can be activated by more than one odorant.²³ Later, a review from Dunkel *et al.* demonstrated that 230 food samples with a different odor were indeed the combination in different ratios of 3 to 40 key odorants.³³ They suggested that food-related olfactory signals have co-evolved with human's 350 olfactory receptors to provide nuanced perceptions from a limited number of odorants.

At this point, a distinction between the activation of the receptors and how the smell is perceived needs to be made. Perception is “the process of using information and the individual's understanding [...] so that sensations become a meaningful experience”.³⁴ It is the result of a cognitive process of the brain, related to the subject's history, memory and even expectations, rather than the simple activation of receptors. The difference between the two is so complex, especially when it comes to olfaction, that considerable research has been performed on neurocognitive limitations of olfactory language. A recent paper synthesizes “behavioral and neuroimaging data to develop a framework for olfactory lexical processing in the human brain”.³⁵ In fact, the perception of an odorant is subjected to neuroprocessing, inducing variations in the description of the same odorant by naive subjects. Neuroscientists have shown that the description of one odorant can vary between individuals, but also over time and according to the concentration of the odorant. Regardless of the process by the brain, individuals are very unlikely to have identical sets of ORs thanks to different gene silencing patterns.³⁶ Moreover, *in vivo* alteration of the odorant during “pre-smell” enzymatic reactions can occur in the mucus. The perception of an odorant is therefore more complex than the activation of one or more receptors.

Problems with the numerous studies on smell are often derived from a lack of purity. The perception threshold of certain odorants is so low that contamination is easy. However, older work³⁷ already pointed at

this fact: smelling is a subjective perception, delivered after a semantic process, and not a combination of biochemical reactions. Investigators of the OR-odorant interactions should bear this important bias in mind.

5.1.2 (Bio)chemistry and theories of olfaction

As explained above, the overall process of an odorant being perceived by the brain is mostly understood, but the interaction between the odorant and the receptor and how this interaction is translated in the depolarization of the OSN remains an important missing piece of the puzzle.

The receptors belong to the class A rhodopsin-like family of G protein-coupled receptors (GPCRs), which are known for being a molecular modeling challenge.³⁸ GPCRs contain seven trans-membrane domains, which make them extremely hard to crystallize. In the absence of an X-ray structure, the shape of the active site remains unknown. This question is so central that books are published on that specific topic,³⁹ as well as numerous structure-function studies (reviewed by de March *et al.*⁴⁰). An alternative to understand the molecular mechanisms of a biological system is site-directed mutagenesis. In this technique, the amino acid sequence of the protein is known, and alternative proteins are synthesized with a targeted mutation. The mutation sites are thought to play a key role in the binding or catalytic site, a role that is demonstrated if the function of the protein is lost after the mutation. Site-directed mutagenesis has been successfully applied to the study of mice ORs to identify the binding site of copper.⁴¹ A recent review summarizes the knowledge to date, and deduces a template of the receptor's structure from alignments and site-directed mutagenesis studies.^{42,43}

Once the odorant interacts with the active site of the ORs, a structural change occurs, and the G-protein activates the lyase that induces the adenylyl cyclase signaling cascade. Briefly, ATP is converted by the lyase into cyclic AMP (cAMP), which in turn opens ion channels resulting in calcium and potassium entering the cell and depolarizing the neuron⁴⁴ (Figure 5.3). However, the modalities of the ORs activation remains unsolved, especially since no experimental structures of the receptors have been obtained so far, and before this major discovery is made, research on the ORs-odorant interactions will need to use a different approach.

So how does the odorant activate the ORs? After a first wave of early theories (summarized in Sell's book⁴⁵), two main views have coexisted about what triggers the receptors response, *i.e.*, what is the nature of the interactions between the odorant and the extracellular part of the G-proteins. On one hand, the vibration theory of olfaction (VTO), described by Dyson in 1928⁴⁶ then 1938,⁴⁷ and further developed by Wright in the fifties,⁴⁸ claims that receptors can recognize frequencies of vibration of the chemical bonds in the odorant.

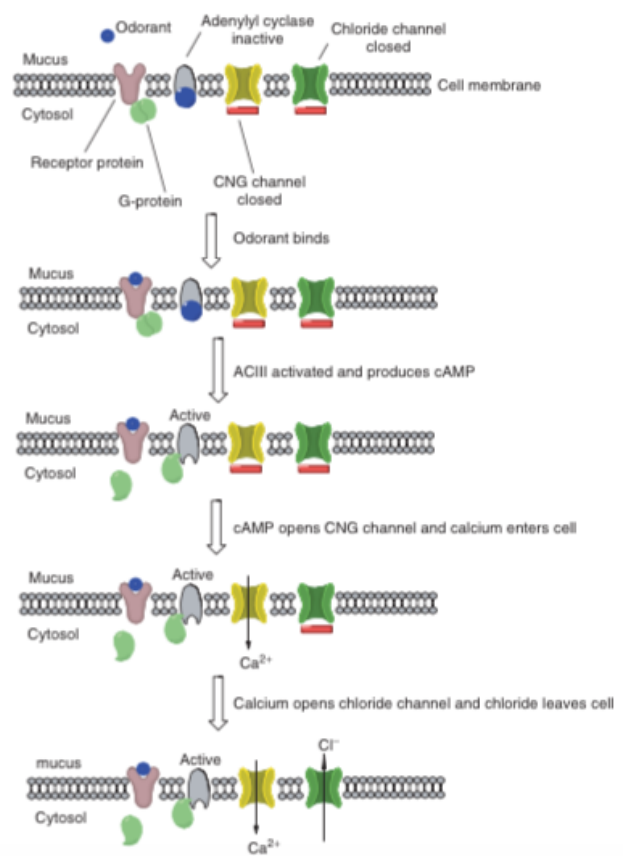


Figure 5.3: Biochemistry at the olfactory receptors (ORs): after activation, the G-protein activates the cAMP-dependent pathway (by Sell⁴⁵)

After years in limbo, the interest in this theory increased when Turin published a more developed version in 1996,¹² in which the vibration energy would allow an electron to activate the G-protein via electron tunneling (Figure 5.4). The vibration frequencies correspond to the infrared region of the electromagnetic spectrum, and so the ORs would work similarly to IR spectrophotometers.

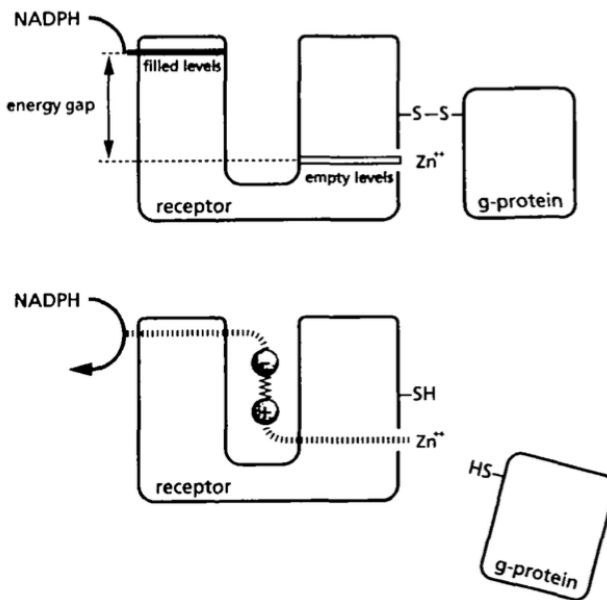


Figure 5.4: Mechanism of activation of the olfactory receptors (ORs) according to the vibration theory of olfaction (VTO) (by Turin).¹²

The shape theory of olfaction (or lock-and-key theory), on the other hand, states that the three-dimensional conformation and the electrostatic properties of the odorant matches the active site of the receptors. The presence of a compound that snugly fits in the active site would change the conformation of the receptor, and therefore activate it. Features such as the molecular shape, molecular size and functional groups would determine the smell character of a compound. The identification of the receptors as part of the GPCR group supports this theory since all known GPCRs proceed via an allosteric conformational change upon binding of a ligand. “Shape” suggests that the form only is taken into account in the interaction with the receptors. This initial simplistic theory – one odorant for one receptor – evolved into the so-called odotope theory of olfaction⁴⁹ that postulates that small parts of the structure of odorants are activating various receptors. The brain processes the information, and the combination leads to perceived smell. The word “odotope” was built as an analogy to “epitope”, the portion of an antigen recognized by the immune system. The odotope theory is also known as the Weak-shape theory.

To overcome the absence of X-ray structures of the receptors, two techniques have been used to structurally characterize them and try to model their interactions with odorants: the *Ab initio* procedure, that uses the amino acid sequence, followed by the application of classical laws of physics to predict the 3D structure of the protein, and homology modeling methods, based on a set of experimentally known similar structures. This second approach has been applied to model the interactions between odorants and ORs, and enables the accessing of information such as binding affinity estimations, the nature of the residues in the binding pocket, and the orientation of the odorant. An example of such a molecular model is presented on Figure 5.5. This modeling is of course limited, and no real assumptions can be made before crystallographers can provide a decent structure of the receptors or site-directed mutagenesis provides enough information on the active site of the ORs.



Figure 5.5: Example of molecular modeling of the OR-odorant interaction: view of the binding site of OR1G1 bound to camphor (by Charlier et al.³⁸)

The two theories of olfaction have been in competition ever since. In *Chemical & Engineering News*, Everts describes the “shape” and “vibration” controversy as an “acrimonious, nearly two-decade-long [controversy]... on the one side are a majority of sensory scientists who argue that our odorant receptors detect specific scent molecules on the basis of their shapes and chemical properties. On the other side are a handful of scientists who posit that an odorant receptor detects an odor molecule’s vibrational frequencies.”¹⁶ Notably, the work from Turin and co-workers,^{12,50,51} and Brookes *et al.*⁵² support the VTO. The “shape” or odotope theory is supported by most authors including Keller and Vosshall,⁵³ and a recent computational paper emphasizes the importance of the molecular volume of odorants.⁵⁴

5.1.3 Interactions of musk-related compounds and the olfactory receptors

The approach chosen in our study is very fundamental. Because one musk human OR, OR5AN1, was identified and the receptor activity could be measured by the OR-luciferase complex, we saw an opportunity to reassess the results of Gane *et al.*⁵¹ on smelling deuterated and undeuterated musk-related compounds, namely muscone (3-methylcyclopentadecanone, **77**, Figure 5.6). The latter presents many advantages: it is commercially available, well-characterized and used in the cosmetic industry. Moreover, this human OR had just been identified by our coworkers, and by others, in two recent publications.^{5,55} Since muscone is chiral, with (*R*)-muscone being the naturally occurring enantiomer, it should be possible to determine the enantioselectivity of the human musk OR, if an enantiomerically pure sample of (*R*)-muscone can be obtained.

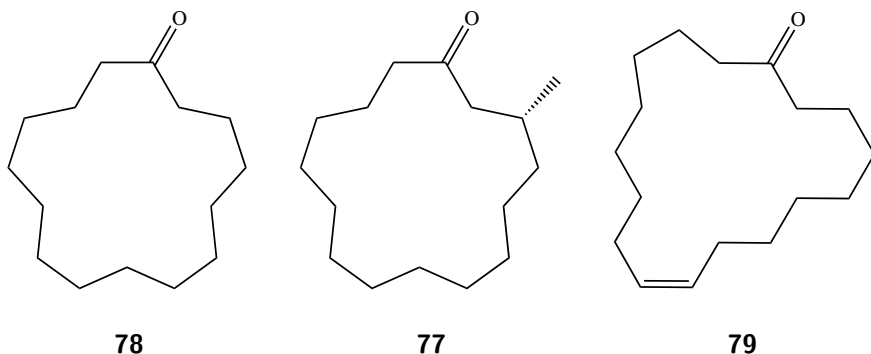


Figure 5.6: Macroyclic ketones related to musk odor: cyclopentadecanone or Exaltone®(**78**), muscone (**77**) from musk deer, and civetone (**79**) from civet cat.

Musks, historically macrocyclic ketones and lactones, have been mentioned by the Arabs since the 8th century,⁵⁶ and have been broadly used in perfume since then. The mixture was originally extracted from the musk deer glands, and was so popular in the 19th century that the specie became threatened with extinction. Today, synthetic musk is still widely used in the perfume and cosmetic industries for its smell but mainly as an odor-fixating and enhancing agent (summarized by Sell⁴⁵). Interestingly, another animal, the civet cat, was known for its pleasant smelling secretion. Civetone (**79**, (*Z*)-9-cycloheptadecen-1-one) is the main compound extracted from the civet cat anal glands. Like muscone, it is a macrocyclic ketone, but it contains seventeen carbons in the ring and a *Z* double bond (Figure 5.6). Strong activation of OR5AN1 has also been detected for civetone.

Instead of working on muscone (**77**, Figure 5.6), Gane and coworkers⁵¹ used cyclopentadecanone (**78**, Figure 5.6), commercially known as Exaltone®, a cyclic 15-carbon ketone related to muscone (**77**). As

one of its analogues, it presents strong activity at the receptor without the complications related to the stereocenter. According to their study, undeuterated and deuterated **78** have a different odor, as perceived by an expert panel, which they attributed to the differences in their bond vibration frequencies.

By repeating the deuteration of **78**, we had two aims: first, to reach a higher organoleptic purity to make sure the conclusions are not based on traces of other chemicals, and second to compare the activity at the receptor level via a luciferase assay to avoid the bias introduced by perception. A difference in the activities measured at the OR level would confirm Gane's group claims.

However, other concerns can be identified in our approach, and we summarize and address them in the next section as well as in the conclusion.

5.1.4 Designing olfactory reception experiments: challenges

Designing experiments demonstrating what happens at the receptor level is not an easy task. Comparing perception of odors to draw conclusions on the receptors' activation would be a mistake, because it neglects the anatomy, genetics, physiology and history of the subjects. Furthermore, concluding that an odor perception describes the OR's activation by an odorant in its original form is questionable.

The study of isotopologues represents a convenient way to better understand the chemistry of olfaction, especially in the case of hydrogen–deuterium exchange. In fact, the C–D bond has a different vibrational frequency thanks to the mass of deuterium, twice as big as ^1H ; therefore the IR spectrum is different. The shape, however, is almost not affected: the carbon–deuterium bond is slightly shorter but the overall conformation of the compound is identical. Multiple studies have been performed over time,^{50,51,53} with different conclusions. In these investigations, the difference between deuterated and undeuterated odorants has been assessed by smell panels. Two problems can be identified in this approach. Firstly, organoleptic purity is hard to achieve, and slight traces of contaminants such as solvents can drastically modify the perception. Furthermore, as explained above, the process of olfaction as a whole is not taken into account: perceptions are compared, but not the mechanism at the receptor. We need to keep all these concerns in mind while designing an experiment to understand the chemistry at the receptor.

In this complex context, the study we have designed is holistic and will focus on the shape vs. vibration theory of olfaction **at the receptor level**. To reach this goal, test odorants have been evaluated using **in vitro activation of receptors**. Measuring the activity of one single receptor to evaluate a whole theory is questionable, since odors are known to be perceived as the combination of the multiple receptors' activation.

To address this issue, the model odorants chosen are musk isotopologues: one unique human receptor, OR5AN1, has been identified to be sensitive to musk compounds in previous studies.^{5,57} The unusual size of the cycle and the ketone group that would function as a hydrogen bond acceptor explain the exclusive specificity of the corresponding mouse receptor to C15 and C16 macrocyclic ketones.⁵⁵ We have thus prepared a series of isotopologues and compared their vibrational properties (e.g., IR bands) and the recognition by the receptor OR5AN1. Organoleptic purity was ensured by repeated crystallization to constant melting point of each isotopologue, and the comparison of the commercial sample with a control (sham synthesis with water). To complete the work, the validity of the model of the vibration theory of olfaction (VTO) is assessed by a computational study.

Charles Sell summarizes the challenging points in describing olfaction in four false assumptions made in most studies on olfaction in his recent book.⁴⁵ Our work needs to address each of them. For clarity, they are enumerated as mistakes to avoid and not false assumptions, and our response to the concern is written in italics.

- 1. Odor is not a molecular property:** we know that it's the activation of a set of receptors, and not the interaction between one odorant and a single receptor, that leads to the perception. Each individual has a different repertoire of receptors, therefore the activation pattern and the signal sent to the brain will be different for each of us. *In our study, we do not measure a perception, but rather the odorant-OR interaction. The activation of OR5AN1 might not be representative of the perceived odor: our approach is more fundamental.*
- 2. The odorant delivered to the nose is not the substance detected by the receptors:** after neglecting the processing of the signal from the receptors by the brain, another mistake is commonly made. The metabolism in the nose (OBP interacting with the odorants, enzymatic reactions occurring in the mucus) are ignored. *Should preolfaction events occur or not, we focus on the activation of the ORs. Again, what we measure could be different than the overall process of smelling musk.*
- 3. Olfactory receptors are not tuned to odor:** investigations of the receptive ranges of ORs shows that the tuning is not to odor but to stereo-electronic properties of the ligands (odorants with a different smell can activate the same receptor if they share common stereoelectronic features).⁵⁸⁻⁶⁰ *Our study focuses on a known odorant-OR interaction rather than a receptive range, and the choice of the macrocyclic musk-OR5AN1 pair should limit this bias. As a matter of fact, very few other*

ORs recognizes cyclopentadecanone (78) according to recent studies.^{5,55} Nonetheless, a screening of the human OR repertoire has been performed to ensure the specificity of OR5AN1.

4. **Odorant-receptor interaction is not the only significant event in the process of olfaction:** even if the odorant-receptor interaction is the most significant step of the overall process of olfaction, neuroscientists believe the input signal is used to construct a mental image. This process is affected by events other than the activation of the receptor. *Again, our approach is more fundamental and exclusively seeks to measure the OR activation, not the overall olfaction of musk compounds.*

As a test of the vibration theory, we have prepared a series of isotopologues of musks and other compounds, containing up to 30 C–H or C–D bonds as test odorants, which are evaluated using in vitro activation of receptors identified by us and other groups as being highly responsive to these isotopologues. We consider the confounding effects of impurities and isotope effects in interpreting odorant perception, as well as the validity of requirements for specific IR bands for recognition of musks by their receptors.

5.2 Results and discussion

As mentioned in the introduction, the challenge in understanding the interactions between odorants and the ORs stems from the lack of available X-ray structures of the receptors. In order to circumvent this issue, a multidisciplinary approach has been adopted. Odorants are synthesized with structural or isotopic modifications, then submitted to a receptor activation assay. A computational model in which the musk carbonyl functions as a hydrogen bond acceptor completes the study.

The model compounds chosen for our study are muscone (77) and cyclopentadecanone (78, Figure 5.6). Deuterated compounds have been synthesized and the properties of each of them has been assessed. The cyclopentadecanones tested were the following: undeuterated cyclopentadecanone (78a), cyclopentadecanone-2,2,15,15-d₄ (78b), cyclopentadecanone-3,3,4,4,5,5,6,6,7,7,8,8,9,9,10,10,11,11,12,12,13,13,14,14-d₂₄ (78c), and cyclopentadecanone-d₂₈ (78d, Figure 5.7). Cyclopentadecanol and cyclopentadecane were byproducts of our reactions and were tested too.

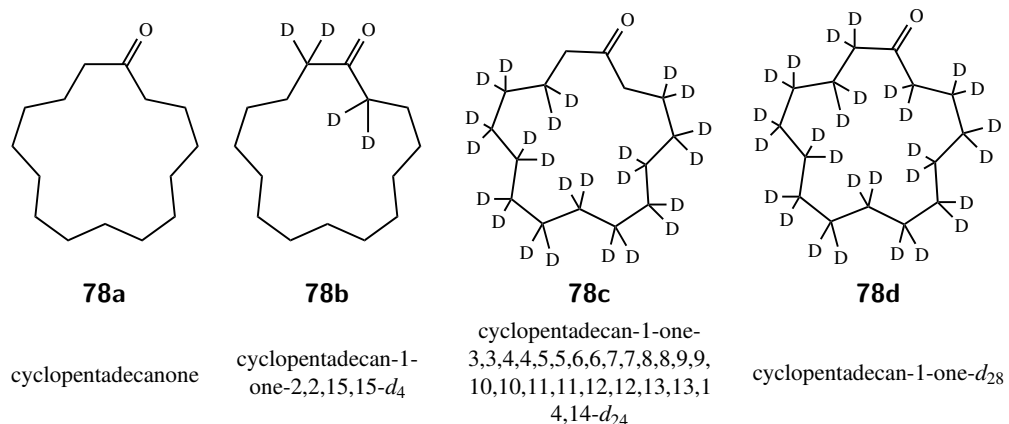


Figure 5.7: Deuteration patterns of cyclopentadecanone isotopologues studied in this work.

5.2.1 Synthesis of musk derivatives

Deuteration procedures

Base catalysed exchange reaction (wash-out) The protons in the α -position of the carbonyl in **78** are more acidic, and can be exchanged (or “washed out”) by deuterium in the presence of a base (Figure 5.8). The product of this reaction, 2,2,15,15-tetradeca^{2,2}terocyclopentadecanone (**78b**), is obtained in 85% yield after three reaction cycles (needed to reach a good deuteration rate, e.g., 94% of the desired hydrogens exchanged).

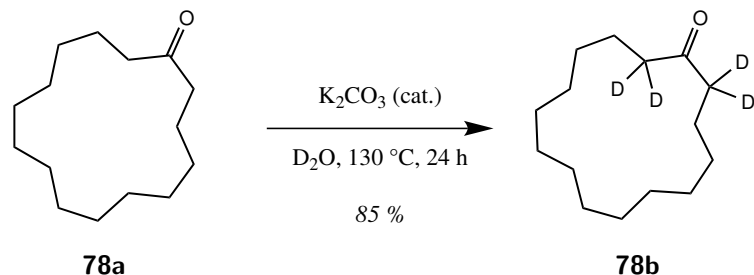


Figure 5.8: Wash-out reaction: base-catalyzed replacement of four hydrogens by four deuteriums in the α -position of the carbonyl.

Heterogenous metal catalysis Pd and Pt catalyzed hydrogen/deuterium isotope exchange has been known for decades but its application was limited due to the formation of byproducts (hydrogenation, dehalogenation, etc.).⁶¹ The reaction is carried out in a triphasic system: solid catalyst, solution of the substrate and gaseous deuterium at elevated temperature (150 °C). It generally leads to high levels of uniform deuter-

ation.⁶¹ The mechanism of the reaction is not fully understood, but the formation of D₂ is thought to be the first step⁶² (Figure 5.9).

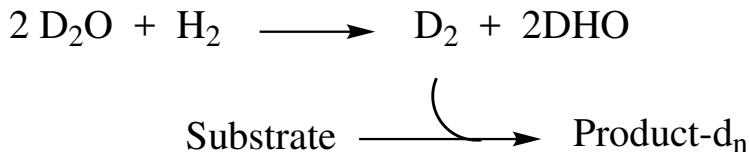


Figure 5.9: First step of the deuteration reaction: proposed mechanism for the formation of D₂ from deuterium oxide and H₂.

In 2008, Maegawa *et al.*⁶³ used rhodium on carbon and obtained a higher deuteration rate than with the traditional noble metals. This method was successfully applied by Gane *et al.*⁵¹ to deuterate cyclopentadecanone (**78**). However their deuteration cycle did not lead to a fully deuterated product (as determined by NMR). The rate depends on the position in the molecule: 95% of the α -keto and 94% of the β -keto hydrogens have been exchanged, but only 90% of the remaining positions.

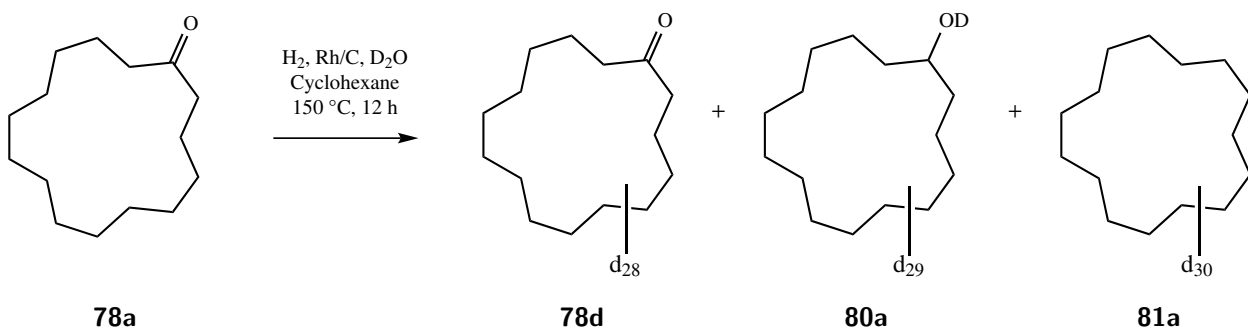


Figure 5.10: Rhodium-catalyzed deuteration reaction leads to the exchange of hydrogens at all positions of the cyclopentadecanone **82a**. Under these conditions, reduction occurs leading to deuterated products **80a** (alcohol) and **81a** (alkane).

After obtaining similar results as well as reduction byproducts (Figure 5.10), we treated the crude product of the reaction under the same conditions to improve the proportion of deuterium. This second cycle lead to higher deuteration and a narrower distribution of the masses of the products, *i.e.*, a higher purity. Mass spectra will be described below.

However, performing a second deuteration cycle also increased reduction of the ketone to the corresponding alcohol and to the alkane. The proportion of ketone (**78d**), alcohol (**80a**) and alkane (**81a**) are 48:48:4 and 2:94:4 after one and two deuteration cycles, respectively (Figure 5.11). Deuterated cyclopentadecanol (**80a**) is obtained as the main product in 30% yield. Cyclopentadecane-d₃₀ (**81a**) is recovered with a yield of 8%,

which is higher than the GC-MS proportion (Figure 5.11), highlighting that the GC-MS proportions are not directly proportional to the concentration: the response factor may vary and is smaller for cyclopentadecane (**81**) than for cyclopentadecanol (**80**) or cyclopentadecanone (**78**).

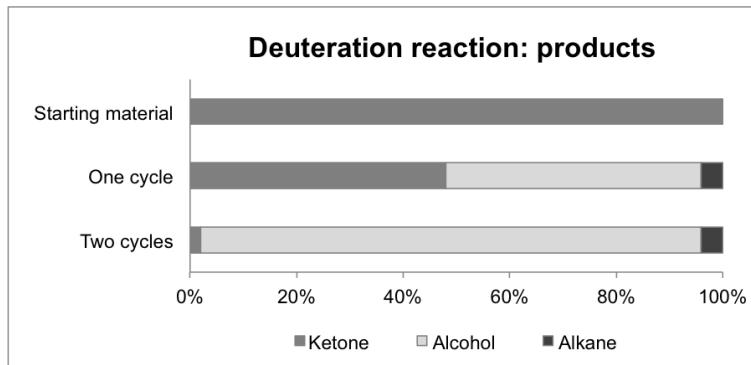


Figure 5.11: Deuteration reaction: proportion of the products.

A sham reaction has also been performed on cyclopentadecanone **78a** in the exact same conditions but with H_2O instead of D_2O . Testing this sample against commercial cyclopentadecanone was conducted to confirm that no undetected by-products of the reaction were present in the samples, affecting the bioassay results.

Reoxidation of the alcohol Considerable material would have been lost if the alcohol **80a** had not been used. Figure 5.12 presents the oxidation reaction, converting a by-product into the desired ketone. This simple reaction affords the ketone **78d** in 97% GC-MS purity. Organoleptic purity is crucial in our analysis and a recrystallization is performed in pentane:EtOH before use in biological assays.

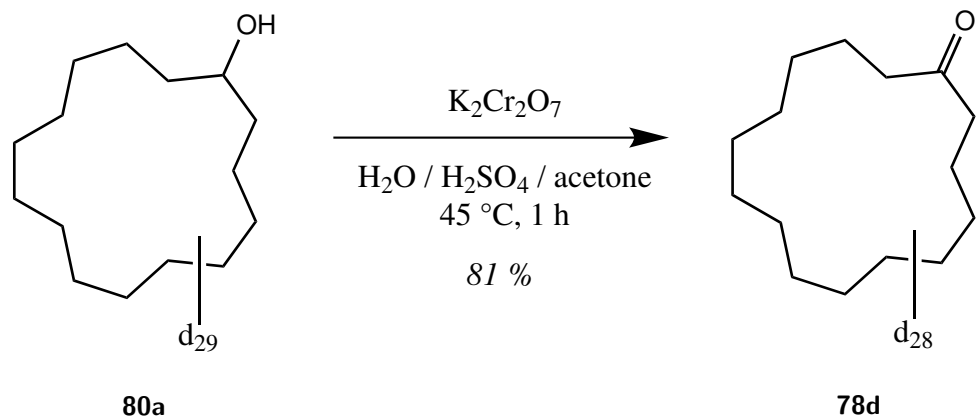


Figure 5.12: Recycling the reduced cyclopentadecanone by oxidation of the alcohol.

Inverted Wash-out In order to check if some carbon-hydrogen bonds were more crucial than others in the recognition of **78** by the receptor, we synthesized cyclopentadecanone with a third deuteration pattern. This was done by washing-out fully deuterated **78d** in H_2O following the wash-out procedure. Again, the α -carbonyl deuteriums, more acidic, are replaced by hydrogens in basic conditions, leading to cyclopentadecanone-3,3,4,4,5,5,6,6,7,7,8,8,9,9,10,10,11,11,12,12,13,13,14,14-d₂₄ (**78c**, Figure 5.13).

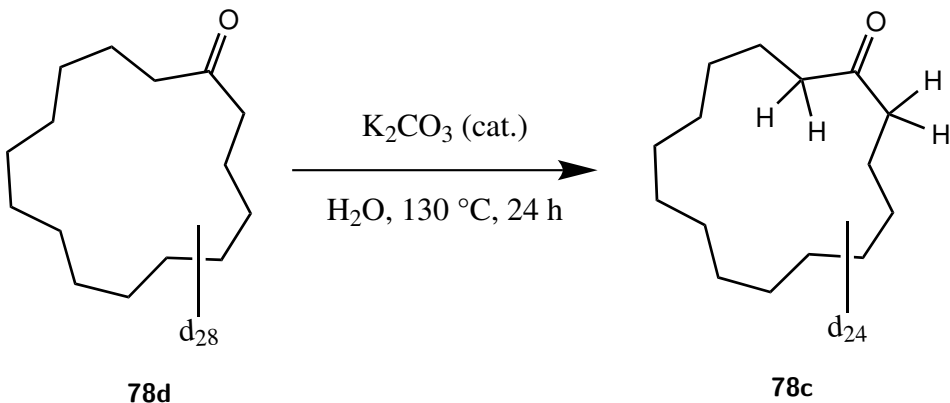


Figure 5.13: Inverted wash-out reaction: base catalyzed exchange of four deuteriums.

Comparison of the spectral data of deuterated cyclopentadecanones

According to the vibration theory of olfaction (VTO), the difference of vibrational energy between C–H and C–D bonds would induce a different recognition of the compound at the receptor level. Hence, the quality of the deuteration and the organoleptic purity are crucial in this project. IR is the first choice technique to assess the absence of vibrations that could interfere with the receptor (still according to the VTO). Two other techniques were used in the evaluation of the purity: GC-MS (indicates the extent of deuteration for each synthesized compound) and NMR (indicates all protons present in the sample). The three techniques and the corresponding results are described in the following paragraph.

1. IR:

Infrared spectra of undeuterated (black) and fully deuterated (blue) cyclopentadecanone are presented (Figure 5.14). The first comment that can be made is the almost total disappearance of the C–H band upon deuteration: the absorption at 2898 cm^{-1} is limited to a tiny band. Two new C–D bands are present on the deuterated trace at 2197 and 2099 cm^{-1} . The compounds seem suitable to assess the plausibility of the VTO. The absence of bands in the 1380 – 1550 cm^{-1} region is important: Gane

and coworkers⁵¹ claimed that a musk receptor “detects vibrations in the 1380-1550 cm^{-1} range,” and that musk odor requires that “the molecule has intense bands in that region”. The IR spectra of their samples had these intense bands. A lack of purity could therefore explain why samples are perceived differently in Gane’s experiment: they present IR bands that compounds synthesized in our lab do not.

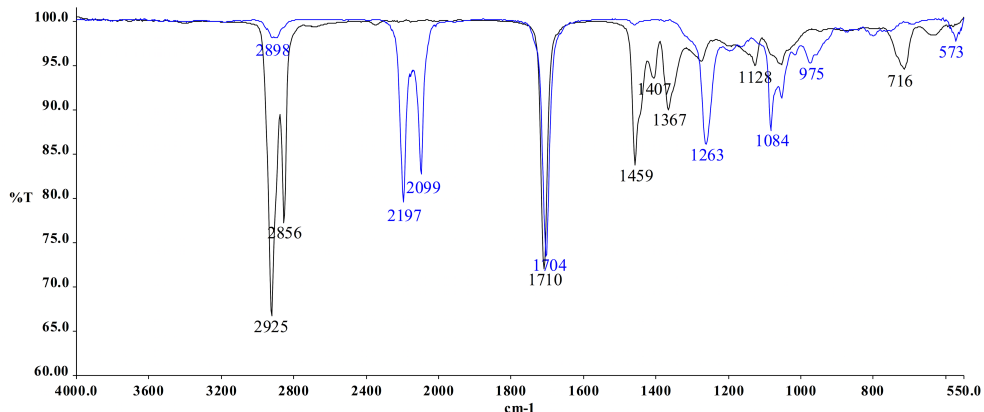


Figure 5.14: Infrared spectra overlay of undeuterated (**78a**, black) and fully deuterated cyclopentadecanone (**78d**, blue), showing C–H bands at 2925 and 2856 cm^{-1} or C–D bands at 2197 and 2099 cm^{-1} , respectively.¹⁵

2. GC-MS:

GC-MS gives us two important pieces of information: the purity can be assessed by the absence of other peaks on the chromatogram, and the level of deuteration can be assessed from the mass spectrum of each peak. Since deuterium has one more neutron than hydrogen, its mass is one unit higher. The m/z ratio of the molecular ion on the mass spectrum therefore indicates how many hydrogens have been replaced, and how isotopologically pure the sample is. As an example, Figure 5.15 displays a portion of the mass spectrum after one and two deuteration cycles of cyclopentadecanone. A very narrow range, leaning toward the molecular weight of **78d** (252), indicates a successful process. The percentage of deuteration has been calculated by comparing the abundance of the peak of fully deuterated **78** (**78d**, 252) to the sum of the abundances of all cyclopentadecanones, regardless of the level of deuteration. By doing that, we assumed that the response factor was identical for all of the isotopologues. The samples used for the luciferase assay showed at least 98.5% of deuterium content.

3. NMR:

The success of the deuteration can be simply measured by the disappearance of proton signals in the ^1H NMR spectra. This procedure also assesses the organoleptic purity by showing other hydrogens from

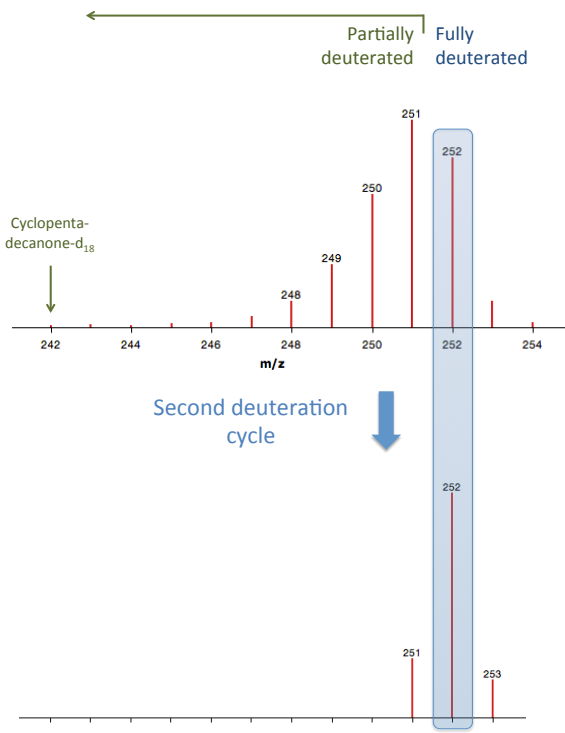


Figure 5.15: Mass spectra of cyclopentadecanone after one (top) or two (bottom) deuteration cycles. Two cycles afford mostly fully deuterated cyclopentadecanone (**78d**), even though the yield is very low.

contaminants. For each deuteration pattern, the NMR spectrum displays the desired residual protons only. Signals of undisplaced hydrogens are observed as traces (Figure 5.16).

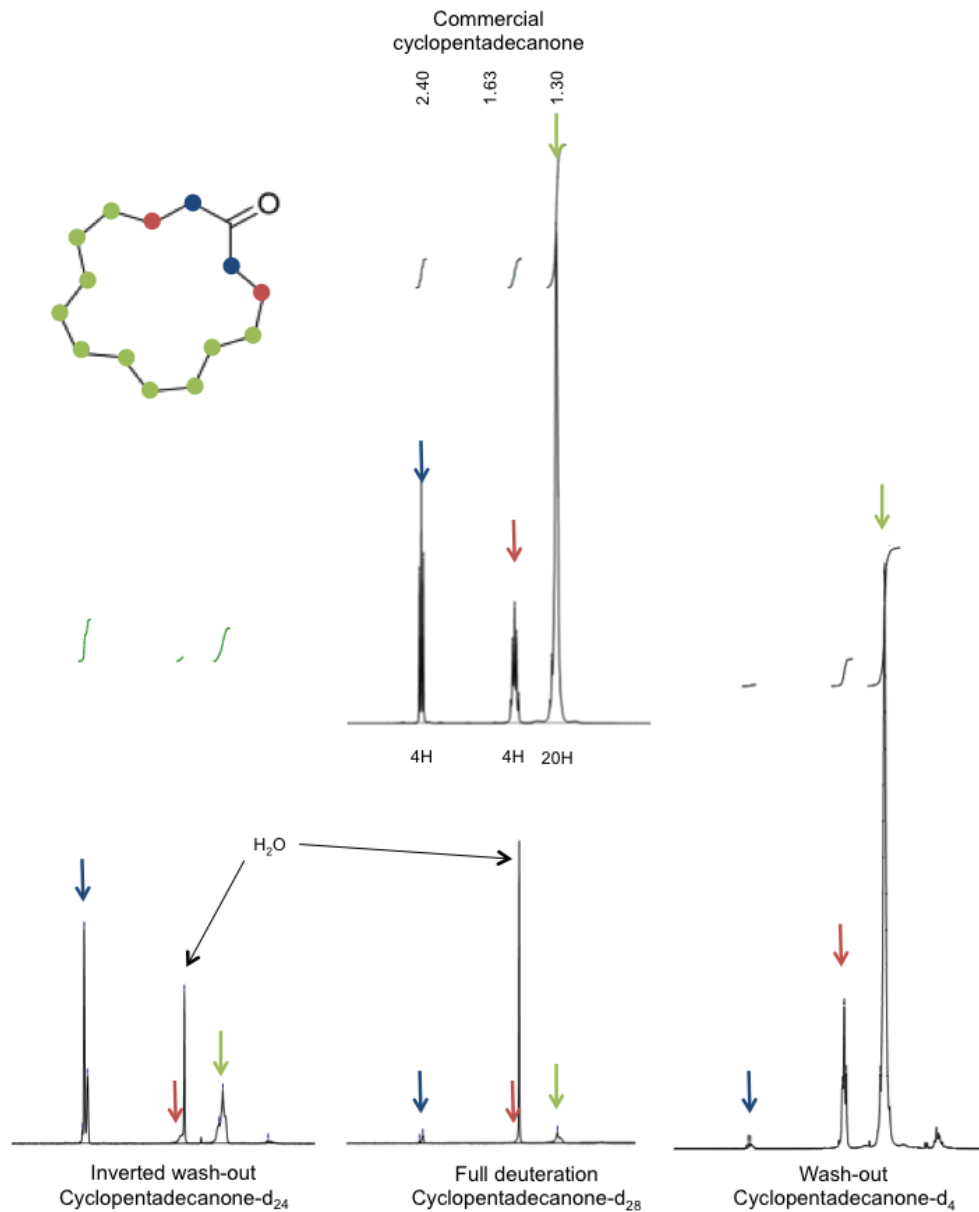


Figure 5.16: The success of the deuteration procedures can be assessed by NMR: the signal decreases for each of the displaced hydrogens.

The level of deuteration was assessed more formally by using anthracene as an internal standard. Anthracene was chosen for its easy handling (solid) and lack of interactions with the signal of compound

78. For example, deuterium accounts for 96.7% of the former hydrogens in cyclopentadecanone-d₂₈ according to this method, which compares well with the less tedious GC-MS assessment for the same sample (98.5%).

These three techniques allowed us to characterize the synthetic products. The organoleptic purity is high, as well as the level of deuteration. The cyclopentadecanone samples are ready for testing in the luciferase assay. Later, the same procedure was applied to muscone (**77**) by coworker Dr. Sivaji Gundala, with similar levels of purity found.

5.2.2 Interactions at the receptors: in vitro testing and computational study

All of these samples have been prepared to perform a receptor activation assay in vitro. Firstly, using a heterologous OR expression system,^{64,65} neurobiology coworkers on this project performed parallel screenings of all deuterated and non-deuterated versions of **78** on the human OR repertoire. Among all 330 human ORs screened, OR5AN1 was identified as a bona fide receptor for cyclopentadecanone (**78**) and its isotopologues. These results are consistent with the recent identification of OR5AN1 as the human muscone OR (based on homology with the corresponding mouse muscone OR)⁵⁵ and identification of OR5AN1 as the only functional human homolog of mouse muscone ORs *in vivo*.⁵⁷ Furthermore, as mentioned above, only a small number of receptors are thought to be involved in sensing musk odor,⁵ confirming the choice of cyclopentadecanone/OR5AN1 interaction for this study. By-product of the reaction cyclopentadecanol (**80**), as well as the Baeyer-Villiger oxidation product, ω -pentadecalactone (**83**), also display an interesting activity toward OR5AN1 according to our screening. The following confirmation experiments did not reveal any human OR that responded to only one, two, or three of the four isotopologues of **78**.

Luciferase assays showed no significant difference between undeuterated and fully deuterated compounds, neither in the example of cyclopentadecanone (**78**) nor of muscone (**77**, Figure 5.17). This result invalidates the VTO, since no discrimination exists between isotopologues at the molecular level. Furthermore, undeuterated and deuterated cyclopentadecanol (**80**) and cyclopentadecane (**81**) induced a small response of OR5AN1 or no response at all, respectively.

The computational study attempts to assess if the theoretical aspects of the VTO, electron transfer at the receptor, is plausible in current computational modeling. This work has been done at at Queens College of the City University of New York and Yale University. Theoretical studies had attempted to support the electron transfer model of the VTO.^{52,66,67} Electron tunneling is a phenomenon in quantum mechanics

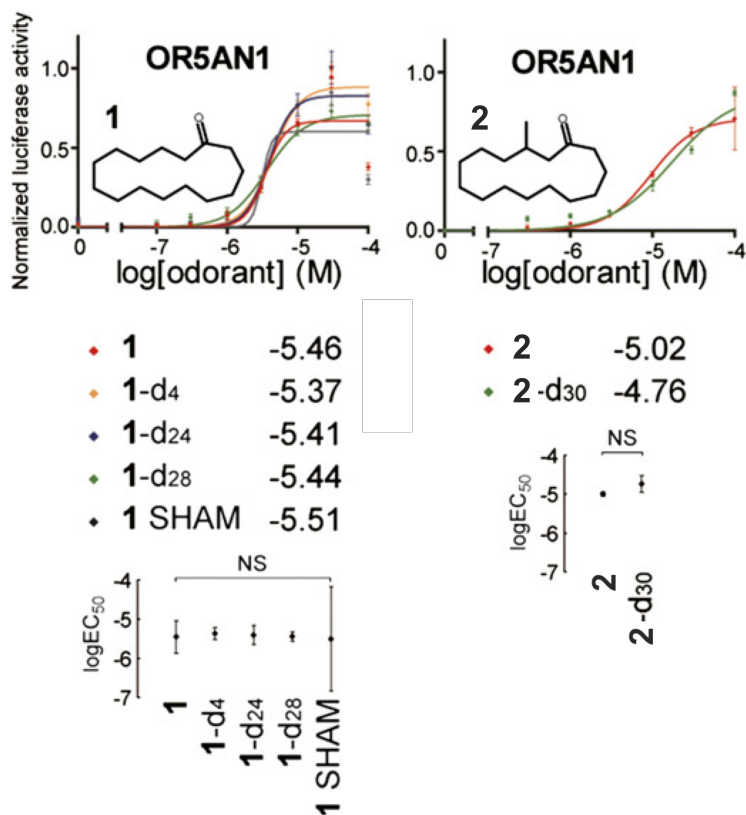


Figure 5.17: Dose-response curves of OR5AN1 to isotopologues of cyclopentadecanone (**78**) and muscone (**77**). Best-fit logEC₅₀ values of the curves are shown alongside the graph legends (placed below the graphs). Scatter plots with 95% confidence interval logEC₅₀ values and indicating statistical significances between the logEC₅₀ values among isotopologues are also shown below the corresponding graphs. “SHAM” indicates non-deuterated cyclopentadecanone subjected to the same chemical synthetic procedures as the deuterated samples without D₂O addition. NS, not significant. For all dose-response curve graphs, the chemical structures of the respective compounds are shown within the graphs and normalized responses are shown as mean \pm SEM (n = 3).¹⁵

in which the electron passes an energy barrier that couldn't be crossed according to classical physics. In the context of the VTO, an odorant with the appropriate vibrational properties would allow the electron transfer (as described above, Figure 5.4, and Figure 5.18). However, these theoretical studies admittedly rely on unconfirmed assumptions, lacking experimental evidence, to make the proposal appear to be feasible. Quantum contributions from molecular vibrational modes other than those molecular vibrational modes of the odorant oscillator are also neglected.

The work of our collaborators includes such modes as well as the effects of disorder, dynamical fluctuations, and the sensitivity of electron couplings to bonding characteristics. Their conclusions are that electron transfer is unlikely to amplify small vibrational contributions of odorants due to the presence of complicating effects typical of electron transfer in biological environments. Activation of OR5AN1 with the carbonyl of macrocyclic ketone being a hydrogen bond acceptor, as suggested by Shirasu,⁵⁵ appears as a more plausible model.

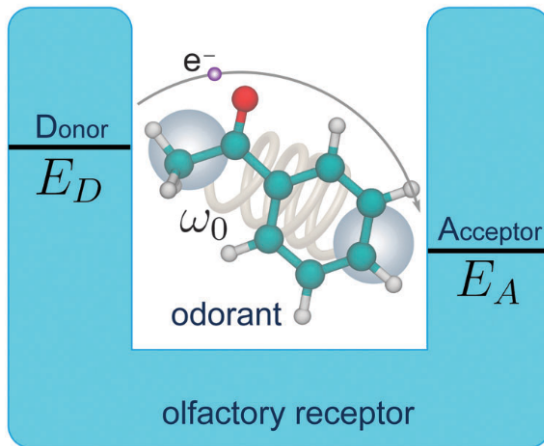


Figure 5.18: Schematic representation of the electron tunneling phenomenon as described by the vibration theory of olfaction (VTO). From Solov'yov et al.⁶⁷

5.2.3 Connection with previous work: could a kinetic isotope effect explain the difference in perception?

A potential kinetic isotope effect (KIE) for a reaction in the nasal mucus could explain the fact that the deuterated and undeuterated compounds are perceived differently when smelled, and therefore the apparent inconsistency between Gane's work⁵¹ and our experiments. The Baeyer-Villiger (BV) reaction is known to

be mediated⁶⁸ by oxidative enzymes (e.g., cytochrome P450), which are present in the nasopharyngeal mucus layer.^{45,65,69,70} The BV reaction of deuterated cyclic ketones forming deuterated lactones shows an isotope effect.⁷¹ A primary KIE involves the breaking of a C–H or C–D bond, which does not occur in the Baeyer–Villiger reaction. In this case, a secondary KIE is observed. Oxidation in the nasal mucus might affect odor perception of pairs such as **78a** and **78d**. An oxidation, a common metabolic reaction, could occur in a pre-olfaction step. To assess the behavior of cyclopentadecanone toward oxidation, undeuterated (**78a**) and fully deuterated cyclopentadecanone (**78d**) have been treated with *m*CPBA in dichloromethane leading to a lactone (Baeyer–Villiger oxidation, Figure 5.19). The amount of product and starting material have been measured over time by GC-MS.

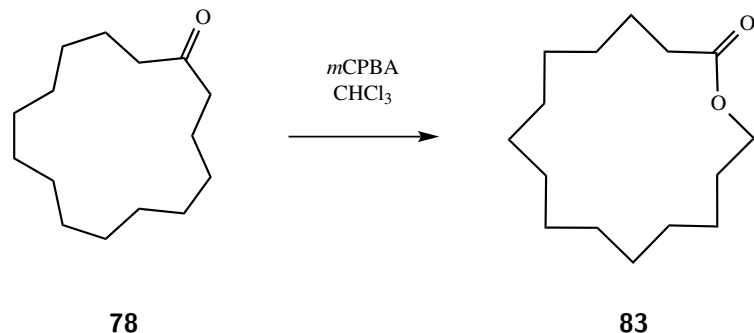


Figure 5.19: Baeyer–Villiger oxidation of cyclopentadecanone (**78**) by *m*CPBA leads to ω -pentadecalactone (**83**). This reaction will be used to assess an eventual KIE.

A preliminary study consists of the GC-MS analysis of the above reaction and a comparison of the peak area of the starting material versus starting material plus product for each level of deuteration. It indicates that cyclopentadecanone-d₂₈ is oxidized faster than the corresponding undeuterated cyclopentadecanone, but also shows a strong variability between injections (Figure 5.20). The comparison of the tangents at the origin (which is mimicking the method of initial rates) gives a slope ratio $\frac{m_H}{m_D}$ of 0.65, which is a significant difference. However, the absence of a valid calibration makes the assessment of the kinetics parameters impossible. These results need to be taken with care, since differences between the response factor for deuterated and undeuterated compounds on one hand, and ketone and lactone on the other hand, could be significant.

A second comparison has been made at higher concentrations and over a longer time (Figure 5.21). An approach similar to the method of initial rates can be adopted considering this reaction as a pseudo-first order reaction (thanks to the large excess of *m*CPBA). In these conditions, *k* is calculated from the plot of

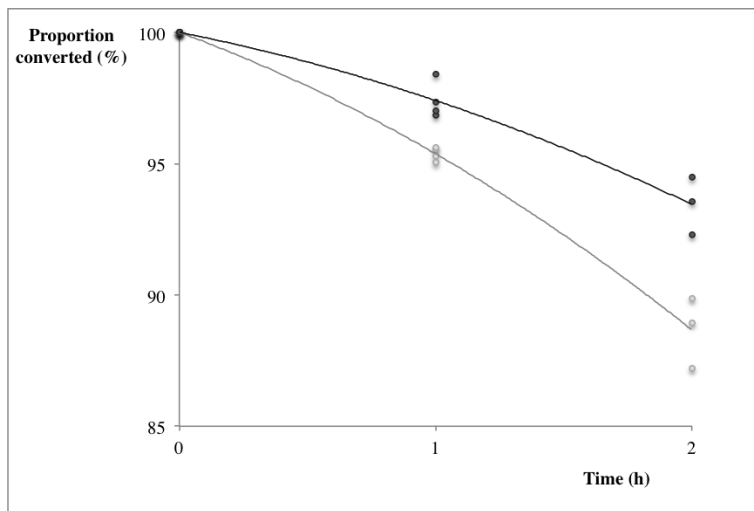


Figure 5.20: Baeyer-Villiger oxidation of cyclopentadecanone-d₀ (**78a**) and -d₂₈ (**78d**) by *m*CPBA occurs at a different rate, the deuterated compound being oxidized faster. The KIE itself has not been measured, the rate equation being unknown, but the ratio between the slopes of the two tangents is 0.65 (repetitions: 3).

$\ln[C] = f(t)$ and $\frac{k_H}{k_D}$ equals 0.955, indicating a slight difference in the Baeyer-Villiger oxidation between CH₂ and CD₂ groups next to the carbonyl. Establishing a kinetic isotope effect would need a more complete study. The C–H bond is weaker than the C–D bond, and KIE are usually greater than 1.⁷² However our two preliminary studies tend to indicate ratios smaller than 1. Examples of $\frac{k_H}{k_D} < 1$ are found with H₂O or D₂O as solvents, in a phenomenon called inverse solvent deuterium isotope effect.⁷³ The results above should be considered carefully because the different rates observed for the oxidation (that cannot be called a KIE) need a more complete study to be fully understood.

5.3 Conclusions

Designing an adequate experiment is a difficult task, as explained in the introduction. Some elements of our work can be highlighted:

1. We consider the concepts of shape vs. vibration theory and odorant perception vs. reception. As a test of the vibration theory, we have prepared a series of isotopologues of musks and other compounds, containing up to 30 C–H or C–D bonds as test odorants, which have been evaluated using *in vitro* activation of receptors identified by us and other groups as being highly responsive to these isotopologues. No significant difference has been measured in the response of the receptors for the test odorants.

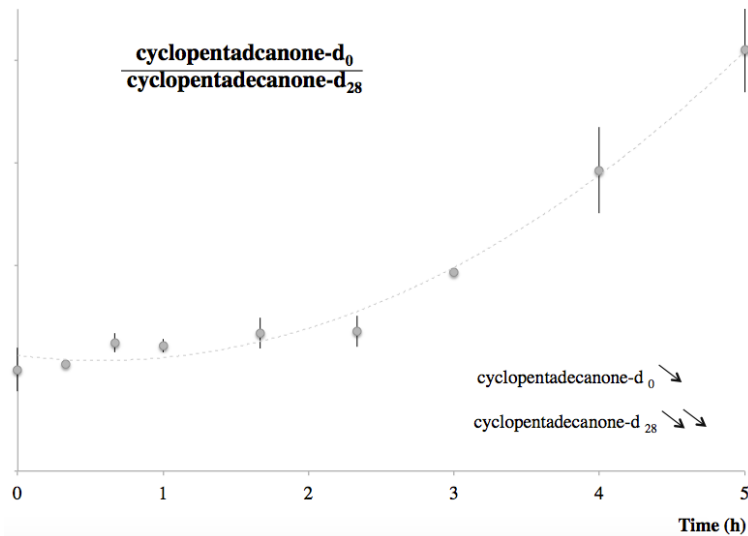


Figure 5.21: Baeyer-Villiger oxidation of cyclopentadecanone-d₀ (**78a**) and -d₂₈ (**78d**) by *m*CPBA occurs at a different rate, the deuterated compound being oxidized faster. The KIE has not been measured, the rate equation being unknown, but in an attempt to assess $\frac{k_H}{k_D}$, the ratio of the peak areas of the two cyclopentadecanones is plotted. This ratio is not constant, cyclopentadecanone-d₂₈ is being oxidized faster relatively to cyclopentadecanone-d₀ (average of two repetitions, error bar: standard deviation).

2. We consider the confounding effects of impurities and isotope effects in interpreting odorant perception, as well as the validity of requirements for specific IR bands for recognition of musks by their receptors. Our test odorants have been purified and the spectral data were clean.
3. The physical validity of the models developed to support the vibration theory has been judged implausible by a computational study.
4. We consider the specific limitations of our *in vitro* approach using isotopologues to evaluate the vibration theory, based primarily on results obtained with a single identified human musk OR, in addition to other OR/ligand pairs. Perhaps other receptors, missed in the screening, could be involved. This study was performed on the most accurate OR/odorant pair to the best of our knowledge.

Our results demonstrate the same level of activation of OR5AN1 by deuterated and undeuterated musk compounds, challenging the vibration theory of olfaction (VTO). Instead of an electron transfer (as postulated in the VTO), we support the theory of Baud *et al.*[60] that the musk carbonyl could be involved in the OR-musk interaction as a hydrogen bond acceptor. This is confirmed by the reduced activity of cyclopentadecanol and lack of activity for cyclopentadecane.

This conclusion does not contradict Gane's results and needs to be qualified. The actual perception of the compounds can be different due to other phenomena, including reactions in the nasal mucus (pre-olfaction) that could be different for isotopologues (*i.e.*, a kinetic isotope effect is present). However, at the fundamental receptor level, the vibration theory of olfaction (VTO) is no longer plausible in the light of these results.

Luca Turin, the main supporter of the VTO, criticized our study in a letter in PNAS.¹⁹ He pointed out a few elements of the experimental procedure that have been addressed in a response,²⁰ and arguing that we used "cells in a dish rather than within whole organism" and that "expressing an olfactory receptor in human embryonic kidney cells doesn't adequately reconstitute the complex nature of olfaction...". Vosshall, however, agrees on the adequacy of kidney cells to model the response of ORs, naming it "the best system in the world" if you are looking at the receptors.¹⁷

Even if the way odorants activate the receptors remains unsolved, "important insights into structure-activity relationships in olfaction, one of the most important problems facing the field" are brought to the table, according to L. Vosshall's comment on our work.¹⁷ Site-directed mutagenesis and a better characterization of the 3D structure at the active site of the ORs (ideally by crystallographers) will eventually lead to the keys of the molecular mechanisms of olfaction in the future.

The initial focus of our work, olfaction involving thiols and sulfides, such as those associated with garlic, were not pursued in my work because the olfactory receptors (ORs) corresponding to these compounds were not known. Since the beginning of my project, human thiol receptors have been identified, and a manuscript on human olfactory receptors for thiols has been submitted by our group.

5.4 Experimental

NMR spectra were recorded in CDCl_3 , unless otherwise indicated, on a Bruker 400 UltrashieldTM, operating at 400 MHz for proton and 100 MHz for carbon. The chemical shifts (δ) are indicated in ppm downfield from tetramethylsilane, with the internal standard being the residual CHCl_3 (7.27 ppm). Infrared spectra of the neat compounds were recorded on a Perkin Elmer UATR 2 FTIR. Mass spectra were obtained using the Hewlett Packard 6890 GC and a 5972A selective mass detector. CH_2Cl_2 and ethyl acetate was purchased from Pharmaco-Aaper and used without further purification. Hexane and pentane were purchased from Sigma-Aldrich and distilled before use. Throughout the study 100% *m*CPBA was employed. The reagent was obtained by washing a dichloromethane solution of the commercial sample, purchased from Sigma-Aldrich as

a 70% mixture with *m*-chlorobenzoic acid, with pH 7.5 phosphate buffer followed by drying and evaporation of the solvent. The drying agent employed was anhydrous magnesium sulfate unless indicated otherwise. Analytical TLC was performed on precoated silica gel plates (Merck) with a 254 nm fluorescent indicator and was visualized under a UV lamp and by staining with a KMnO₄ solution.

Percentatge of deuteration. The percentage is determined by two different methods for validation. A GC-MS procedure is applied as follows for a compound containing *n* hydrogens or deuteriums:

$$\%D = \frac{Total_{(D)}}{Total_{(D)} + Total_{(H)}}$$

with

$$Total_{(D)} = \sum_{i=0}^n abundance_{([M-d_i])} \times i$$

and

$$Total_{(H)} = \sum_{i=0}^n abundance_{([M-d_i])} \times (n - i)$$

The deuterium content is also assessed by NMR: an internal standard is added in precise amount, and the integration values of the standard is compared to the integration values of the residual hydrogens of the sample on the ¹H spectrum. Anthracene has been chosen for its ease of handling (solid that can be weighted) and lack of confusion with the samples in terms of chemical shifts. The deuterium content measured for a sample varies from 96.7% (anthracene procedure) to 98.5% (calculation from the GC-MS). The results are close enough to validate both methods in the context of our experiments, but the GC-MS method is easier to carry and more reproducible (weighting small amounts of anthracene and handling chloroform solutions at low concentration might introduce errors).

Commercial cyclopentadecanone (78a) Spectral data are recorded for future comparison. ¹H NMR (400 MHz, CDCl₃) δ 2.41 (t, *J* = 6.7 Hz, 4H), 1.73–1.56 (m, 4H), 1.31 (dd, *J* = 20.5, 6.9 Hz, 20H) ppm. ¹³C NMR (100 MHz, CDCl₃) δ 42.30, 27.77, 26.96, 26.91, 26.62, 26.48, 23.65 ppm. MS: *m/z* = 224 (M). IR (neat): 2923, 2853 (sp³ C–H), 1707 (s, carbonyl) cm⁻¹.

Deuteration of cyclopentadecanone (78) A mixture of commercial cyclopentadecanone (1 g, 4.46 mmol), rhodium on carbon (200 mg), cyclohexane (0.8 mL) and 27 mL of D₂O is stirred in a sealed tube under H₂ atmosphere at 150 °C for 15 h. After filtration of the rhodium on Celite, the mixture was diluted in saturated aqueous NH₄Cl and extracted three times by CH₂Cl₂. The organic layer was dried (MgSO₄) and concentrated under vacuum. The GC-MS analysis showed the presence of cyclopentadecanone, cyclopentadecanol and

cyclopentadecane in 10:10:1 proportions, respectively. Mass recovered = 1.2 g. The material was then stirred without further purification in a sealed tube with 27 mL of fresh D₂O, 0.8 mL cyclohexane and 200 mg rhodium on carbon under H₂ atmosphere at 150 °C for 15 h. After dilution in saturated aqueous NH₄Cl, the products are extracted by CH₂Cl₂. The organic layer was dried and concentrated as above, then analyzed by GC-MS. The mixture of cyclopentadecanone-d₂₈ (**78d**, 2%), cyclopentadecanol-d₃₀ (**80a**, 94%) and cyclopentadecane-d₃₀ (**81-d₃₀**) (4%, all GC-MS purity) is purified by column chromatography using a 10:1 hexanes : Et₂O mixture as eluent.

Cyclopentadecanol-d₂₉ (80a**)**: The alcohol was isolated as a white solid in 30% yield (332 mg). Mp = 80-81 °C (commercial compound: Mp = 79-80 °C). Overall deuterium content = 96.7% (determined by NMR with anthracene as an internal standard). ¹H NMR (400 MHz, CDCl₃) δ 1.27 (d, *J* = 8.4 Hz). MS: *m/z* = 236 (100, [M-HDO]⁺), 253 (1, [M]⁺). IR (neat): 3279 (br, O–H bond), 2992 (w, residual sp³ C–H), 2195, 2097 (sp³ C–D) cm⁻¹. Deuterium content: 98.5% by GC-MS, 96.7% by NMR.

Cyclopentadecanone-d₂₈ (78d**)**. Cyclopentadecanol-d₂₉ (**80a**) (120 mg, 0.468 mmol) is dissolved in 6 mL of a 2:1 acetone:H₂O mixture. A 65 mg/mL solution of K₂Cr₂O₇ in H₂O + H₂SO₄ conc. (12.5% v/v) is prepared, and 8.8 mL (0.656 mol, 1.4 eq) is then added dropwise to the mixture. The mixture is stirred at RT for 3 h, until a dark green coloration appears, then the solution is extracted three times by hexanes. The combined organic layers are dried over MgSO₄ and evaporated under reduced pressure. The product is isolated as a white solid in 77 % yield and identified as cyclopentadecanone-d₂₈ by GC-MS (purity: 97.9%). The solid is recrystallized for even better purity in a H₂O/MeOH mixture. Mp = 61-62 °C (undeuterated **78a**: Mp = 62-63 °C). ¹H NMR (400 MHz, CDCl₃) δ 2.38 (d, *J* = 10.2 Hz, 5H), 1.25 (s, 9H) as traces. MS: *m/z* = 252 ([M]⁺). IR (neat): 2892 (w, residual sp³ C–H), 2196, 2098 (sp³ C–D), 1702 (s, carbonyl) cm⁻¹. Deuterium content: 98.9% by GC-MS.

Cyclopentadecane-d₃₀ (81-d₃₀**)** This compound is a by-product of the deuteration of cyclopentadecanone (**78**) described above. The hydrocarbon was isolated as a white solid in 8 % yield (87 mg). Mp = 52-55 °C (commercial compound: Mp = 60-63 °C). ¹H NMR (400 MHz, CDCl₃) δ 1.26 (traces). ¹³C NMR (100 MHz, CDCl₃): δ 25.97, 25.78, 25.59, 25.41, 25.22. MS: *m/z* = 240 ([M]⁺). IR (neat): 2918, 2850 (w, residual sp³ C–H), 2194, 2097 (sp³ C–D) cm⁻¹.

Cyclopentadecanone-d₄ (78b**)** A procedure from the literature⁷⁴ is adapted as follows: A mixture of D₂O (9 mL) and cyclopentadecanone (1 g, 4.46 mmol) in the presence of a catalytic amount of K₂CO₃ was refluxed at 130 °C in a sealed tube for 24 h. The reaction mixture was cooled to RT, diluted with saturated aqueous

NH_4Cl and extracted three times with CH_2Cl_2 . The organic layers were combined, dried over anhydrous Na_2SO_4 and the volatiles removed under reduced pressure. The residue was then re-dissolved in fresh D_2O (9 mL), catalytic K_2CO_3 was added and the mixture was stirred in a sealed tube at 130 °C for another 24 h. This process was repeated two more times until an aliquot analyzed by GC-MS showed complete deuteration at the desired positions. The crude mixture was purified by column chromatography using hexanes : Et_2O (15:1) as eluent. The product was isolated as a white solid in 85 % yield (813 mg). $\text{Mp} = 54\text{--}56$ °C. ^1H NMR (400 MHz, CDCl_3) δ 1.62 (t, $J = 6.9$ Hz, 4H), 1.29 (s, 20H). ^{13}C NMR (100 MHz, CDCl_3) δ 212.8, 41.4 (t, $1\text{JCD} = 19.3$ Hz), 27.5, 26.8, 26.7, 26.5, 26.3, 23.3. Deuterium content: 13.4 % by GC-MS (should be 14.3% if four hydrogens had been replaced by deuteriums, so 94% of the desired positions have been deuterated).

Cyclopentadecanone-d₂₄ (78c) A mixture of H_2O (9 mL) and cyclopentadecanone-d₂₈ (78d) (150 mg, 0.6 mmol) in the presence of a catalytic amount of K_2CO_3 was refluxed at 130 °C in a sealed tube for 24 h. The reaction mixture was cooled to RT, diluted with saturated aqueous NH_4Cl and extracted three times with CH_2Cl_2 . The organic layers were combined, dried over anhydrous Na_2SO_4 and the volatiles removed under reduced pressure. The residue was then re-dissolved in fresh H_2O (9 mL), catalytic K_2CO_3 was added and the mixture was stirred in a sealed tube at 130 °C for another 24 h. This process was repeated two more times until an aliquot analyzed by GC-MS showed complete D - H exchange at the desired positions. The crude mixture was purified by column chromatography using pentane : Et_2O (20:1) as eluent. The product was isolated as a white solid in 40% yield (60 mg). ^1H NMR (400 MHz, CDCl_3) δ 2.46–2.32 (m, 4H), 1.27 (d, $J = 12.4$ Hz, 3H) (peak at 1.6 not integrated due to confusion with H_2O) ^{13}C NMR (100 MHz, CDCl_3): not taken MS: $m/z = 247$ ($[\text{M-d}_{23}]^+$), 248 ($[\text{M-d}_{24}]^+$), 249 ($[\text{M-d}_{25}]^+$), 250 ($[\text{M-d}_{26}]^+$). Deuterium content: 88.3% by GC-MS (should be 85.7% if twenty-four hydrogens had been replaced by deuteriums, so 97% of the desired positions have been hydrogenated).

Evaluation of the presence of a kinetic isotope effect (KIE): *Experiment 1:* About 10 mg (about 0.05 mmol) of commercial cyclopentadecanone 78a and 10 mg (0.04 mmol) of fully deuterated cyclopentadecanone 78d are dissolved in 10 mL of chloroform. About 10 mg of recrystallized mCPBA (0.06 mmol, 1.2 eq) are added and the solution is stirred under argon under reflux. Samples are collected after 1 h and 2 h and kept at 0 °C until injection on the GC-MS. Percentage of starting material consumed is calculated as follows:

$$\frac{\text{Peak area}_{\text{SM}}}{\text{Peak area}_{\text{SM}} + \text{Peak area}_{\text{product}}} \times 100 \text{ for each of the two starting materials and products.}$$

Experiment 2 : 9.6 mg (0.0428 mmol) of commercial cyclopentadecanone 78a and 8.6 mg (0.0341 mmol) of fully deuterated cyclopentadecanone 78d are dissolved in 2.5 mL of chloroform dried over molecular

sieve with 9.5 mg (0.0452 mmol) of cyclopentadecane (as the internal standard). 60 mg of recrystallized mCPBA (0.35 mmol, 10 eq) are added and the solution is stirred under argon under reflux. Samples are collected following the schedule and kept at 0 °C until injection on the GC-MS. Cyclopentadecane was later rejected as the internal standard due to limited reproducibility, since the standard deviation of the ratio $\frac{\text{Peak area}_{\text{cyclopentadecane}}}{\text{Peak area}_{\text{cyclopentadecanone}}}$ between the injections is large and inconsistent.

References

- (1) Bushdid, C.; Magnasco, M. O.; Vosshall, L. B.; Keller, A. Humans can discriminate more than 1 trillion olfactory stimuli. *Science* **2014**, *343*, 1370–1372.
- (2) Gerkin, R. C.; Castro, J. B. The number of olfactory stimuli that humans can discriminate is still unknown. *eLife* **2015**, *4*, DOI: 10.7554/eLife.08127.001.
- (3) Meister, M. On the dimensionality of odor space. *eLife* **2015**, *4*, DOI: 10.7554/eLife.07865.
- (4) Magnasco, M. O.; Keller, A.; Vosshall, L. B. On the dimensionality of olfactory space. *bioRxiv* **2015**, DOI: 10.1101/022103.
- (5) Nara, K.; Saraiva, L. R.; Ye, X.; Buck, L. B. A large-scale analysis of odor coding in the olfactory epithelium. *J. Neurosci.* **2011**, *31*, 9179–9191.
- (6) Buck, L.; Axel, R. A novel multigene family may encode odorant receptors: A molecular basis for odor recognition. *Cell* **2014**, *65*, 175–187.
- (7) Andersen, K. K.; Bernstein, D. T. Some chemical constituents of the scent of the striped skunk (*Mephitis mephitis*). *J. Chem. Ecol.* **1975**, *1*, 493–499.
- (8) Hasegawa, Y.; Yabuki, M.; Matsukane, M. Identification of new odoriferous compounds in human axillary sweat. *Chem. Biodivers.* **2004**, *1*, 2042–2050.
- (9) Milligan, B.; Swan, J. M. 1140. Unsymmetrical dialkyl disulphides from Bunte salts. *J. Chem. Soc.* **1963**, 6008–6012.
- (10) Lin, D. Y.; Zhang, S.-Z.; Block, E.; Katz, L. C. Encoding social signals in the mouse main olfactory bulb. *Nature* **2005**, *434*, 470–477.
- (11) Duan, X.; Block, E.; Li, Z.; Connelly, T.; Zhang, J.; Huang, Z.; Su, X.; Pan, Y.; Wu, L.; Chi, Q.; Thomas, S.; Zhang, S.; Ma, M.; Matsunami, H.; Chen, G.-Q.; Zhuang, H. Crucial role of copper in detection of metal-coordinating odorants. *Proc. Natl. Acad. Sci. U.S.A.* **2012**, *109*, 3492–3497.
- (12) Turin, L. A spectroscopic mechanism for primary olfactory reception. *Chem. Senses* **1996**, *21*, 773–791.
- (13) Turin, L. Smells, spanners, and switches. *Inference Rev.* **2016**, *2*.
- (14) Cai, X.-J.; Block, E.; Uden, P. C.; Quimby, B. D.; Sullivan, J. J. *Allium* chemistry: identification of natural abundance organoselenium compounds in human breath after ingestion of garlic using gas chromatography with atomic emission detection. *J. Agric. Food Chem.* **1995**, *43*, 1751–1753.

(15) Block, E.; Jang, S.; Matsunami, H.; Sekharan, S.; Dethier, B.; Ertem, M. Z.; Gundala, S.; Pan, Y.; Li, S.; Li, Z.; Lodge, S. N.; Ozbil, M.; Jiang, H.; Penalba, S. F.; Batista, V. S.; Zhuang, H. Implausibility of the vibrational theory of olfaction. *Proc. Natl. Acad. Sci. U.S.A.* **2015**, *112*, E2766–E2774.

(16) Everts, S. Receptor research reignites a smelly debate. *Chem. Eng. News* **2015**, *93*, 29–30.

(17) Vosshall, L. B. Laying a controversial smell theory to rest. *Proc. Natl. Acad. Sci. U.S.A.* **2015**, *112*, 6525–6526.

(18) In This Issue. *Proc. Natl. Acad. Sci. U.S.A.* **2015**, *112*, 6519–6520.

(19) Turin, L.; Gane, S.; Georganakis, D.; Maniati, K.; Skoulakis, E. M. C. Plausibility of the vibrational theory of olfaction. *Proc. Natl. Acad. Sci. U.S.A.* **2015**, *112*, E3154–E3154.

(20) Block, E.; Jang, S.; Matsunami, H.; Batista, V. S.; Zhuang, H. Reply to Turin et al.: Vibrational theory of olfaction is implausible. *Proc. Natl. Acad. Sci. U.S.A.* **2015**, *112*, E3155–E3155.

(21) Block, E. What's that smell? A controversial theory of olfaction deemed implausible; 2015.

(22) Joseph, J.; Dunn, F. A.; Stopfer, M. Spontaneous olfactory receptor neuron activity determines follower cell response properties. *J. Neurosci.* **2012**, *32*, 2900–2910.

(23) Mori, K.; Takahashi, Y. K.; Igarashi, K. M.; Yamaguchi, M. Maps of odorant molecular features in the mammalian olfactory bulb. *Physiol. Rev.* **2006**, *86*, 409–433.

(24) Stevens, C. F. What the fly's nose tells the fly's brain. *Proc. Natl. Acad. Sci. U.S.A.* **2015**, DOI: 10.1073/pnas.1510103112.

(25) Bahrami, K.; Khodaei, M. M.; Khedri, M. A novel method for the deoxygenation of sulfoxides with the PPh₃/Br₂/CuBr system. *Chem. Lett.* **2007**, *36*, 1324–1325.

(26) Malnic, B.; Hirono, J.; Sato, T.; Buck, L. B. Combinatorial receptor codes for odors. *Cell* **1999**, *96*, 713–723.

(27) Buck, L. B. Unraveling the sense of smell (Nobel lecture). *Angew. Chem. Int. Ed.* **2005**, *44*, 6128–6140.

(28) Débat, H.; Eloit, C.; Blon, F.; Sarazin, B.; Henry, C.; Huet, J.-C.; Trotier, D.; Pernollet, J.-C. Identification of human olfactory cleft mucus proteins using proteomic analysis. *J. Proteome Res.* **2007**, *6*, 1985–1996.

(29) Regnier, F. E. Semiochemicals-structure and function. *Biol. Reprod.* **1971**, *4*, 309–326.

(30) Pelosi, P.; Mastrogiacomo, R.; Iovinella, I.; Tuccori, E.; Persaud, K. C. Structure and biotechnological applications of odorant-binding proteins. *Appl. Microbiol. Biotechnol.* **2014**, *98*, 61–70.

(31) Schilling, B.; Kaiser, R.; Natsch, A.; Gautschi, M. Investigation of odors in the fragrance industry., English *Chemoecology* **2010**, *20*, 135–147.

(32) Crasto, C. J.; Marenco, L. N.; Skoufos, E.; Healy, M.; Singer, M.; Nadkarni, P.; Miller, P.; Shepherd, G. The olfactory receptor database; <http://senselab.med.yale.edu/ORDB/>, 2015.

(33) Dunkel, A.; Steinhaus, M.; Kotthoff, M.; Nowak, B.; Krautwurst, D.; Schieberle, P.; Hofmann, T. Nature's chemical signatures in human olfaction: a foodborne perspective for future biotechnology. *Angew. Chem. Int. Ed.* **2014**, *53*, 7124–7143.

(34) Bernstein, D., *Essentials of Psychology*; Cengage Learning: Boston, 2010, p 864.

(35) Olofsson, J. K.; Gottfried, J. A. The muted sense: neurocognitive limitations of olfactory language. *Trends Cogn. Sci.* **2015**, *19*, 314–321.

(36) Gilad, Y.; Man, O.; Pääbo, S.; Lancet, D. Human specific loss of olfactory receptor genes. *Proc. Natl. Acad. Sci. U.S.A.* **2003**, *100*, 3324–3327.

(37) Ohloff, G.; Vial, C.; Wolf, H. R.; Job, K.; Jégou, E.; Polonsky, J.; Lederer, E. Stereochemistry-odor relationships in enantiomeric ambergris fragrances. *Helv. Chim. Acta* **1980**, *63*, 1932–1946.

(38) Charlier, L.; Topin, J.; Claire, A.; Lai, P. C.; Crasto, C. J.; Golebiowski, J., *Molecular Modelling of Odorant/Olfactory Receptor Complexes*; Springer: New York, 2013, pp 53–65.

(39) Eleonora, A.; Aeaneda, R. C.; Baghaei, K. A.; Bahl, G.; Ben-Shahar, Y.; Benton, R.; Castro, A.; Charlier, L.; Cook, B.; Corin, K.; Crasto, C. J.; De March, C. A.; Golebiowski, J.; Gu, X.; Hyland, L.; Katsanis, N.; Kotthoff, M.; Krautwurst, D.; Lai, P. C.; Lancet, D.; Lucas, P.; Luetje, C. W.; Mainland, J. D.; Malnic, B.; Marenco, L. N.; Matarazzo, V.; Matsunami, H. U.; Miller, P.; Nativ, N.; Nichols, A. S.; Niimura, Y.; Olander, T.; Pajot-Augy, E.; Peterlin, Z.; Pousset, J.; Reggiani, L.; Renou, M.; Ronin, C.; Saina, M.; Sanz, G.; Sheperd, G. M.; Sherman, B. L.; Shi, J.; Smith, R. S.; Topin, J.; Wang, R.; Willer, J. R.; Zhang, S., *Olfactory Receptors. Methods and Protocols*, 1st ed.; Crasto, C. J., Ed.; Humana Press: New York, 2013, p 259.

(40) De March, C. A.; Ryu, S.; Sicard, G.; Moon, C.; Golebiowski, J. Structure-odour relationships reviewed in the postgenomic era. *Flavour Fragr. J.* **2015**, DOI: 10.1002/ffj.3249.

(41) Sousa, C. M.; Berthet, J.; Delbaere, S.; Coelho, P. J. Acid-catalyzed domino reactions of tetraarylbut-2-yne-1,4-diols. *Synthesis of conjugated indenes and inden-2-ones*. *J. Org. Chem.* **2014**, *79*, 5781–5786.

(42) De March, C. A.; Kim, S.-K.; Antonczak, S.; Goddard, W. A.; Golebiowski, J. G protein-coupled odorant receptors: From sequence to structure. *Protein Sci.* **2015**, DOI: 10.1002/pro.2717.

(43) De March, C. A.; Yu, Y.; Ni, M. J.; Adipietro, K. A.; Matsunami, H.; Ma, M.; Golebiowski, J. Conserved residues control activation of mammalian G protein-coupled odorant receptors. *J. Am. Chem. Soc.* **2015**, DOI: 10.1021/jacs.5b04659.

(44) Jones, D. T.; Reed, R. R. Golf: an olfactory neuron specific-G protein involved in odorant signal transduction. *Science* **1989**, *244*, 790–795.

(45) Sell, C., *Chemistry and the Sense of Smell*; Wiley: Hoboken, 2014.

(46) Dyson, G. M. Some aspects of the vibration theory of odor. *Perfum. Essent. Oil Rec.* **1928**, *19*, 456–459.

(47) Dyson, G. M. The scientific basis of odour. *J. Soc. Chem. Ind.* **1938**, *57*, 647–651.

(48) Wright, R. H.; Reid, C.; Evans, H. G. V. Odour and molecular vibration. 3. A new theory of olfaction simulation. *Chem. Ind.* **1956**, 973–977.

(49) Shepherd, G. M. A molecular vocabulary for olfaction. *Ann. N. Y. Acad. Sci.* **1987**, *510*, 98–103.

(50) Franco, M. I.; Turin, L.; Mershin, A.; Skoulakis, E. M. C. Molecular vibration-sensing component in *Drosophila melanogaster* olfaction. *Proc. Natl. Acad. Sci. U.S.A.* **2011**, *108*, 3797–3802.

(51) Gane, S.; Georganakis, D.; Maniati, K.; Vamvakias, M.; Ragoussis, N.; Skoulakis, E. M. C.; Turin, L. Molecular vibration-sensing component in human olfaction. *PLoS One* **2013**, *8*, e55780.

(52) Brookes, J. C.; Hartoutsiou, F.; Horsfield, A. P.; Stoneham, A. M. Could humans recognize odor by phonon assisted tunneling? *Phys. Rev. Lett.* **2007**, *98*, 38101.

(53) Keller, A.; Vosshall, L. B. A psychophysical test of the vibration theory of olfaction. *Nat. Neurosci.* **2004**, *7*, 337–338.

(54) Saberi, M.; Seyed-allaei, H. Odorant receptors of *Drosophila* are sensitive to the molecular volume of odorants. *Sci. Rep.* **2016**, *6*, 25103.

(55) Shirasu, M.; Yoshikawa, K.; Takai, Y.; Nakashima, A.; Takeuchi, H.; Sakano, H.; Touhara, K. Olfactory receptor and neural pathway responsible for highly selective sensing of musk odors. *Neuron* **2014**, *81*, 165–78.

(56) Sell, C., *The Chemistry of Fragrances: From Perfumer to Consumer*; RSC Paperbacks; Royal Society of Chemistry: London, 2006.

(57) McClintock, T. S.; Adipietro, K.; Titlow, W. B.; Breheny, P.; Walz, A.; Mombaerts, P.; Matsunami, H. In vivo identification of eugenol-responsive and muscone-responsive mouse odorant receptors. *J. Neurosci.* **2014**, *34*, 15669–15678.

(58) Triller, A.; Boulden, E. A.; Churchill, A.; Hatt, H.; Englund, J.; Spehr, M.; Sell, C. S. Odorant-receptor interactions and odor percept: a chemical perspective. *Chem. Biodivers.* **2008**, *5*, 862–886.

(59) Sanz, G.; Schlegel, C.; Pernollet, J.-C.; Briand, L. Comparison of odorant specificity of two human olfactory receptors from different phylogenetic classes and evidence for antagonism. *Chem. Senses* **2005**, *30*, 69–80.

(60) Baud, O.; Etter, S.; Spreafico, M.; Bordoli, L.; Schwede, T.; Vogel, H.; Pick, H. The mouse eugenol odorant receptor: structural and functional plasticity of a broadly tuned odorant binding pocket. *Biochemistry* **2011**, *50*, 843–853.

(61) Junk, T.; Catallo, W. J. Hydrogen isotope exchange reactions involving C-H (D, T) bonds. *Chem. Soc. Rev.* **1997**, *26*, 401–406.

(62) Hirota, K.; Sajiki, H.; Ito, N. Method for producing deuterium gas and catalytic deuteration method using deuterium gas obtained thereby; US 20080145303 A1., 2006.

(63) Maegawa, T.; Fujiwara, Y.; Inagaki, Y.; Esaki, H.; Monguchi, Y.; Sajiki, H. Mild and efficient H/D exchange of alkanes based on C-H activation catalyzed by rhodium on charcoal. *Angew. Chem. Int. Ed.* **2008**, *47*, 5394–5397.

(64) Saito, H.; Kubota, M.; Roberts, R. W.; Chi, Q.; Matsunami, H. RTP family members induce functional expression of mammalian odorant receptors. *Cell* **2004**, *119*, 679–691.

(65) Zhuang, H.; Matsunami, H. Evaluating cell-surface expression and measuring activation of mammalian odorant receptors in heterologous cells. *Nat. Protoc.* **2008**, *3*, 1402–1413.

(66) Bittner, E. R.; Madalan, A.; Czader, A.; Roman, G. Quantum origins of molecular recognition and olfaction in *Drosophila*. *J. Chem. Phys.* **2012**, *137*, 22A551.

(67) Solov'yov, I. A.; Chang, P.-Y.; Schulten, K. Vibrationally assisted electron transfer mechanism of olfaction: myth or reality? *Phys. Chem. Chem. Phys.* **2012**, *14*, 13861–13871.

(68) Renz, M.; Meunier, B. 100 years of Baeyer-Villiger oxidations. *European J. Org. Chem.* **1999**, *1999*, 737–750.

(69) Thiebaud, N.; Veloso Da Silva, S.; Jakob, I.; Sicard, G.; Chevalier, J.; Ménétrier, F.; Berdeaux, O.; Artur, Y.; Heydel, J.-M.; Le Bon, A.-M. Odorant metabolism catalyzed by olfactory mucosal enzymes influences peripheral olfactory responses in rats. *PLoS One* **2013**, *8*, e59547.

(70) Nagashima, A.; Touhara, K. Enzymatic conversion of odorants in nasal mucus affects olfactory glomerular activation patterns and odor perception. *J. Neurosci.* **2010**, *30*, 16391–16398.

(71) Winnik, M. A.; Stoute, V.; Fitzgerald, P. Secondary deuterium isotope effects in the Baeyer-Villiger reaction. *J. Am. Chem. Soc.* **1974**, *96*, 1977–1979.

(72) Sykes, P., *A Guidebook to Mechanism in Organic Chemistry*; Longman: Essex, 1986, p 416.

(73) Clayden, J., *Organic Chemistry*; Oxford University Press: Oxford, 2001.

(74) Wesslén, B. Aldol reactions of formaldehyde in non-aqueous media. IV. The mechanism of the acid-catalyzed reaction of 2-butanone with formaldehyde. *Acta Chem. Scand.* **1968**, *22*, 2085–2100.

Chapter 6

General conclusions and perspectives

In the first part of this thesis (Chapter 2), we have screened higher-mass organosulfur compounds in garlic extracts by UPLC-MS and DART-MS. Among these novel molecules, two compounds have been isolated and characterized (Chapter 2). Ajothiolane (**20**) is a thiolane-containing derivative, whereas methylisoajoene (**8**) is linear. Synthesis of analogues have been proposed in Chapter 3, but the total synthesis was unsuccessful. Less common techniques such as INADEQUATE NMR were applied to confirm the structure of ajothiolane. Both compounds had been identified in previous reports¹ but the structures proposed were questionable in terms of functional groups and biosynthesis. This illustrates the complexity of these organosulfur compounds, and the importance of less common methods such as INADEQUATE NMR in solving multi-heteroatom structures in which the atom-connectivity is conceivable in multiple ways. To extend this project, ideas for total synthesis are suggested in Chapter 3. The stereochemistry of ajothiolane could be investigated as well. Furthermore, these compounds have shown bioactivity, in the immune system for example.^{1,2} More applications as therapeutics could be considered.

Next, we have isolated and analyzed three important garlic metabolites: alliin (**1a**), alliinase and vinyldithiins (**5**). A validated HPLC method for the analysis of the diastereoisomers of alliin was published.³ The conditions for the preparation of alliin and alliinase have been optimized, and published for the vinyldithiins.⁴ As a result, convenient, ready-to-use procedures are available for future studies.

Finally, in the context of a project on the olfaction of garlic-related compounds (thiols and sulfides), we used isotopologues of macrocyclic ketones to assess the response of a human olfactory receptor, OR5AN1, to deuterated and undeuterated versions of the odorant.⁵ The response from the receptor was not significantly

different for the isotopologues, invalidating the vibrational theory of olfaction. Future work will focus on identifying the features of compounds triggering a response from the olfactory receptors, in particular for odorants such as thiols and sulfides.

References

- (1) Nohara, T.; Kiyota, Y.; Sakamoto, T.; Manabe, H.; Ono, M.; Ikeda, T.; Fujiwara, Y.; Nakano, D.; Kinjo, J. Garlicnins B1, C1, and D, from the fraction regulating macrophage activation of *Allium sativum*. *Chem. Pharm. Bull.* **2012**, *60*, 747–751.
- (2) El-Aasr, M.; Fujiwara, Y.; Takeya, M.; Ono, M.; Nakano, D.; Okawa, M.; Kinjo, J.; Ikeda, T.; Miyashita, H.; Yoshimitsu, H.; Nohara, T. Garlicnin A from the fraction regulating macrophage activation of *Allium sativum*. *Chem. Pharm. Bull.* **2011**, *59*, 1340–1343.
- (3) Dethier, B.; Laloux, M.; Hanon, E.; Nott, K.; Heuskin, S.; Wathelet, J. P. Analysis of the diastereoisomers of alliin by HPLC. *Talanta* **2012**, *101*, 447–452.
- (4) Dethier, B.; Hanon, E.; Maayoufi, S.; Nott, K.; Fauconnier, M.-L. Optimization of the formation of vinyldithiins, therapeutic compounds from garlic. *Eur. Food Res. Technol.* **2013**, *237*, 83–88.
- (5) Block, E.; Jang, S.; Matsunami, H.; Sekharan, S.; Dethier, B.; Ertem, M. Z.; Gundala, S.; Pan, Y.; Li, S.; Li, Z.; Lodge, S. N.; Ozbil, M.; Jiang, H.; Penalba, S. F.; Batista, V. S.; Zhuang, H. Implausibility of the vibrational theory of olfaction. *Proc. Natl. Acad. Sci. U.S.A.* **2015**, *112*, E2766–E2774.

Chapter 7

Appendices

7.1 Extraction and purification of thiolane-containing natural products from processed genus *Allium* plants

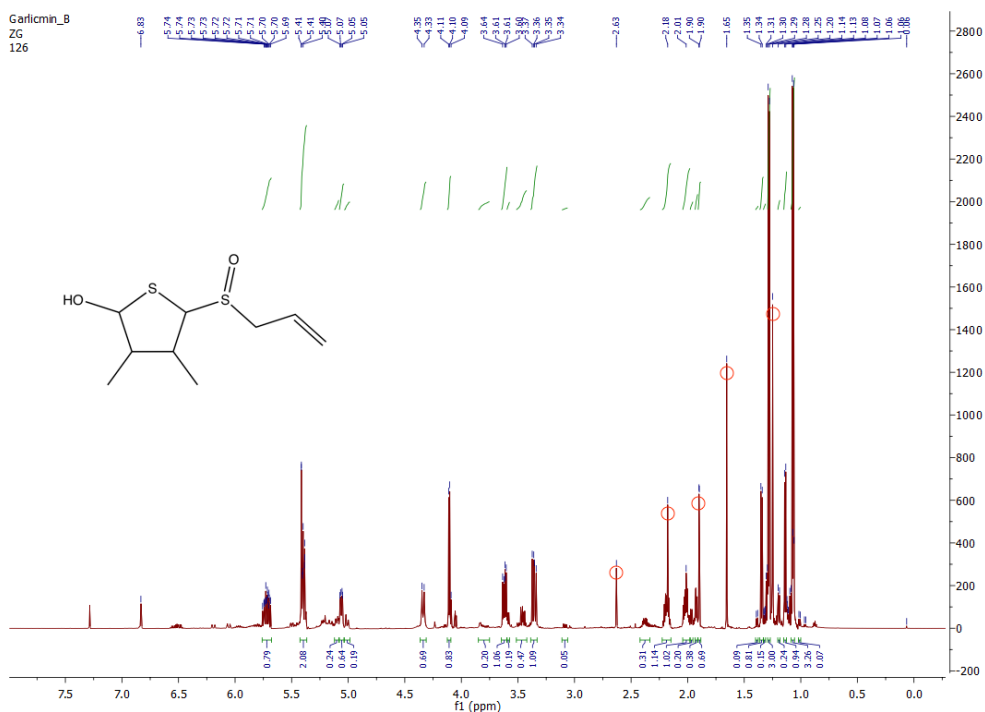


Figure 7.1: ¹H NMR spectrum (600 MHz, CDCl₃) of purified ajothiolane (**20**). One stereoisomer is major. Impurities are present in the spectrum (singlets at 1.25, 1.65, 1.90, 2.18 and 2.63 ppm).

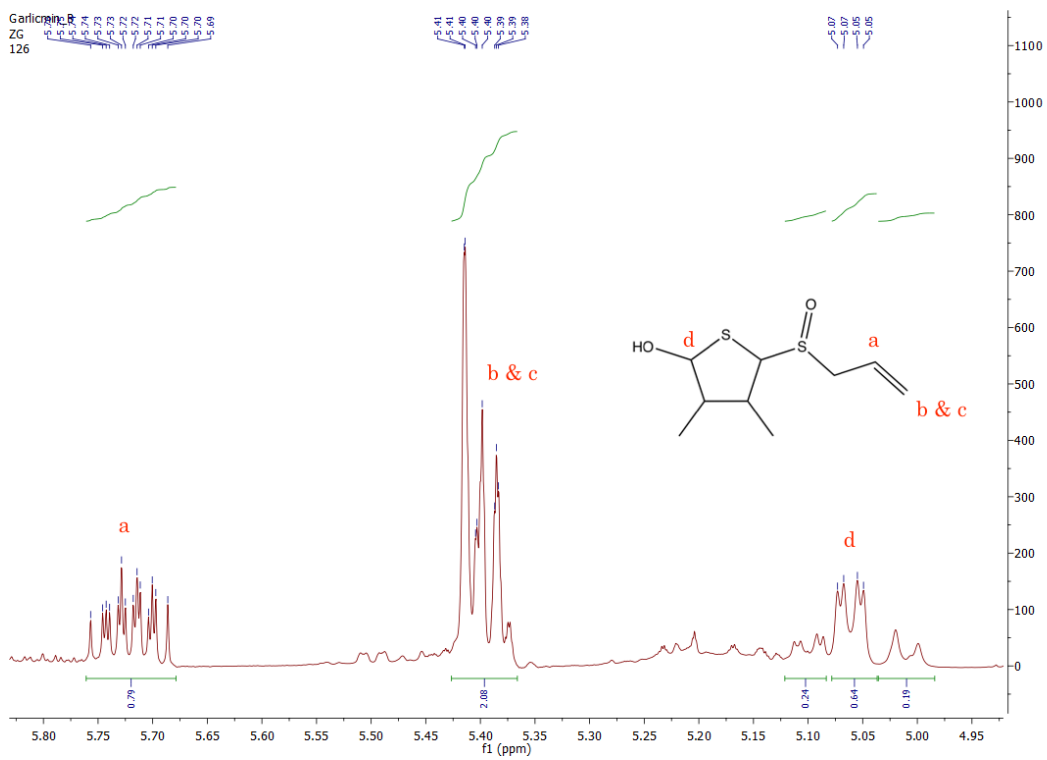


Figure 7.2: ^1H NMR spectrum (600 MHz, CDCl_3) of purified ajothiolane (**20**), detailed view of the olefinic region.

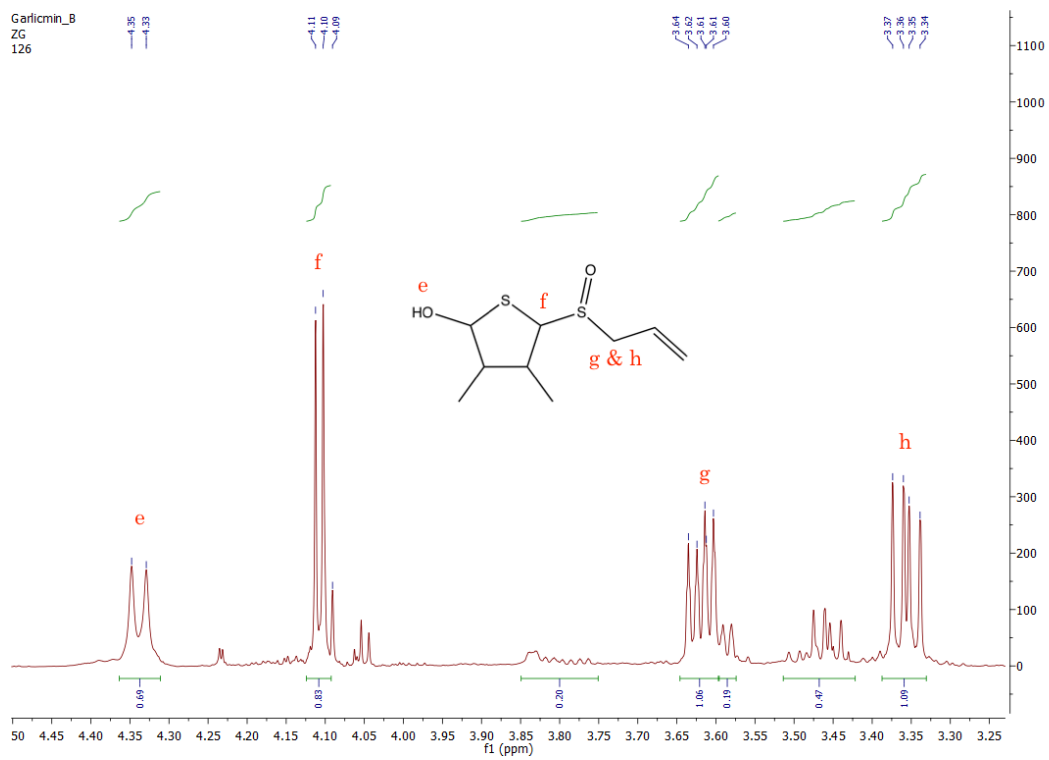


Figure 7.3: ^1H NMR spectrum (600 MHz, CDCl_3) of purified ajothiolane (**20**), detailed view.

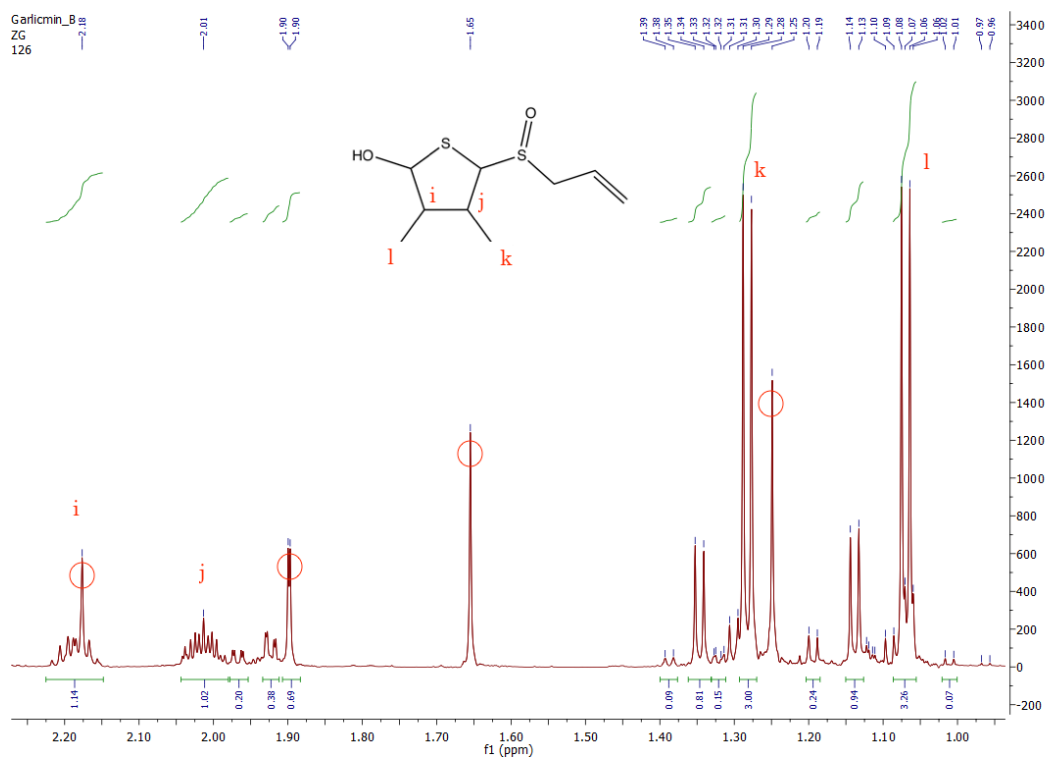


Figure 7.4: ^1H NMR spectrum (600 MHz, CDCl_3) of purified ajothiolane (**20**), detailed view. Impurities are present as a singlets at 1.25, 1.65, 1.90 and 2.18 ppm.

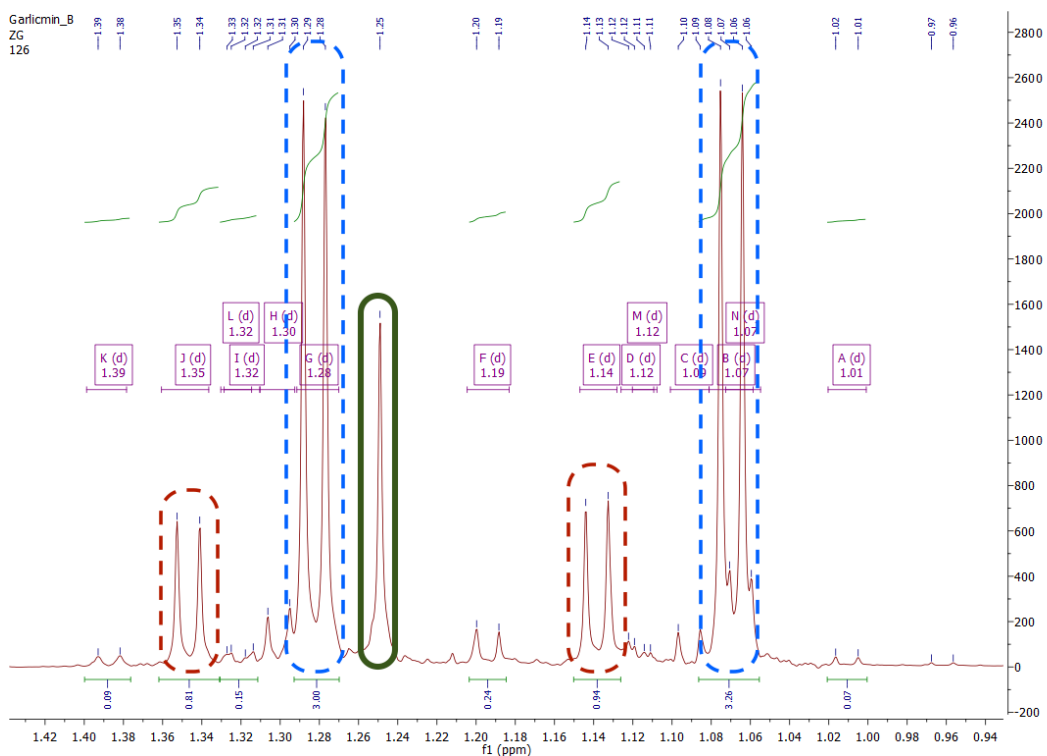


Figure 7.5: ^1H NMR spectrum (600 MHz, CDCl_3) of purified ajothiolane (**20**). View of the methyl region. Fourteen doublets appear for the methyl groups (two per compounds), indicating the presence of at least seven stereoisomers in this sample. The coupling constants are indicated in the parentheses for the following chemical shifts: 1.39 (d, $J = 6.7$ Hz, 1H), 1.35 (d, $J = 7.0$ Hz, 11H), 1.32 (d, $J = 5.6$ Hz, 2H), 1.32 (d, $J = 6.7$ Hz, 2H), 1.30 (d, $J = 6.7$ Hz, 5H), 1.28 (d, $J = 6.7$ Hz, 43H), 1.19 (d, $J = 6.8$ Hz, 4H), 1.14 (d, $J = 6.9$ Hz, 13H), 1.12 (d, $J = 4.8$ Hz, 3H), 1.12 (d, $J = 4.9$ Hz, 2H), 1.09 (d, $J = 6.8$ Hz, 3H), 1.07 (d, $J = 6.7$ Hz, 46H), 1.07 (d, $J = 6.6$ Hz, 26H), 1.01 (d, $J = 6.9$ Hz, 1H). Singlet at 1.25 ppm is an impurity.

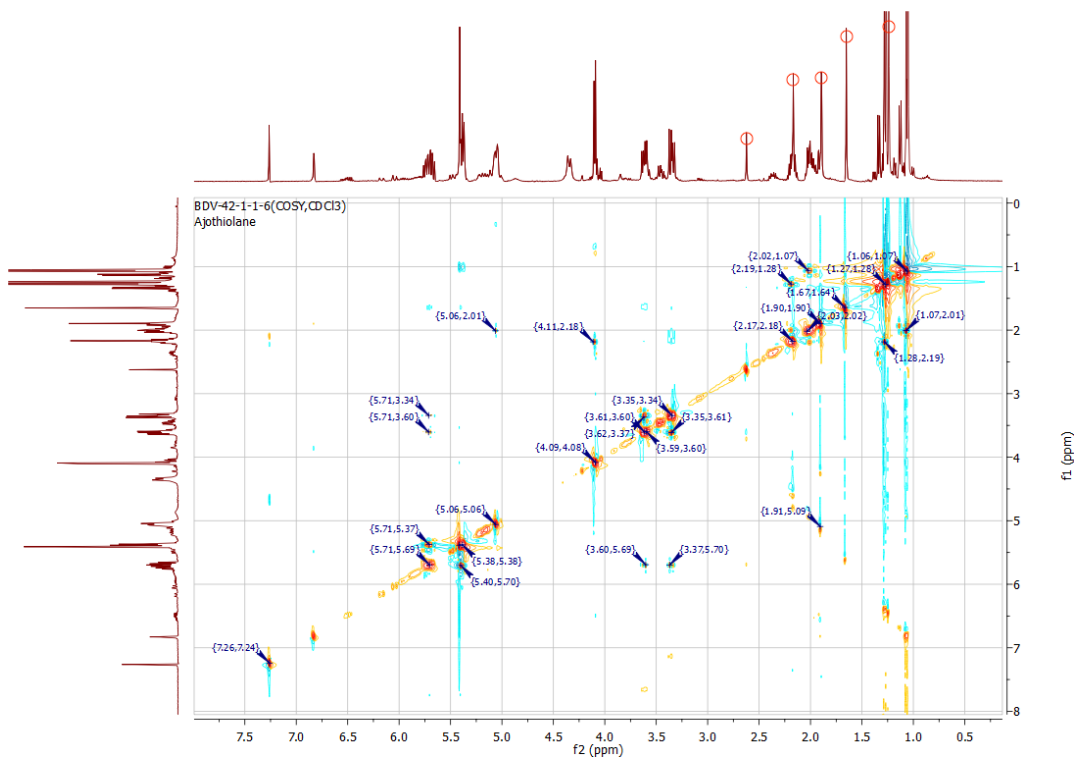


Figure 7.6: COSY NMR spectrum (400 MHz, CDCl_3) of purified ajothiolane (**20**). Impurities (plasticizers) and other stereoisomers are present.

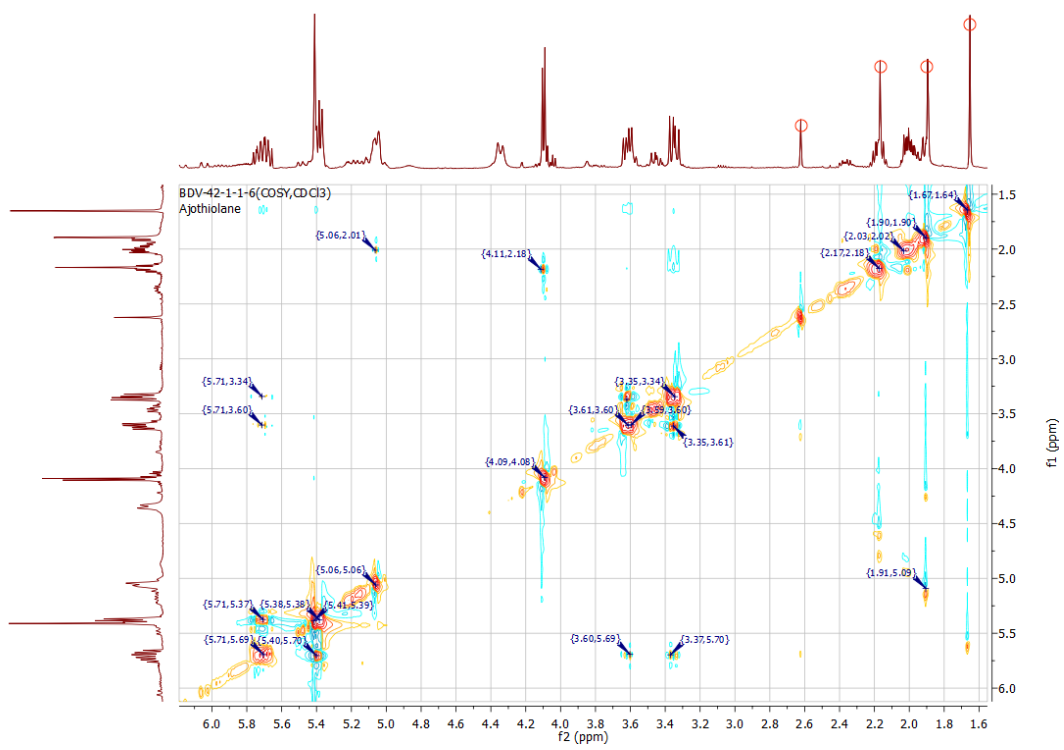


Figure 7.7: COSY NMR spectrum (400 MHz, CDCl_3) of purified ajothiolane (**20**), detailed view.

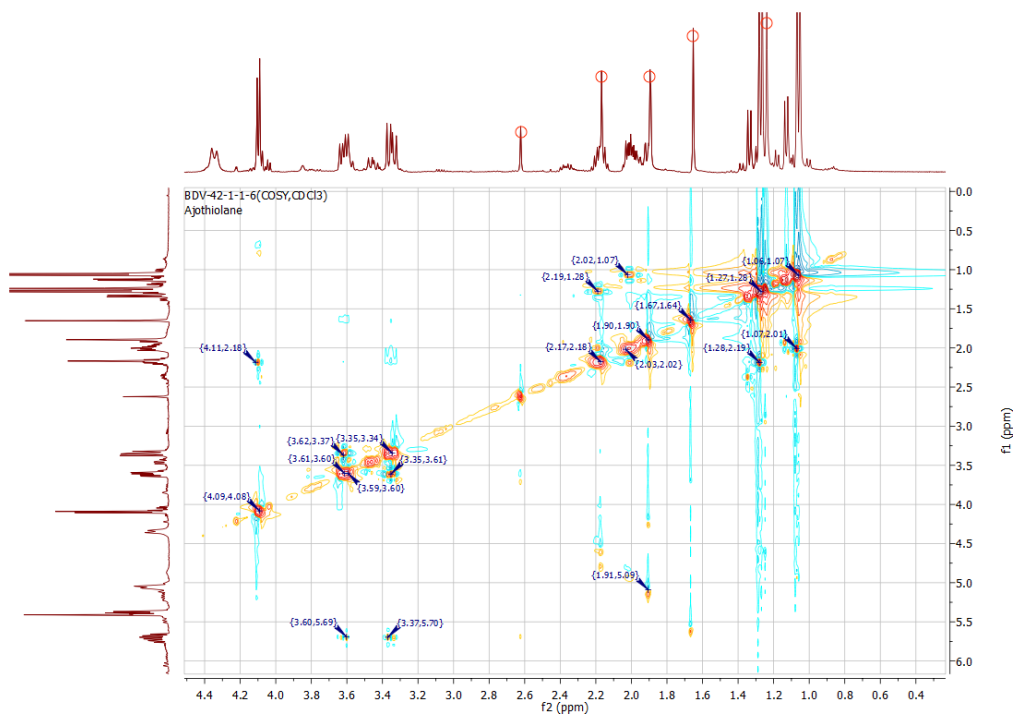


Figure 7.8: COSY NMR spectrum (400 MHz, CDCl₃) of purified ajothiolane (**20**). Impurities (plasticizers, singlets at 1.25, 1.65, 1.90, 2.18 and 2.63 ppm) and other stereoisomers are present.

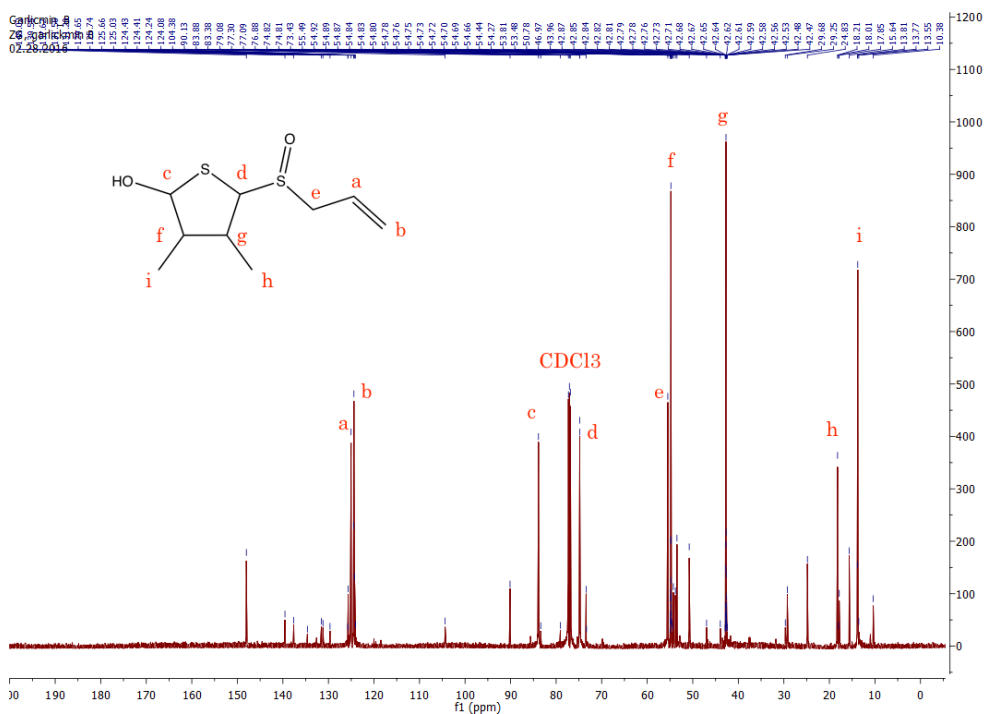


Figure 7.9: ^{13}C NMR spectrum (125 MHz, CDCl_3) of purified ajothiolane (**20**). Impurities (plasticizers) and other stereoisomers are present. This sample (40 mg) was prepared from 6 kg of garlic.

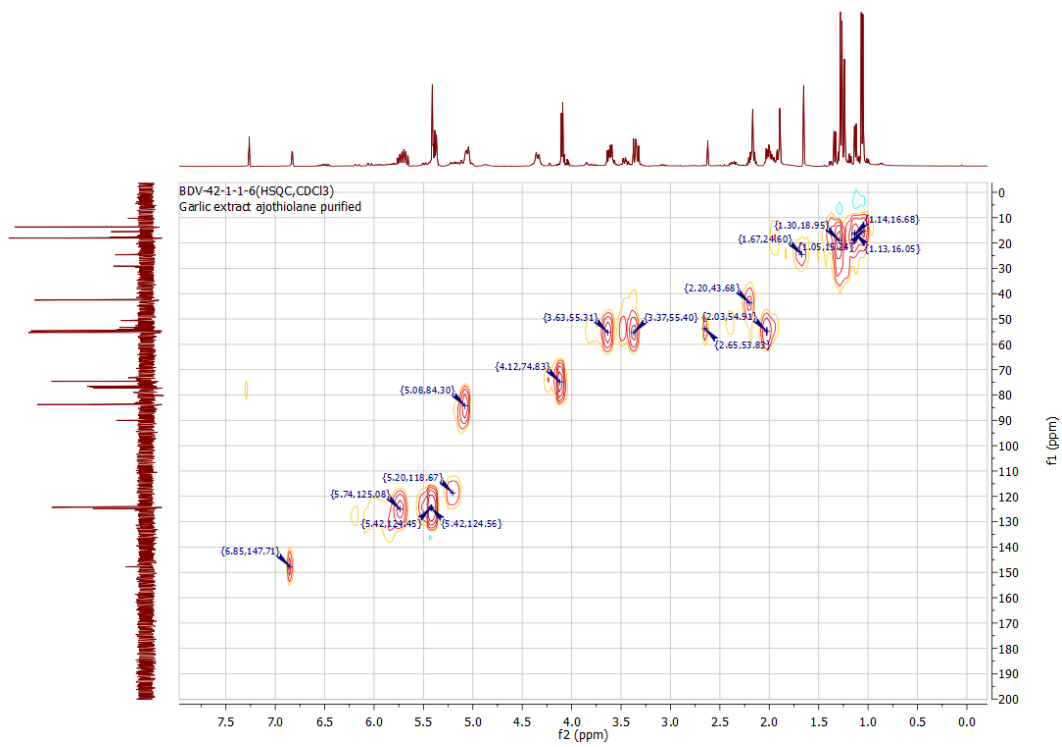


Figure 7.10: HSQC NMR spectrum (CDCl₃) of purified ajothiolane (**20**). Impurities (plasticizers) and other stereoisomers are present.

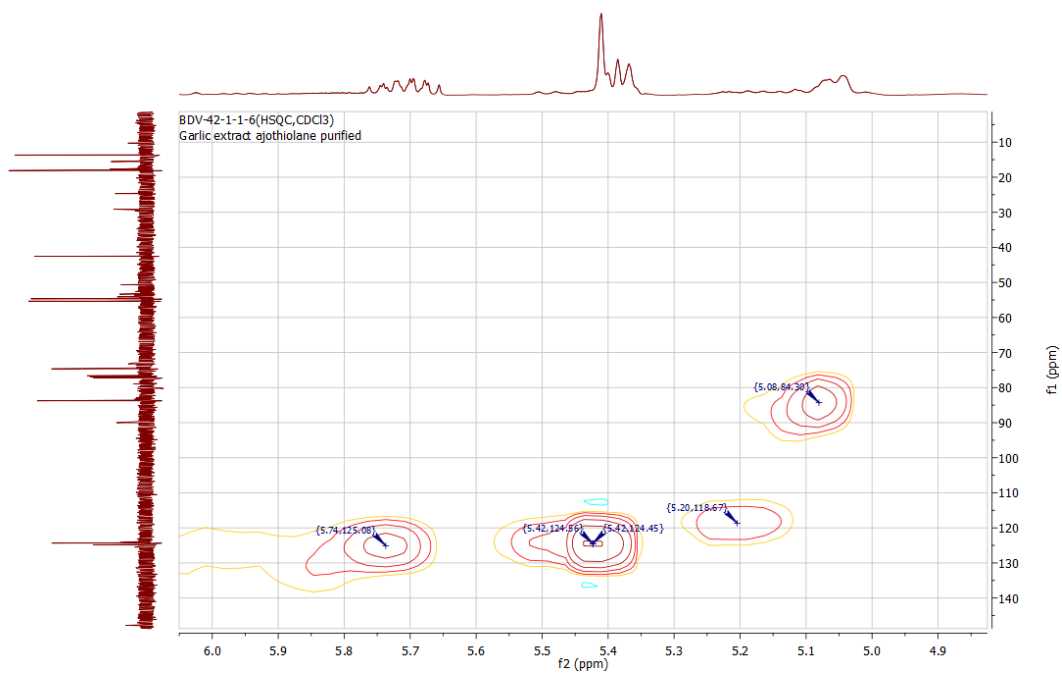


Figure 7.11: HSQC NMR spectrum (CDCl_3) of purified ajothiolane (**20**), detailed view of the olefinic region. Impurities (plasticizers) and other stereoisomers are present.

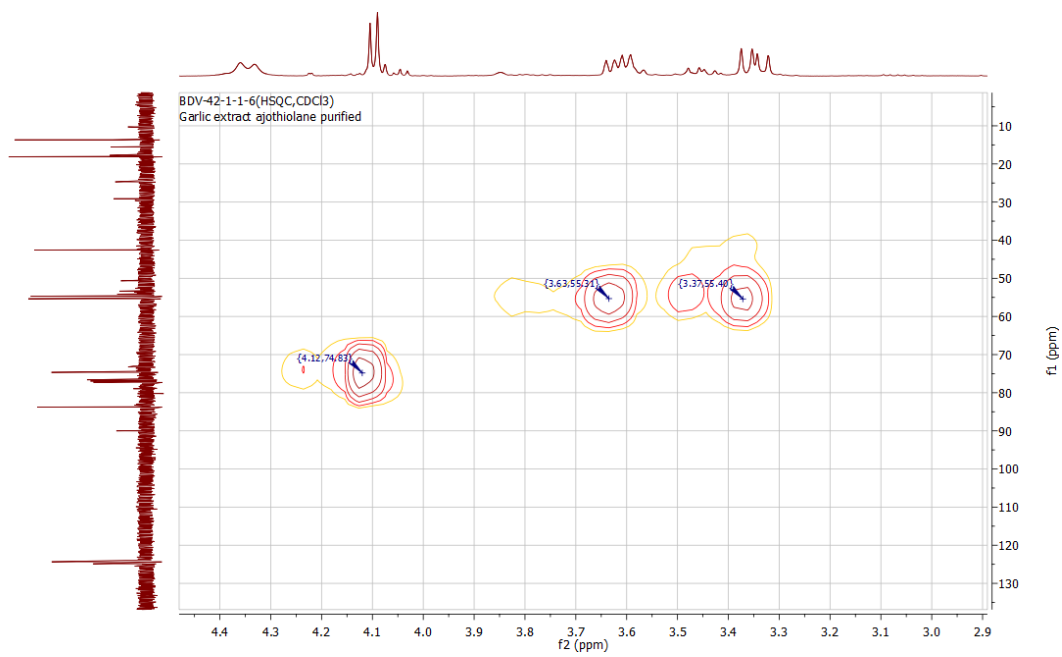


Figure 7.12: HSQC NMR spectrum (CDCl_3) of purified ajothiolane (**20**), detailed view. Impurities (plasticizers) and other stereoisomers are present.

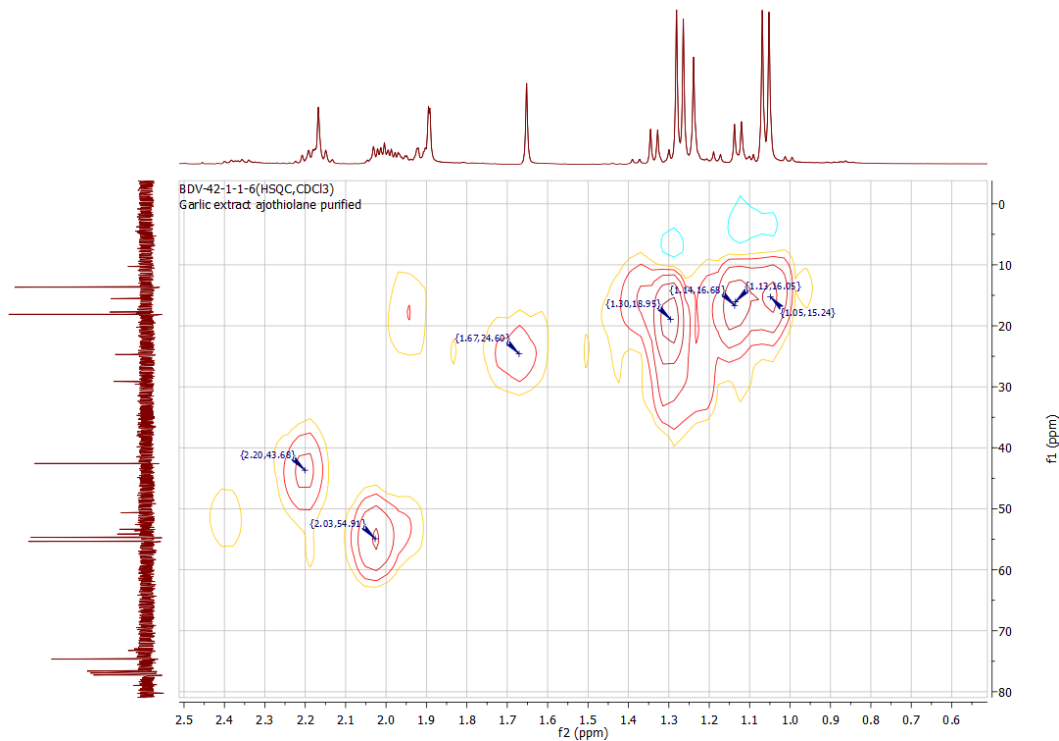


Figure 7.13: HSQC NMR spectrum (CDCl₃) of purified ajothiolane (**20**), detailed view of the methyl region. Impurities (plasticizers) and other stereoisomers are present.

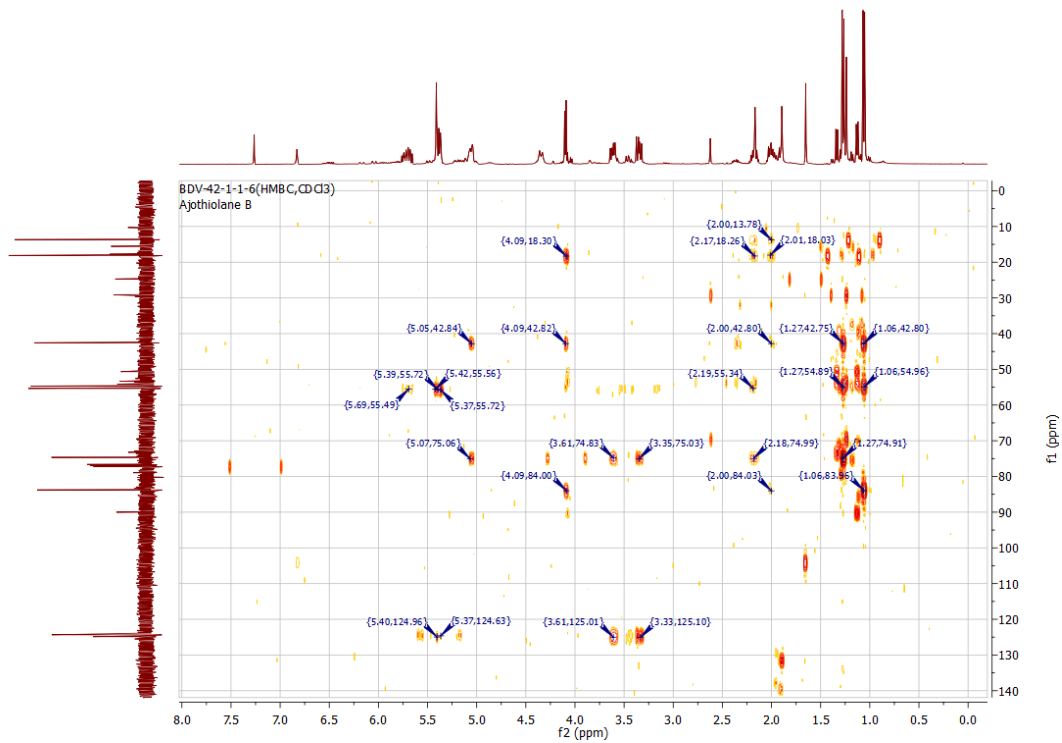


Figure 7.14: HMBC NMR spectrum (CDCl_3) of purified ajothiolane (**20**). Impurities (plasticizers) and other stereoisomers are present.

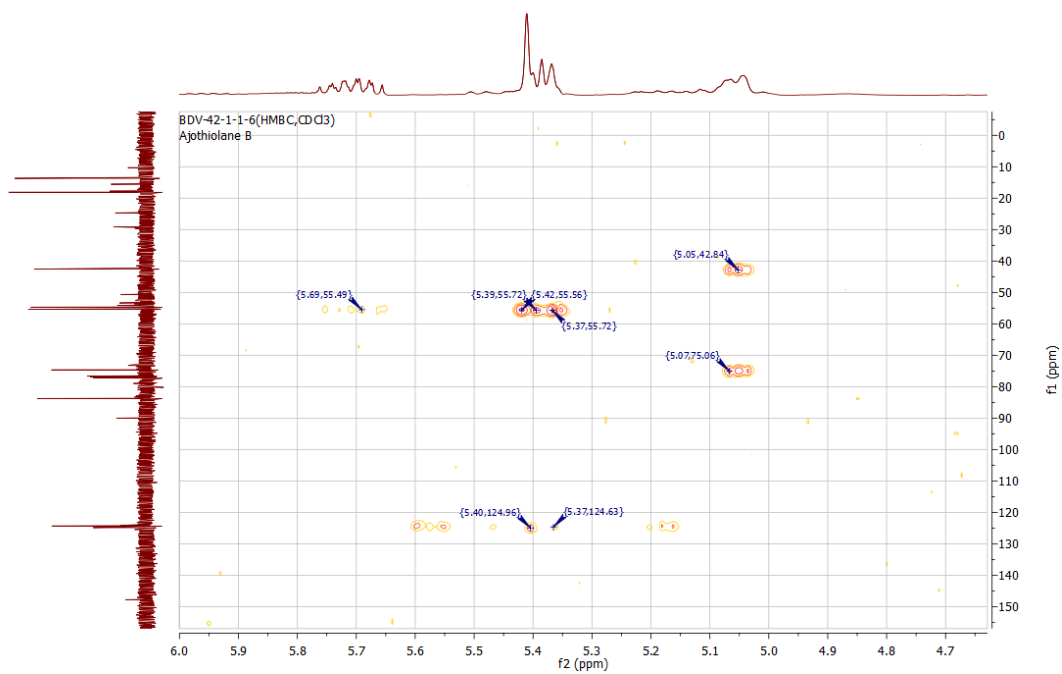


Figure 7.15: HMBC NMR spectrum (CDCl_3) of purified ajothiolane (**20**), detailed view of the olefinic region. Impurities (plasticizers) and other stereoisomers are present.

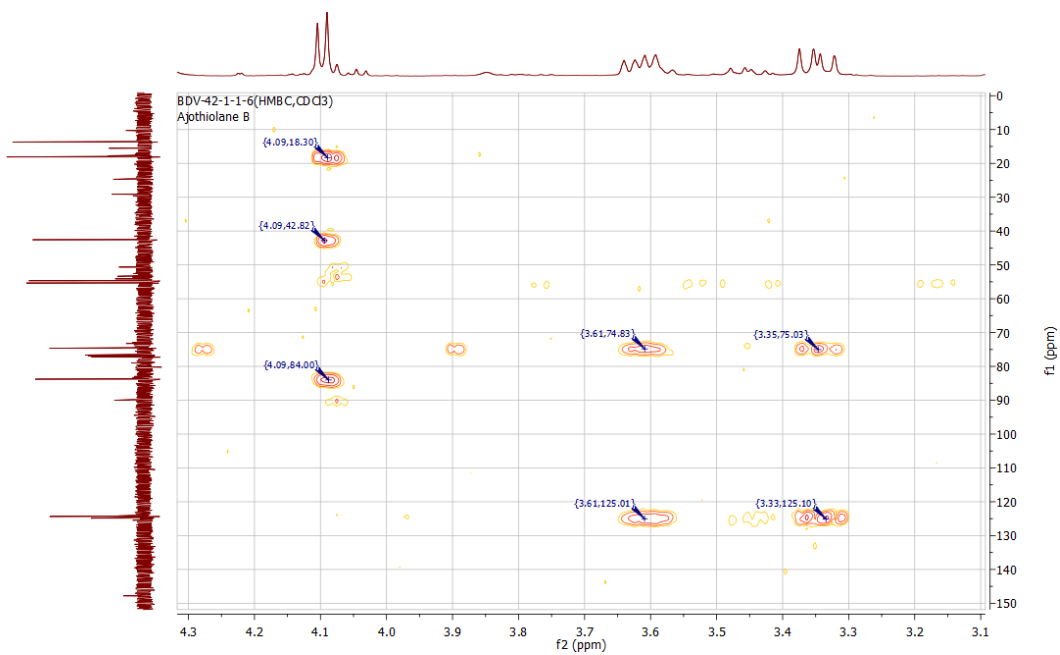


Figure 7.16: HMBC NMR spectrum (CDCl_3) of purified ajothiolane (**20**), detailed view. Impurities (plasticizers) and other stereoisomers are present.

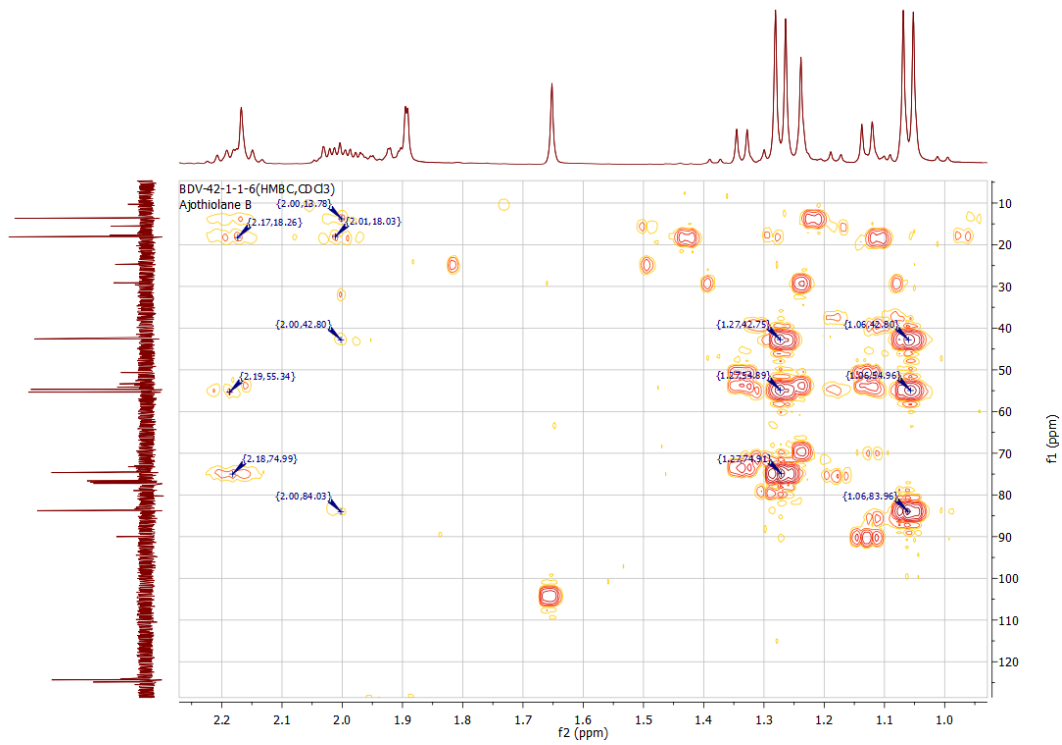


Figure 7.17: HMBC NMR spectrum (CDCl_3) of purified ajothiolane (**20**), detailed view of the methyl region. Impurities (plasticizers) and other stereoisomers are present.

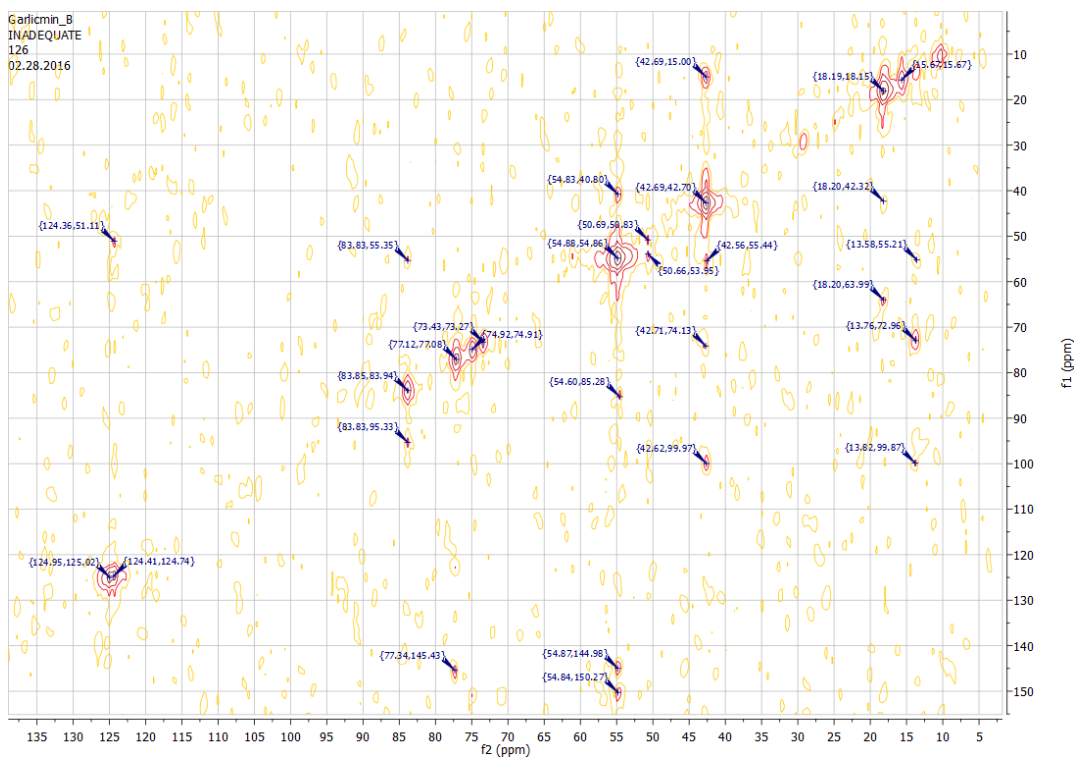


Figure 7.18: INADEQUATE NMR spectrum (125 MHz, CDCl_3) of purified ajothiolane (**20**). Impurities (plasticizers) and other stereoisomers are present.

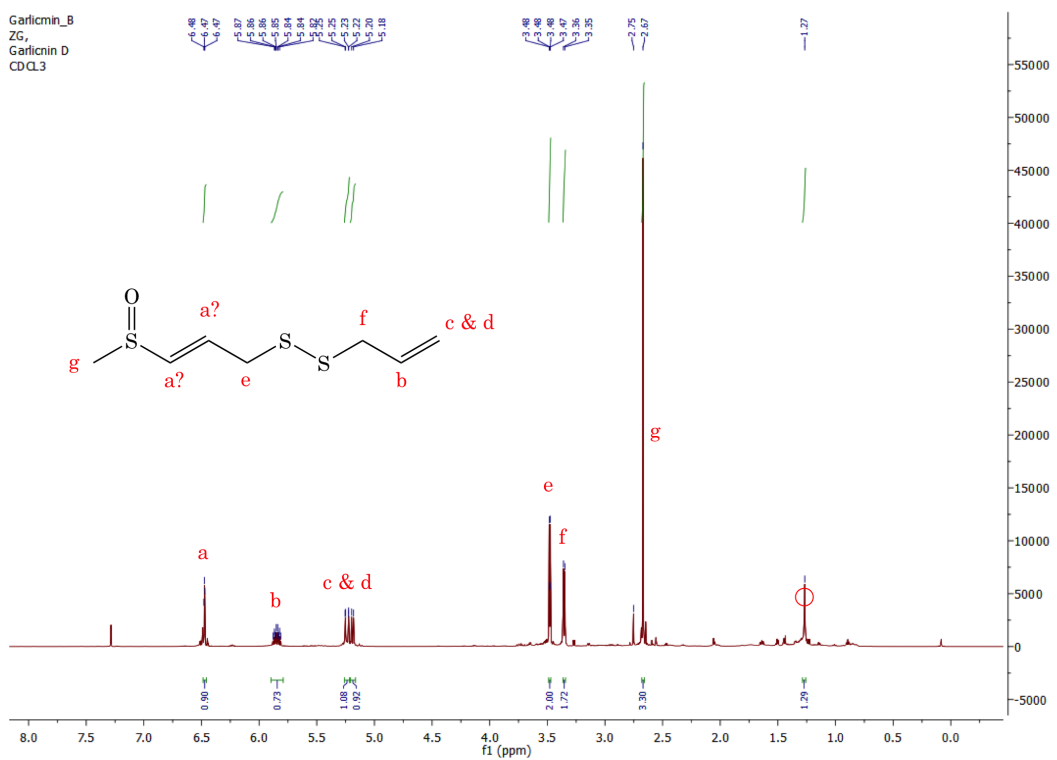


Figure 7.19: ¹H NMR spectrum (600 MHz, CDCl₃) of purified methylisoajoene (**8**). In deuterated chloroform, only four olefinic protons are visible. Grease is present in the spectrum (singlets at 1.25, 1.65, 1.90, 2.18 and 2.63 ppm).

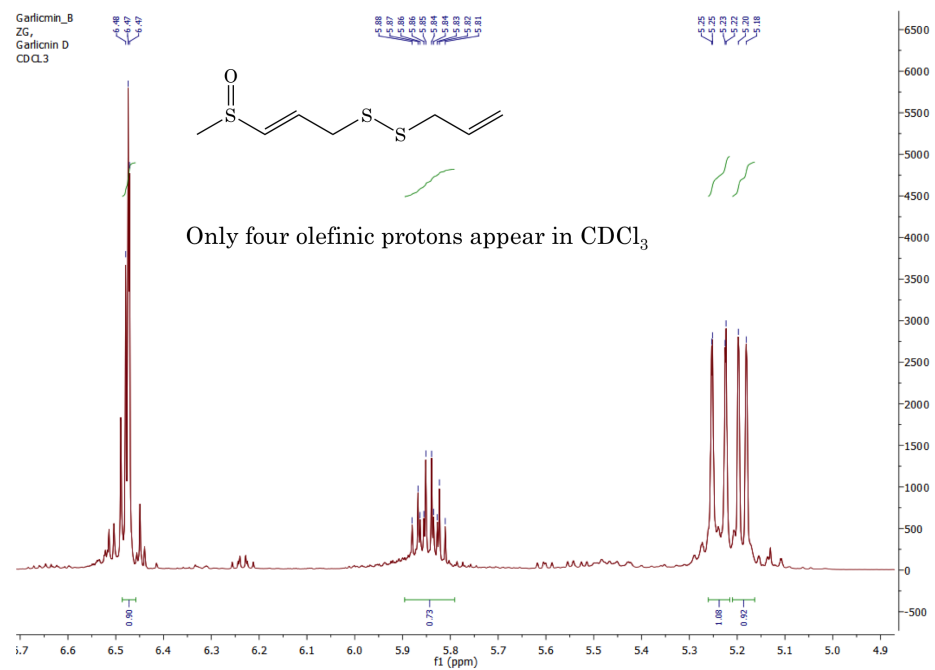


Figure 7.20: ¹H NMR spectrum (600 MHz, CDCl₃) of purified methylisoajoene (8), detailed view of the olefinic region. In deuterated chloroform, only four olefinic protons are visible.

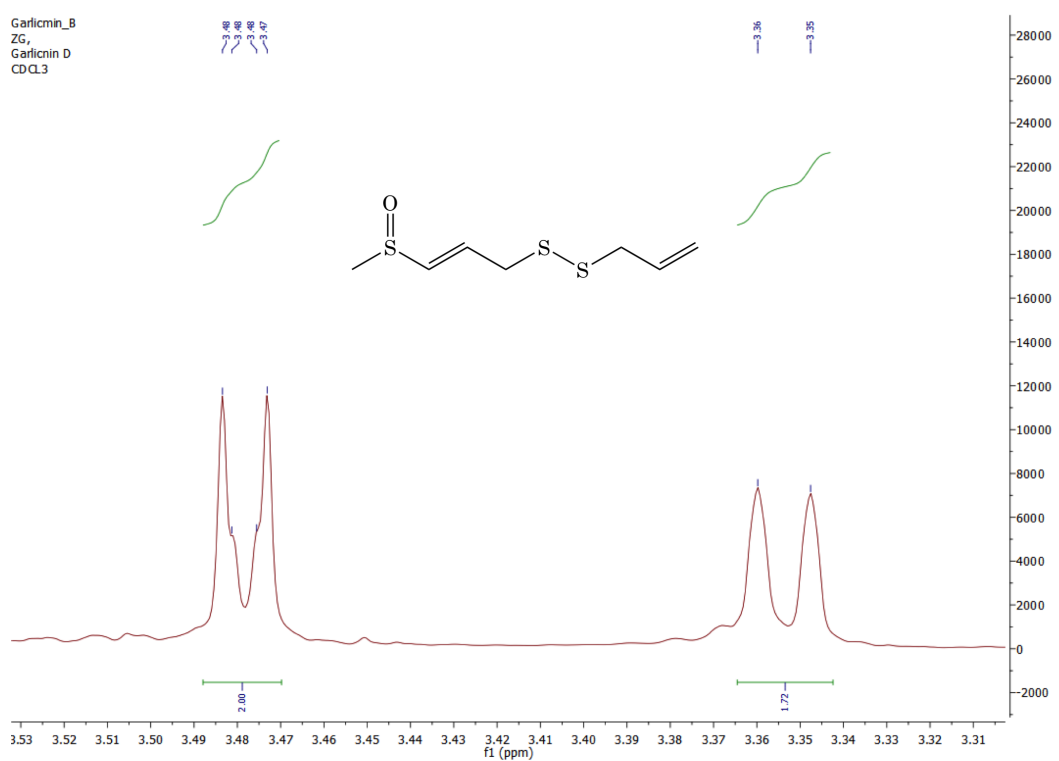


Figure 7.21: ¹H NMR spectrum (600 MHz, CDCl₃) of purified methylisooajoene (8), detailed view.

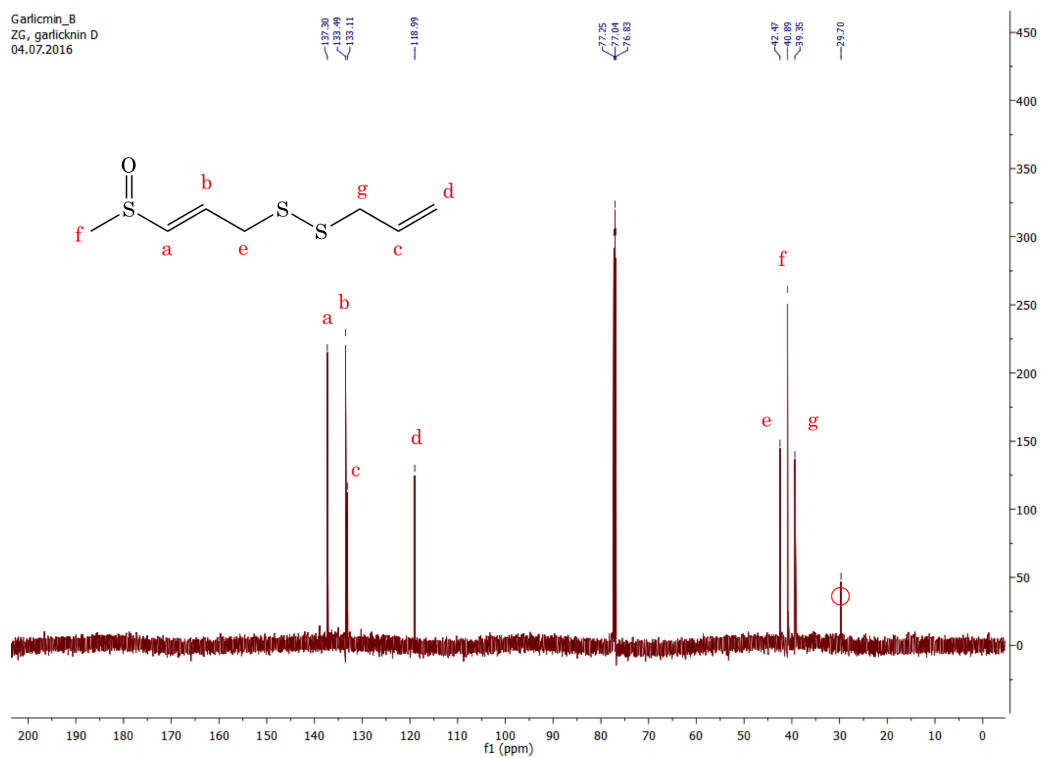


Figure 7.22: ^{13}C NMR spectrum (125 MHz, CDCl_3) of purified methylisoajoene (8). Grease (red circle) is present in the sample.

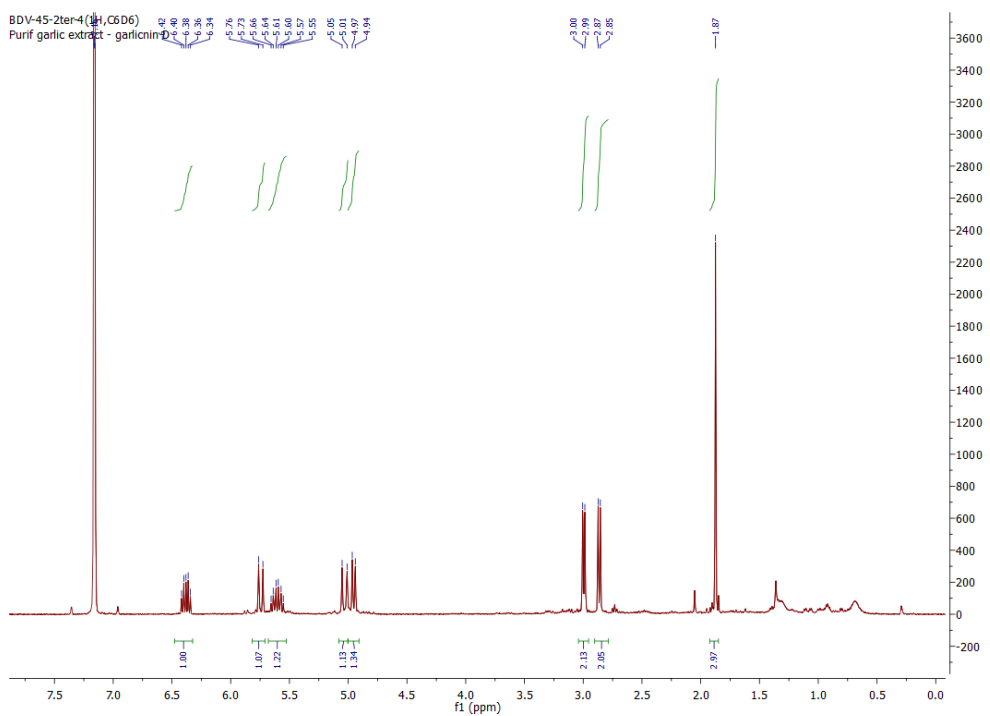


Figure 7.23: ^1H NMR spectrum (400 MHz, C_6D_6) of purified methylisoajoene (8).

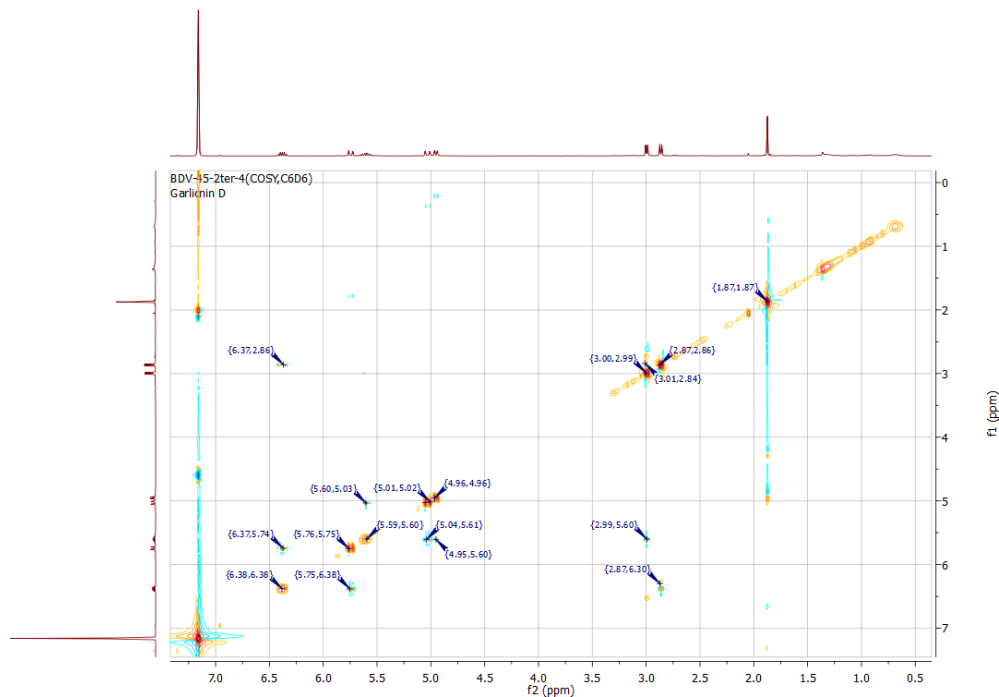


Figure 7.24: COSY NMR spectrum (400 MHz, C_6D_6) of purified methylisoajoene (8).

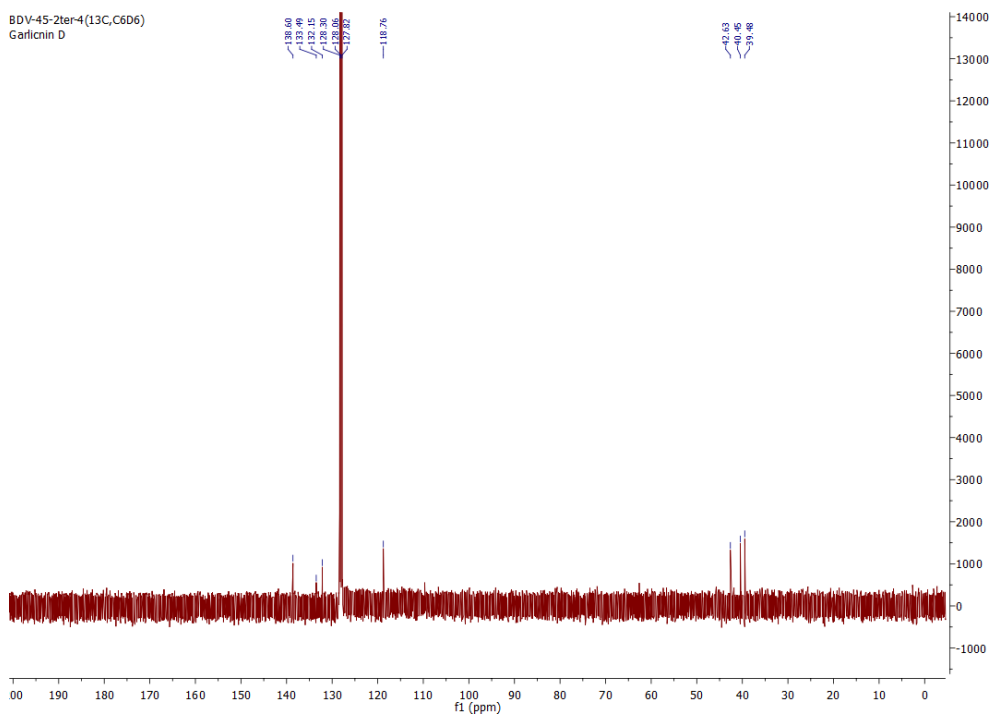


Figure 7.25: ^{13}C NMR spectrum (100 MHz, C_6D_6) of purified methylisoajoene (8).

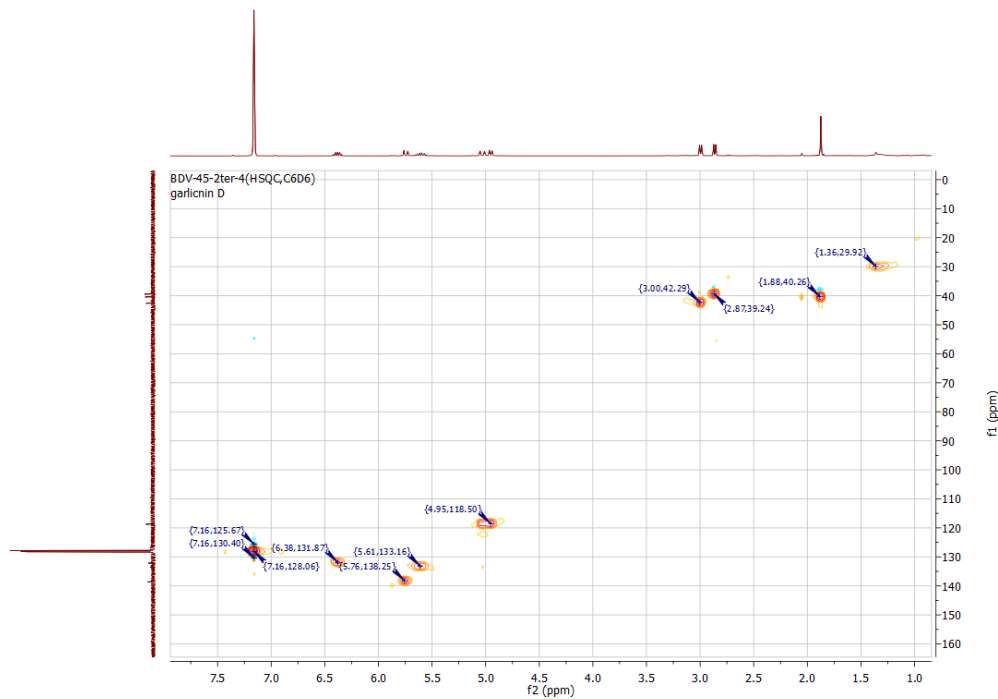


Figure 7.26: HSQC NMR spectrum (C_6D_6) of purified methylisoajoene (8).

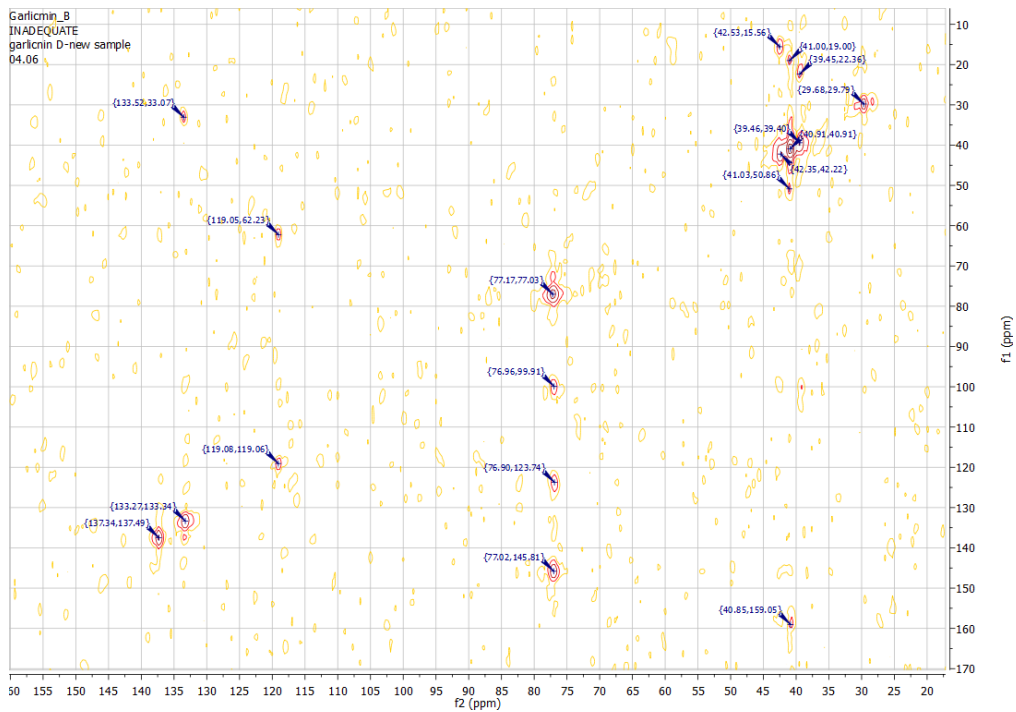


Figure 7.27: INADEQUATE NMR spectrum (600 MHz, CDCl_3) of purified methylisoajoene (**8**). No correlations are visible because the instrument was tuned to show $\text{sp}^3\text{-sp}^3$ correlations.

7.2 Chemistry of thiolane-containing natural products from processed plants of the genus *Allium*

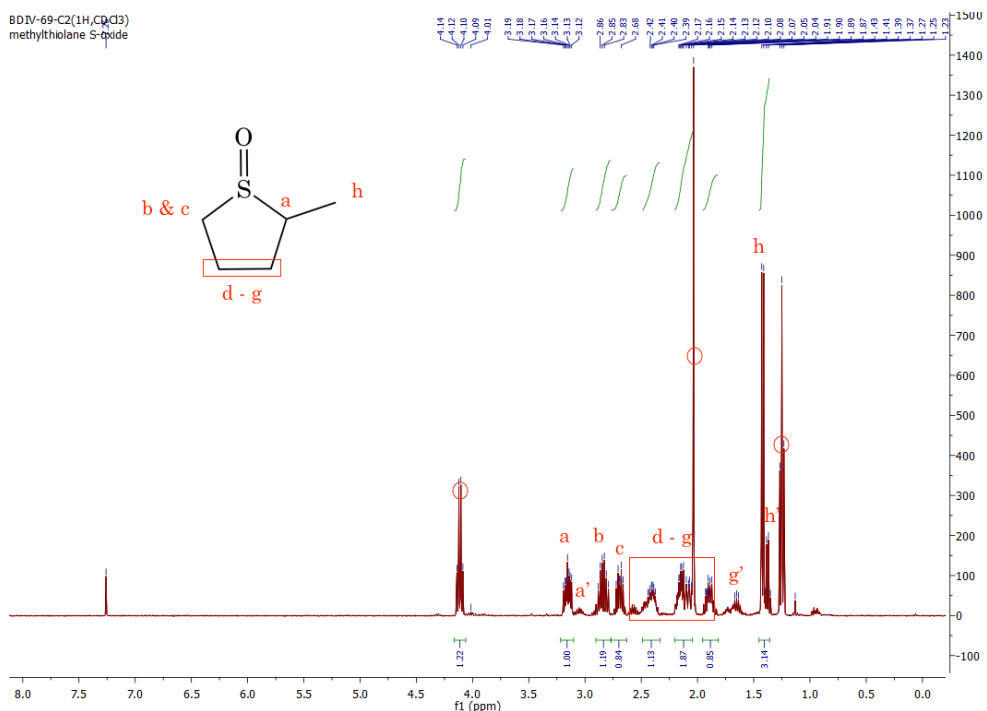


Figure 7.28: ^1H NMR spectrum (400 MHz, CDCl_3) of 2-methylthiolane sulfoxide (**33a**), mixture of stereoisomers in 4:1 ratio, detailed view (prime labels: minor stereoisomer). Ethyl acetate peaks are circled in red.

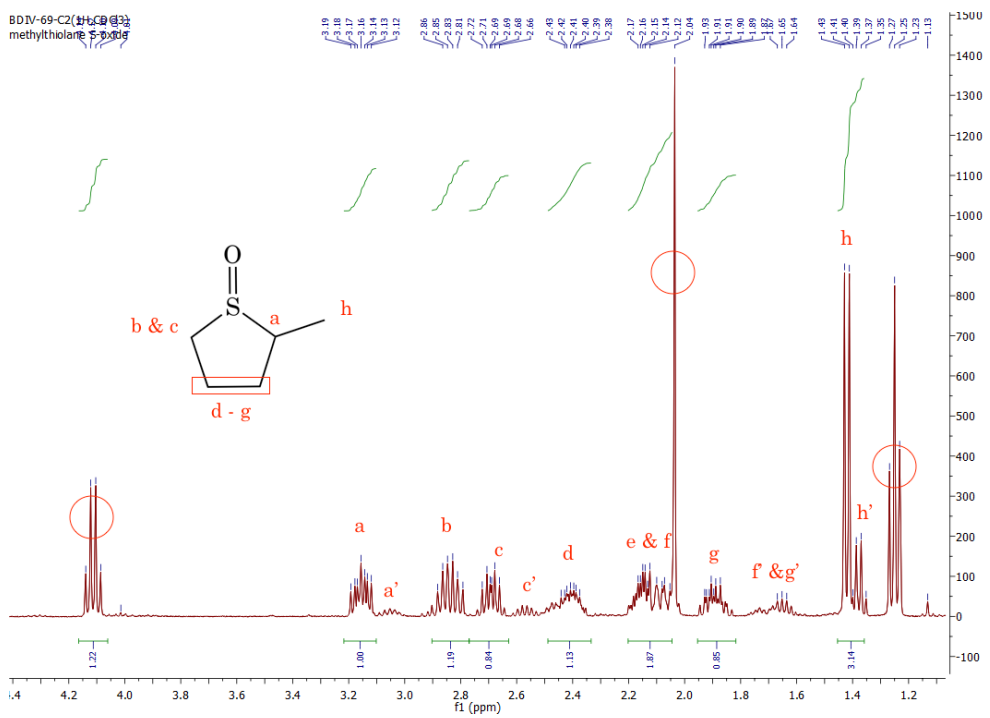


Figure 7.29: ¹H NMR spectrum (400 MHz, CDCl₃) of 2-methylthiolane sulfoxide (**33a**), mixture of stereoisomers in 4:1 ratio, detailed view (prime labels: minor stereoisomer). Ethyl acetate peaks are circled in red.

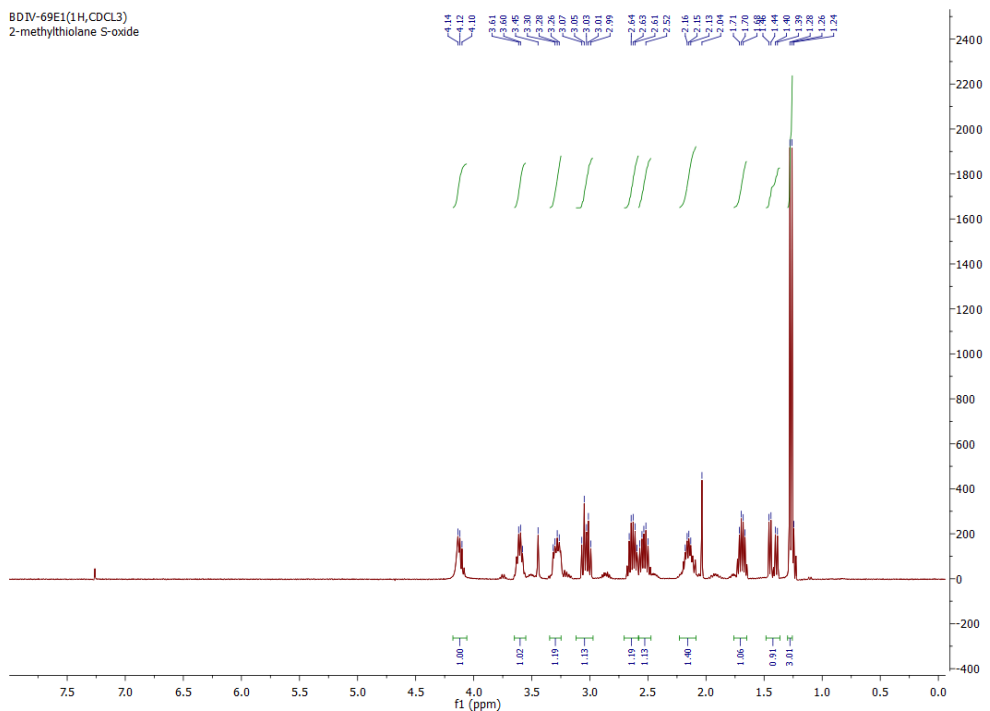


Figure 7.30: ¹H NMR spectrum (400 MHz, CDCl₃) of 2-methylthiolane sulfoxide (**33a**), pure stereoisomers.

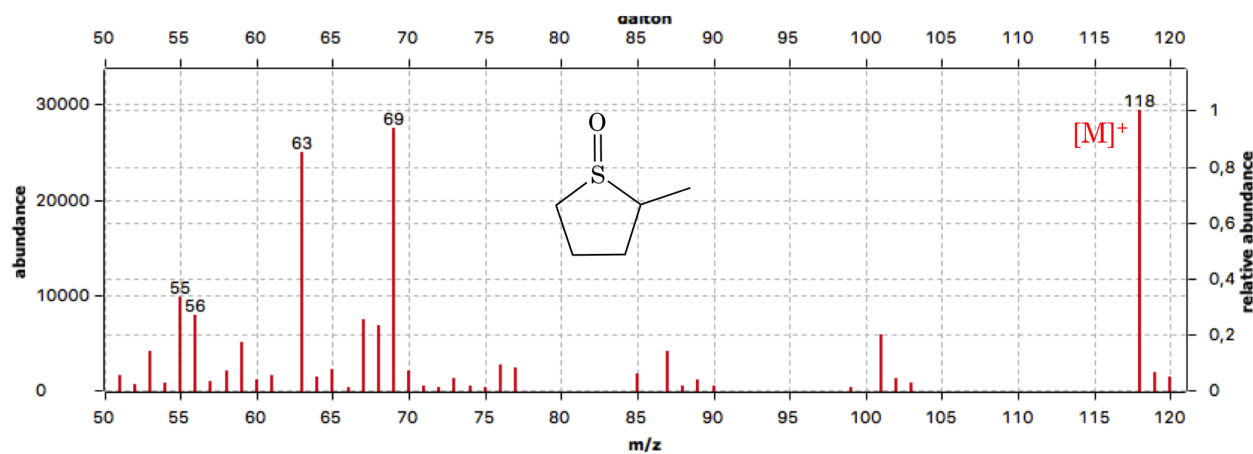


Figure 7.31: Mass spectrum of 2-methylthiolane sulfoxide (33a) recorded by GC-MS.

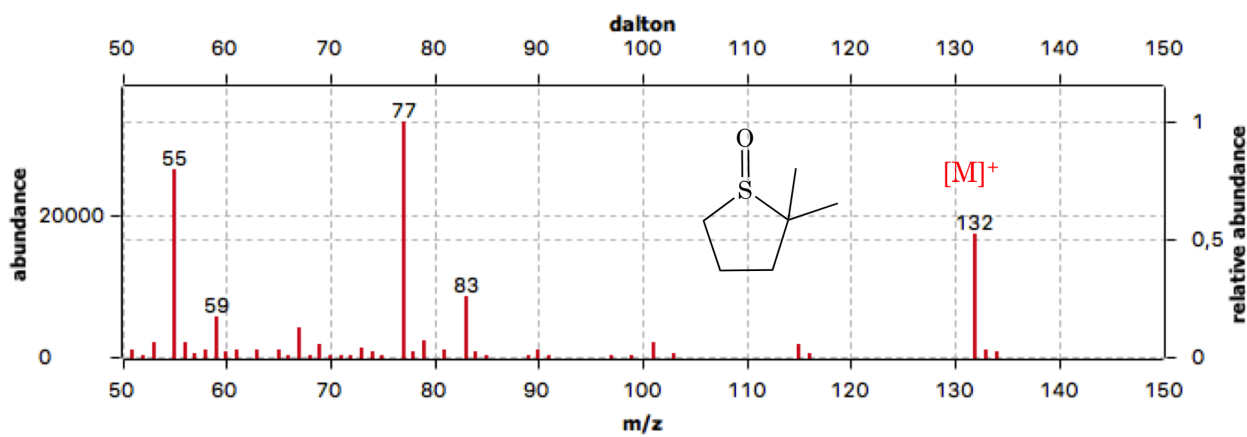


Figure 7.32: Mass spectrum of 2,2-dimethylthiolane sulfoxide recorded by GC-MS.

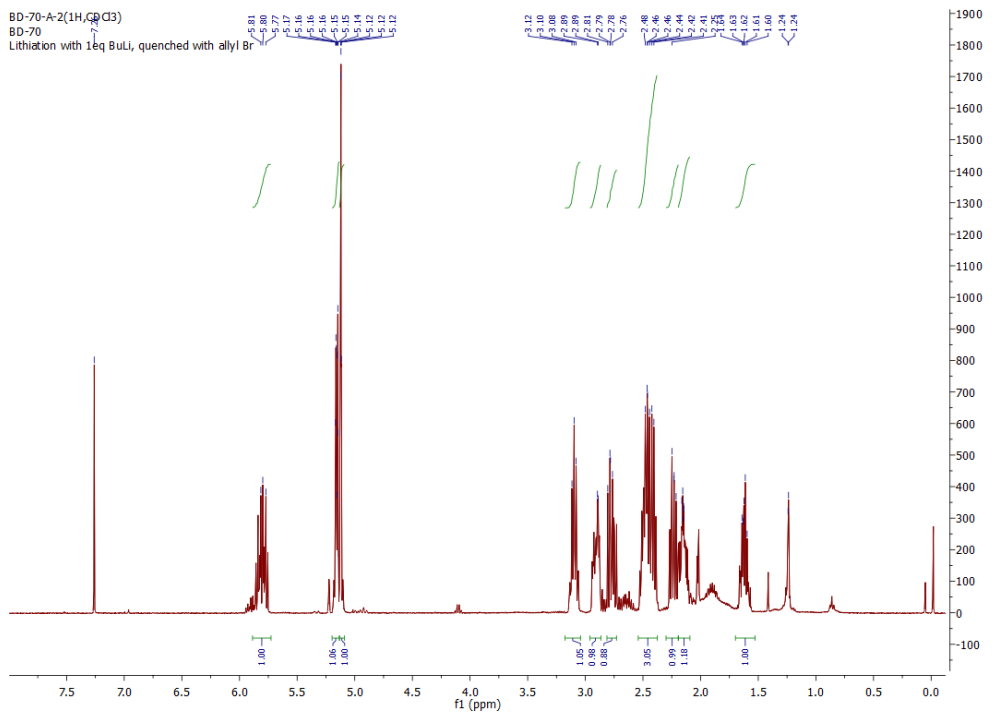


Figure 7.33: ^1H NMR spectrum (400 MHz, CDCl_3) of 2-allylthiolane sulfoxide (**33b**).

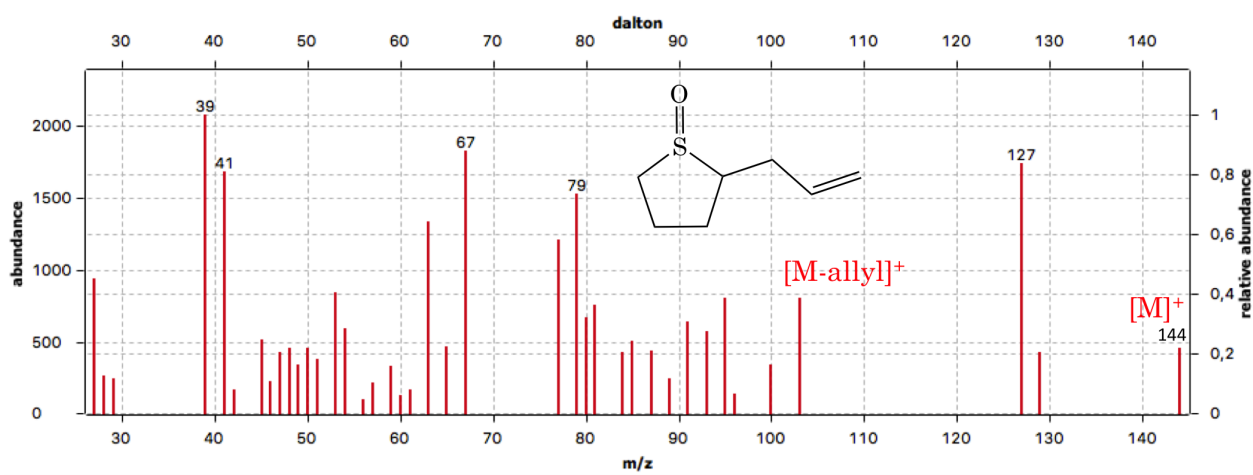


Figure 7.34: Mass spectrum of 2-allylthiolane sulfoxide (**33b**) recorded by GC-MS.

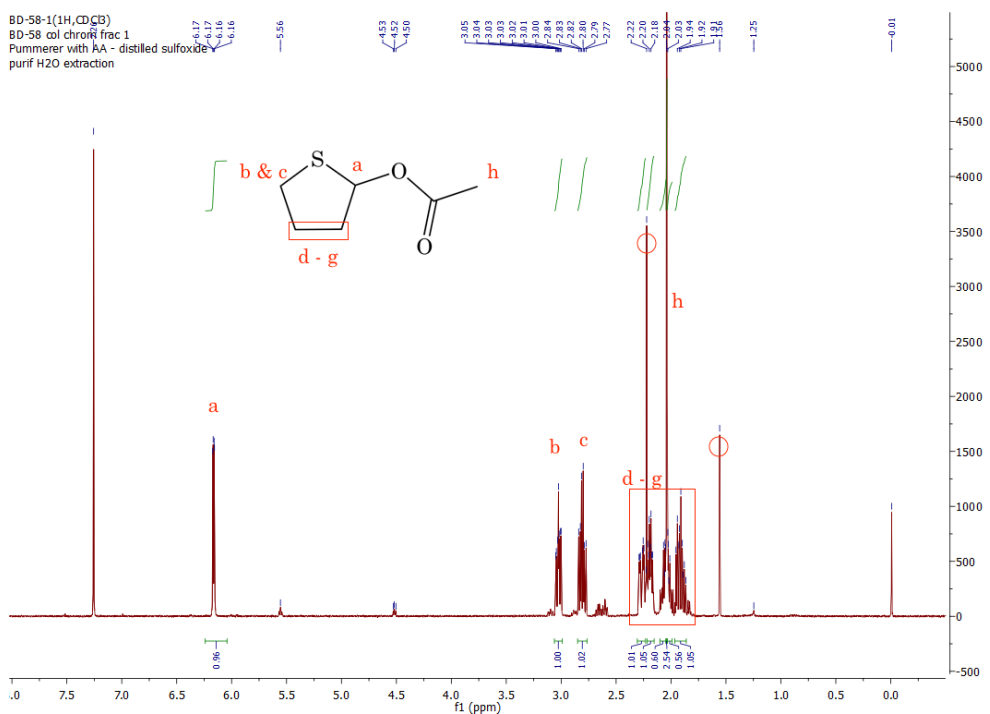


Figure 7.35: ^1H NMR spectrum (400 MHz, CDCl_3) of 2-acetoxythiolane (**34**). Traces of water (1.56 ppm) and acetic anhydride (2.21 ppm) are present in the spectrum and circled in red.

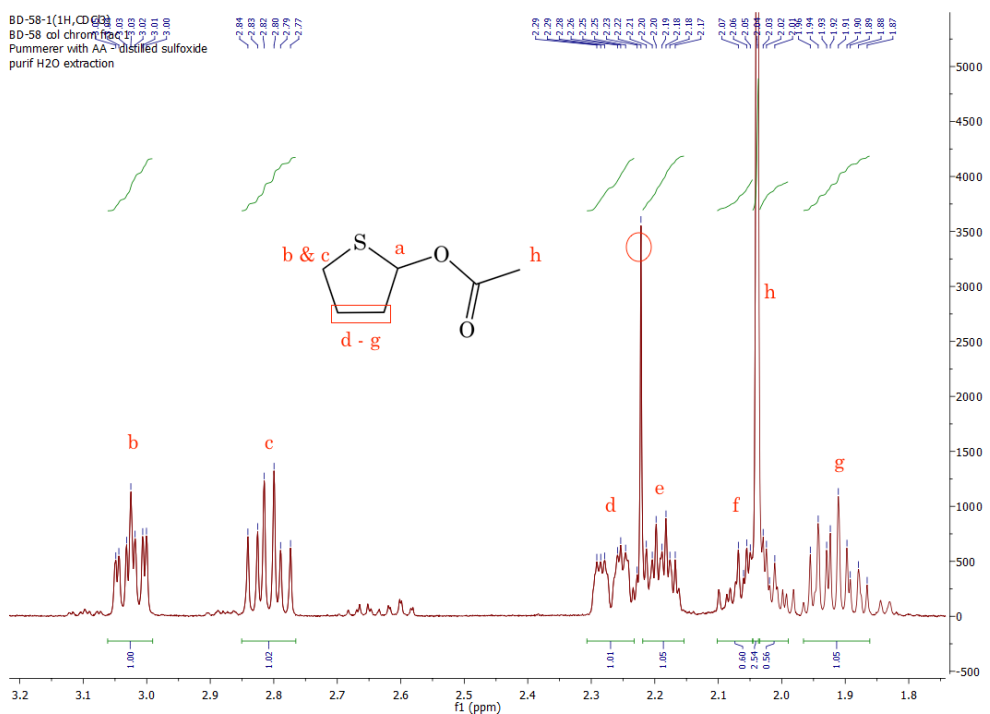


Figure 7.36: ¹H NMR spectrum (400 MHz, CDCl₃) of 2-acetoxythiolane (**34**). Acetic anhydride is present in the spectrum (2.21 ppm, circled in red).

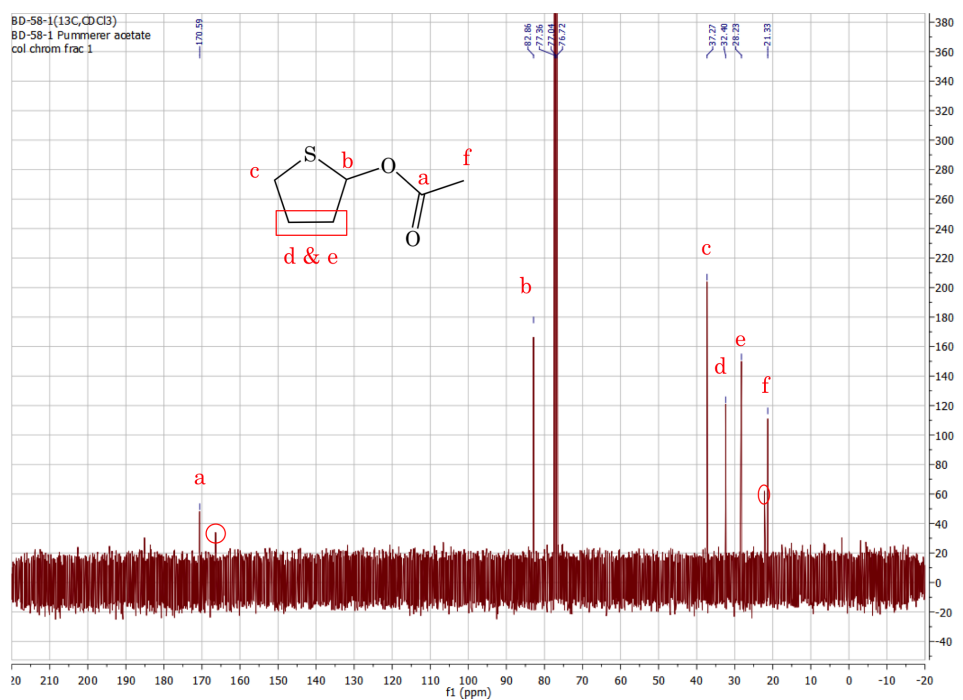


Figure 7.37: ¹³C NMR spectrum (400 MHz, CDCl₃) of 2-acetoxythiolane (**34**). Acetic anhydride is present in the spectrum (circled in red).

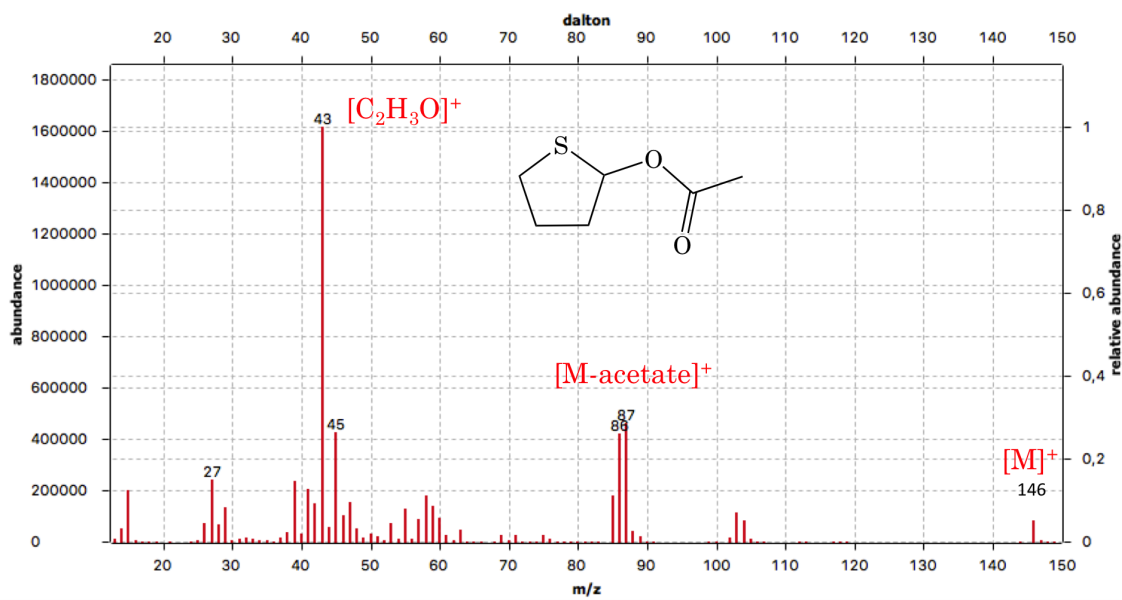


Figure 7.38: Mass spectrum of 2-acetoxythiolane (**34**) recorded by GC-MS.

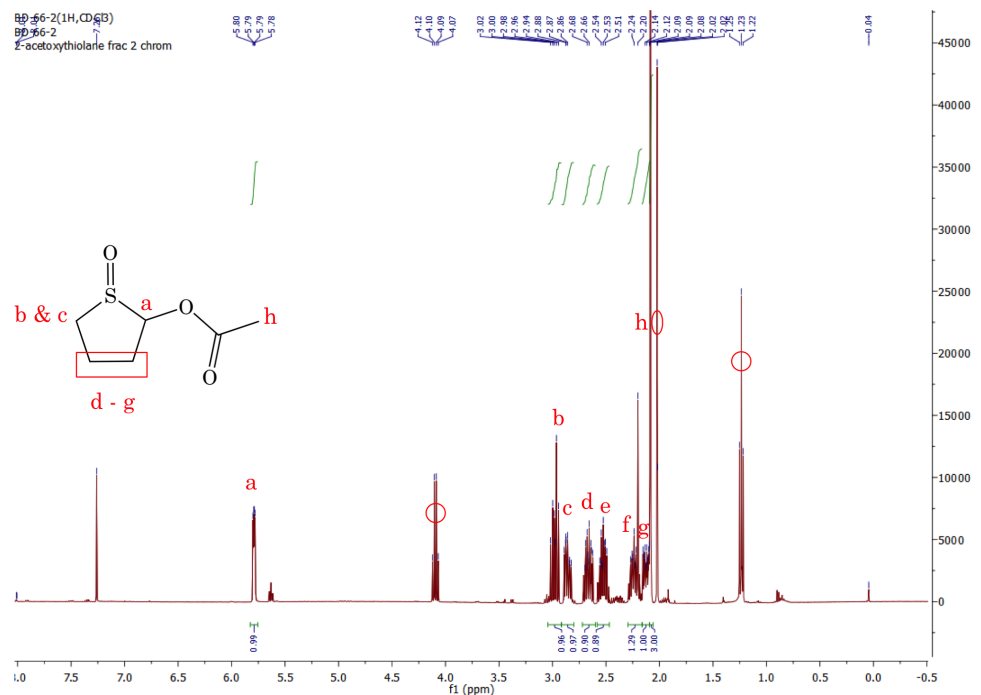


Figure 7.39: ^1H NMR spectrum (400 MHz, CDCl_3) of 2-acetoxythiolane sulfoxide (**35**). Traces of ethyl acetate are circled in red.

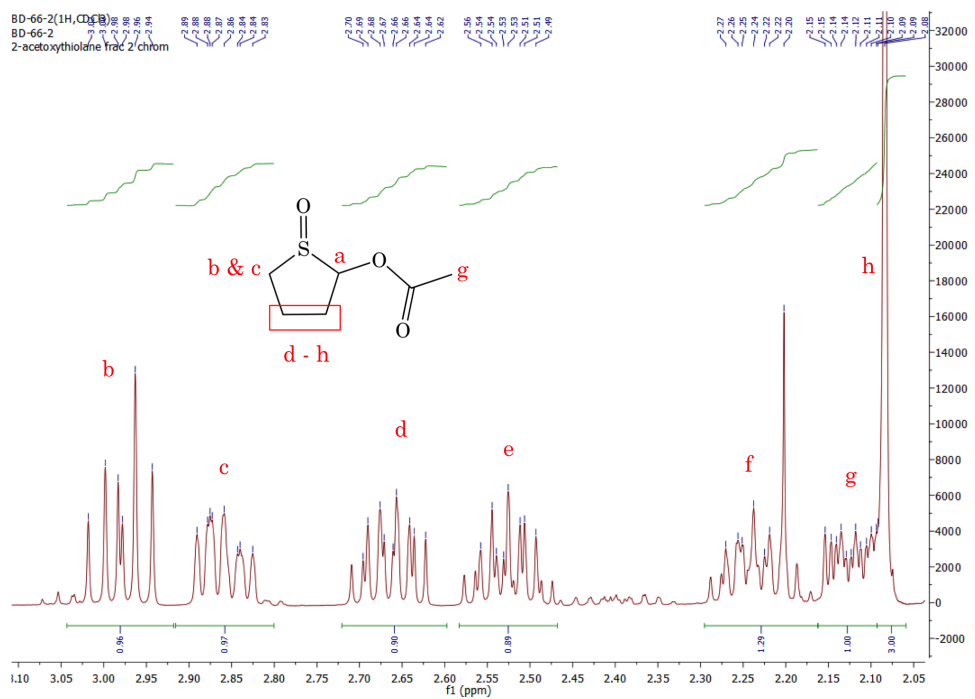


Figure 7.40: ¹H NMR spectrum (400 MHz, CDCl₃) of 2-acetoxythiolane sulfoxide (**35**), detailed view.

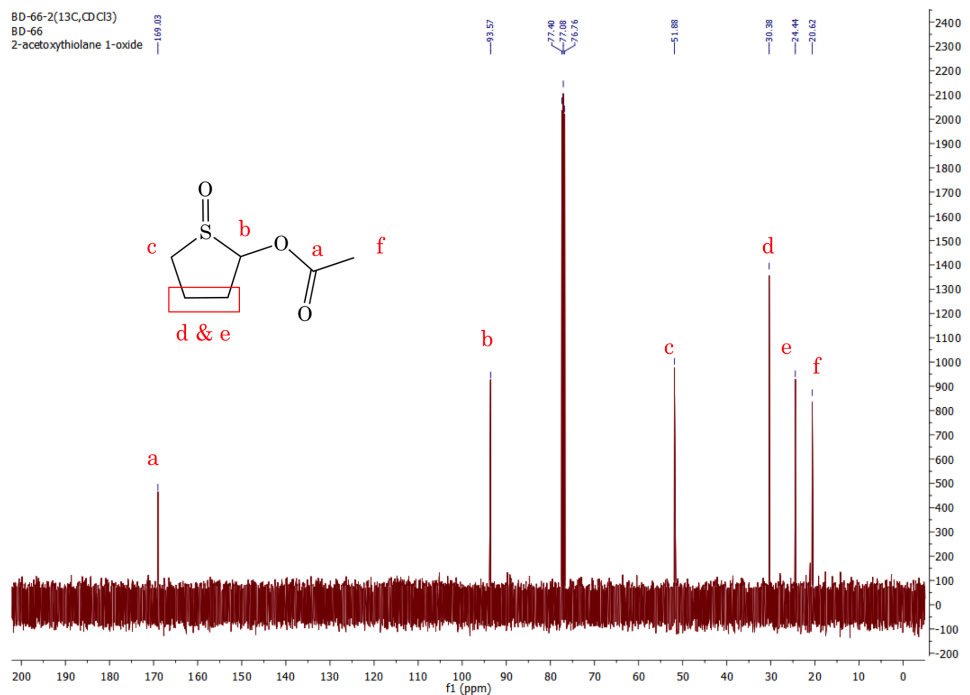


Figure 7.41: ¹³C NMR spectrum (400 MHz, CDCl₃) of 2-acetoxythiolane sulfoxide (**35**).

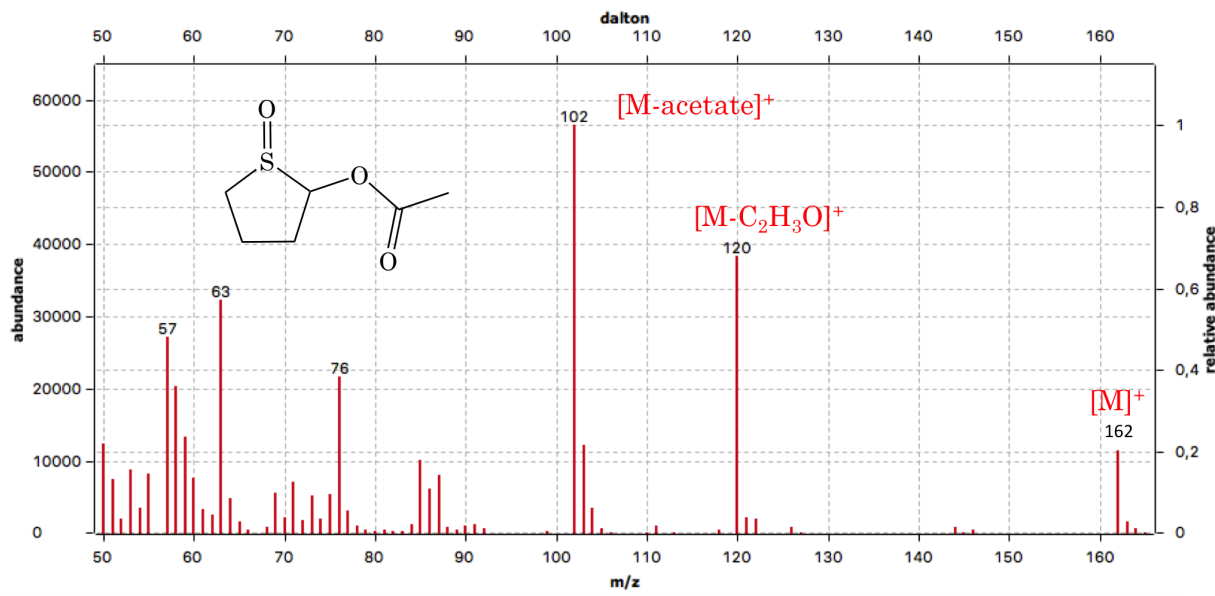


Figure 7.42: Mass spectrum of 2-acetoxythiolane sulfoxide (**35**) recorded by GC-MS.

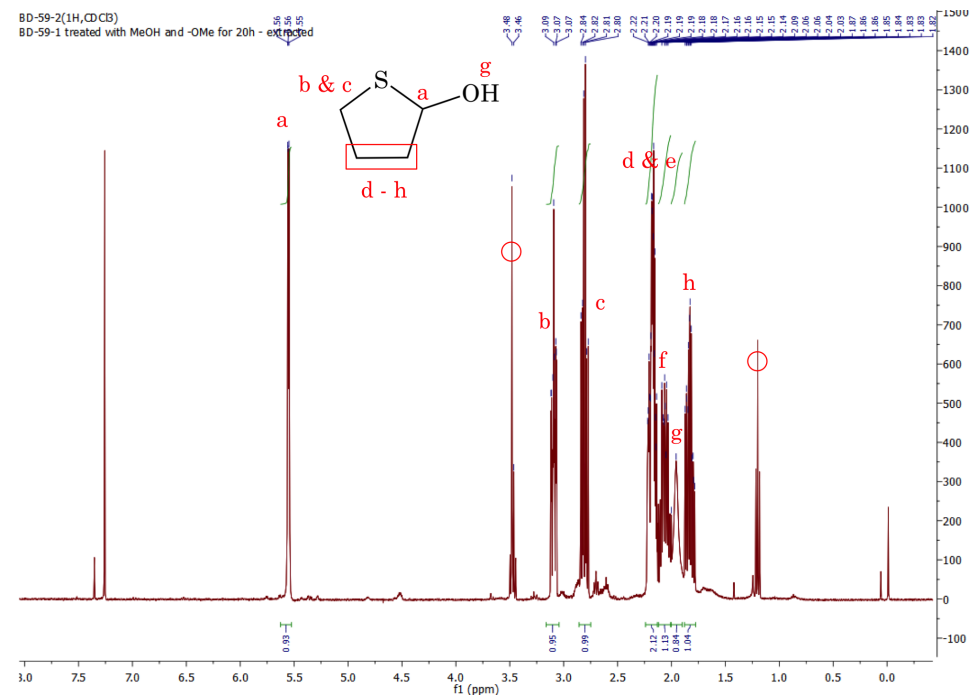


Figure 7.43: ¹H NMR spectrum (400 MHz, CDCl_3) of 2-hydroxythiolane (**29**). Methanol is the impurity circled in red.

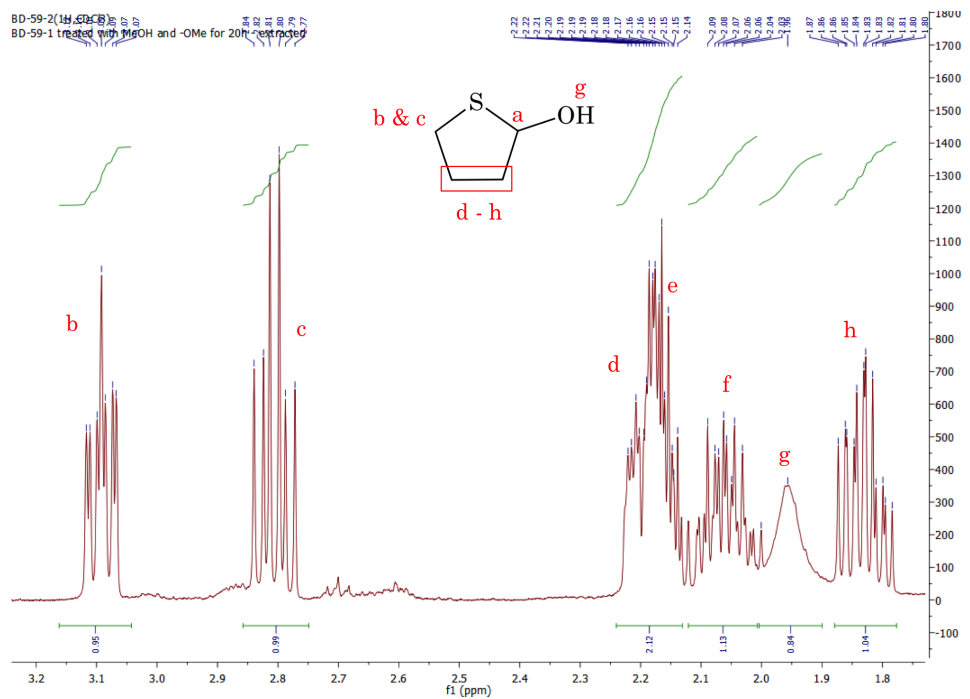


Figure 7.44: ^1H NMR spectrum (400 MHz, CDCl_3) of 2-hydroxythiolane (**29**), detailed view.

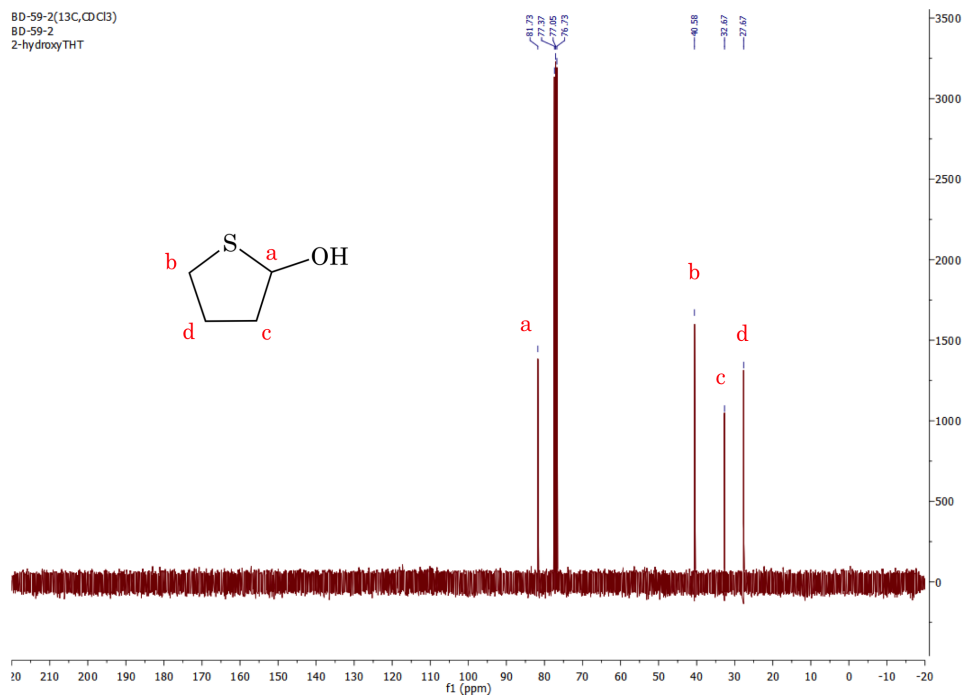


Figure 7.45: ^{13}C NMR spectrum (400 MHz, CDCl_3) of 2-hydroxythiolane (**29**).

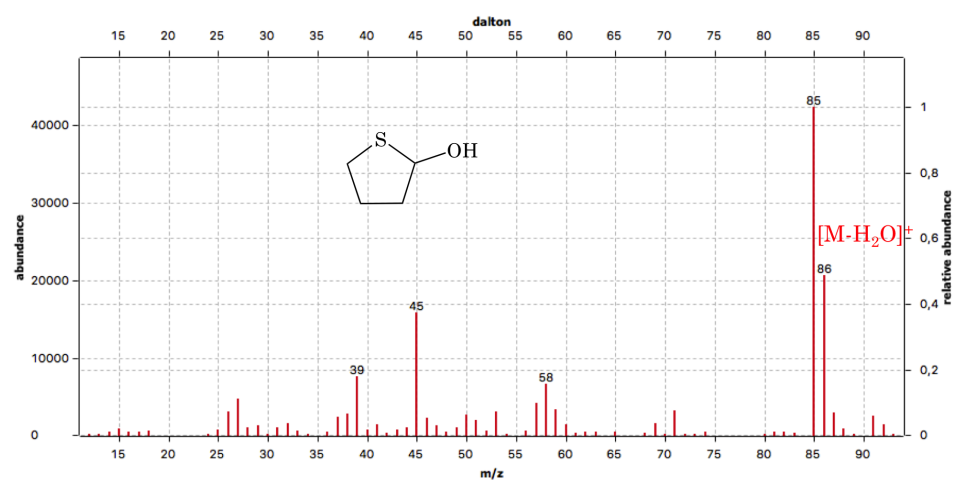


Figure 7.46: Mass spectrum of 2-hydroxythiolane (**29**) recorded by GC-MS. The molecular ion is not visible in the spectrum because loss of water occurs rapidly.

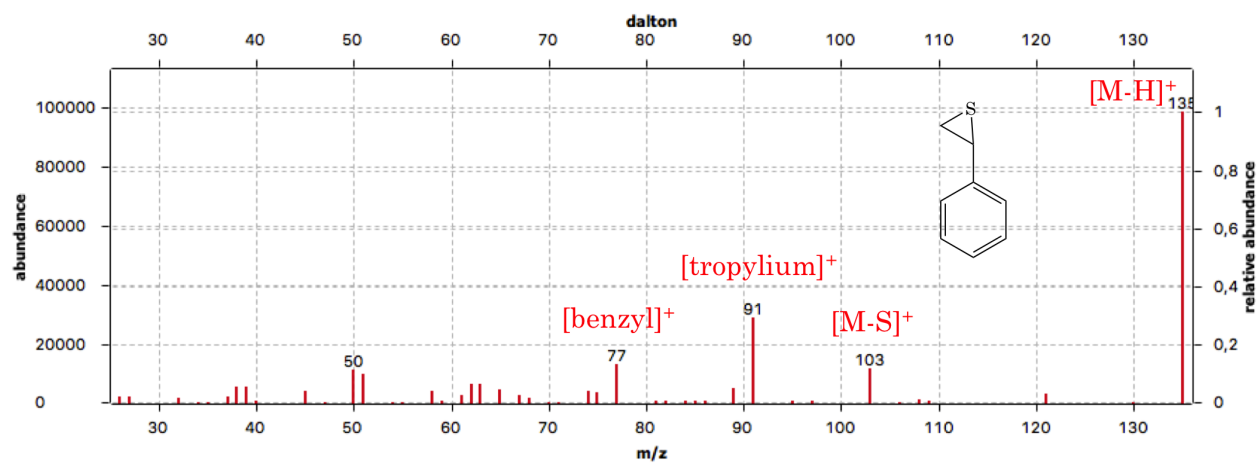


Figure 7.47: Mass spectrum of 2-phenylthiirane (39) recorded by GC-MS.

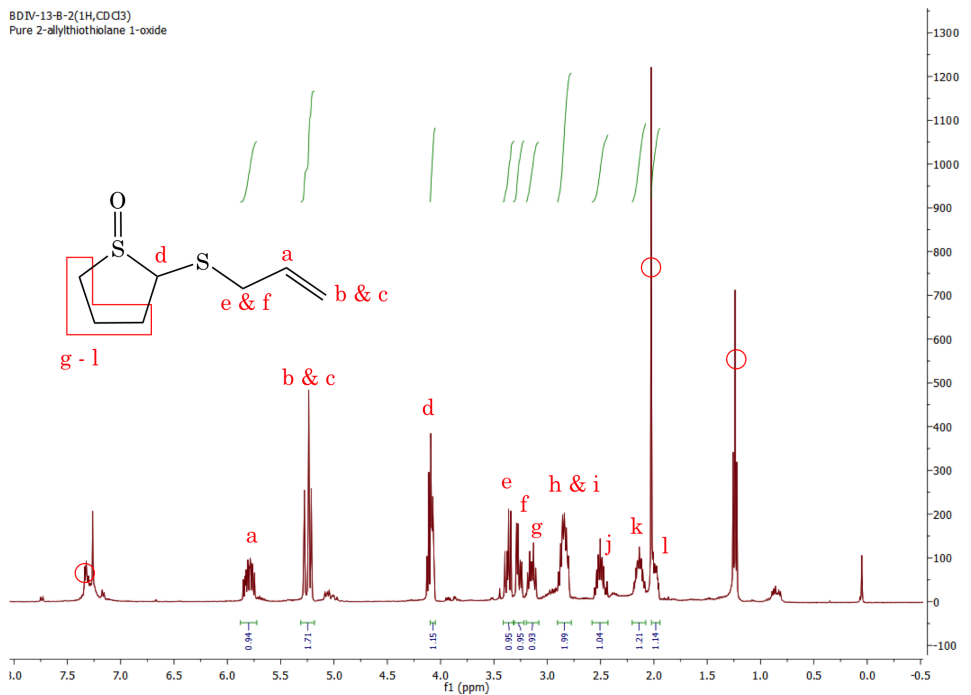


Figure 7.48: ¹H NMR spectrum (400 MHz, CDCl₃) of 2-allylthioliolane sulfoxide (**41**). Ethyl acetate is present in the spectrum and the peaks are circled in red. Traces of styrene also appear.

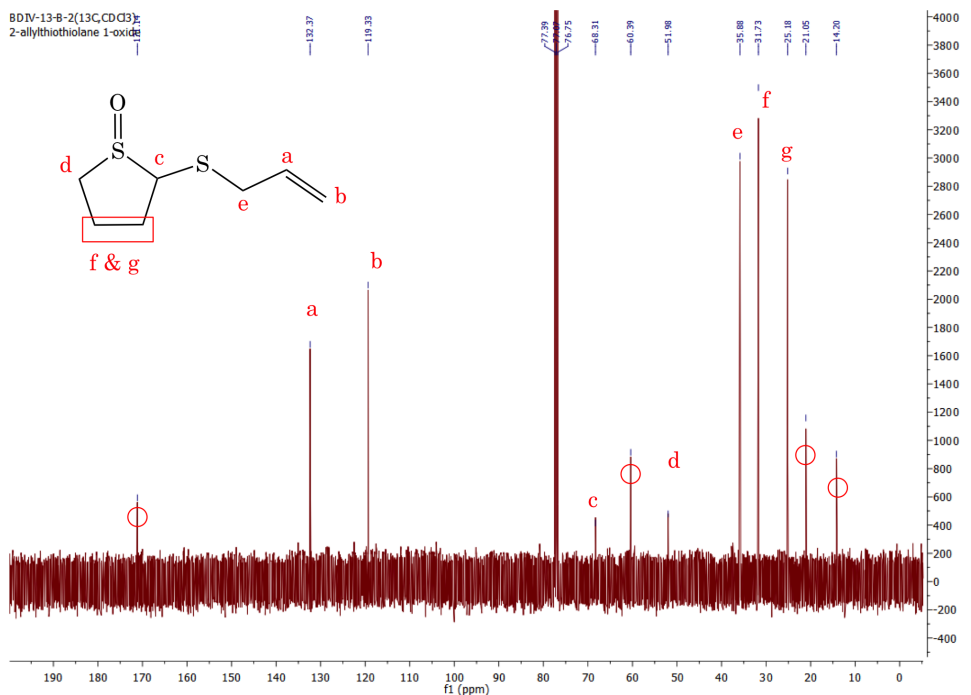


Figure 7.49: ¹³C NMR spectrum (400 MHz, CDCl₃) of 2-allylthioliolane sulfoxide (**41**). Ethyl acetate is present in the spectrum and the peaks are circled in red.

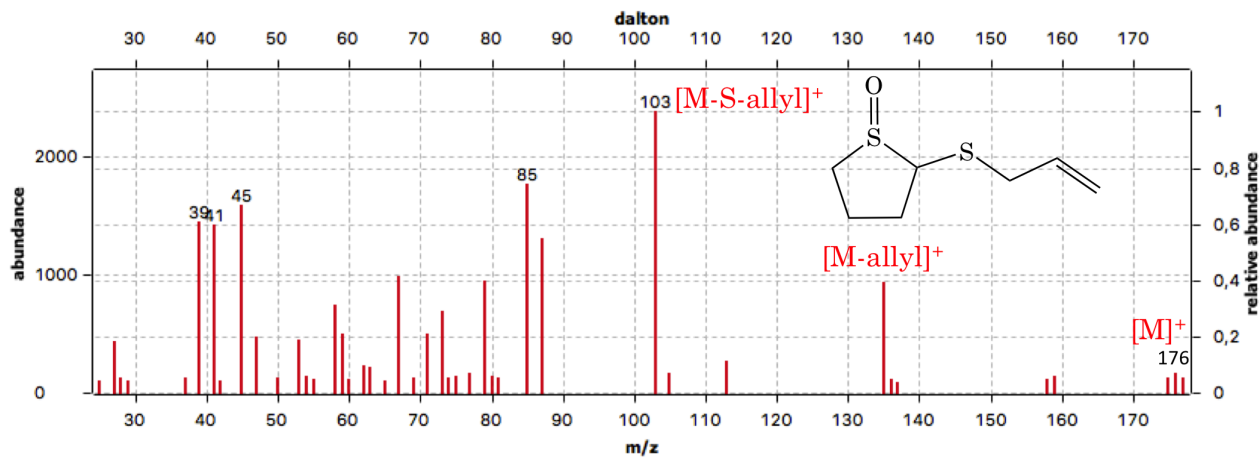


Figure 7.50: Mass spectrum of 2-allylthiothiolane sulfoxide (**41**) recorded by GC-MS.

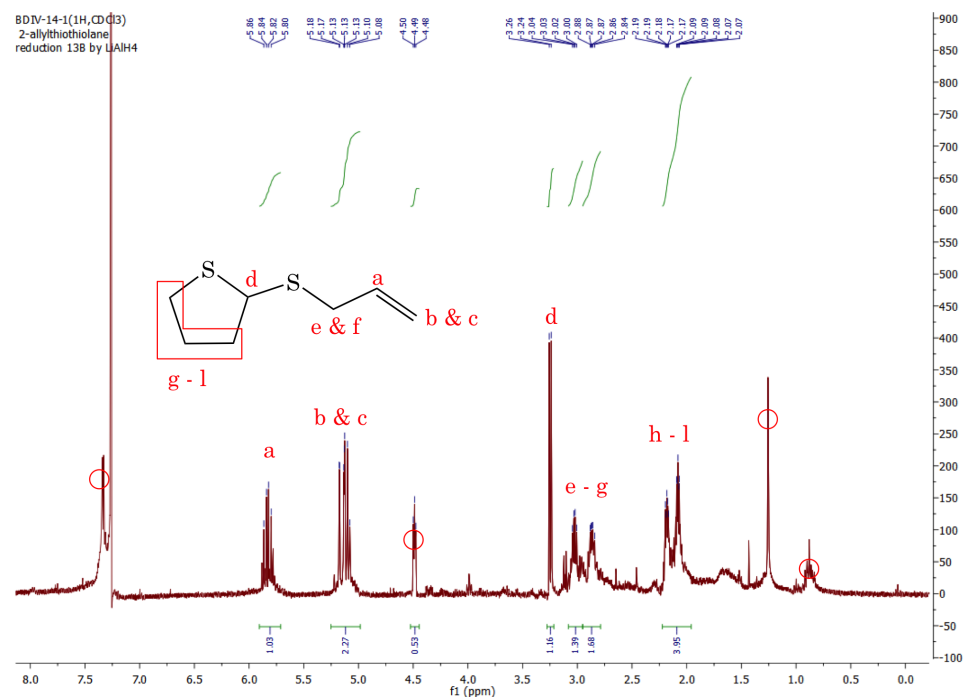


Figure 7.51: ^1H NMR spectrum (400 MHz, CDCl_3) of 2-allylthiothiolane (**43**). Styrene and other unknown impurities are present.

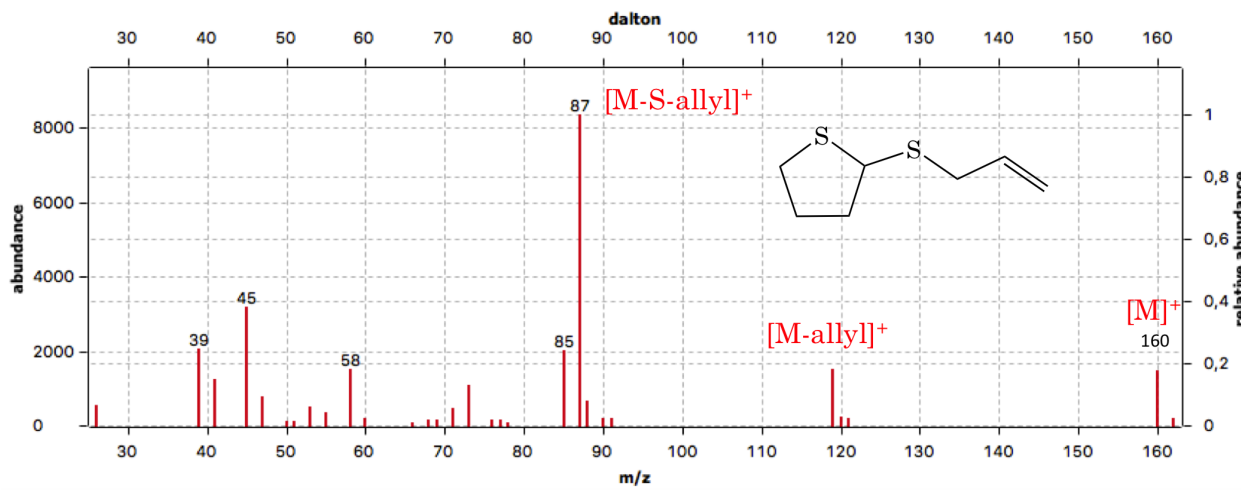


Figure 7.52: Mass spectrum of 2-allylthiothiolane (43) recorded by GC-MS.

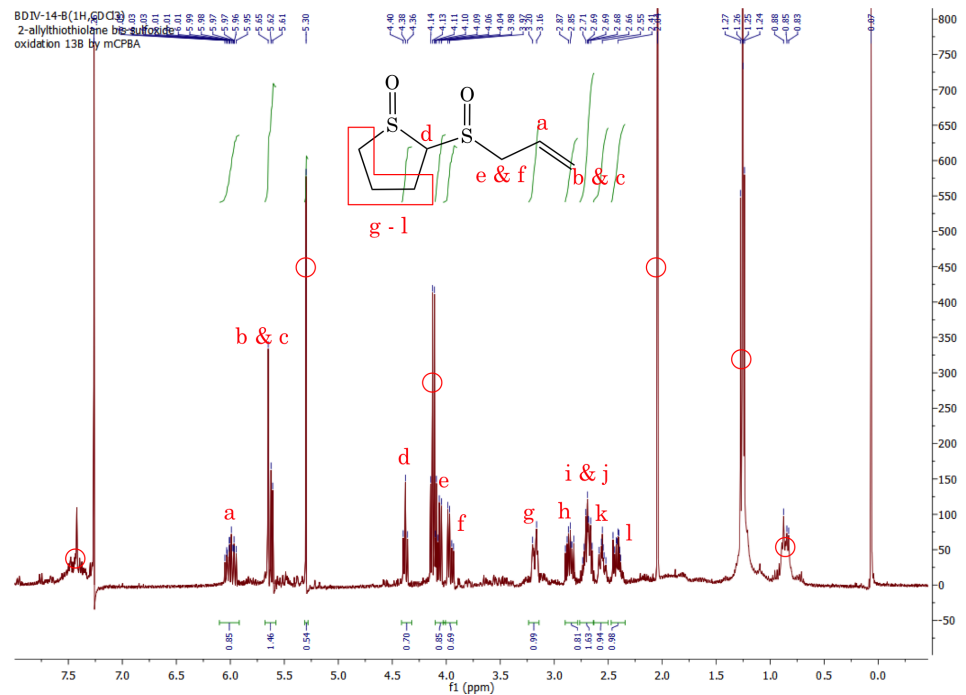


Figure 7.53: ^1H NMR spectrum (400 MHz, CDCl_3) of 2-allylthiothiolane bissulfoxide (44). Impurities circled in red include styrene, ethyl acetate and methylene chloride.

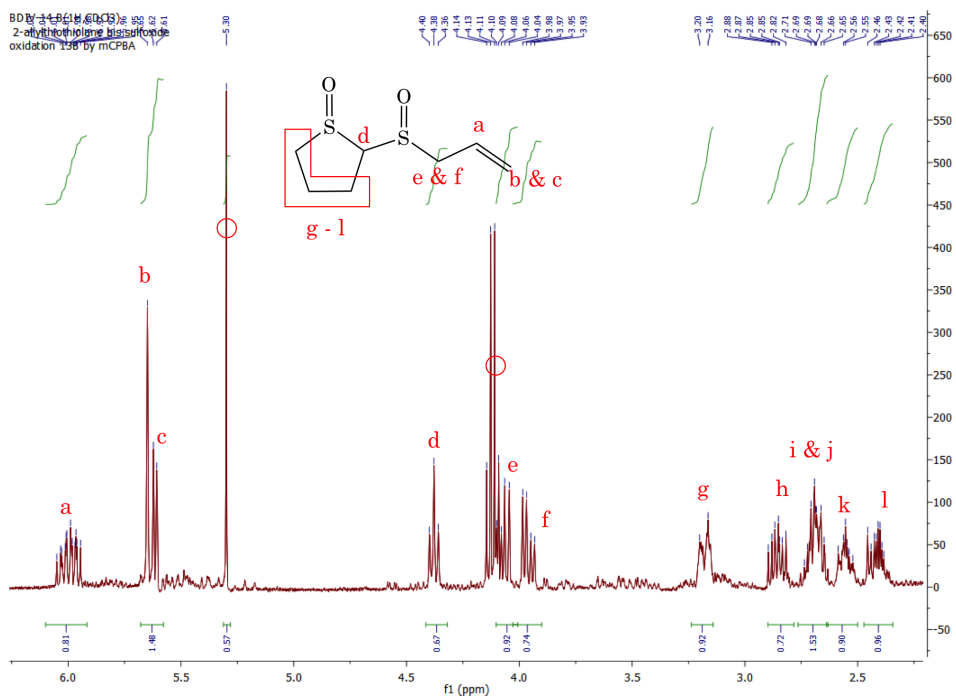


Figure 7.54: ^1H NMR spectrum (400 MHz, CDCl_3) of 2-allylthiolane bissulfoxide (**44**), detailed view. Impurities circled in red include ethyl acetate and methylene chloride.

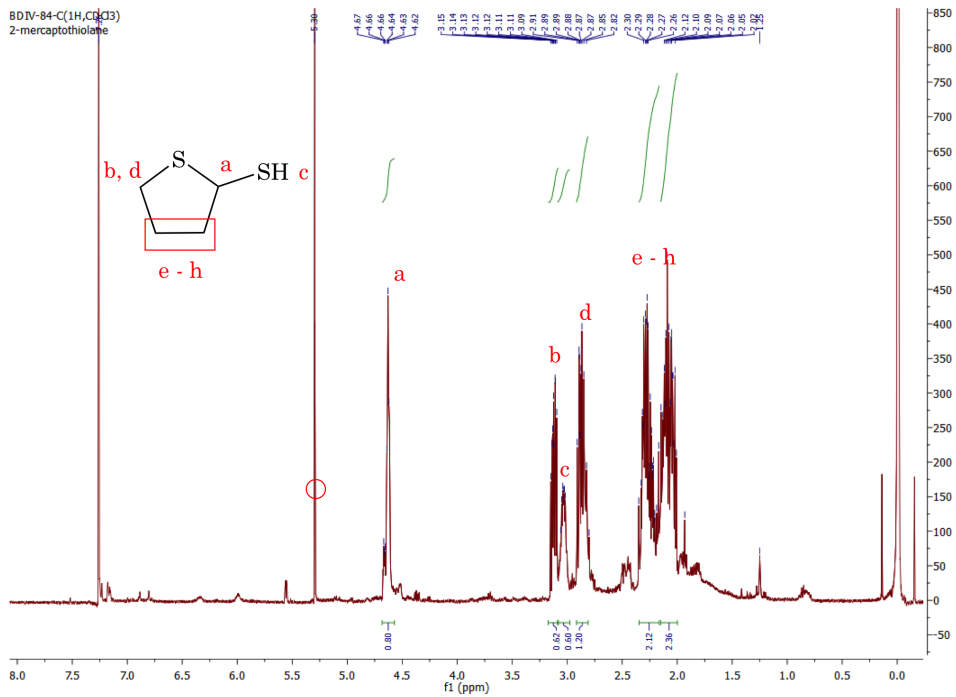


Figure 7.55: ^1H NMR spectrum (400 MHz, CDCl_3) of 2-mercaptopthiolane (**46**). The dichloromethane peak is circled in red.

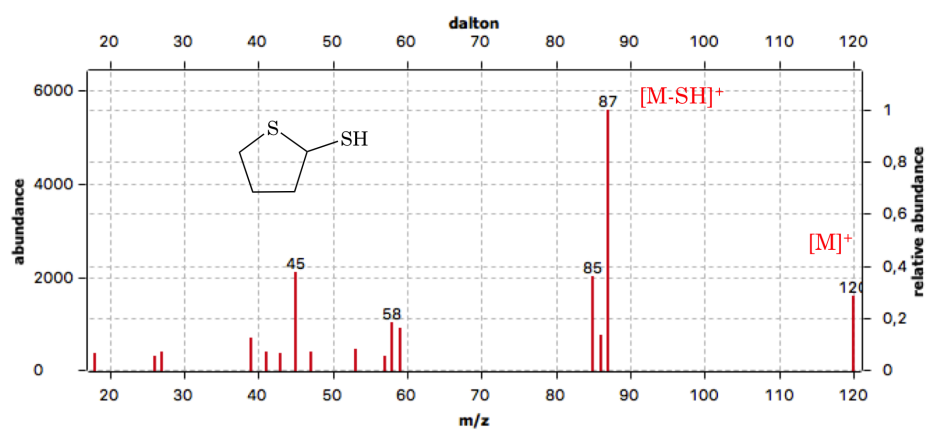


Figure 7.56: Mass spectrum of 2-mercaptopthiolane (**46**) recorded by GC-MS.

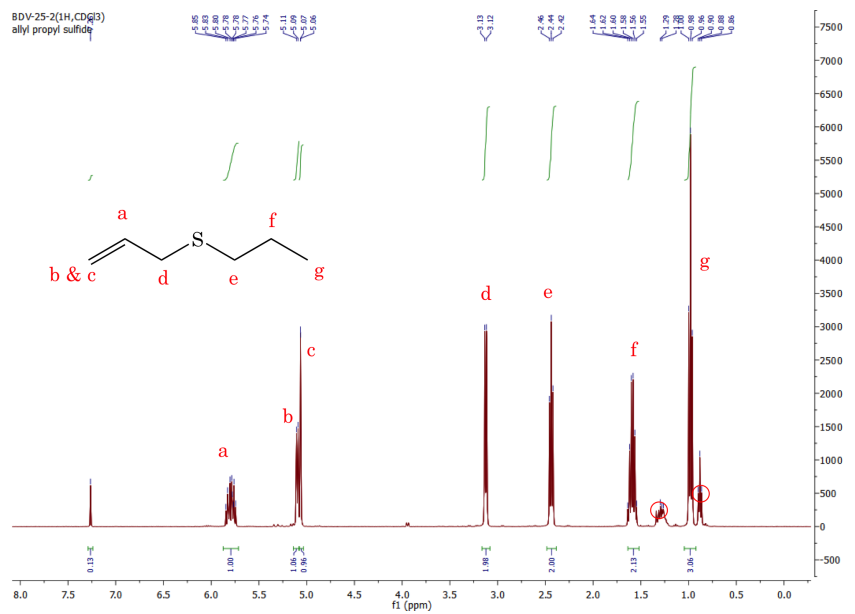


Figure 7.57: ^1H NMR spectrum (400 MHz, CDCl_3) of allyl propyl sulfide (**50b**). Some pentane was left in the sample (circled in red).

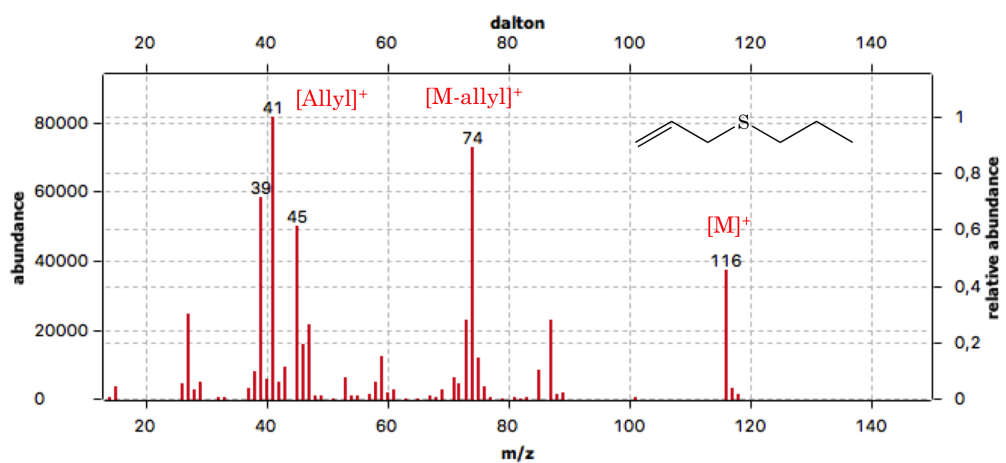


Figure 7.58: Mass spectrum of allyl propyl sulfide (**50b**) recorded by GC-MS.

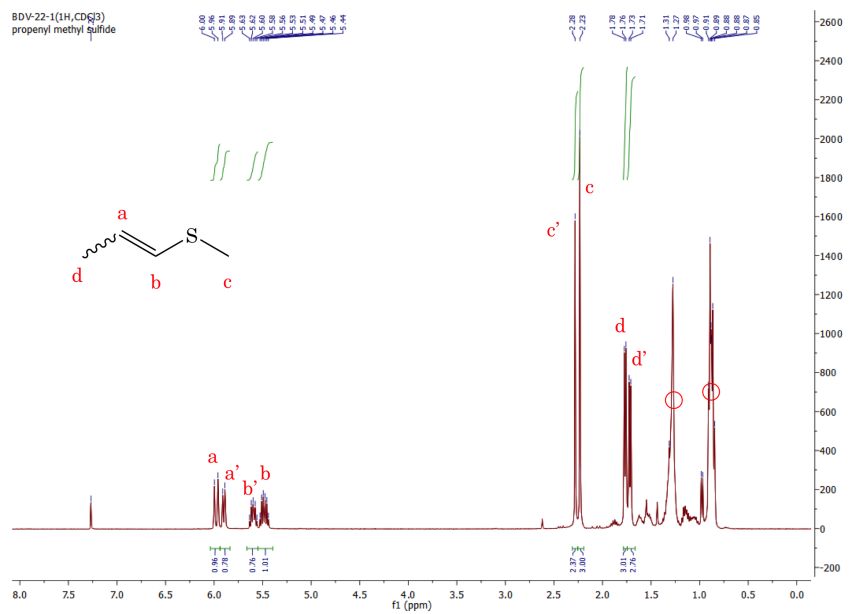


Figure 7.59: ¹H NMR spectrum (400 MHz, CDCl₃) of methyl 1-propenyl sulfide (mixture of stereoisomers, **49b**). Some pentane was left in the sample (circled in red).

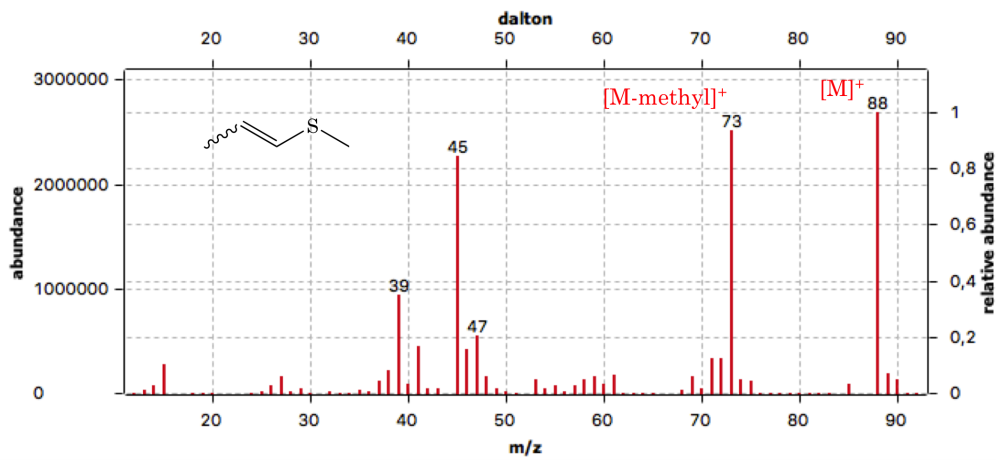


Figure 7.60: Mass spectrum of methyl 1-propenyl sulfide (**49b**) recorded by GC-MS.

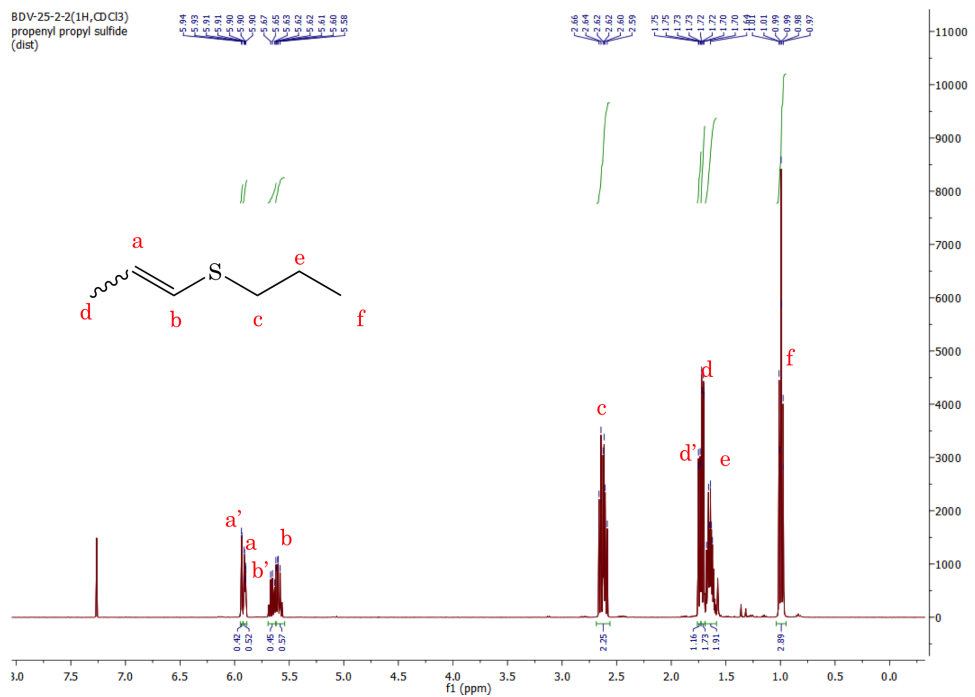


Figure 7.61: ^1H NMR spectrum (400 MHz, CDCl_3) of 1-propenyl propyl sulfide (mixture of stereoisomers, **49a**). Minor stereoisomer is marked with prime letters.

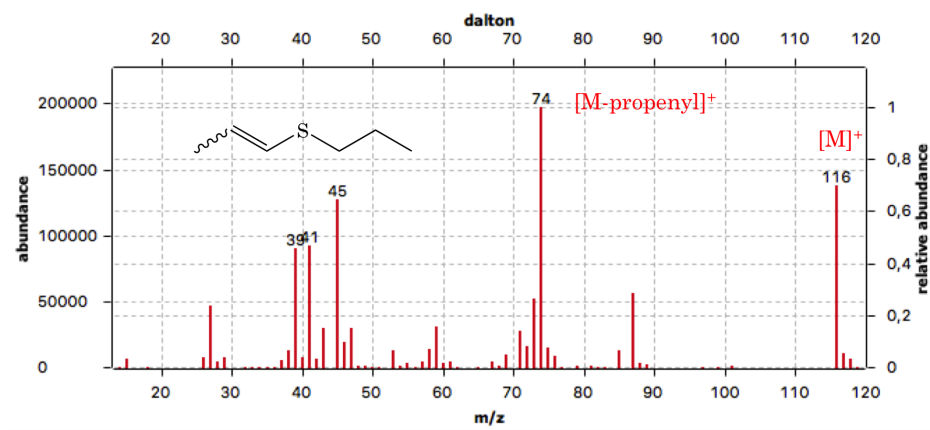


Figure 7.62: Mass spectrum of 1-propenyl propyl sulfide (49a) recorded by GC-MS.

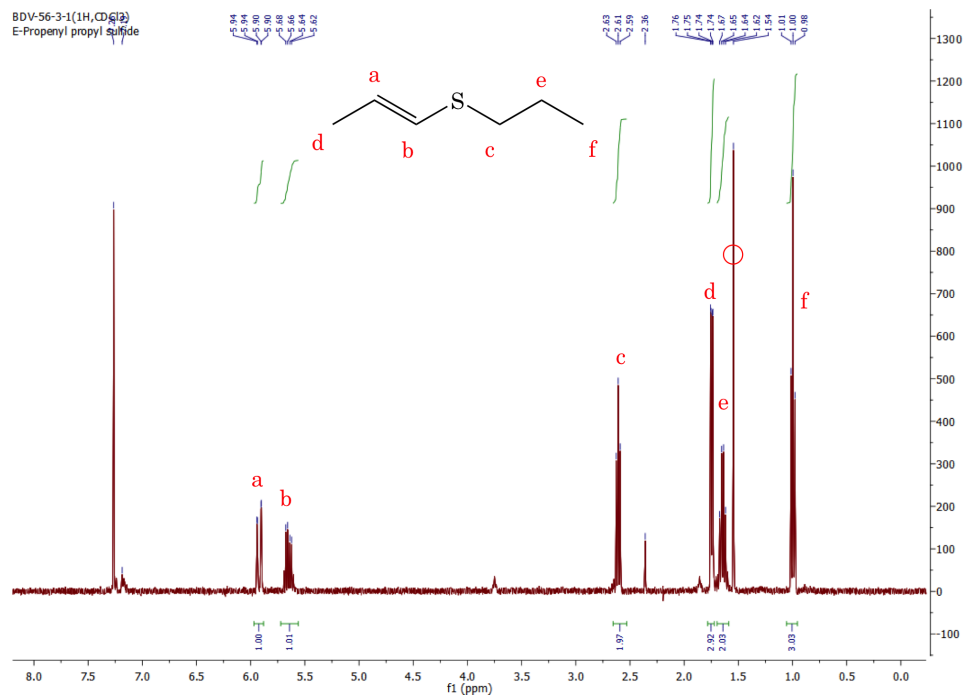


Figure 7.63: ¹H NMR spectrum (400 MHz, CDCl_3) of (E)-1-propenyl propyl sulfide ((E)-49a). Water was present in the chloroform (circled in red).

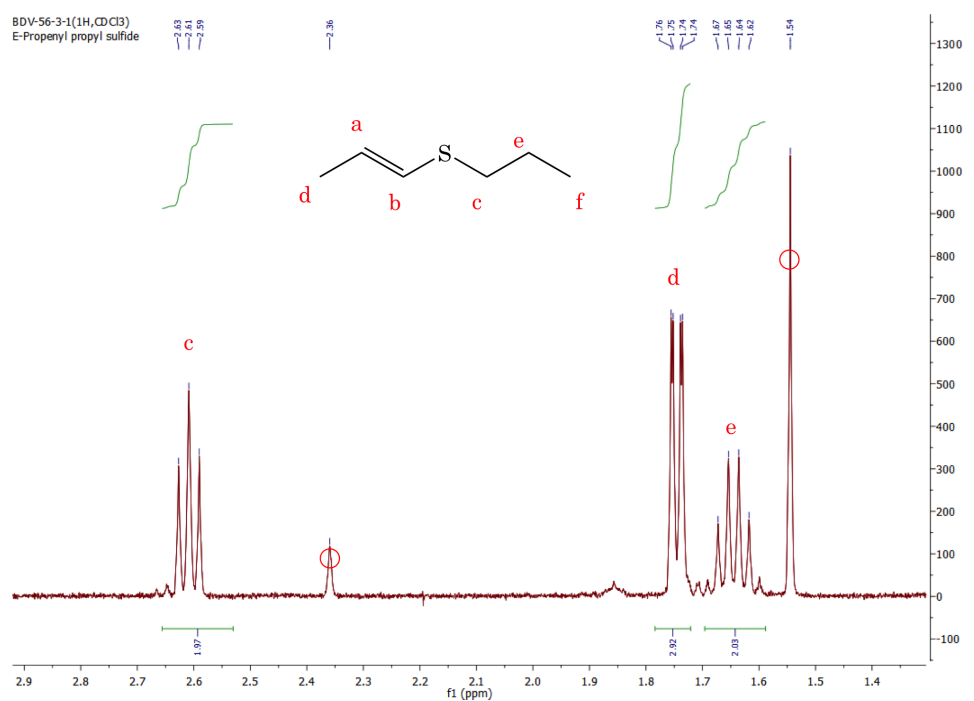


Figure 7.64: ^1H NMR spectrum (400 MHz, CDCl₃) of (E) -1-propenyl propyl sulfide ((E) -49a), detailed view. Water was present in the chloroform (peak circled in red).

BDIV-94-B($^1\text{H}_2\text{CDCl}_3$)
propenyl disulfide oxidation by mCPBA in $^1\text{H-NMR}$ $\delta = 73$

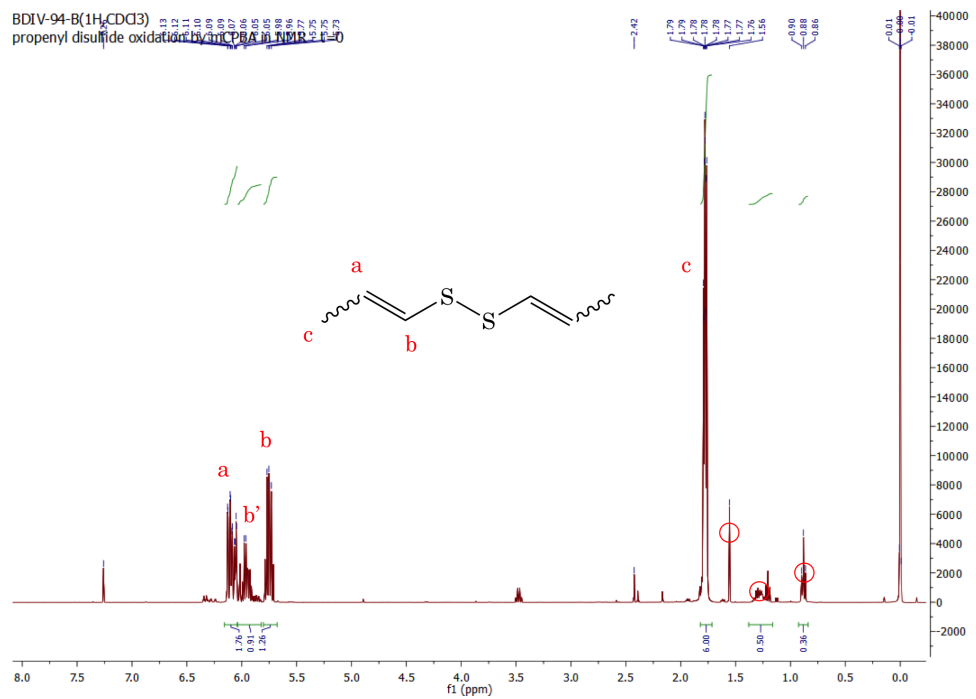


Figure 7.65: ^1H NMR spectrum (400 MHz, CDCl_3) of propenyl disulfide (mixture of stereoisomers, **23**).

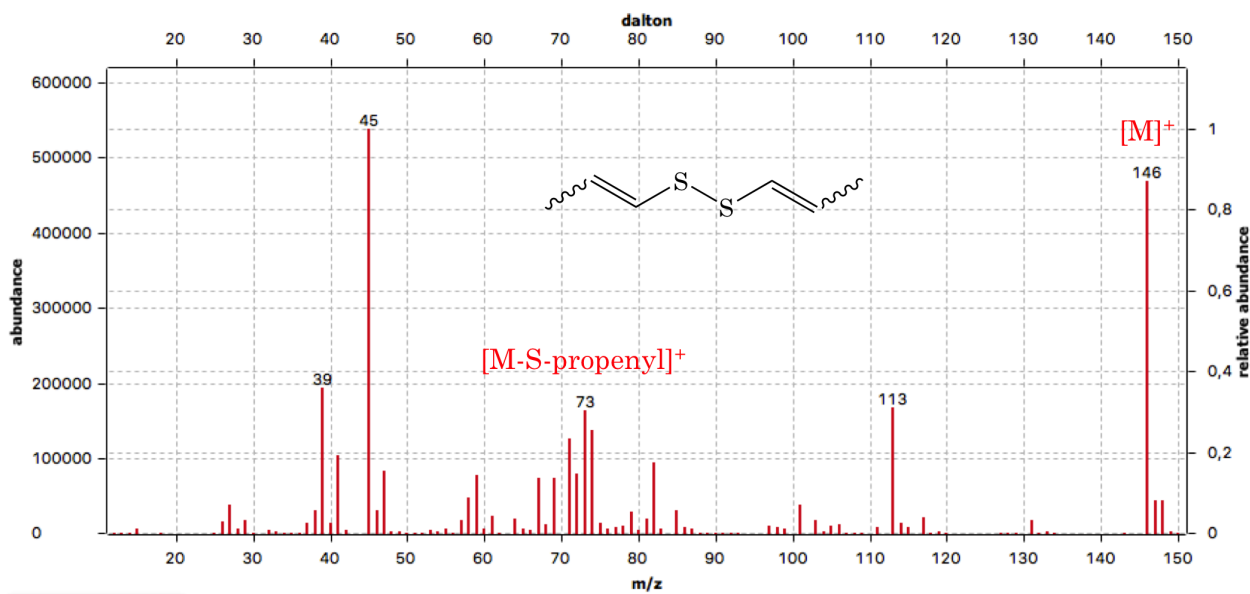


Figure 7.66: Mass spectrum of bis-1-propenyl disulfide (**23**) recorded by GC-MS.

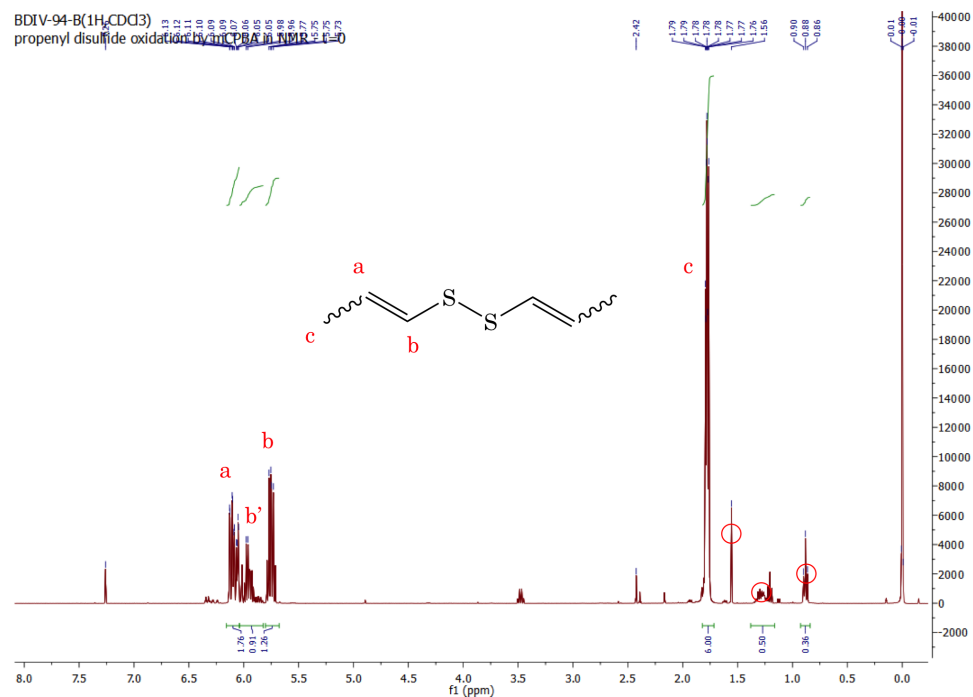


Figure 7.67: ^1H NMR spectrum (400 MHz, CDCl_3) of the low temperature oxidation of propenyl disulfide. Signals corresponding the thiosulfinate are visible, as well as mCPBA, pentane and rearrangement products; zwiebelanes (**9**) and sultenes (**10**). The gray trace is the starting material (**23**).

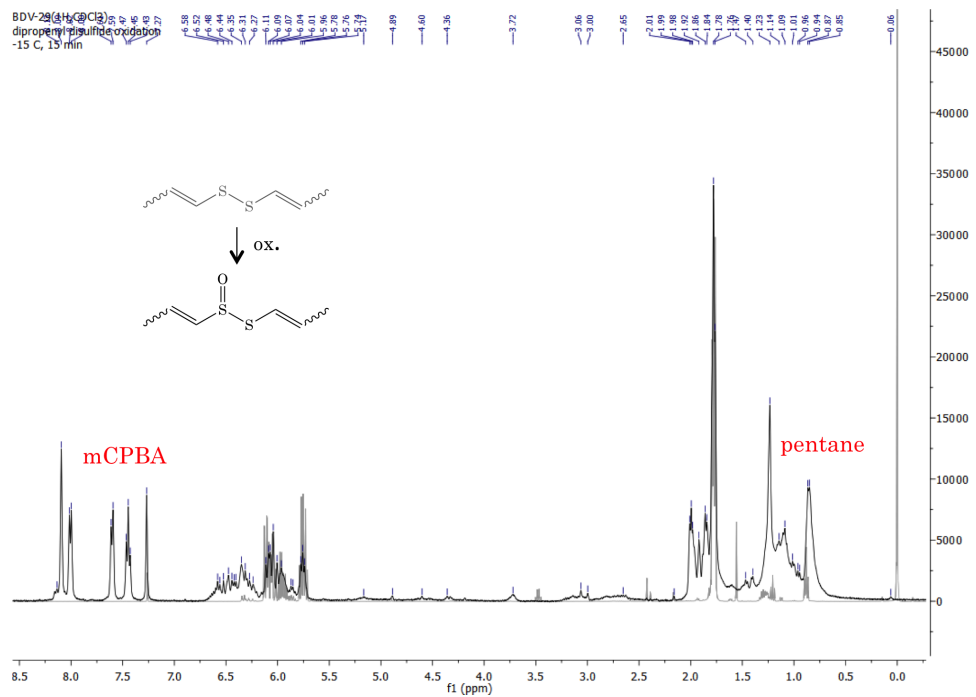


Figure 7.68: Olefinic region of the ^1H NMR spectrum (400 MHz, CDCl_3), low temperature oxidation of propenyl disulfide. Signals corresponding the thiosulfinate are visible (6.7–6.2 ppm) and rearrangement products, zwiebelanes (**9**) and sultenes (**10**) between 5 and 4 ppm. The gray trace is the starting material (**23**).

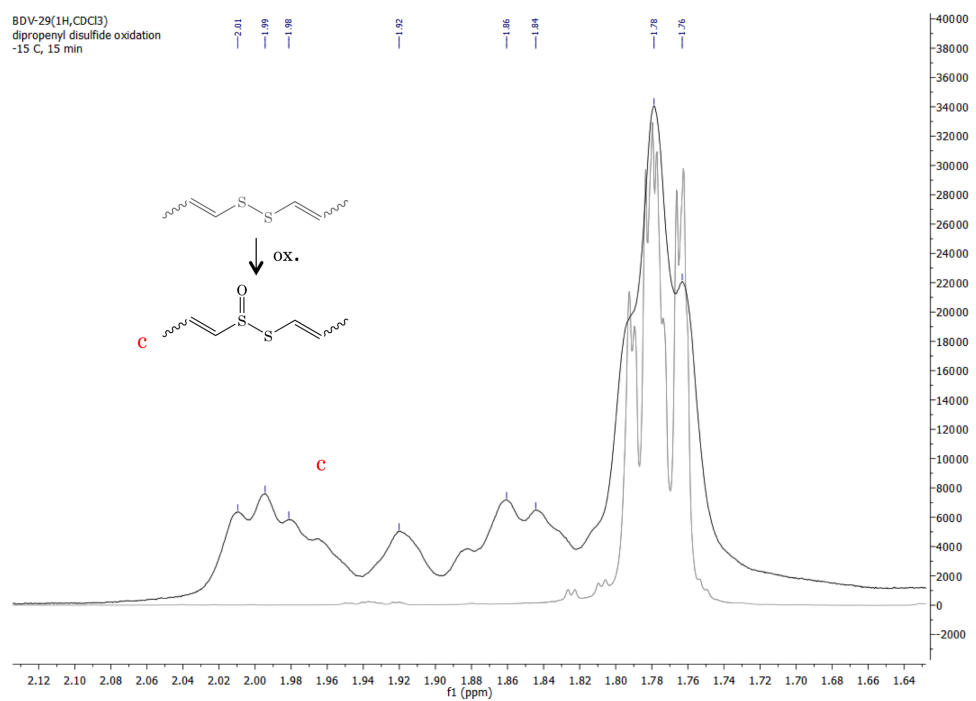


Figure 7.69: Methyl region of the ¹H NMR spectrum (400 MHz, CDCl₃), low temperature oxidation of propenyl disulfide. Signals corresponding the thiosulfinate are visible (2.05–1.80 ppm). The gray trace is the starting material (**23**). Precipitated *m*-chlorobenzoic acid makes the shimming challenging and is responsible for the low resolution.

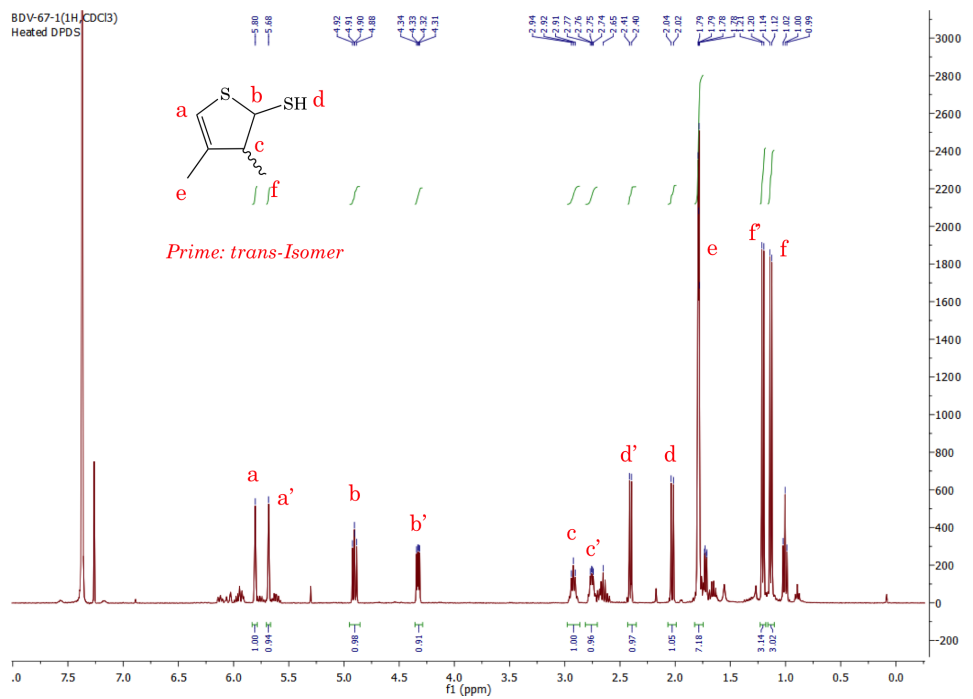


Figure 7.70: ¹H NMR spectrum (400 MHz, CDCl₃) of 3,4-dimethyl-2,3-dihydrothiophene-2-thiol (**58**), mixture of stereoisomers.

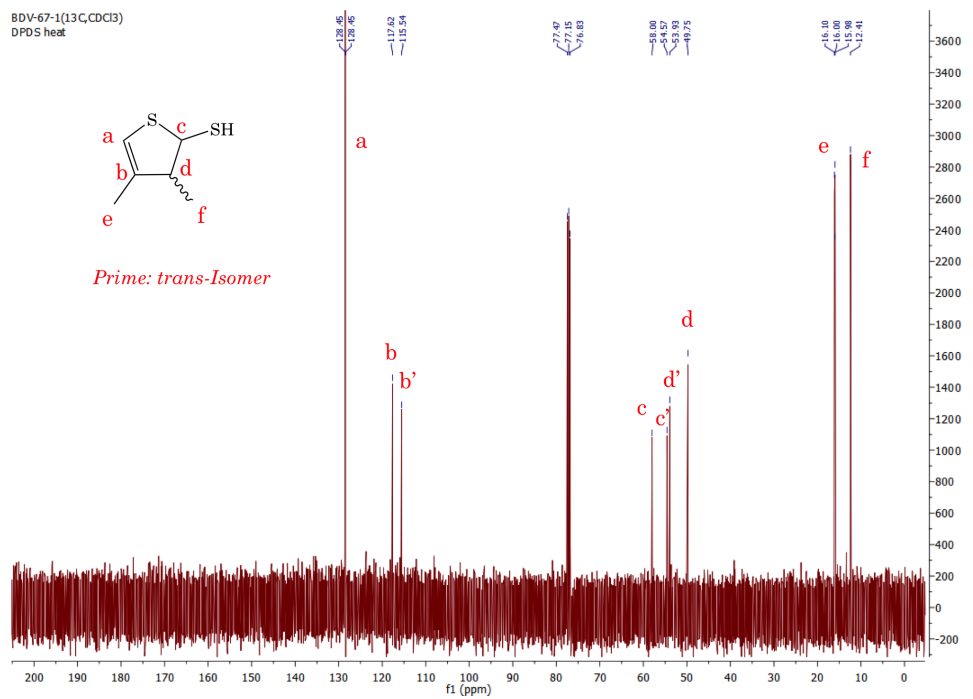


Figure 7.71: ¹³C NMR spectrum (100 MHz, CDCl₃) of 3,4-dimethyl-2,3-dihydrothiophene-2-thiol (**58**), mixture of stereoisomers.

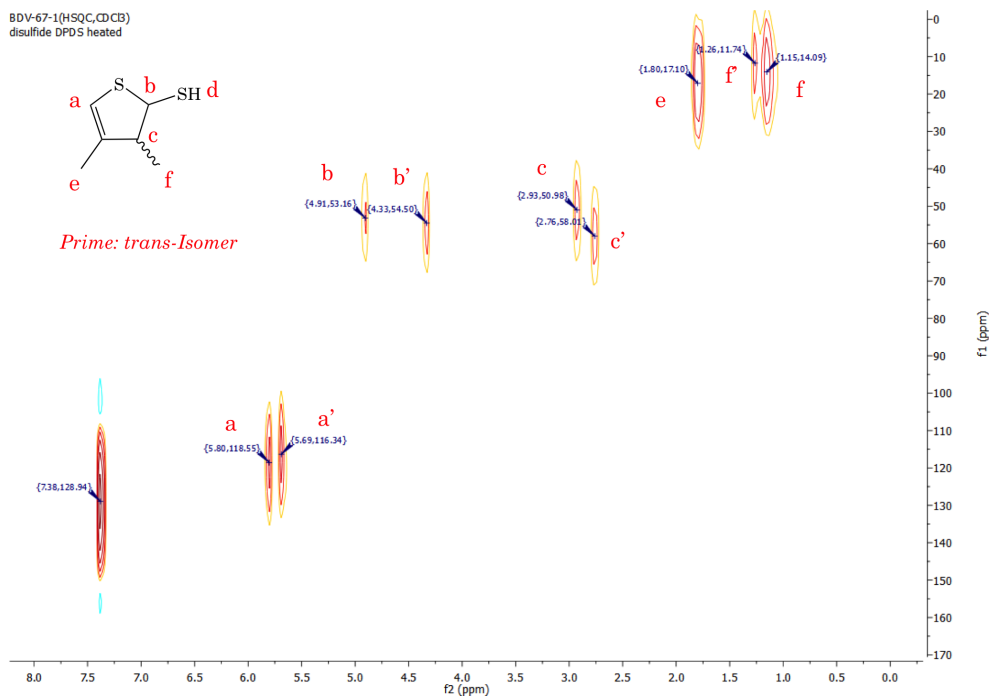


Figure 7.72: HSQC NMR spectrum of 3,4-dimethyl-2,3-dihydrothiophene-2-thiol (**58**), mixture of stereoisomers.

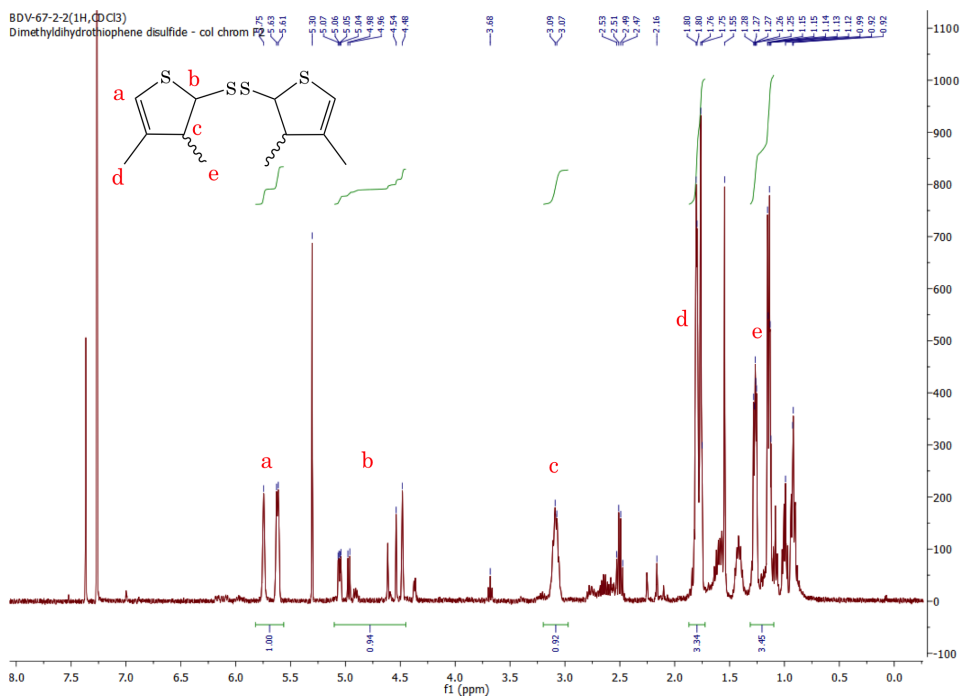


Figure 7.73: ^1H NMR spectrum (400 MHz, CDCl_3) of 1,2-bis(3,4-dimethyl-2,3-dihydrothiophene-2-yl)disulfane (**59**), mixture of stereoisomers.

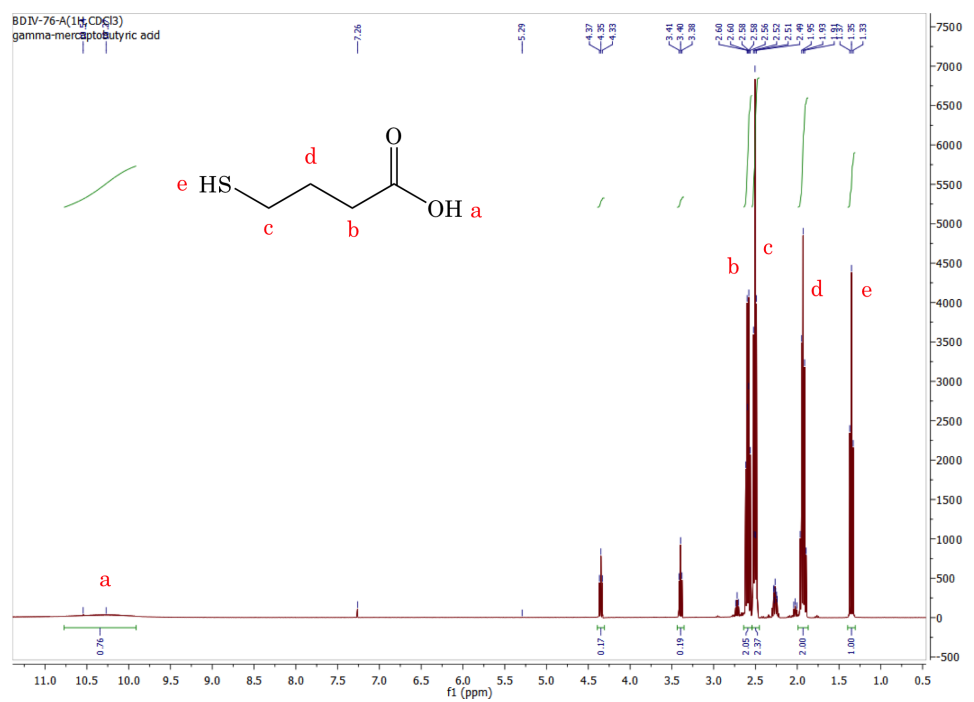


Figure 7.74: ^1H NMR spectrum (400 MHz, CDCl_3) of γ -mercaptopbutyric acid (68).

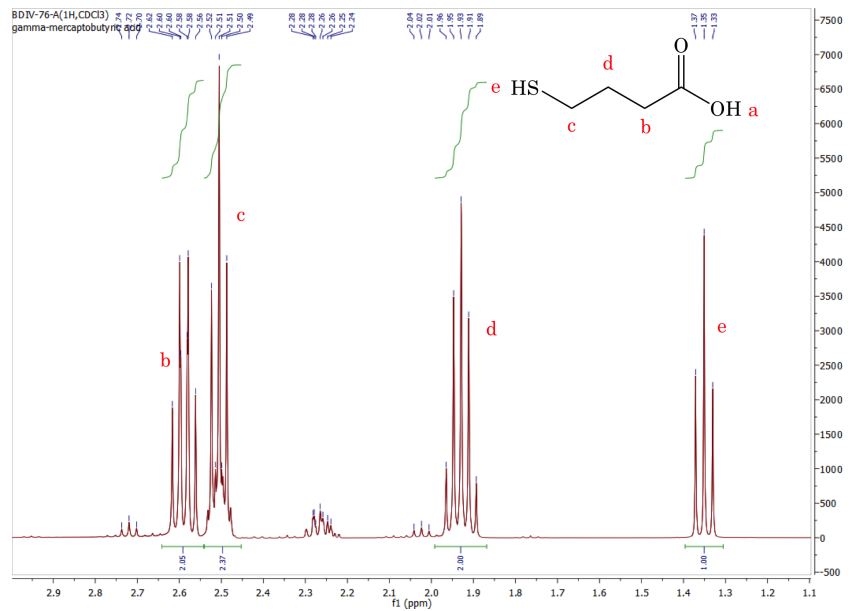


Figure 7.75: ^1H NMR spectrum (400 MHz, CDCl_3) of γ -mercaptopbutyric acid (**68**), detailed view.

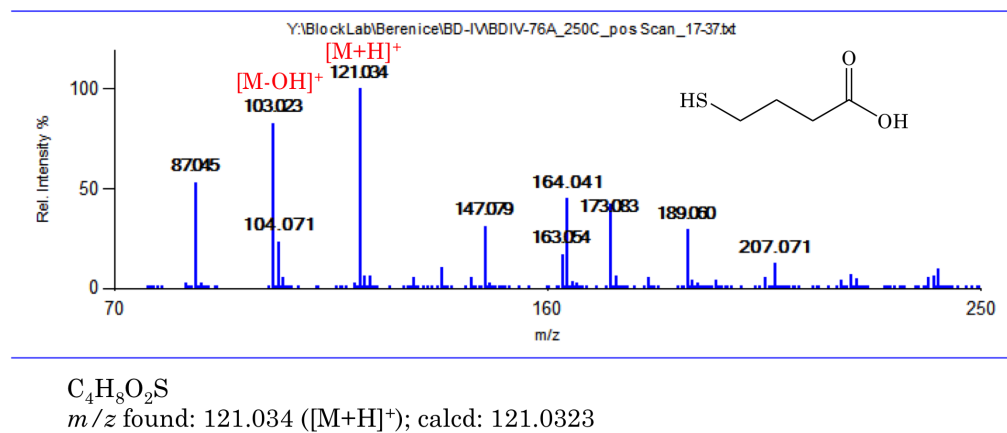


Figure 7.76: Mass spectrum of γ -mercaptopbutyric acid (**68**) recorded by DART-MS. $\text{C}_4\text{H}_8\text{O}_2\text{S}$, m/z found: 121.034 ($[\text{M}+\text{H}]^+$), calcd: 121.0323.

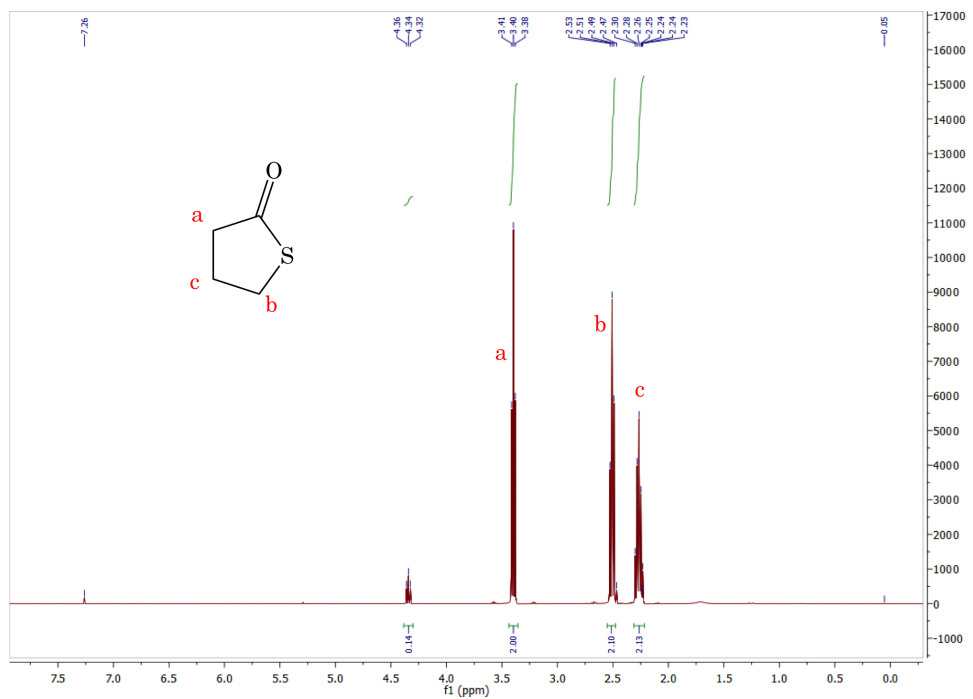


Figure 7.77: ^1H NMR spectrum (400 MHz, CDCl_3) of γ -thiobutyrolactone (67).

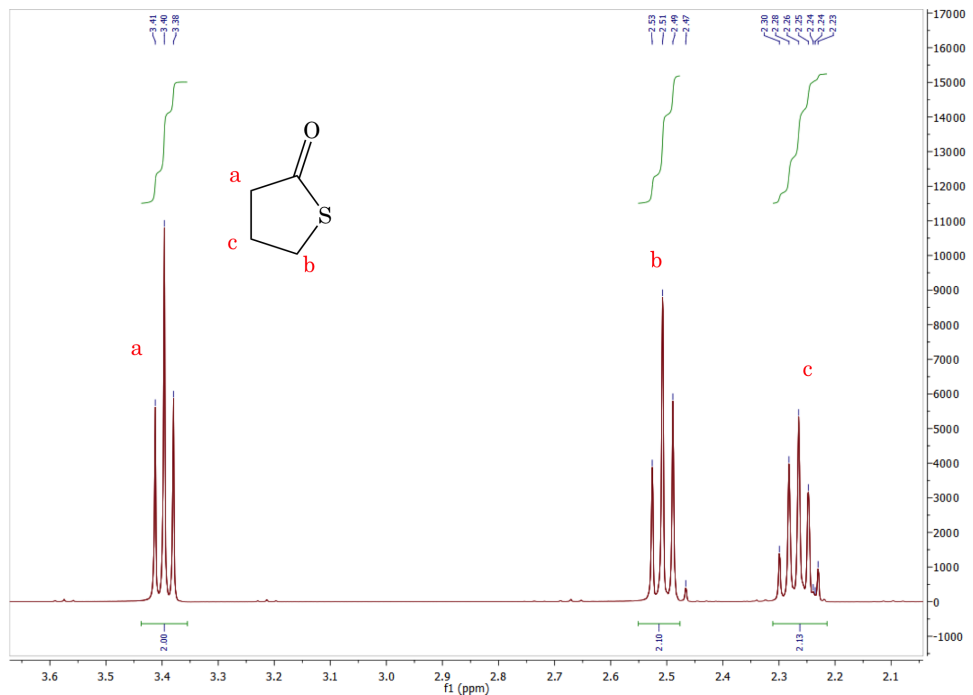


Figure 7.78: ^1H NMR spectrum (400 MHz, CDCl_3) of γ -thiobutyrolactone (67), detailed view.

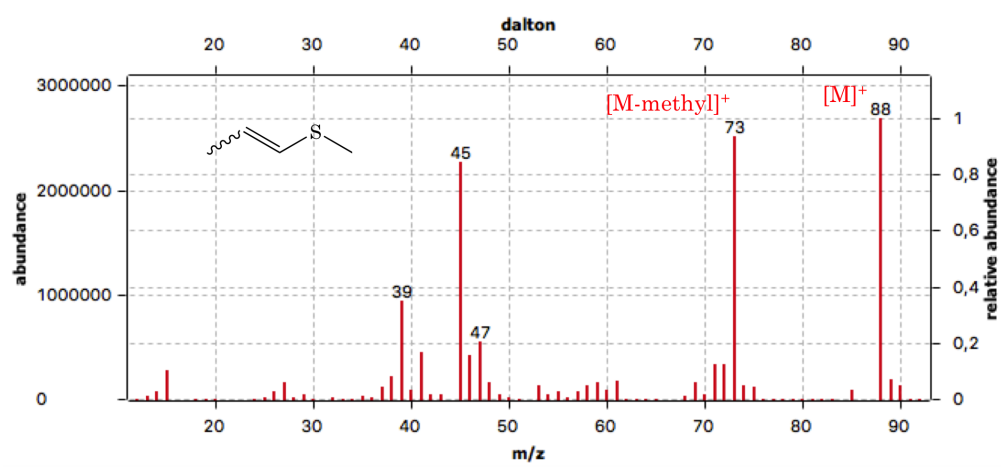


Figure 7.79: Mass spectrum of γ -thiobutyrolactone (67) recorded by DART-MS. C_4H_7OS , m/z found: 103.022 ($[M+H]^+$); calcd: 103.0218.

7.3 Alliin, the precursor: analytical and preparative study

7.3.1 Deoxyalliin

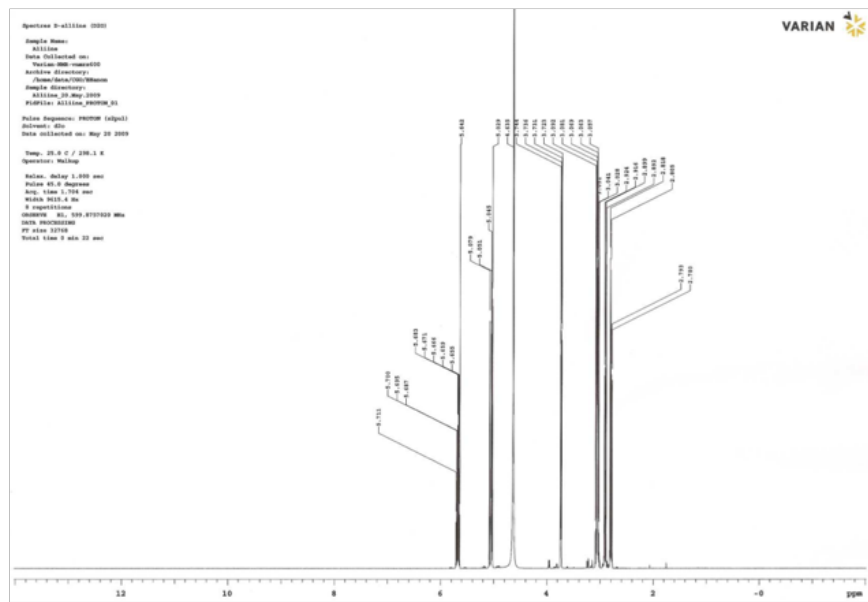


Figure 7.80: ^1H NMR spectrum (600 MHz, D_2O) of deoxyalliin (**71**).

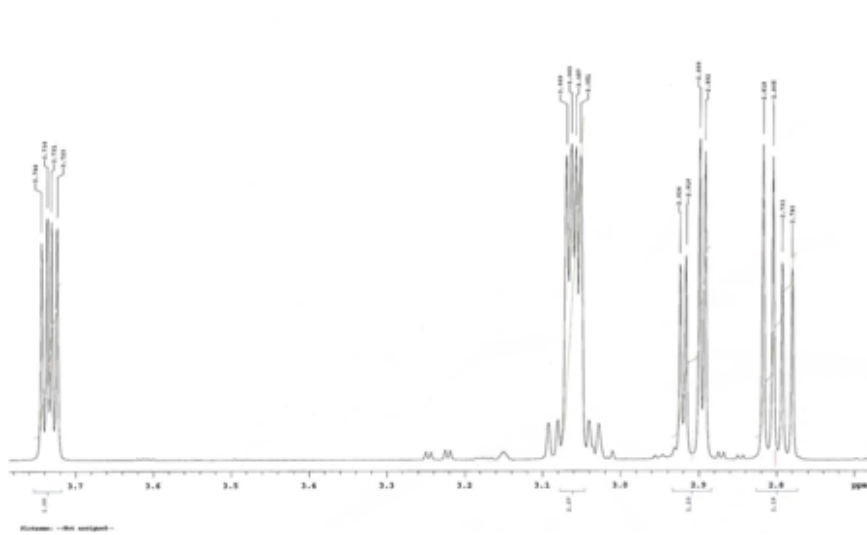


Figure 7.81: ^1H NMR spectrum (600 MHz, D_2O) of deoxyalliin (**71**), detailed view.

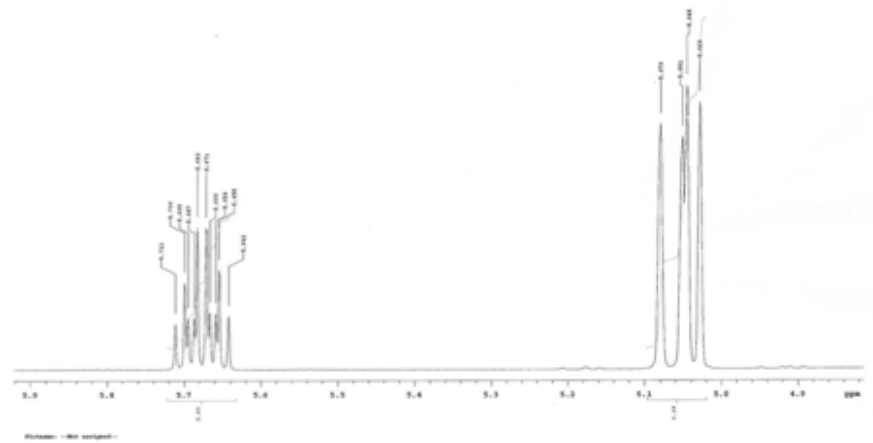


Figure 7.82: ^1H NMR spectrum (600 MHz, D_2O) of deoxyalliin (**71**), detailed view.

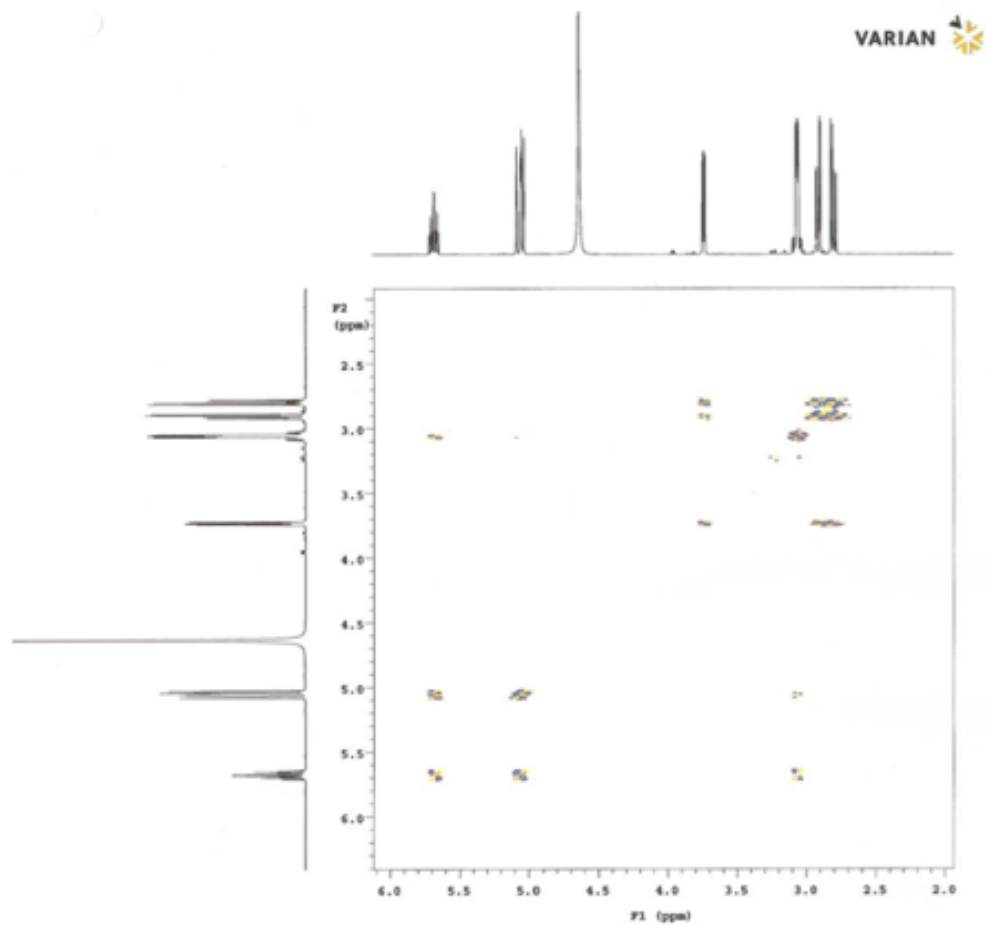


Figure 7.83: COSY NMR spectrum (600 MHz, D_2O) of deoxyalliin (**71**).

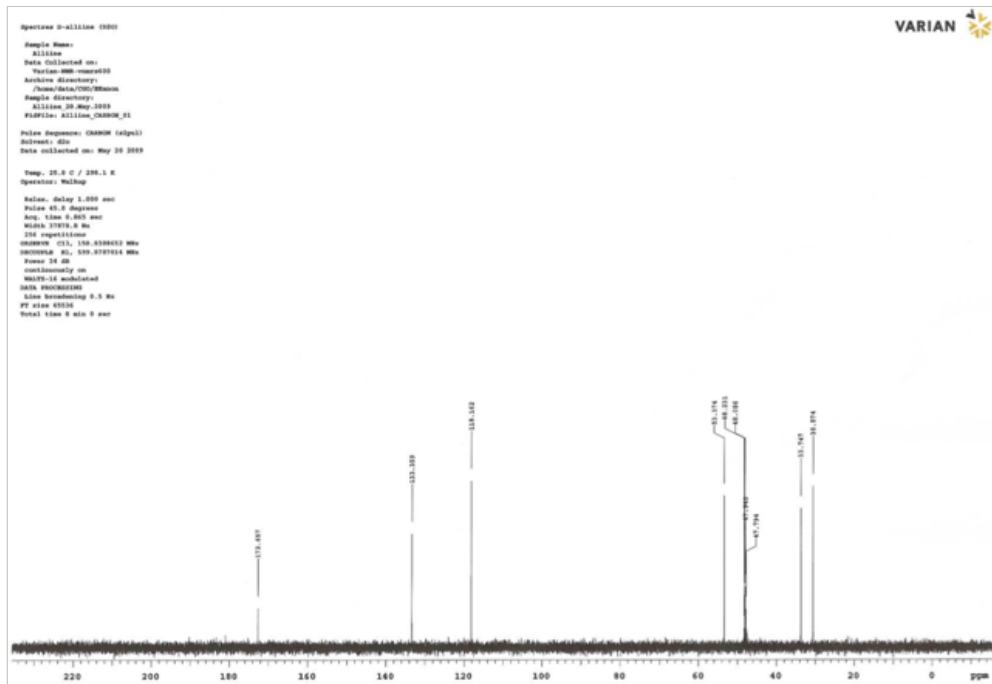


Figure 7.84: ^{13}C NMR spectrum (125 MHz, D_2O) of deoxyalliin (**71**).

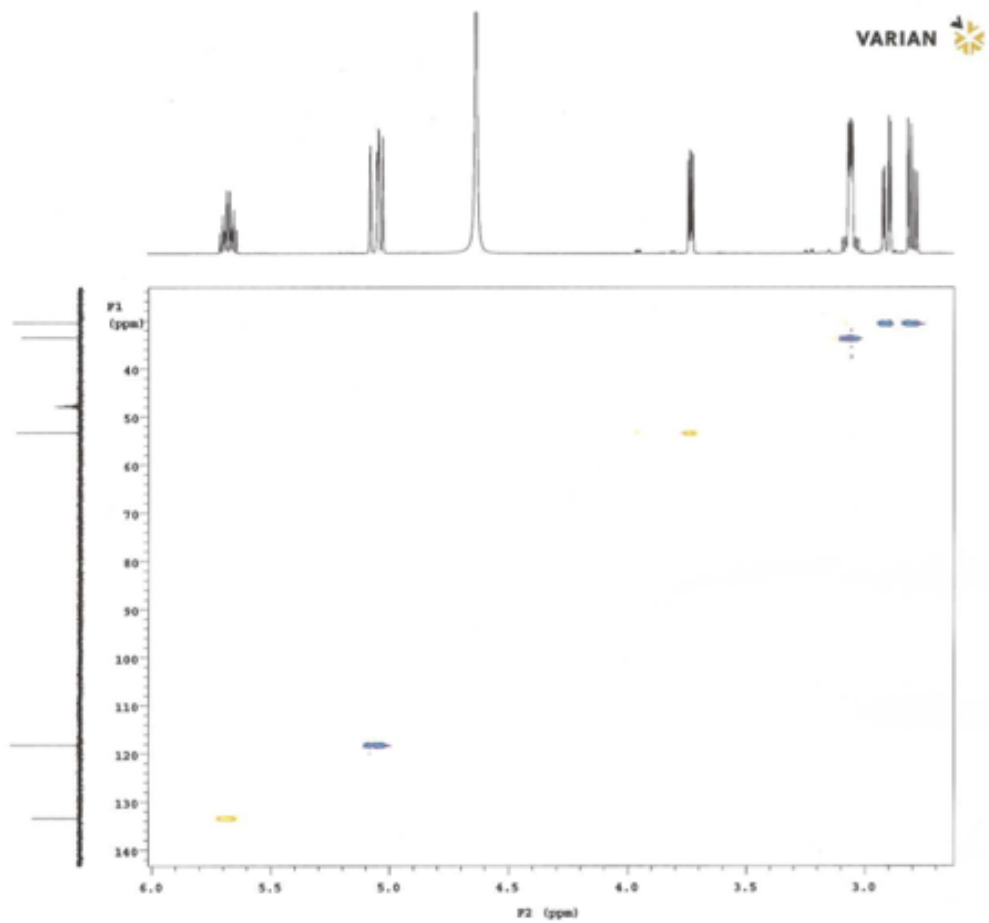


Figure 7.85: HSQC NMR spectrum (D_2O) of deoxyalliin (**71**).

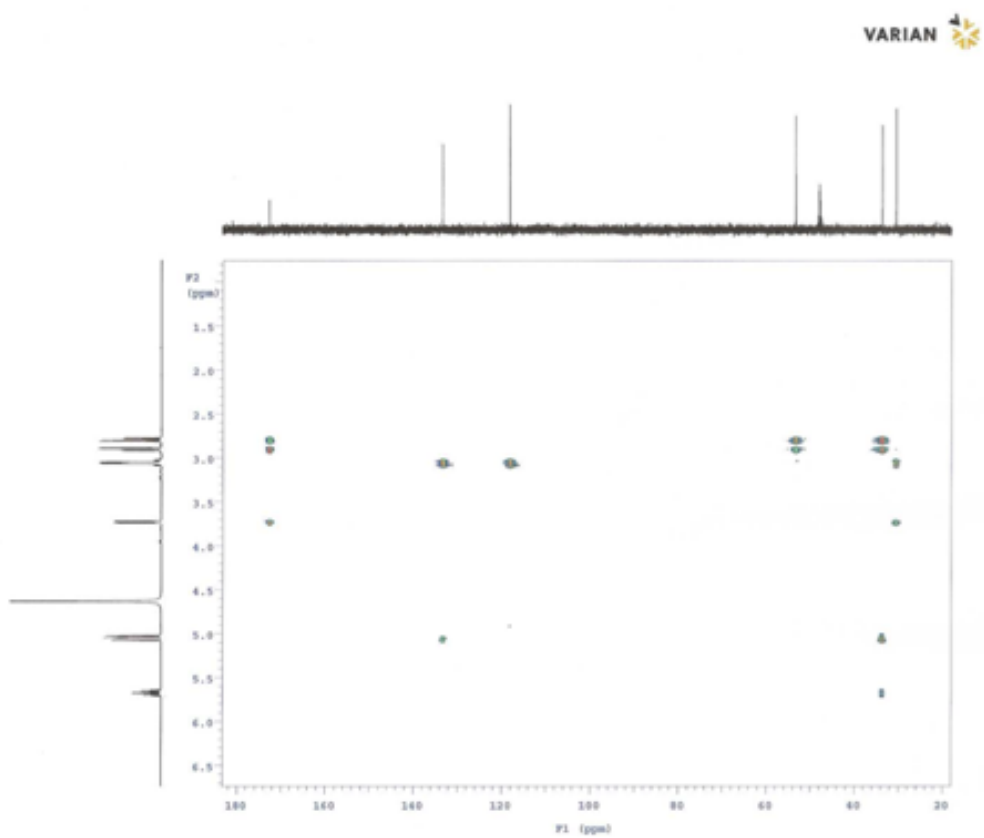


Figure 7.86: HMBC NMR spectrum (D_2O) of deoxyalliin (71).

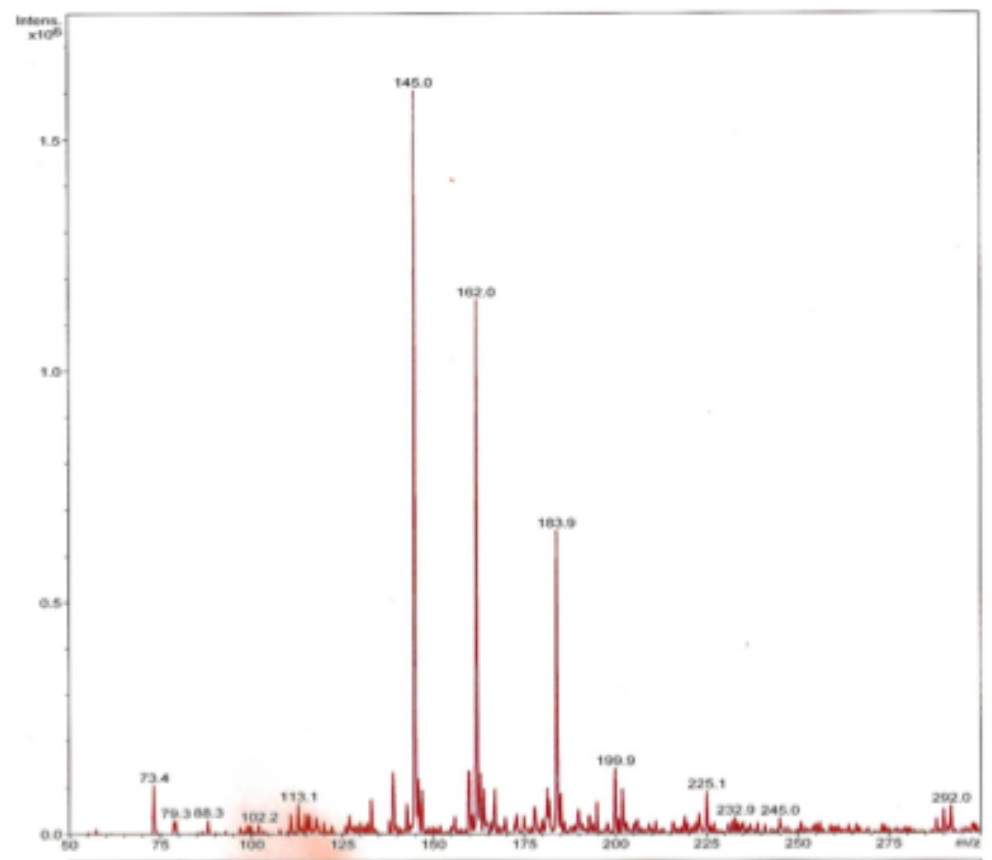


Figure 7.87: Mass spectrum of deoxyalliin (**71**), positive mode (infusion, electrospray: Bruker Esquire HCT with ion trap).

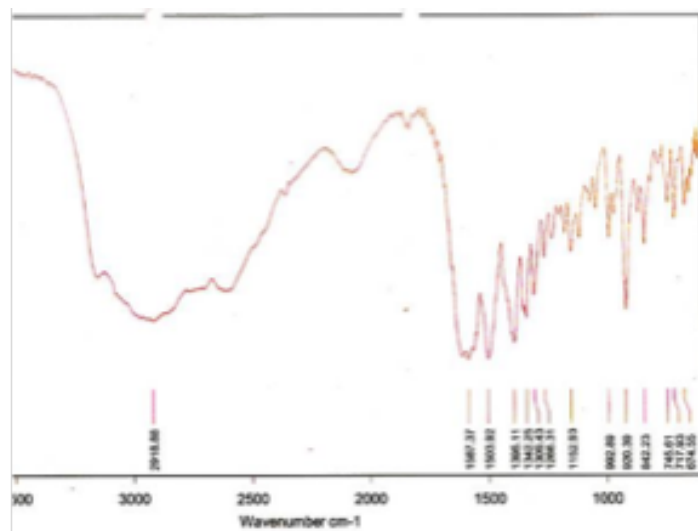


Figure 7.88: Infrared spectrum of deoxyalliin (**71**) (Bruker IFS 48).

7.3.2 Alliin

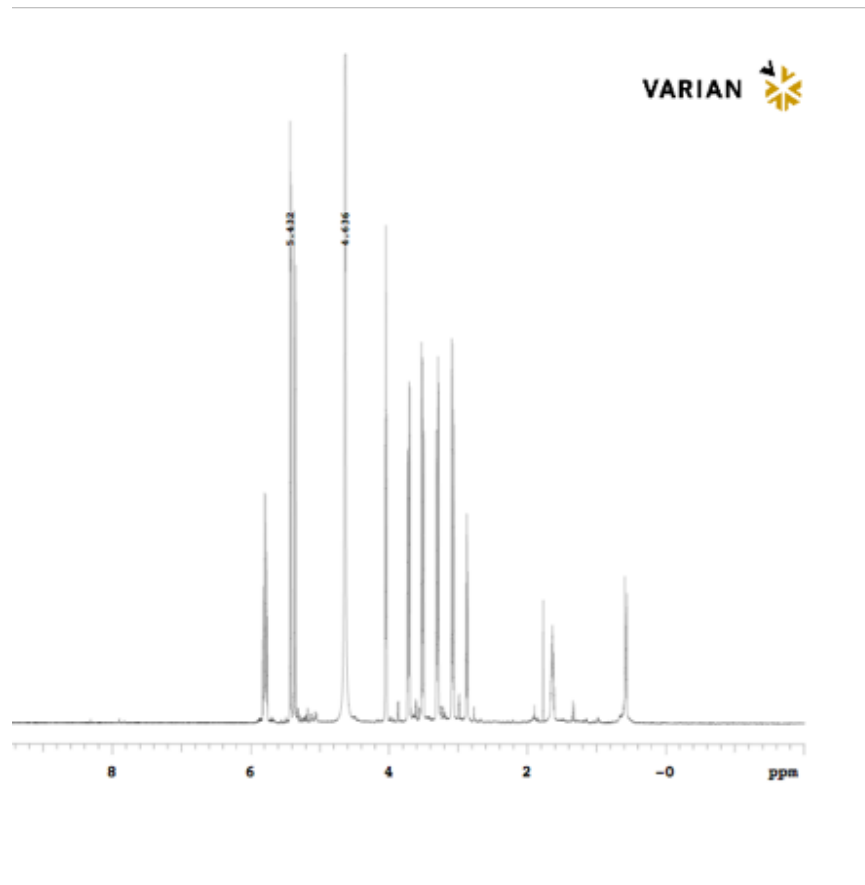


Figure 7.89: ${}^1\text{H}$ NMR spectrum (600 MHz, D_2O) of (+)-alliin (1a).

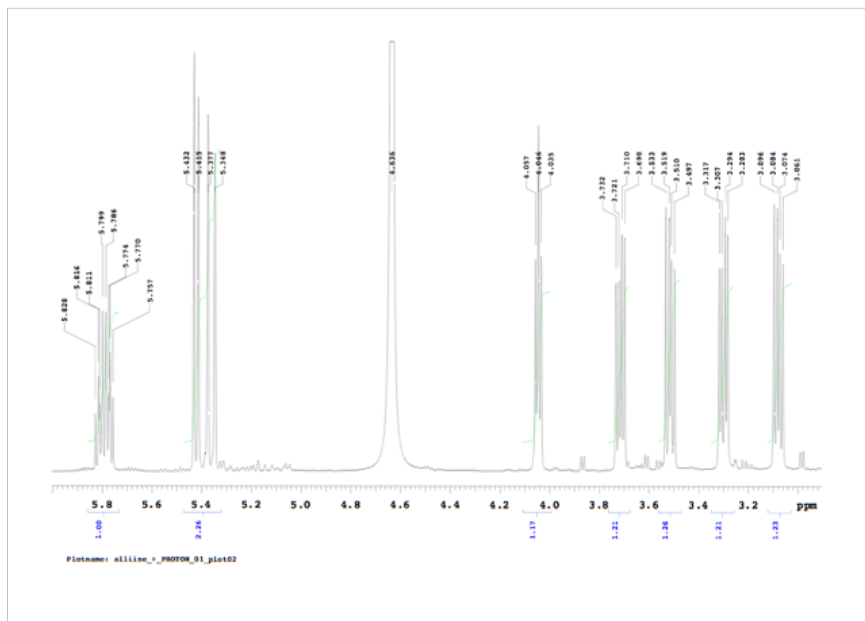


Figure 7.90: ^1H NMR spectrum (600 MHz, D_2O) of (+)-alliin (**1a**), detailed view.

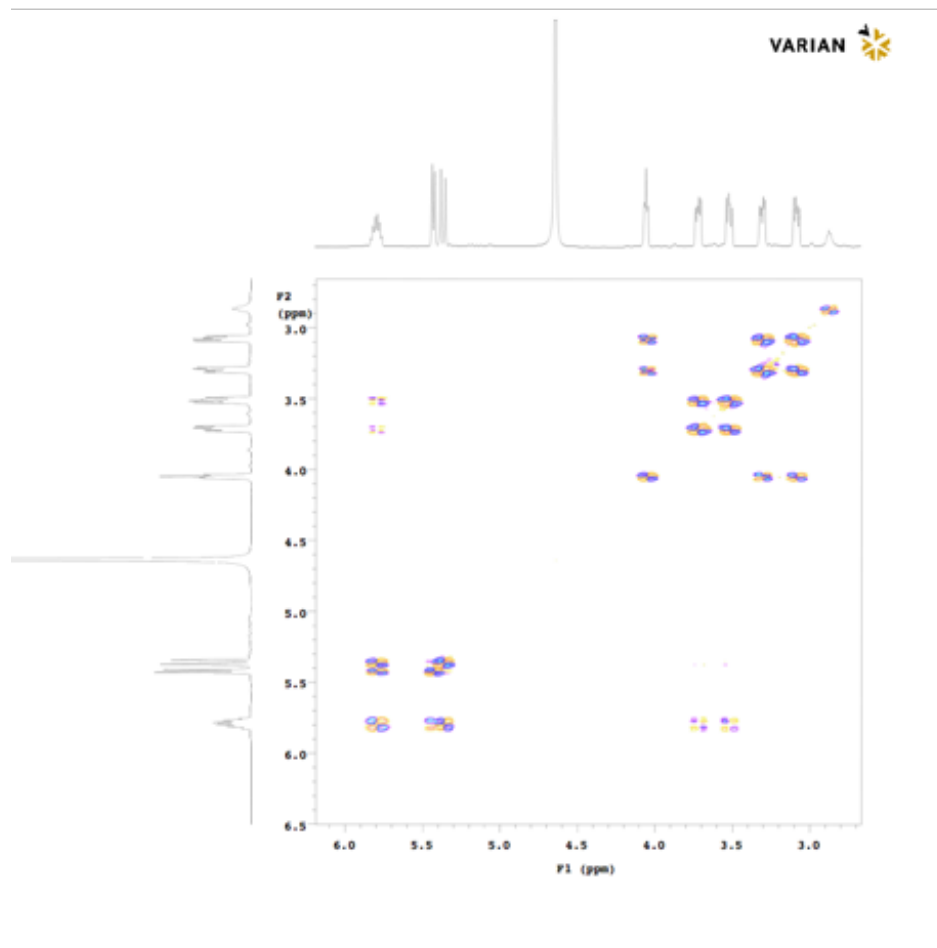


Figure 7.91: COSY NMR spectrum (600 MHz, D_2O) of (+)-alliin (**1a**).

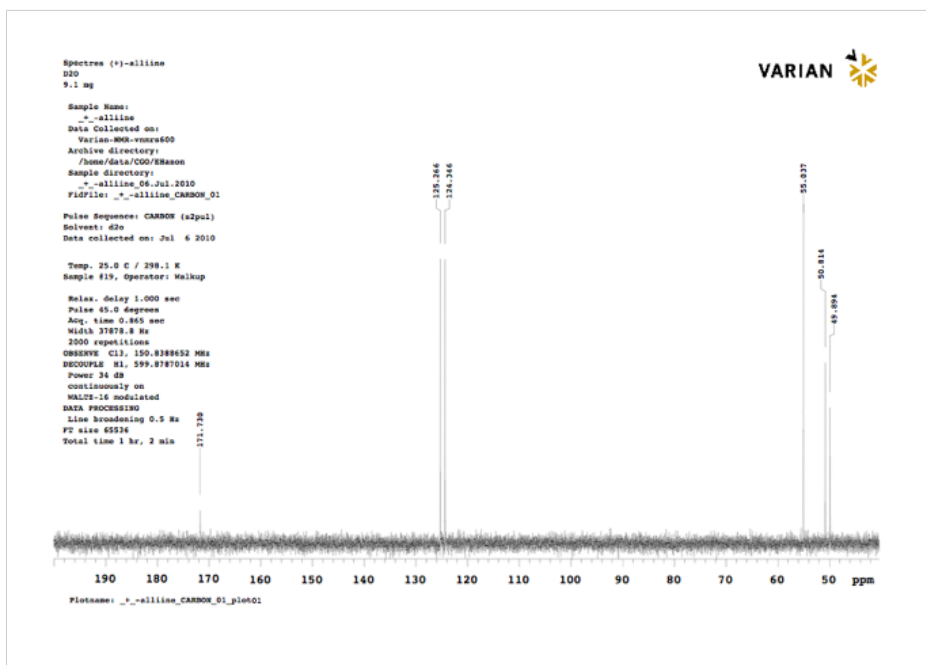


Figure 7.92: ¹³C NMR spectrum (125 MHz, D₂O) of (+)-alliin (**1a**).

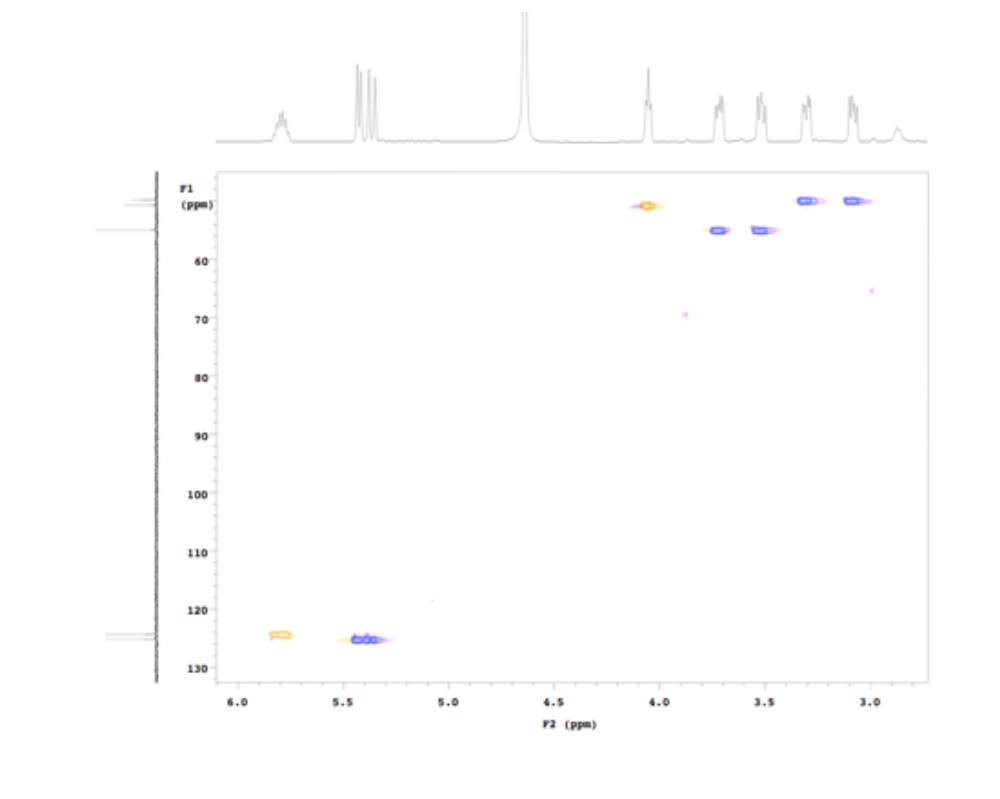


Figure 7.93: HSQC NMR spectrum (D_2O) of (+)-alliin (**1a**).

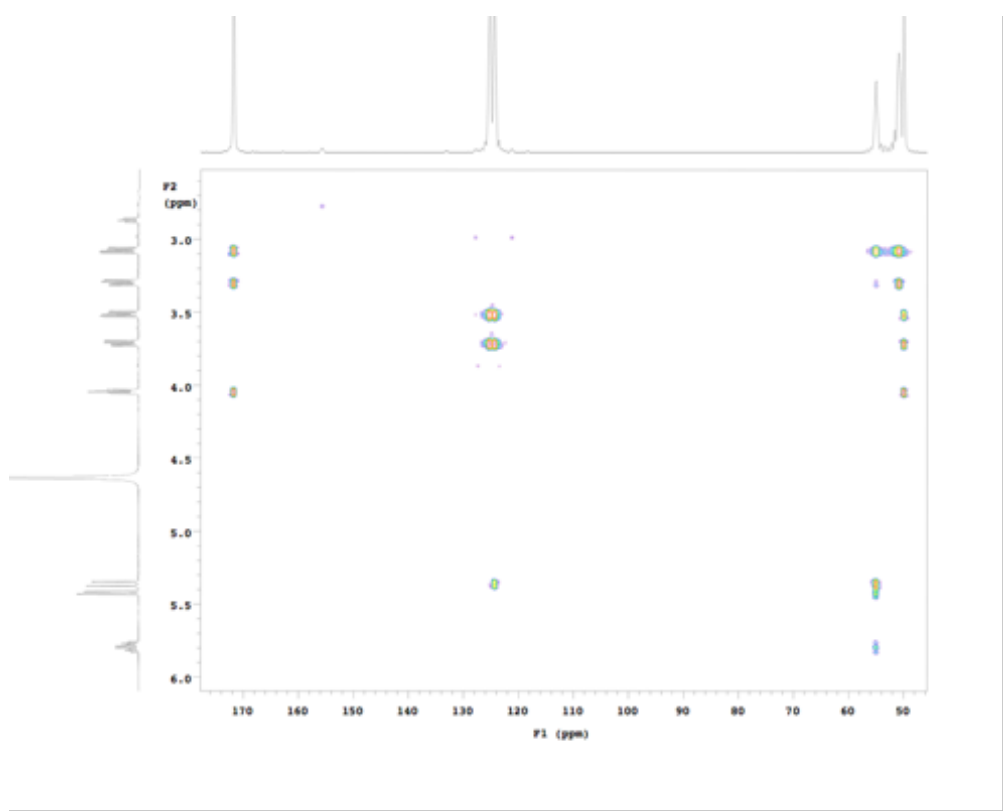


Figure 7.94: HMBC NMR spectrum (D_2O) of (+)-alliin (**1a**).

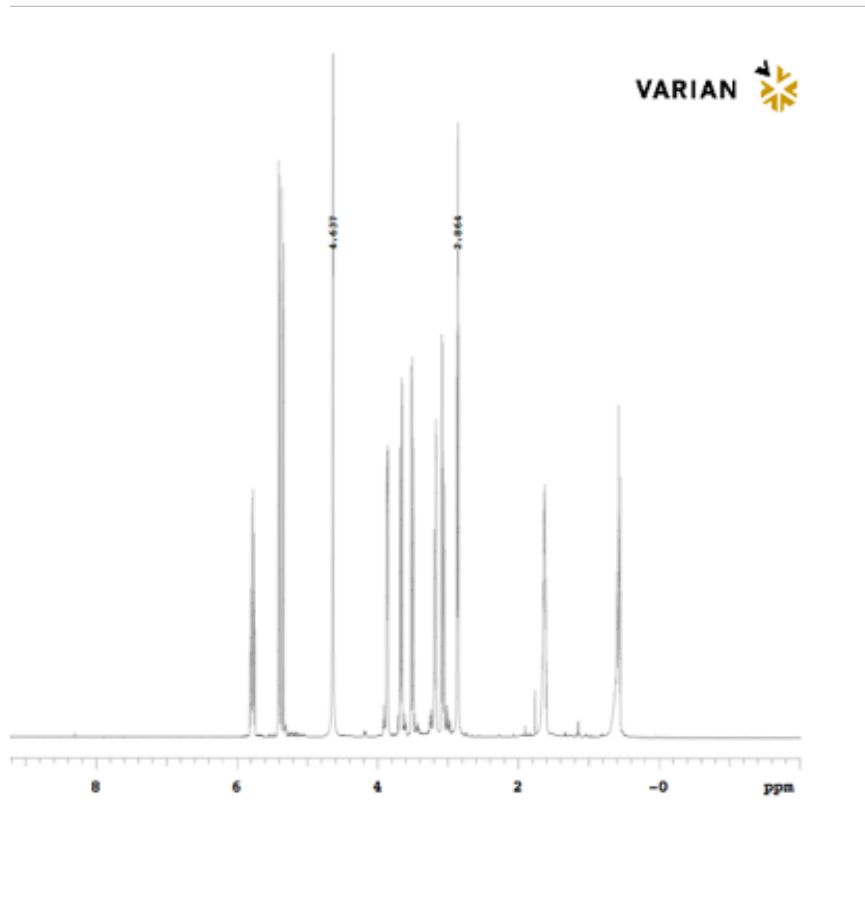


Figure 7.95: ^1H NMR spectrum (600 MHz, D_2O) of (-)-alliin (**1a**).

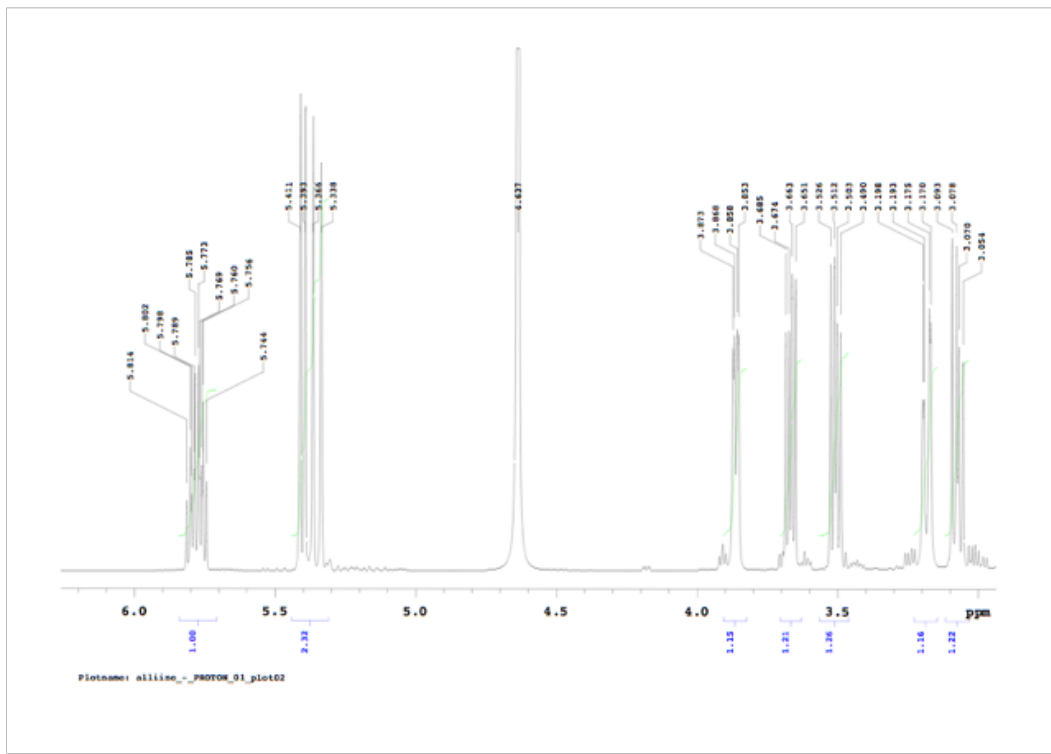


Figure 7.96: ^1H NMR spectrum (600 MHz, D_2O) of (-)-alliin (**1a**), detailed view.

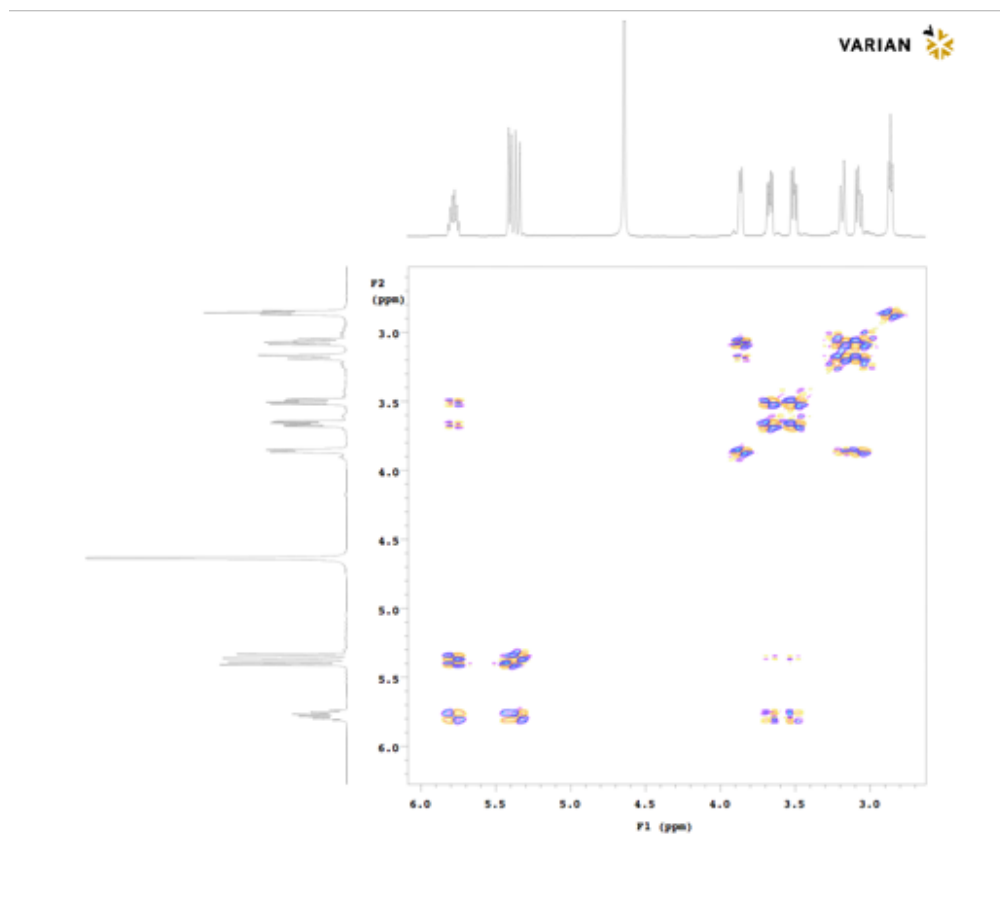


Figure 7.97: COSY NMR spectrum (600 MHz, D_2O) of (-)-alliin (**1a**).

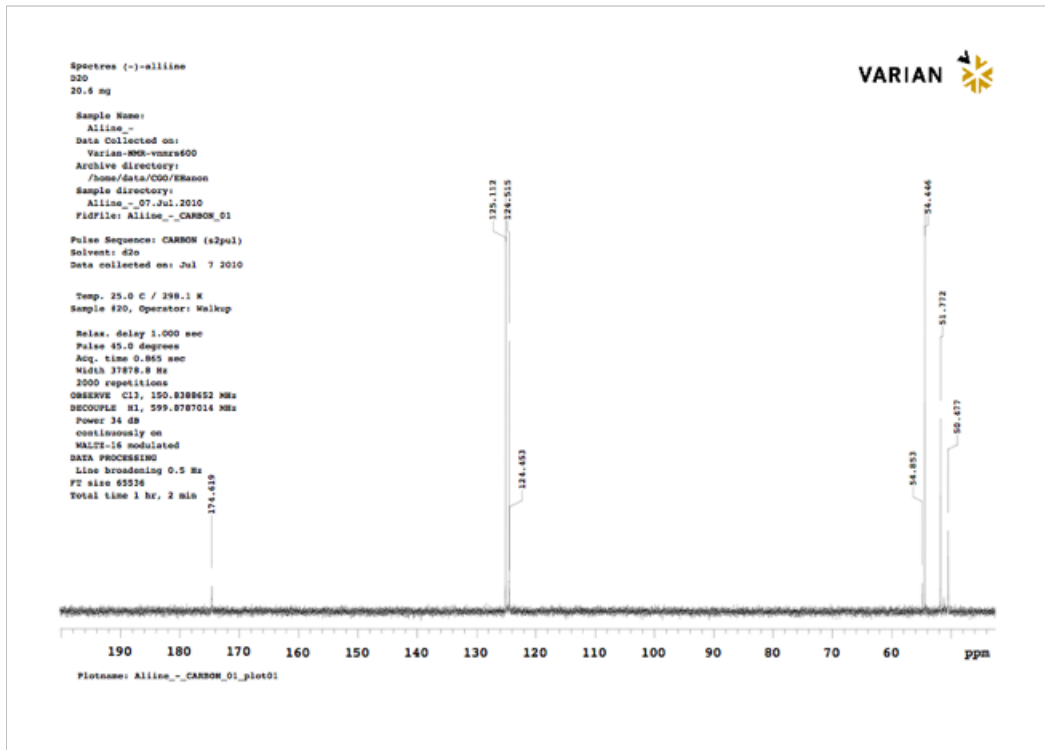


Figure 7.98: ^{13}C NMR spectrum (125 MHz, D_2O) of (-)-alliin (**1a**).

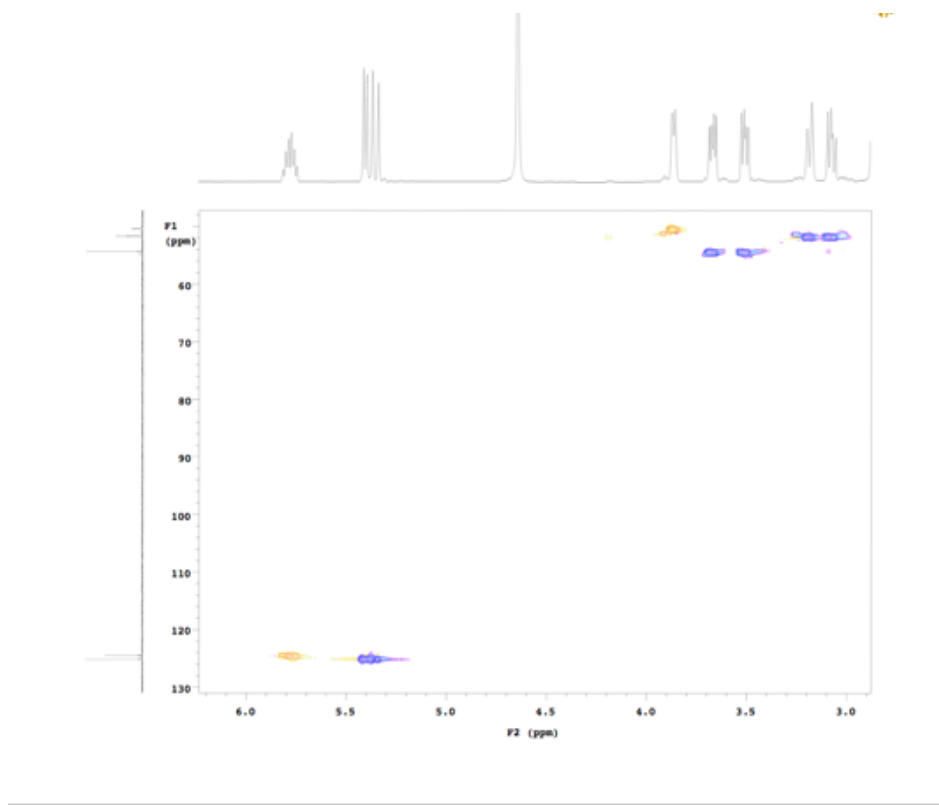


Figure 7.99: HSQC NMR spectrum (D_2O) of (-)-alliin (**1a**).

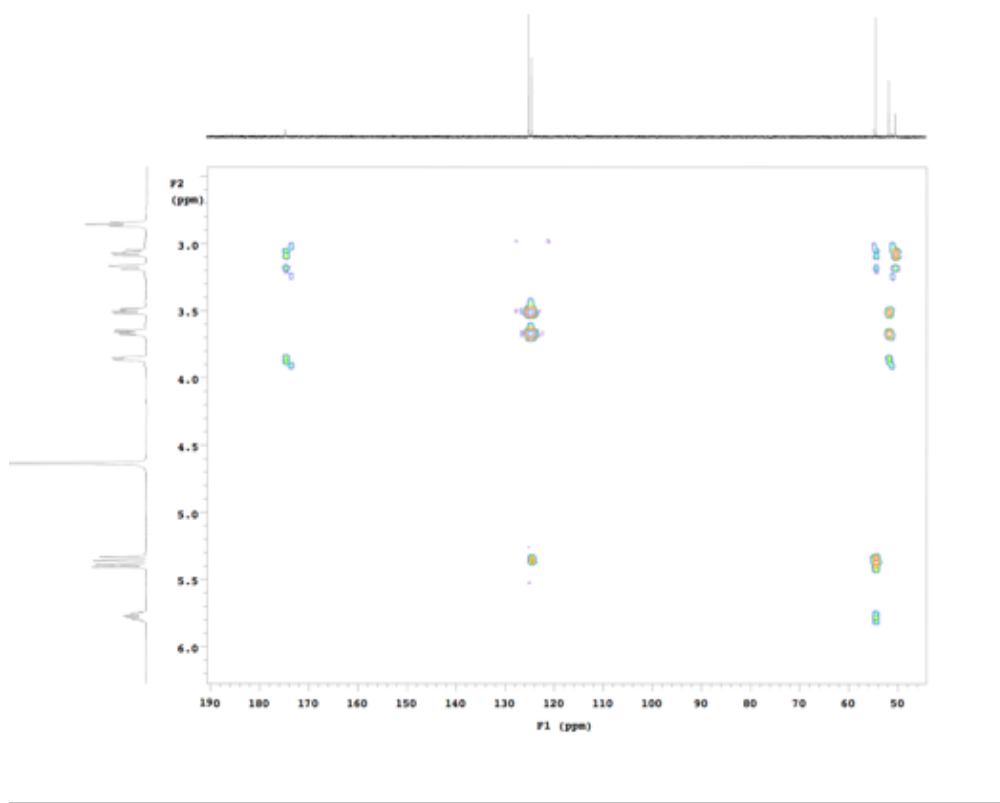


Figure 7.100: HMBC NMR spectrum (D_2O) of (-)-alliin (**1a**).

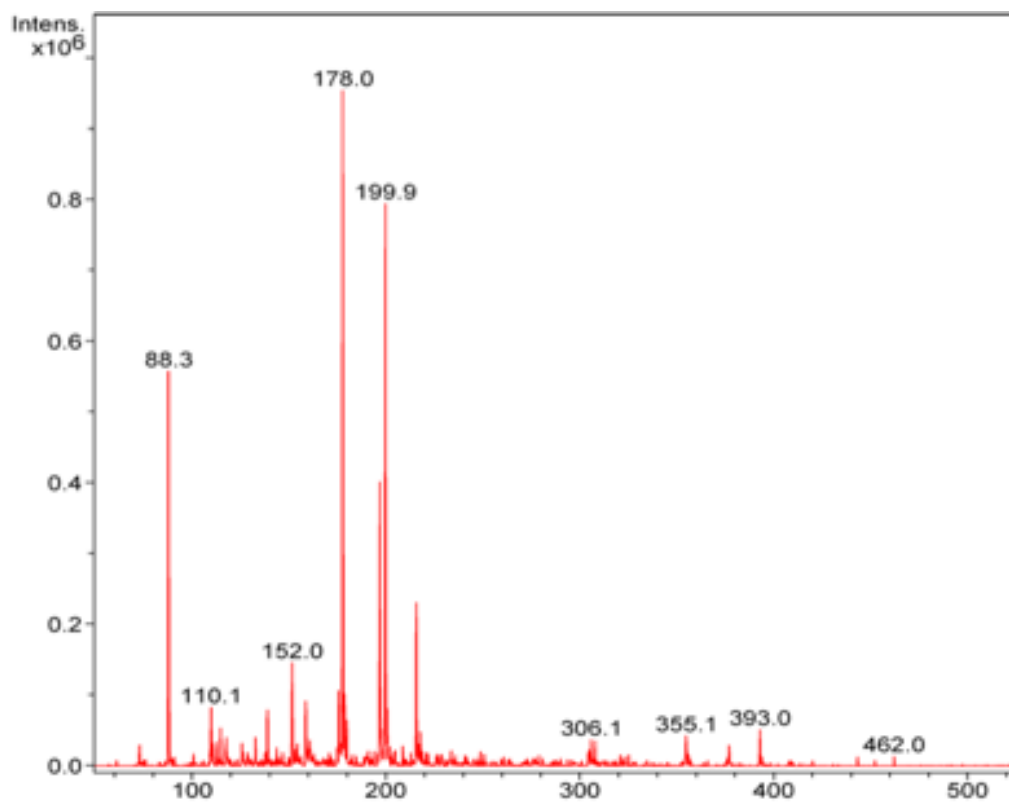


Figure 7.101: Mass spectrum of alliin (**1a**), positive mode (infusion, electrospray: Bruker Esquire HCT with ion trap).

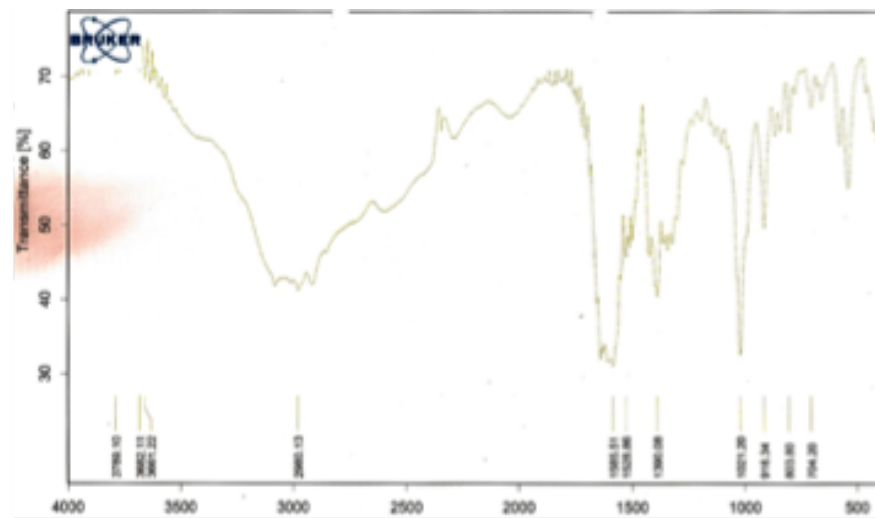


Figure 7.102: Infrared spectrum of alliin (**1a**) (Bruker IFS 48).

7.4 The chemistry of smell

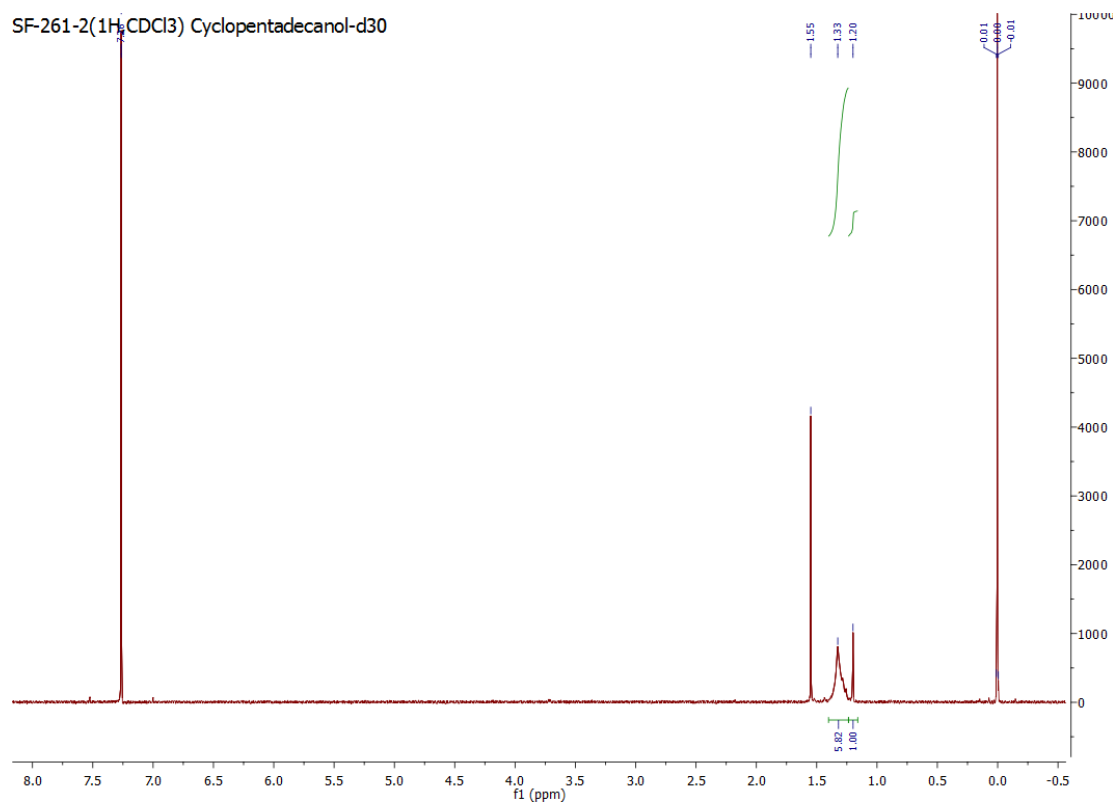


Figure 7.103: ¹H NMR spectrum (400 MHz, CDCl₃) of cyclopentadecanol-d₂₉ (**80a**).

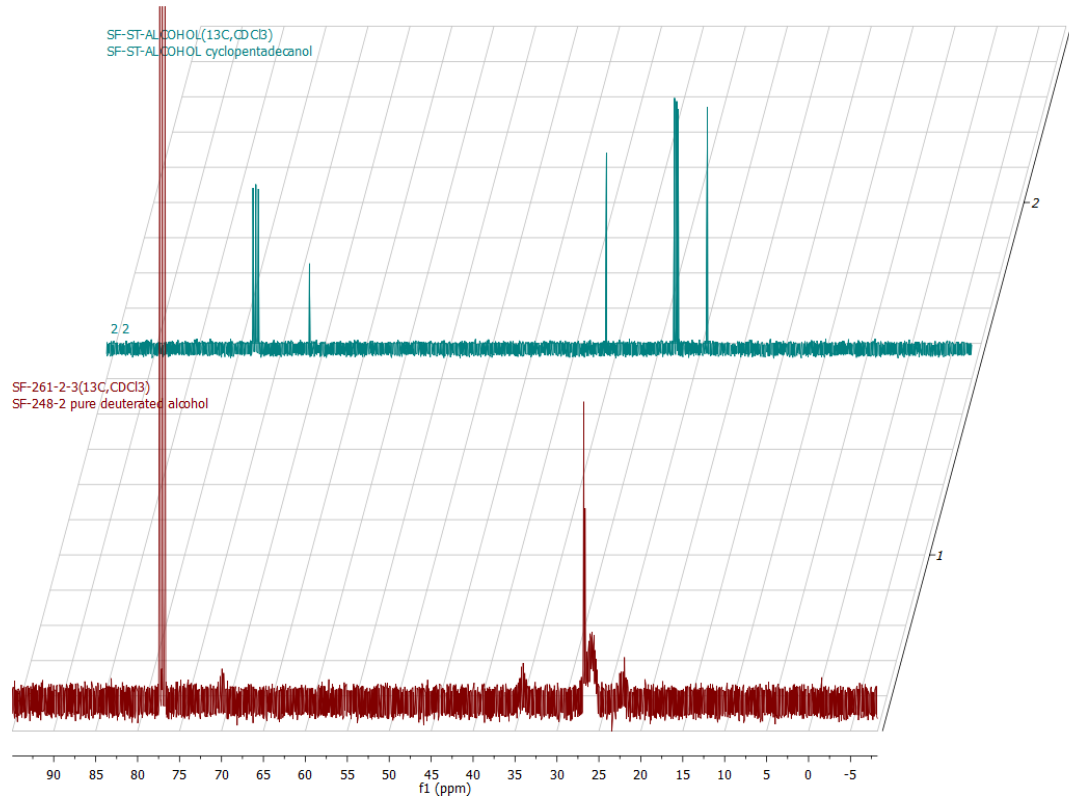


Figure 7.104: ¹³C NMR spectrum (100 MHz, CDCl₃) of cyclopentadecanol-d₂₉ (**80a**). The standard is provided in the back for comparison.

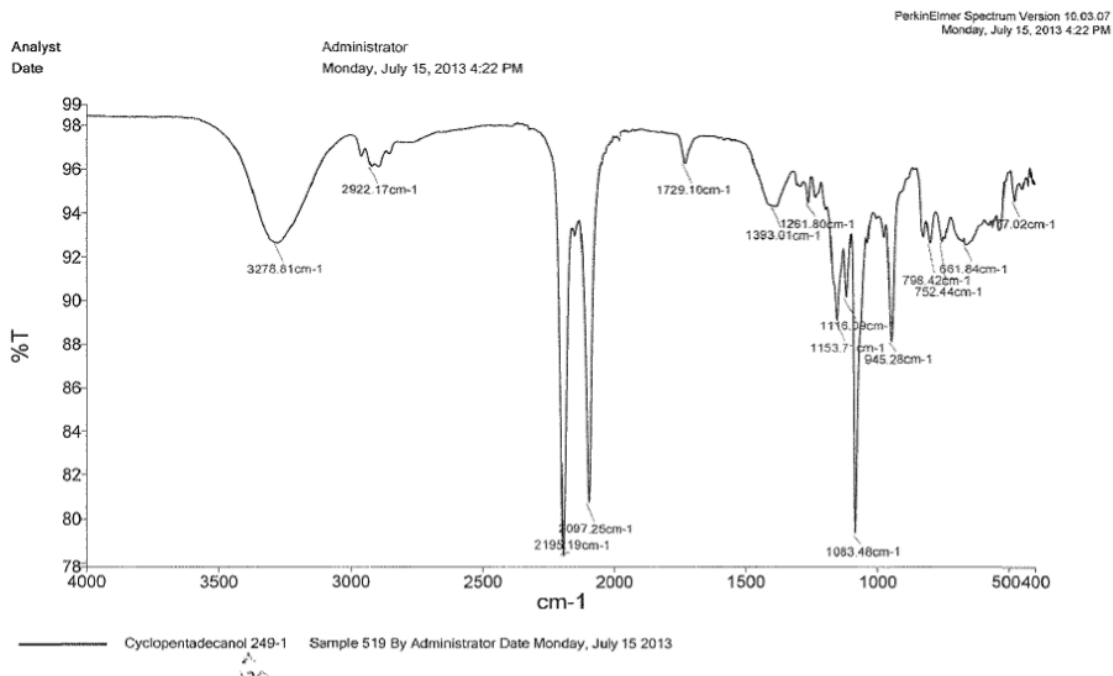


Figure 7.105: Infrared spectrum of cyclopentadecanol-d₂₉ (**80a**).

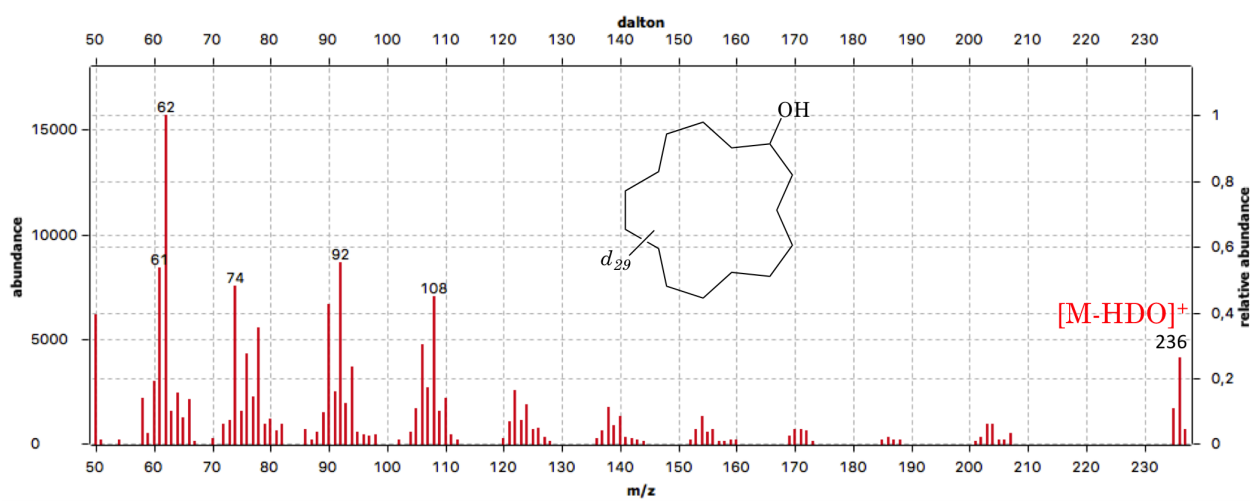


Figure 7.106: Mass spectrum of cyclopentadecanol-d₂₉ (**80a**) recorded by GC-MS. Only the ion with loss of water is seen.

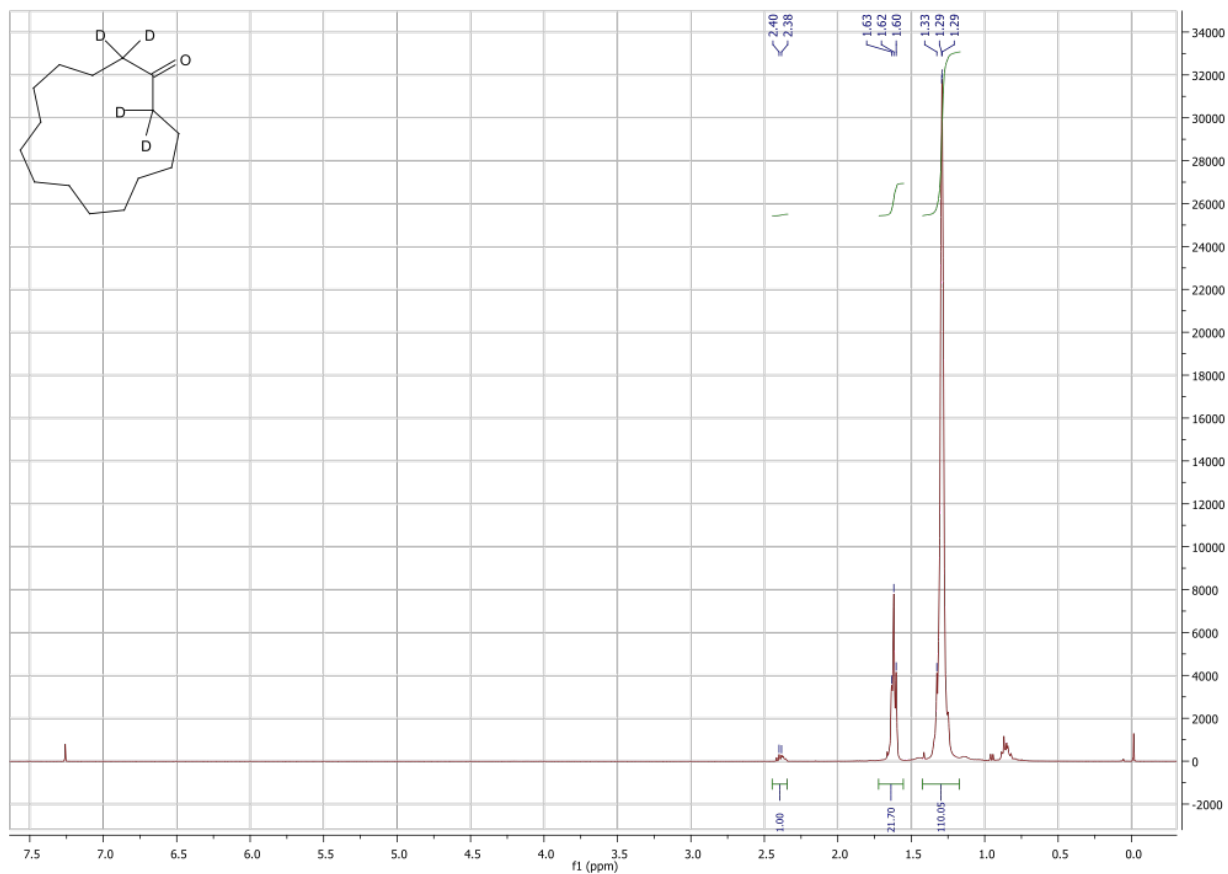


Figure 7.107: ^1H NMR spectrum (400 MHz, CDCl_3) of cyclopentadecanone-d₄ (**78b**).

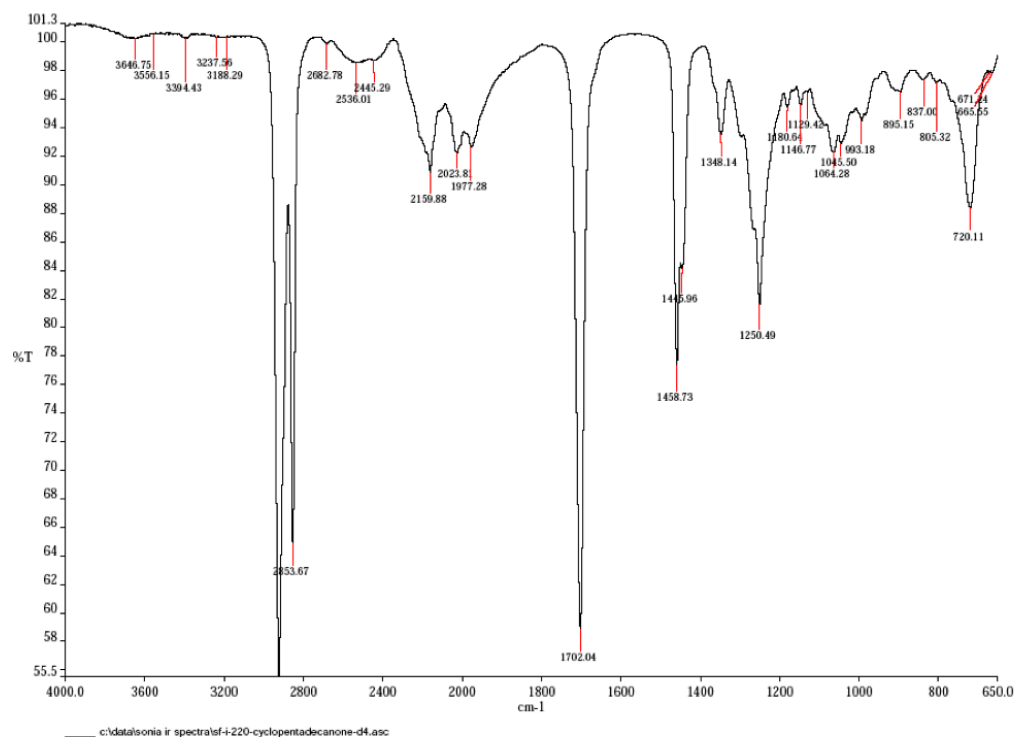


Figure 7.108: Infrared spectrum of cyclopentadecanone-d₄ (**78b**).

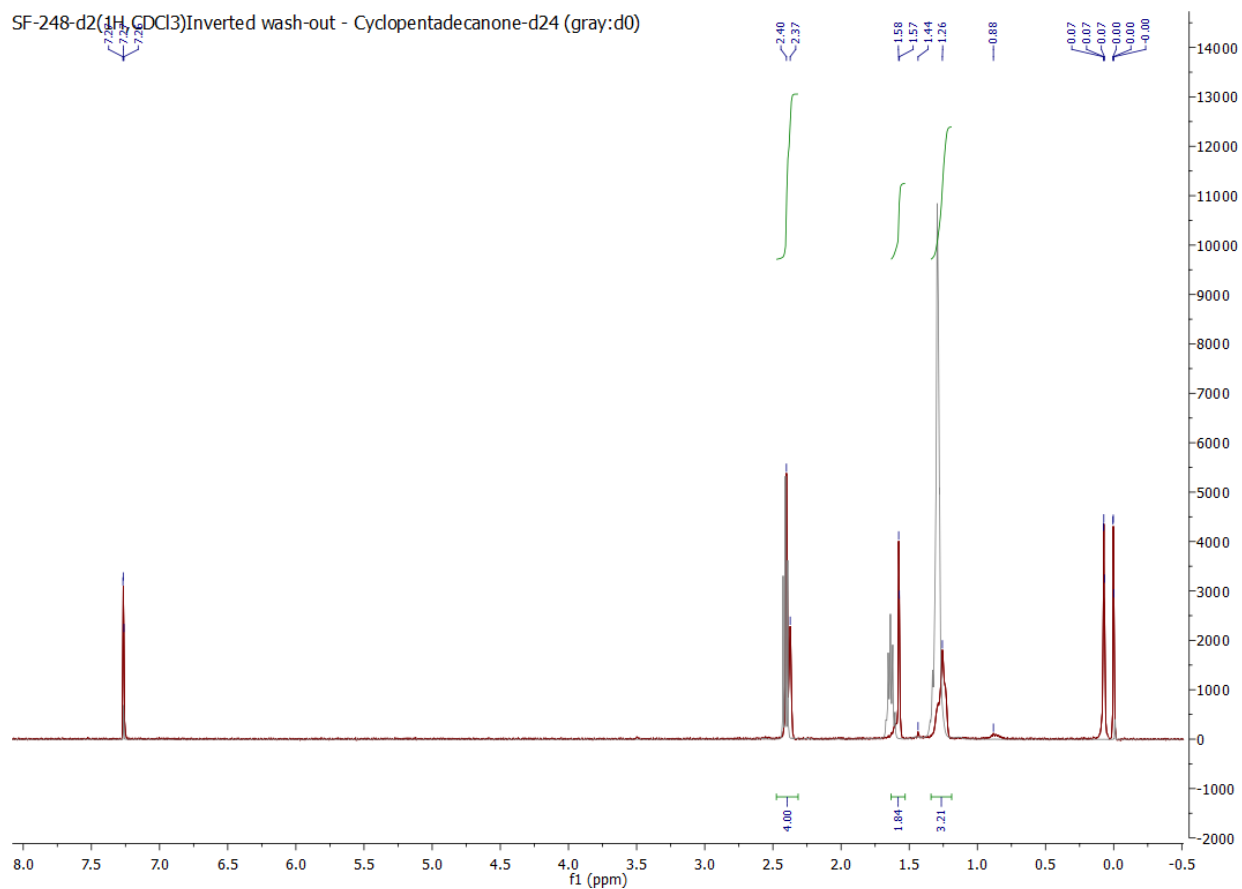


Figure 7.109: ¹H NMR spectrum (400 MHz, CDCl₃) of cyclopentadecanone-d₂₄ (**78c**). Undeuterated compound appears as the gray trace for comparison.

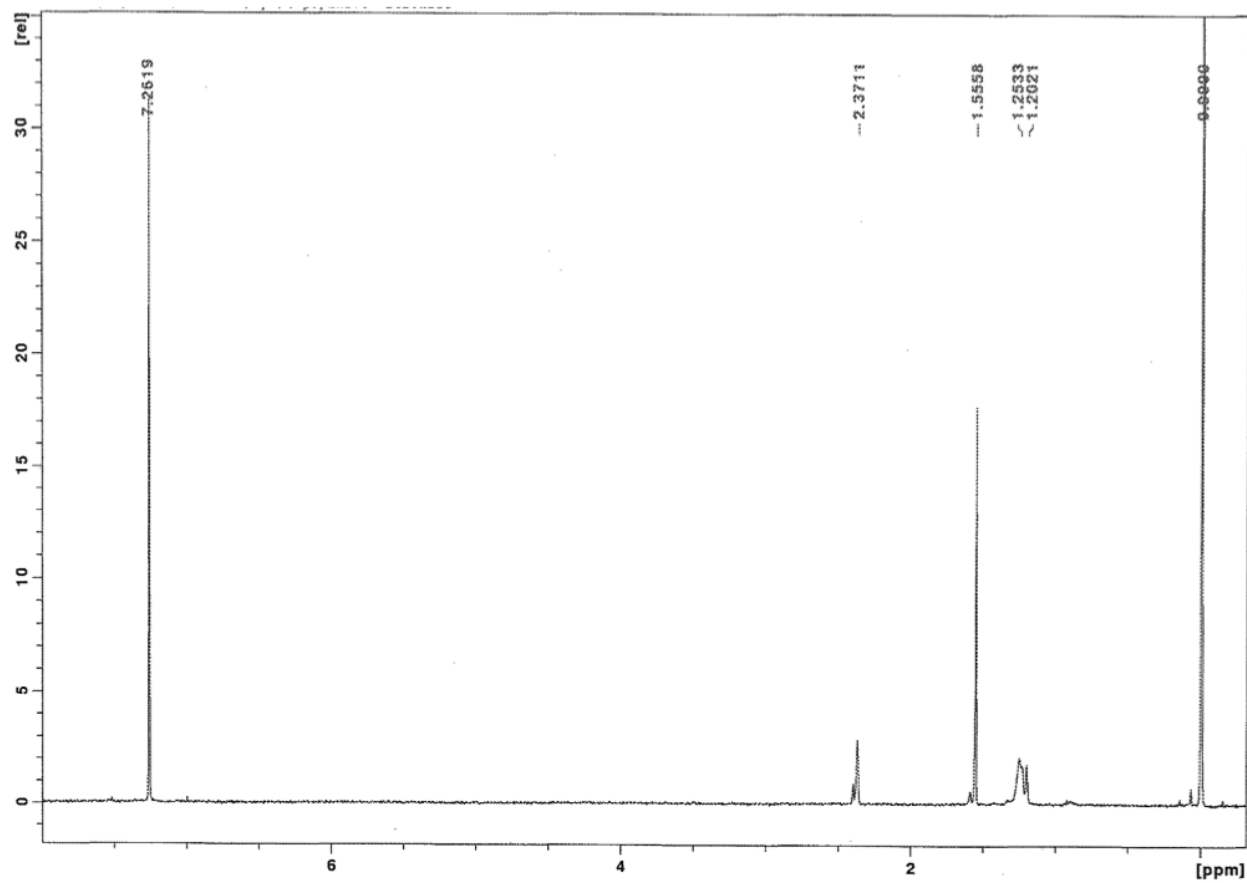


Figure 7.110: ^1H NMR spectrum (400 MHz, CDCl_3) of cyclopentadecanone-d₂₈ (**78d**).

Date: 9/5/2014

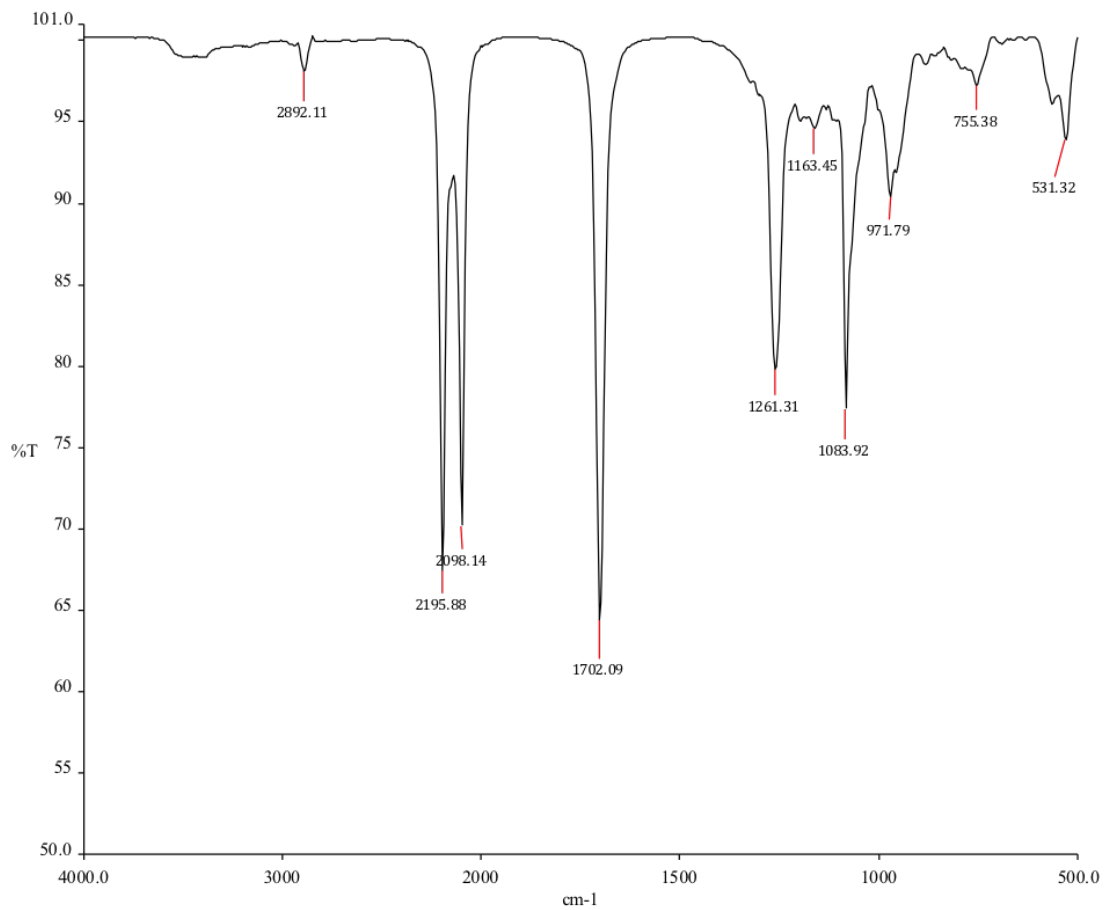


Figure 7.111: Infrared spectrum of cyclopentadecanone-d₂₈ (**78d**).

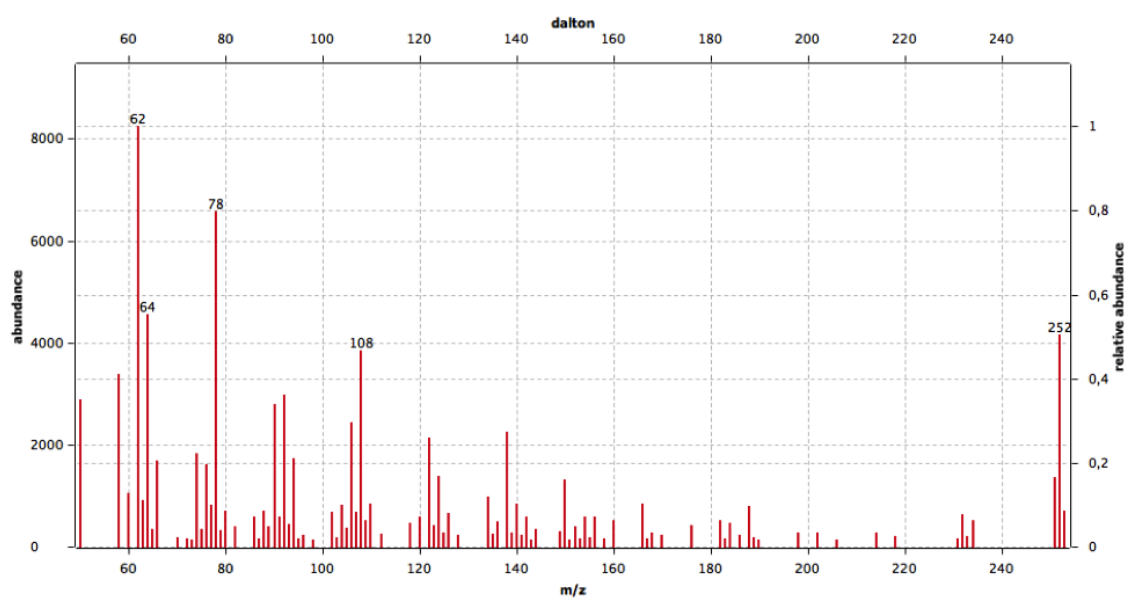


Figure 7.112: Mass spectrum of cyclopentadecanone-d₂₈ (**78d**) recorded by GC-MS. Peak at $m/z = 252$ is the parent ion. Traces of C₁₅HD₂₇O are present (peak at $m/z = 251$).